University of Sussex

Exploring Mechanisms For Pattern Formation Through Coupled Bulk-Surface PDEs

Muflih Alhazmi

Submitted for the degree of Doctor of Philosophy

University of Sussex

June 2018

Declaration

I hereby declare that this thesis has not been and will not be submitted in whole or in part to another University for the award of any other degree.

Signature:

Muflih Alhazmi

UNIVERSITY OF SUSSEX

Muflih Alhazmi, Doctor of Philosophy

Exploring Mechanisms For Pattern Formation Through Coupled Bulk-Surface PDEs

Summary

This work explores mechanisms for pattern formation through coupled bulk-surface partial differential equations of reaction-diffusion type. Reaction-diffusion systems posed both in the bulk and on the surface on stationary volumes are coupled through linear Robin-type boundary conditions. In this framework we study three different systems as follows (i) non-linear reactions in the bulk and surface respectively, (ii) non-linear reactions in the bulk and linear reactions on the surface and (iii) linear reactions in the bulk and non-linear reactions on the surface. In all cases, the systems are non-dimensionalised and rigorous linear stability analysis is carried out to determine the necessary and sufficient conditions for pattern formation. Appropriate parameter spaces are generated from which model parameters are selected. To exhibit pattern formation, a coupled bulk-surface finite element method is developed and implemented. We implement the numerical algorithm by using an open source software package known as deal.II and show computational results on spherical and cuboid domains. Theoretical predictions of the linear stability analysis are verified and supported by numerical simulations. The results show that non-linear reactions in the bulk and surface generate patterns everywhere, while non-linear reactions in the bulk and linear reactions on the surface generate patterns in the bulk and on the surface with a pattern-less thin boundary layer. However, linear reactions in the bulk do not generate patterns on the surface even when the surface reactions are non-linear. The generality, robustness and applicability of our theoretical computational framework for coupled system of bulk-surface reaction-diffusion equations set premises to study experimentally driven models where coupling of bulk and surface

chemical species is prevalent. Examples of such applications include cell motility, pattern formation in developmental biology, material science and cancer biology.

Acknowledgements

I would like to give great thanks to my supervisor Prof. Anotida Madzvamuse for his continuous support, encouragement and patience throughout my research and preparation of this thesis. His kind and excellent support led me to the successful completion of this work. Also I wish to thank Dr. Chandrasekhar Venkataraman and Dr. Filippo Cagnetti for their support and help as my secondary supervisors. I am grateful to the University of Sussex, in particular to the Department of Mathematics for providing the resourceful and equipped environment for research. I wish to thank all the staff members of the School of Mathematical and Physical Sciences at the Sussex University. I am grateful to the Northern Borders University in Saudi Arabia for funding my PhD studies. I would like to give many thanks to Prof. James Hirschfeld for his helpful suggestions and advice during my annual reviews. Many thanks go to the Maths postgraduate students for all the chats and discussions especially with my office mates Benard Kiplangat, Laura Murphy and Eduard Cmpillo-Funollet. I wish to also thank Wakil Sarfafaz, Davide Cusseddu and Victor Ogessa Juma for all the relevant department seminars and group meetings. I would like to further thank my family for their enormous support, kindness, love and patience during my studies.

Contents

List of Tables

List of Figures

Chapter 1

Introduction and Literature Review

1.1 Introduction

Most biological and chemical processes that can be explored through reaction and diffusion of chemical species, are often modelled by systems of partial differential equations Kondo and Asai (1995); Janssen (1981); Hutson (1988). A special class of these are reaction-diffusion equations, which are used to analyse and quantify various biological processes such as the natural evolution of pattern formation on animal coats, developmental embryology, immunology, ecological dynamics Murray (1981); Mullins et al. (1996); De Boer et al. (1992); Segel and Jackson (1972). The study of reaction-diffusion systems in general has been and continues to be an interesting topic for research in various branches of scientific studies. In order to quantify the evolution of chemical reaction kinetics associated to biological processes, it is a usual approach to employ a system of partial differential equations describing the chemical reactions, which is investigated through mathematical techniques to reveal the long-term behaviour of the evolving kinetics Keener and Sneyd (1998); Logan (2008).

Alan Turing was one of the first scientists to suggest in 1952 the use of a system of reaction-diffusion equations to model how two or more chemical substances evolve when they are simultaneously subject to a specific reaction rate and each one of them diffuses independently of the other. Alan Turing suggested that the theory of biolo-

gical pattern formation can be mathematically formulated by a system of partial differential equations Turing (1952). The work presented in Turing (1952) contains an elegant and detailed study on the evolution and interaction of morphogenesis, which are modelled as a discrete set of chemical concentrations coupled through a specific given reaction kinetics and independent diffusion rates. Turing's work turned out to be one of the most motivational studies for applied mathematicians to rigorously explain the evolution and properties of reaction-diffusion systems. The seminal work of Turing Turing (1952) also proved as a motivational ground for experimental and theoretical biologists to search for experimental evidence of pattern formation satisfying Turing's mathematical theory of reaction-diffusion systems. A few examples of Turing models being tested by experimental biologists are Castets et al. (1990); Levine and Rappel (2005), whose results indicate strong evidence supporting Turing's theory of pattern formation. In Castets et al. (1990) a detailed chemical experiment is conducted to show similar evidence to that predicted by Alan Turing as a result of specific chemical reaction and diffusion. The results pertained by Castets et al. (1990) are claimed by authors to be the first unambiguous experimental evidence of Turing pattern. However, Turing theory of pattern formation as the solution of a reaction-diffusion system has still not been proven as a scientific fact. Researchers have also studied the bulk excursion of a particle when it intermittently unbinds from a planar surface into the bulk Chechkin et al. (2012). The study in Chechkin et al. (2012) is a theoretical set-up through coupling reaction-diffusion system to provide insight on the trajectory of a particle during the process of bulk excursion, when it unbinds from the surface without a regular occurrence. Turing's theory suggests that pattern formation occurs, when a system experiences diffusion-driven instability Turing (1952); Murray (2001), which is a concept that is hypothetically responsible for the emergence of spatial variation in the concentration density of a chemical species. Diffusion-driven instability takes place in the evolution of a system, when a uniform stable steady state is destabilised by including the effects of the diffusion process in the system. It is a non-trivial property of the diffusion operator that it can be responsible to destabilise a stable steady state of a system of partial differential equations, because a diffusion operator by itself has the property to homogenise small spatial perturbations, therefore, intuitively if diffusion is added

to a system of reaction kinetics that is stable in the absence of diffusion, then small perturbations near a uniform steady state are expected to ensure that the evolution of the reaction-kinetics converges to the uniform steady state. It is rather unexpected to find that a stabilising process such as diffusion can be capable to destabilise a steady state that is also stable. Such a transition from a uniform steady state in the absence of diffusion to diffusion-driven instability was observed by scientists and presented with detailed elaboration on the process in Ouyang and Swinney (1991). Reaction-kinetics without diffusion are usually modelled by a system of ordinary differential equations, which becomes a system of partial differential equations, when diffusion is added to the system. This makes the analysis and computation of such systems a very challenging task.

Researchers in applied mathematics and computational science also explore bulk-surface reaction-diffusion systems (BSRDSs), which are employed in special kinds of models for biological processes, where species react and diffuse in the bulk of a domain and these are coupled with other species that react and diffuse on the surface of the domain. Bulk-surface reaction-diffusion systems are employed as a framework to model the chemical interaction of bulk-surface problems arising in cell biology Novak et al. (2007). In particular the framework proposed by Novak et al. (2007) aims to provide improved computational and algorithmic efficiency, which is mainly achieved, through employing the usual diffusion on local tangential planes as an approximation of Laplace-Beltrami operator. The framework proposed by Novak et al. (2007) is applied to a realistic cell-like geometry, which produces results that are in agreement with quantitative experimental analysis on fluorescence-loss in photo-bleaching. Another example of a computational approach to solving coupled systems of BSRDEs is the work presented in Hansbo et al. (2016), where they proposed a computational approach to bulk-surface reaction-diffusion systems on time-dependent domains.

In general there are two main aspects to the study of bulk-surface reaction-diffusion equations. The first approach is to solve systems of bulk-surface numerically. Finite element method is the usual choice of the numerical method in the literature, for example there is a detailed study in Elliott and Ranner (2013), suggesting some results on the numerical analysis, existence and convergence of finite

element approximation when bulk-surface reaction-diffusion equations (BSRDEs) are posed with Robin-type boundary conditions. A priori error bounds on the finite element approximate numerical solution are also both derived in certain norms and verified numerically. The work in Elliott and Ranner (2013) is concentrated mainly on the numerical analysis side of the particular scheme they present, which lacks to provide any insight on the stability analysis of the proposed system. Although it is a reasonable decision to exclude stability analysis due to consistency and relevance of contents, with improvements in computational efficiency of BSRDEs, it is crucial that attention is given to stability analysis of such systems. Bulk-surface systems with a single PDE posed in the bulk and coupled with another PDE on the surface also play a vital role in the understanding of receptor-ligand in the process of a signalling cascade Elliott et al. (2017). The study in Elliott et al. (2017) is mainly focused on the numerical analysis through finite element method (FEM) of a two-component system of single equations posed in the bulk and on the surface. In Elliott et al. (2017) the existence of solutions is proven with some computational results associated to the theoretical problem, again lacking to provide insight on the stability behaviour of the dynamics modelled by the coupled system. Even though the results achieved in Elliott et al. (2017) are mathematically sound from a numerical analysis and computational viewpoint, it would provide a complementary back-up to the work if it is equipped with detailed results of stability analysis.

The non-linearities associated with reaction-diffusion system were treated by IMEX and 1-SBEM (a first order semi-implicit backward Euler differentiation formula). Each of these schemes has associated drawbacks that are either related to accuracy or computational efficiency. With the attempt to resolve these drawbacks scientists used a fully implicit, with fractional θ scheme, to improve the computational efficiency as well as to obtain sufficient accuracy. Numerical solutions of reaction-diffusion equations are studied in Madzvamuse and Chung (2014) with a single Newton iteration and compared the convergence rate with the use of a single Picard iteration and it is found that a single Newton's iteration can only prove more efficient if a fractional θ-scheme is applied in the particular case when $\theta = 1 - \sqrt{2}$. The work contained in Madzvamuse and Chung (2014) is not conducted on the actual bulk-surface set-up, instead the numerical schemes are rigorously compared

through investigating the results obtained for a two component reaction-diffusion equation on stationary volumes of rectangular and spherical geometries. This comparison and the results therein can potentially be employed to solve a system of coupled bulk-surface reaction-diffusion equations. One of the computational extensions associated to this thesis is that we apply the fully implicit scheme to an actual four component bulk-surface reaction-diffusion system. The numerical solution of BSRDEs are obtained through this extension on two types of stationary volumes and on the corresponding surfaces. We execute the algorithm to solve the four component BSRDEs on a cuboid and on sphere, where two of the equations are posed on the bulk and the remaining two equations are posed on the boundary surface.

Stability and bifurcation analysis are two other usual analytical approaches to understanding the dynamical properties of reaction-diffusion system near a uniform steady state Krischer and Mikhailov (1994); Hagberg and Meron (1994); Iron et al. (2004); Madzvamuse et al. (2015a); Wei and Winter (2015). It is evident from the literature on the subject of stability analysis that a very limited amount of work is done on stability analysis in a coupled bulk-surface set-up. This is mainly due to the extensive complexity associated in deriving the relevant conditions for diffusion-driven instability when equations from the bulk are coupled with equations on the surface. One of the first detailed studies on stability analysis of BSRDEs is conducted in Madzvamuse et al. (2015a), where it is analytically proven that a certain suitable parameter range exists for equations in the bulk that can induce spatial pattern on the surface. For example Madzvamuse et al. (2015a) found that if a suitable set of reaction kinetics are posed in the bulk, with appropriate choice of parameters, then it is possible that the reaction-diffusion process inside the bulk causes the pattern to emerge on the surface as well, which is found to occur regardless of the type of governing reaction kinetics on the surface. However, if a system of reaction-diffusion equations is posed on the surface with parameters from Turing spaces, then a spatial pattern can evolve on the surface, which may induce the same pattern on a layer of the bulk that is closest to the boundary. It means that such case scenario initiates a patterned boundary layer of certain thickness, beyond which the pattern is not induced in the interior of the bulk. This happens even if the reaction kinetics or parameter values are not suitable for pattern formation

for reaction-diffusion system posed inside the bulk. It is also evident from findings in Madzvamuse et al. (2015a), that the properties of pattern formation in the bulk and on the surface have a continuous influence on each other during the process of reaction and diffusion. The findings of Madzvamuse et al. (2015a) may be further summarised by stating that no choice of reaction kinetics posed on the surface can induce patterning in the whole volume of the bulk, however a certain reaction kinetics with suitable parameter values can induce a boundary layer in which patterning can be emerged without extension of the pattern to the interior of the bulk. All the results in Madzvamuse et al. (2015a) are numerically supported by the finite element method through a library called **deal.II** Bangerth et al. (2016). The current thesis extends the approach taken in Madzvamuse et al. (2015a) to explore different combinations of reaction kinetics on the surface and in the bulk. In particular, combinations of linear and non-linear reaction kinetics are investigated to understand the pattern formation properties of reaction-diffusion equations posed on a coupled bulk-surface type setting.

1.2 Biological motivation

Coupled systems of bulk-surface reaction-diffusion equations (BSRDEs) are one of the several generalisations of reaction-diffusion theory to explore numerous applications in mathematical biology. Processes that involve bulk-surface reaction and/or diffusion are found in various research disciplines such as experimental research in organic chemistry, where a bulk-surface photografting process is used as an efficient tool to create thick grafted layers of hydrophobic polymers in a very short span of time Yang and Rånby (1996a,b). Bulk-surface reaction kinetics are also used to investigate the behaviour of chemical reactions in the interior of a cell, and to explore how a set of specific reaction kinetics in the interior of a cell evolve to influence the surface of the cell Levine and Rappel (2005). We also find bulk-surface reaction-diffusion equations that model a particular aspect of cellular functions with relevance to chemical signalling. In Rätz and Röger (2014) a detailed mathematical model is developed for this particular investigation, to explore the dynamics of pattern formation in the consequences of bulk-surface coupling reaction kinetics.

Moreover, bulk-surface reaction-diffusion equations help to reveal the mechanism of symmetry breaking which is one of the essential steps before the emergence of polarisation of biological cells or buds in yeast cells, the direction of cell motility Rätz and Röger (2014). Bulk-surface reaction-diffusion system are also used to model how surface active agents (surfactants) evolve on the surface of a system, in which the chemical concentration is coupled through a given reaction with the substance in the bulk Hahn et al. (2014). BSRDSs also arise in mathematical models for the dynamics of lipid raft formation on biological membranes Garcke et al. (2016), where the formation of the layer on a biological membrane is modelled as the consequence of coupling conditions with species that react and diffuse in the bulk. A further example of biological application employing bulk-surface reaction-diffusion systems is presented in Bruce et al. (2007), where they model the mediation of cellular metabolism and signalling in part by trans-membrane receptors that undergo the process of diffusion in cell membrane. From the variety of applications that employ BSRDSs, one realises that a robust study of such systems can provide solutions to a great number of important questions in mathematical biology. This in turn requires in-depth and rigorous study of BSRDSs in an attempt to achieve extensive insight on the evolving properties of these models. Most of the published work presented in the current section on the study of BSRDSs either investigate an over-simplified case scenario with the aim of mathematical tractability or a complex model with limitations on the robustness of analytical and numerical findings. This study is therefore, motivated to explore BSRDSs with a realistic degree of complexity through a four-component reaction-diffusion system, two of which are posed on the surface and the other two are posed the bulk. The equations in the bulk and on the surface also satisfy coupling conditions through the evolution dynamics on the surface is influenced by the reaction-diffusion process inside the bulk. It can prove of great importance to obtain insight on the pattern formation properties of such systems. The tools to achieve this in the current thesis are the combined application of linear stability theory, mode isolation and the finite element method.

1.3 Notation and mathematical preliminaries

We start by introducing the required mathematical notations that are consistently used throughout the thesis. Most of the mathematical notation conventions are standard and used globally throughout the entire length of the thesis, unless otherwise stated. We also present some definitions and theorems to serve as the mathematical requirement associated with the derivations and proofs contained in the body on this thesis.

1.3.1 Notations

Consider the set of real numbers $\mathbb{R}$, we define the following concepts:

- A two-dimensional real space denoted by $\mathbb{R}^2$ and defined by $\mathbb{R}^2 = \{\mathbf{x} = (x, y) : x, y \in \mathbb{R}\}$.
- A three-dimensional real space denoted by $\mathbb{R}^3$ and expressed by $\mathbb{R}^3 = \{\mathbf{x} = (x, y, z) : x, y, z \in \mathbb{R}\}$.

Let $u(x, y, z)$ denote a scalar valued function defined on a three-dimensional real space and $\mathbf{w} = (w_1, w_2, w_3)$ to be a vector valued function. The following operators are defined as in Arfken and Weber (2005):

- The gradient operator is given by $\nabla u = \left(\frac{\partial u}{\partial x}, \frac{\partial u}{\partial y}, \frac{\partial u}{\partial z}\right)^T$.
- The divergence operator is defined by $\nabla \cdot \mathbf{w} = \frac{\partial w_1}{\partial x} + \frac{\partial w_2}{\partial y} + \frac{\partial w_3}{\partial z}$.

We denote ordinary derivatives using both the Leibniz notation $\frac{du}{dx}$, $\frac{d^2u}{dx^2}, \ldots$, or the prime notation $y', y'', \ldots$. depending on the notational convenience.

1.3.2 Definitions in $\mathbb{R}^3$

Definition 1.3.1 (Laplace operator) *Gilbarg and Trudinger (2015) Let $\Omega \subset \mathbb{R}^3$ be a connected domain and u a $C^2(\Omega)$ scalar function. The Laplace of u denoted by Δu, is given by*

$$\Delta u = \nabla \cdot \nabla u = \frac{\partial^2 u}{\partial x^2} + \frac{\partial^2 u}{\partial y^2} + \frac{\partial^2 u}{\partial z^2}.$$

Definition 1.3.2 (Outward flux) *Evans (1998) If $\boldsymbol{\nu}$ denotes a unit vector in the outward normal direction, then $\nabla\varphi\cdot\boldsymbol{\nu}$ represents the outward flux which is also called the directional derivative of the scalar valued function φ in the direction $\boldsymbol{\nu}$, which is defined by*

$$\nabla\varphi\cdot\boldsymbol{\nu}=\frac{\partial\varphi}{\partial\boldsymbol{\nu}}.$$

Theorem 1.3.1 (Divergence theorem in $\mathbb{R}^n$) *Gantmacher et al. (1960) Let Ω be a bounded domain with C^1 boundary $\partial\Omega$ and let $\boldsymbol{\nu}$ denote the unit outward normal to $\partial\Omega$. For any vector field $\mathbf{u}\in C^1(\bar{\Omega})$ we have*

$$\int_\Omega \nabla\cdot\mathbf{u}\ \mathrm{d}\Omega=\int_{\partial\Omega}\mathbf{u}\cdot\boldsymbol{\nu}\ \mathrm{d}S \tag{1.1}$$

where $\mathrm{d}S$ indicates the $(n-1)$ dimensional area element in $\partial\Omega$. In particular, if w is a $C^2(\bar{\Omega})$ function, we have by taking $\mathbf{u}=\nabla w$

$$\int_\Omega \Delta w\ \mathrm{d}\Omega=\int_{\partial\Omega}\nabla w\cdot\boldsymbol{\nu}\ \mathrm{d}S=\int_{\partial\Omega}\frac{\partial w}{\partial\boldsymbol{\nu}}\ \mathrm{d}S. \tag{1.2}$$

Definition 1.3.3 (Green's formula in $\mathbb{R}^n$) *Gantmacher et al. (1960) Let Ω be a domain in $\mathbb{R}^n$ with C^1 boundary $\partial\Omega$ for which the divergence theorem holds and let u be $C^2(\bar{\Omega})$ function. If we select $\mathbf{w}=v\nabla u$ in the divergence theorem above, we will have*

$$\int_\Omega v\Delta u\ d\Omega+\int_\Omega \nabla u\cdot\nabla v\ d\Omega=\int_{\partial\Omega}v\frac{\partial u}{\partial\boldsymbol{\nu}}\ \mathrm{d}S, \tag{1.3}$$

which is Green's formula.

1.3.3 Definitions on surface

Definition 1.3.4 (Hypersurfaces) *Dziuk and Elliott (2013a) Γ is called a hypersurface if it is defined by a C^2 function in $\mathbb{R}^2$, such that there exists an open subset U in $\mathbb{R}^2$ and a function $f\in C^2(U)$, with the properity that $\nabla f\neq 0$ on U and*

$$\Gamma=\{x\in U: f(x)=0\}.$$

Definition 1.3.5 (The tangential gradient) *Dziuk and Elliott (2013a) For a scalar valued function $u:\Omega\times(0,T]\to\mathbb{R}$ we denote by the $\nabla_\Gamma u$ the tangential gradient of u and it is defined by*

$$\nabla_\Gamma u=\nabla\bar{u}-(\nabla\bar{u}\cdot\boldsymbol{\nu})\boldsymbol{\nu}$$

where $\bar{u}$ is an smooth extension of u, $\nabla\bar{u}$ is the ordinary gradient of $\bar{u}$ and $\boldsymbol{\nu}$ is the outward normal to the surface Γ.

Definition 1.3.6 (The Laplace-Beltrami operator) *Dziuk and Elliott (2013a) If tangential divergence denoted by $\nabla_\Gamma\cdot$ is applied to the tangential gradient of u, that is, $\nabla_\Gamma u$, this will provide us with The Laplace-Beltrami operator which is*

$$\Delta_\Gamma u = \nabla_\Gamma \cdot \nabla_\Gamma u,$$

where the tangential divergence of a vector valued function is defined by

$$\nabla_\Gamma \cdot \mathbf{u} = \nabla \cdot \mathbf{u} - \sum_{i=1}^{N+1} (\nabla u_i \cdot \boldsymbol{\nu})\nu_i.$$

1.3.4 A typical example of reaction kinetics

For illustrative purposes, we consider Schnakenberg reaction kinetics as an example of classical reactions kinetics. It was introduced by Schnakenberg in (1979) and it is also known as *activator-depleted* model or the *Brusselator* model Gierer and Meinhardt (1972); Schnakenberg (1979); Lakkis et al. (2013); Prigogine and Lefever (1968); Venkataraman et al. (2012). It is derived from a series of autocatalytic reactions by given in Schnakenberg (1979) of the form

$$X \underset{k_1}{\overset{k_2}{\rightleftharpoons}} A, \quad B \xrightarrow{k_4} Y, \quad 2X + Y \xrightarrow{k_3} 3X.$$

Consider the concentrations of X, A, B and Y denoted by u, a_1, b_1 and v respectively. By using the Law of Mass Action and non-dimensionalisation Madzvamuse (2000), we obtain

$$f(u,v) = a - u + u^2 v, \qquad \text{and} \qquad g(u,v) = b - u^2 v, \tag{1.4}$$

with positive parameters a and b.

1.4 Thesis overview

This thesis is structured such that in Chapter 2 a detailed study is conducted through the application of rigorous linear stability theory which is applied to analytically explore and predict the pattern formation properties associated to three bulk-surface

reaction-diffusion systems. This is done through investigating the necessary conditions for diffusion-driven instability for each of these systems. Chapter 3 presents deriving a set of sufficient conditions for diffusion-driven instability, which complements the necessary conditions of the previous chapter in order to insure that spatial pattern is obtained. In Chapter 4 the theoretical formulation for the finite element method is presented for each of the three systems in great detail. We also conduct a comparison of two types of time-stepping schemes in this chapter. Chapter 5 contains the numerical simulations obtained using Deal.II library to verify the analytical predictions associated to the pattern formation properties for the three systems. Chapter 6 concludes the thesis with some ideas for future extensions of the current framework.

Chapter 2

Analysis of Coupled System of Bulk-Surface Reaction-Diffusion Equations (BSRDEs)

In this chapter, we formulate and present the coupled systems of bulk-surface reaction-diffusion equations on stationary volumes, in which two of the equations are posed in the bulk and coupled with two other equations that are posed on the surface bounding the corresponding stationary volume. Reaction-diffusion systems posed both in the bulk and on the surface are coupled through linear Robin-type boundary conditions. In this chapter we explore three different systems. In the first system we analyse non-linear reaction kinetics both in the bulk and on the surface. We present the details of the scaling process that makes all the systems studied in this chapter dimensionless. Also, linear stability analysis is carried out both in the absence and presence of diffusion, the necessary and sufficient conditions for steady state to be stable are derived in the absence of diffusion. In the presence of diffusion, the necessary conditions for diffusion-driven instability are derived. The theoretical results for this system show that the bulk dynamics and the surface dynamics drive pattern formation. The second system is non-linear reactions in the bulk and linear reactions on the surface. The process of re-scaling and rigorous linear stability analysis both in absence and presence of diffusion is carried out to determine the necessary conditions for diffusion-driven instability. The theoretical results for this system show that only the bulk dynamics emerge spatial pattern with the surface

dynamics undergoing a pattern-less evolution. In the last part of this chapter we study another system with linear reactions in the bulk, which are coupled with non-linear reactions on the surface. This system is also investigated through a similar approach as the previous two systems and we find that neither equations in the bulk nor those on the surface can emerge spatial pattern. Therefore, a system with such characteristics is shown to always return to its constant and uniform steady state upon small perturbation in the neighbourhood of the same.

2.1 Non-linear reaction kinetics in the bulk and on the surface

Let $\Omega \subset \mathbb{R}^3$ be a stationary domain with boundary that is a compact hypersurface denoted by $\Gamma \subset \mathbb{R}^2$. Let $u : \Omega \times (0,T] \to \mathbb{R}$ and $v : \Omega \times (0,T] \to \mathbb{R}$ denote the concentration of two chemical species which react and diffuse in Ω. Let $r : \Gamma \times (0,T] \to \mathbb{R}$ and $s : \Gamma \times (0,T] \to \mathbb{R}$ denote two chemical species residing on the surface. When the species from the bulk and surface are coupled only through the reaction kinetics and there is no cross-diffusion, it means that all four species diffuse independently of each other, which can be written in dimensional form as a four-component reaction-diffusion system with independent diffusion rates. For the first system we focus a non-linear reaction kinetics posed both in the bulk and on the surface written in the form

$$\begin{cases} \begin{cases} u_t &= D_u \Delta u + f(u,v), \\ v_t &= D_v \Delta v + g(u,v), \end{cases} & \text{in } \Omega \times (0,T] \\ \begin{cases} r_t &= D_r \Delta_\Gamma r + f(r,s) - h_1(u,v,r,s), \\ s_t &= D_s \Delta_\Gamma s + g(r,s) - h_2(u,v,r,s), \end{cases} & \text{on } \Gamma \times (0,T] \end{cases} \tag{2.1}$$

with coupling boundary conditions

$$\begin{cases} \frac{\partial u}{\partial \nu} = h_1(u,v,r,s), \\ d_\Omega \frac{\partial v}{\partial \nu} = h_2(u,v,r,s), \end{cases} \quad \text{on } \Gamma \times (0,T]. \tag{2.2}$$

We take Ω to be a three-dimensional fixed domain bounded by a compact surface denoted by Γ. We assume that it is a boundary-free connected and closed surface. The strictly positive constants $D_u > 0$, $D_v > 0$, $D_r > 0$ and $D_s > 0$ are the

independent diffusion rates corresponding to the variables indicated in the respective subscripts of each D. We assume $f(.,.)$ and $g(.,.)$ to be non-linear functions. The coupling conditions of the system are represented by h_1 and h_2 which are functions of u, v, r and s. h_1 and h_2 denote reactions of substances througth boundary interface, therefore they depend on all four species namely u, v, r and s. We explicitly define $h_1(u, v, r, s)$ and $h_2(u, v, r, s)$ Madzvamuse et al. (2015a) to be

$$h_1(u, v, r, s) = \alpha_1 r - \beta_1 u - \kappa_1 v \tag{2.3}$$

$$h_2(u, v, r, s) = \alpha_2 s - \beta_2 u - \kappa_2 v. \tag{2.4}$$

The constants $\alpha_1, \alpha_2, \beta_1, \beta_2, \kappa_1$ and κ_2 are positive parameters of system (2.1). We also assume that from all the species we initially have some positive quantity present, which we denote by u^0, v^0, r^0 and s^0, which provides the initial conditions for system (2.1) written as

$$u(\mathbf{x}, 0) = u^0(\mathbf{x}), \quad v(\mathbf{x}, 0) = v^0(\mathbf{x}), \quad r(\mathbf{x}, 0) = r^0(\mathbf{x}), \quad \text{and} \quad s(\mathbf{x}, 0) = s^0(\mathbf{x}).$$

In this system, we focus on the widely known *activator-depleted* model also known as the Brusselator model (Gierer and Meinhardt, 1972; Schnakenberg, 1979; Lakkis et al., 2013; Prigogine and Lefever, 1968; Venkataraman et al., 2012). In the Brusselator model the reaction kinetics are non-linear, given by

$$f(u, v) = k_1 - k_2 u + k_3 u^2 v, \quad \text{and} \quad g(u, v) = k_4 - k_3 u^2 v, \tag{2.5}$$

with positive parameters k_1, k_2, k_3 and k_4.

2.1.1 Non-dimensionalisation

Non-dimensionalisation is a process of rescaling in which partial or full removal of units occurs from an equation by appropriate substitution of the rescaled variables (Murray, 2001; Madzvamuse, 2000; George, 2012). We non-dimensionalise the system of equations using a specific scale, in space or time, when we are interested in observing the prospective solution within the specified scale range. In the new system after non-dimensionalisation, the variables and parameters are all unitless and the parameters will be fewer than in system (2.1). We introduce the non-dimensional variables with a hat and these are written as $\hat{u}$, $\hat{v}$, $\hat{r}$ and $\hat{s}$ with the

corresponding scaling factors u^*, v^*, r^* and s^* respectively. We present the process of non-dimensionalisation only for the bulk-equations in three spatial diemnsions, and the process is identical to non-dimensionalise the surface equations where a two-dimensional surface is embedded in three dimensional space. We choose L to denote the scaling factor for length (L_b for the bulk and L_s for the surface) and t^* to denote the scaling factor for time (t_b^* for the bulk and t_s^* for the surface), The dimensional and the non-dimensional variables Madzvamuse (2000), George (2012) are related through

$$u = u^*\hat{u}, \qquad v = v^*\hat{v}, \qquad r = r^*\hat{r}, \qquad s = s^*\hat{s},$$

where for the bulk we use the scaling given by

$$x = L_b\hat{x}, \qquad y = L_b\hat{y}, \qquad z = L_b\hat{z}, \qquad t = t_b^*\tau$$

and for the surface equations we use

$$x = L_s\hat{x}, \qquad y = L_s\hat{y}, \qquad z = L_s\hat{z}, \qquad t = t_s^*\tau.$$

We substitute for each dimensional variable its corresponding product of non-dimensional variable and the scaling factor leading to

$$\frac{u^*}{t_b^*}\frac{\partial\hat{u}}{\partial\tau} = D_u\frac{u^*}{L_b^2}\Delta\hat{u} + k_1 - k_2u^*\hat{u} + k_3u^{*2}v^*\hat{u}^2\hat{v}, \tag{2.6}$$

$$\frac{v^*}{t_b^*}\frac{\partial\hat{v}}{\partial\tau} = D_v\frac{v^*}{L_b^2}\Delta\hat{v} + k_4 - k_3u^{*2}v^*\hat{u}^2\hat{v}, \qquad \text{in } \hat{\Omega}\times(0,\hat{T}] \tag{2.7}$$

$$\frac{r^*}{t_s^*}\frac{\partial\hat{r}}{\partial\tau} = D_r\frac{r^*}{L_s^2}\Delta_{\hat{\Gamma}}\hat{r} + k_1 - k_2r^*\hat{r} + k_3r^{*2}s^*\hat{r}^2\hat{s} - \alpha_1r^*\hat{r} + \beta_1u^*\hat{u} + \kappa_1v^*\hat{v}, \tag{2.8}$$

$$\frac{s^*}{t_s^*}\frac{\partial\hat{s}}{\partial\tau} = D_s\frac{s^*}{L_s^2}\Delta_{\hat{\Gamma}}\hat{s} + k_4 - k_3r^{*2}s^*\hat{r}^2\hat{s} - \alpha_2s^*\hat{s} + \beta_2u^*\hat{u} + \kappa_2v^*\hat{v}, \quad \text{on } \hat{\Gamma}\times(0,\hat{T}]$$

(2.9)

where $\hat{\Omega}$ and $\hat{\Gamma}$ respectively denote unit cube and its six sided surface. The scaling $\hat{T}$ denotes the final time for the non-dimensional system. Multiplying (2.6), (2.7), (2.8) and (2.9) by $\frac{t_b^*}{u^*}$, $\frac{t_b^*}{v^*}$, $\frac{t_s^*}{r^*}$ and $\frac{t_s^*}{s^*}$ respectively, provided that u^*, v^*, r^* and s^* are non-zero, we obtain

$$\begin{cases} \begin{cases} \frac{\partial\hat{u}}{\partial\tau} &= D_u\frac{t_b^*}{L_b^2}\Delta\hat{u} + \frac{t_b^*k_1}{u^*} - k_2t_b^*\hat{u} + k_3t_b^*u^*v^*\hat{u}^2\hat{v}, \\ \frac{\partial\hat{v}}{\partial\tau} &= D_v\frac{t_b^*}{L_b^2}\Delta\hat{v} + \frac{t_b^*k_4}{v^*} - k_3t_b^*u^{*2}\hat{u}^2\hat{v}, \end{cases} & \text{in } \hat{\Omega}\times(0,\hat{T}] \\ \begin{cases} \frac{\partial\hat{r}}{\partial\tau} &= D_r\frac{t_s^*}{L_s^2}\Delta_{\hat{\Gamma}}\hat{r} + \frac{t_s^*}{r^*}k_1 - k_2t_s^*\hat{r} + k_3t_s^*r^*s^*\hat{r}^2\hat{s} - \alpha_1t_s^*\hat{r} + \frac{t_s^*}{r^*}\beta_1u^*\hat{u} + \frac{t_s^*}{r^*}\kappa_1v^*\hat{v}, \\ \frac{\partial\hat{s}}{\partial\tau} &= D_s\frac{t_s^*}{L_s^2}\Delta_{\hat{\Gamma}}\hat{s} + \frac{t_s^*}{s^*}k_4 - k_3t_s^*r^{*2}\hat{r}^2\hat{s} - \alpha_2t_s^*\hat{s} + \frac{t_s^*}{s^*}\beta_2u^*\hat{u} + \frac{t_s^*}{s^*}\kappa_2v^*\hat{v}, \end{cases} & \text{on } \hat{\Gamma}\times(0,\hat{T}]. \end{cases}$$

(2.10)

We may choose to define $t_b^* = \frac{L_b^2}{D_u}$ and $t_s^* = \frac{L_s^2}{D_r}$ to obtain

$$\begin{cases} \begin{cases} \frac{\partial \hat{u}}{\partial \tau} &= \Delta \hat{u} + \frac{L_b^2}{D_u}[\frac{k_1}{u^*} - k_2\hat{u} + k_3 u^* v^* \hat{u}^2 \hat{v}], \\ \frac{\partial \hat{v}}{\partial \tau} &= \frac{D_v}{D_u}\Delta \hat{v} + \frac{L_b^2}{D_u}[\frac{k_4}{v^*} - k_3 u^{*2}\hat{u}^2\hat{v}], \end{cases} & \text{in } \hat{\Omega} \times (0, \hat{T}] \\ \begin{cases} \frac{\partial \hat{r}}{\partial \tau} &= \Delta_{\hat{\Gamma}} \hat{r} + \frac{L_s^2}{D_r}[\frac{k_1}{r^*} - k_2\hat{r} + k_3 r^* s^* \hat{r}^2 \hat{s} - \alpha_1 \hat{r} + \frac{u^*}{r^*}\beta_1 \hat{u} + \frac{v^*}{r^*}\kappa_1 \hat{v}], \\ \frac{\partial \hat{s}}{\partial \tau} &= \frac{D_s}{D_r}\Delta_{\hat{\Gamma}} \hat{s} + \frac{L_s^2}{D_r}[\frac{k_4}{s^*} - k_3 r^{*2}\hat{r}^2\hat{s} - \alpha_2 \hat{s} + \frac{u^*}{s^*}\beta_2 \hat{u} + \frac{v^*}{s^*}\kappa_2 \hat{v}], \end{cases} & \text{on } \hat{\Gamma} \times (0, \hat{T}]. \end{cases} \tag{2.11}$$

Factoring out some parameters will result in writing the system as

$$\begin{cases} \begin{cases} \frac{\partial \hat{u}}{\partial \tau} &= \Delta \hat{u} + \frac{L_b^2 k_2}{D_u}[\frac{k_1}{k_2 u^*} - \hat{u} + \frac{k_3}{k_2} u^{*2} v^* \hat{u}^2 \hat{v}], \\ \frac{\partial \hat{v}}{\partial \tau} &= d_\Omega \Delta \hat{v} + \frac{L_b^2 k_2}{D_u}[\frac{k_4}{k_2 v^*} - \frac{k_3}{k_2} u^{*2}\hat{u}^2\hat{v}], \end{cases} & \text{in } \hat{\Omega} \times (0, \hat{T}] \\ \begin{cases} \frac{\partial \hat{r}}{\partial \tau} &= \Delta_{\hat{\Gamma}} \hat{r} + \frac{L_s^2 k_2}{D_r}[\frac{k_1}{r^* k_2} - \hat{r} + \frac{k_3}{k_2} r^{*2} s^* \hat{r}^2 \hat{s} - \frac{\alpha_1}{k_2}\hat{r} + \frac{u^*}{r^* k_2}\beta_1 \hat{u} + \frac{v^*}{r^* k_2}\kappa_1 \hat{v}], \\ \frac{\partial \hat{s}}{\partial \tau} &= d_\Gamma \Delta_{\hat{\Gamma}} \hat{s} + \frac{L_s^2 k_2}{D_r}[\frac{k_4}{s^* k_2} - \frac{k_3}{k_2} r^{*2}\hat{r}^2\hat{s} - \frac{\alpha_2}{k_2}\hat{s} + \frac{u^*}{s^* k_2}\beta_2 \hat{u} + \frac{v^*}{s^* k_2}\kappa_2 \hat{v}], \end{cases} & \text{on } \hat{\Gamma} \times (0, \hat{T}] \end{cases} \tag{2.12}$$

where $d_\Omega = \frac{D_v}{D_u}$ and $d_\Gamma = \frac{D_s}{D_r}$ express the non-dimensional positive ratios of diffusion parameters. Requiring the terms $\frac{k_3}{k_2}u^{*2} = 1$ and $\frac{k_3}{k_2}r^{*2} = 1$ to be non-dimensional respectively imply defining $u^* = \sqrt{\frac{k_2}{k_3}}$ and $r^* = \sqrt{\frac{k_2}{k_3}}$. The scaling factors v^* and s^* through a similar process may be derived as

$$\frac{k_3}{k_2}\sqrt{\frac{k_2}{k_3}}v^* = 1 \Rightarrow v^* = \sqrt{\frac{k_2}{k_3}} \quad \text{and} \quad \frac{k_3}{k_2}\sqrt{\frac{k_2}{k_3}}s^* = 1 \Rightarrow s^* = \sqrt{\frac{k_2}{k_3}}. \tag{2.13}$$

Substituting (2.13) in system (2.12) results in

$$\begin{cases} \begin{cases} \frac{\partial \hat{u}}{\partial \tau} &= \Delta \hat{u} + \gamma_\Omega[a_2 - \hat{u} + \hat{u}^2\hat{v}], \\ \frac{\partial \hat{v}}{\partial \tau} &= d_\Omega \Delta \hat{v} + \gamma_\Omega[b_2 - \hat{u}^2\hat{v}], \end{cases} & \text{in } \hat{\Omega} \times (0, \hat{T}] \\ \begin{cases} \frac{\partial \hat{r}}{\partial \tau} &= \Delta_{\hat{\Gamma}} \hat{r} + \gamma_\Gamma[a_2 - \hat{r} + \hat{r}^2\hat{s} - \rho_3 \hat{r} + \mu \hat{u} + \delta_2 \hat{v}], \\ \frac{\partial \hat{s}}{\partial \tau} &= d_\Gamma \Delta_{\hat{\Gamma}} \hat{s} + \gamma_\Gamma[b_2 - \hat{r}^2\hat{s} - \rho_4 \hat{s} + \mu_1 \hat{u} + \delta_3 \hat{v}], \end{cases} & \text{on } \hat{\Gamma} \times (0, \hat{T}] \end{cases} \tag{2.14}$$

where the new dimensionless parameters $\gamma_\Omega = \frac{L_b^2 k_2}{D_u}$, $\gamma_\Gamma = \frac{L_s^2 k_2}{D_r}$, $a_2 = \frac{k_1\sqrt{\frac{k_3}{k_2}}}{k_2}$, $b_2 = \frac{k_4\sqrt{\frac{k_3}{k_2}}}{k_2}$, $\rho_3 = \frac{\alpha_1}{k_2}$, $\rho_4 = \frac{\alpha_2}{k_2}$, $\mu = \frac{\beta_1}{k_2}$, $\mu_1 = \frac{\beta_2}{k_2}$, $\delta_2 = \frac{\kappa_1}{k_2}$ and $\delta_3 = \frac{\kappa_2}{k_2}$ are defined as a consequence of the scaling choice used for u^*, v^*, r^* and s^*. The boundary and initial conditions are non-dimensionalised through the same choice of scaling factors for all variables. For notational convenience we drop all the hats from the non-dimensional variables to obtain the full system of BSRDEs given by (2.1) in its

non-dimensional form as

$$\begin{cases} \begin{cases} \frac{\partial u}{\partial t} &= \Delta u + \gamma_\Omega[a_2 - u + u^2 v], \\ \frac{\partial v}{\partial t} &= d_\Omega \Delta v + \gamma_\Omega[b_2 - u^2 v], \end{cases} & \text{in } \Omega \times (0,T] \\ \begin{cases} \frac{\partial r}{\partial t} &= \Delta_\Gamma r + \gamma_\Gamma[a_2 - r + r^2 s - \rho_3 r + \mu u + \delta_2 v], \\ \frac{\partial s}{\partial t} &= d_\Gamma \Delta_\Gamma s + \gamma_\Gamma[b_2 - r^2 s - \rho_4 s + \mu_1 u + \delta_3 v], \end{cases} & \text{on } \Gamma \times (0,T] \end{cases} \tag{2.15}$$

with linear boundary conditions

$$\begin{cases} \nabla u \cdot \nu = \gamma_\Gamma[\rho_3 r - \mu u - \delta_2 v], \\ d_\Omega \nabla v \cdot \nu = \gamma_\Gamma[\rho_4 s - \mu_1 u - \delta_3 v]. \end{cases} \quad \text{on } \Gamma \times (0,T], \tag{2.16}$$

The non-dimensional initial conditions for all equations are given by

$$u(\mathbf{x},0) = u^0(\mathbf{x}), \quad v(\mathbf{x},0) = v^0(\mathbf{x}), \quad r(\mathbf{x},0) = r^0(\mathbf{x}) \quad \text{and} \quad s(\mathbf{x},0) = s^0(\mathbf{x}). \tag{2.17}$$

The parameter γ_Ω is known as the reaction scaling parameter in the bulk and γ_Γ is the reaction scaling parameter on the surface and both are non-dimensional.

2.1.2 Linear stability analysis in the absence of diffusion

Definition 2.1.1 *(Uniform steady state):(Turing, 1952; Murray, 2001) A point* (u_0, v_0, r_0, s_0) *is a uniform steady state of the coupled system of bulk-surface reaction-diffusion equations* (2.15) *if it solves the nonlinear algebraic system given by* $f_i(u_0, v_0, r_0, s_0) = 0$ *, for all* $i = 1, 2, 3, 4$ *and satisfies the boundary conditions given by* (2.16).

We derive the uniform steady state by solving the algebraic system

$$f_1(u,v,r,s) = \gamma_\Omega(a_2 - u + u^2 v) = 0, \tag{2.18}$$

$$f_2(u,v,r,s) = \gamma_\Omega(b_2 - u^2 v) = 0, \tag{2.19}$$

$$f_3(u,v,r,s) = \gamma_\Gamma(a_2 - r + r^2 s - \rho_3 r + \mu u + \delta_2 v) = 0, \tag{2.20}$$

$$f_4(u,v,r,s) = \gamma_\Gamma(b_2 - r^2 s - \rho_4 s + \mu_1 u + \delta_3 v) = 0, \tag{2.21}$$

such that the boundary conditions given by (2.16) are also satisfied:

$$\gamma_\Gamma[\rho_3 r - \mu u - \delta_2 v] = 0, \tag{2.22}$$

$$\gamma_\Gamma[\rho_4 s - \mu_1 u - \delta_3 v] = 0. \tag{2.23}$$

We add (2.18) and (2.19) to obtain

$$a_2 - u_0 - u_0^2 v_0 + b_2 - u_0^2 v_0 = 0 \;\Rightarrow u_0 = a_2 + b_2. \tag{2.24}$$

Upon substituting u_0 into (2.19), we find

$$v_0 = \frac{b_2}{(a_2 + b_2)^2}.$$

Through a similar straightforward algebraic manipulations we also find the steady state expressions for r_0 and s_0 in the form

$$r_0 = a_2 + b_2, \quad \text{and} \quad s_0 = \frac{b_2}{(a_2 + b_2)^2}. \tag{2.25}$$

Therefore, the uniform steady state solution satisfying system (2.15) is of the form

$$(u_0, v_0, r_0, s_0) = \Big(a_2 + b_2, \frac{b_2}{(a_2 + b_2)^2}, a_2 + b_2, \frac{b_2}{(a_2 + b_2)^2}\Big). \tag{2.26}$$

Substituting the uniform steady state (2.26) in (2.20) and (2.21), leads to state condition on the parameters that is required for (2.26) to satisfy Definition 2.1.1. The condition on the parameters is derived by direct substitution of (2.26) and algebraic manipulations through the following steps

$$-\rho_3(a_2 + b_2) + \mu(a_2 + b_2) + \delta_2 \frac{b_2}{(a_2 + b_2)^2} = 0,$$

$$\Rightarrow (a_2 + b_2)^3 = -\frac{b_2 \delta_2}{\mu - \rho_3}. \tag{2.27}$$

$$-\rho_4 \frac{b_2}{(a_2 + b_2)^2} + \mu_1(a_2 + b_2) + \delta_3 \frac{b_2}{(a_2 + b_2)^2} = 0,$$

$$\Rightarrow (a_2 + b_2)^3 = -\frac{b_2(\delta_3 - \rho_4)}{\mu_1}. \tag{2.28}$$

Combining (2.27) and (2.28) we obtain the required condition on the parameters in the form

$$\frac{b_2 \delta_2}{\mu - \rho_3} = \frac{b_2(\delta_3 - \rho_4)}{\mu_1},$$

$$(\mu - \rho_3)(\delta_3 - \rho_4) = \delta_2 \mu_1. \tag{2.29}$$

Therefore, in order for (2.26) to be a steady state of system (2.15), a condition on the parameters is required to hold, which is

$$(\mu - \rho_3)(\delta_3 - \rho_4) - \delta_2 \mu_1 = 0. \tag{2.30}$$

These findings are summarised in the following theorem.

Theorem 2.1.1 *(Existence and uniqueness of the uniform steady state) (Madzvamuse et al., 2015a) The coupled system of BSRDEs (2.15) with conditions (2.16) admits a unique non-zero steady state given by*

$$(u_0, v_0, r_0, s_0) = \Big(a_2 + b_2, \frac{b_2}{(a_2+b_2)^2}, a_2 + b_2, \frac{b_2}{(a_2+b_2)^2}\Big), \tag{2.31}$$

provided the following compatibility condition on the coefficients of the coupling terms is satisfied

$$(\mu - \rho_3)(\delta_3 - \rho_4) - \delta_2\mu_1 = 0. \tag{2.32}$$

Proof 2.1.1 *The proof of this theorem is provided by all the steps from (2.18) to (2.30).* □

The next step is to complete the linearisation in the absence of diffusion, which is achieved by omitting the diffusion terms from system (2.15). It results in a four-component system of ordinary differential equations written as

$$\frac{du}{dt} = f_1(u, v, r, s) = \gamma_\Omega(a_2 - u + u^2 v) \tag{2.33}$$
$$\frac{dv}{dt} = f_2(u, v, r, s) = \gamma_\Omega(b_2 - u^2 v) \tag{2.34}$$
$$\frac{dr}{dt} = f_3(u, v, r, s) = \gamma_\Gamma(a_2 - r + r^2 s - \rho_3 r + \mu u + \delta_2 v) \tag{2.35}$$
$$\frac{ds}{dt} = f_4(u, v, r, s) = \gamma_\Gamma(b_2 - r^2 s - \rho_4 s + \mu_1 u + \delta_3 v). \tag{2.36}$$

We proceed to linearise the system of ordinary differential equations about the steady state (u_0, v_0, r_0, s_0) using the Taylor expansion (Arfken and Weber, 2005) for functions of four variables up to and including the linear terms, where we define $u(t) = u_0 + \varepsilon w_1(t)$, $v(t) = v_0 + \varepsilon w_2(t)$, $r(t) = r_0 + \varepsilon w_3(t)$, $s(t) = s_0 + \varepsilon w_4(t)$, with $0 < \varepsilon << 1$. The next step is to substitute the linear expansion into (2.33)-(2.36) to obtain

$$\begin{aligned}
\varepsilon\frac{dw_1(t)}{dt} &= \frac{du(t)}{dt} = \gamma_\Omega[a_2 - (u_0 + \varepsilon w_1(t)) + (u_0 + \varepsilon w_1(t))^2(v_0 + \varepsilon w_2)] \\
\varepsilon\frac{dw_2(t)}{dt} &= \frac{dv(t)}{dt} = \gamma_\Omega[b_2 - (u_0 + \varepsilon w_1(t))^2(v_0 + \varepsilon w_2(t))]. \\
\varepsilon\frac{dw_3(t)}{dt} &= \frac{dr(t)}{dt} = \gamma_\Gamma[a_2 - (r_0 + \varepsilon w_3(t)) + (r_0 + \varepsilon w_3(t))^2(s_0 + \varepsilon w_4(t)) \\
&\quad - \rho_3(r_0 + \varepsilon w_3(t)) + \mu(u_0 + \varepsilon w_1(t)) + \delta_2(v_0 + \varepsilon w_2(t))] \\
\varepsilon\frac{dw_4(t)}{dt} &= \frac{ds(t)}{dt} = \gamma_\Gamma[b_2 - (r_0 + \varepsilon w_3(t))^2(s_0 + \varepsilon w_4(t)) \\
&\quad - \rho_4(s_0 + \varepsilon w_4(t)) + \mu_1(u_0 + \varepsilon w_1(t)) + \delta_3(v_0 + \varepsilon w_2(t))].
\end{aligned}$$

We can expand the brackets to write

$$\begin{aligned}
\varepsilon\frac{dw_1(t)}{dt} &= \gamma_\Omega[a_2 - u_0 - \varepsilon w_1(t) + u_0^2 v_0 + v_0\varepsilon^2 w_1^2(t) + 2u_0 v_0 \varepsilon w_1(t) \\
&\quad + u_0^2\varepsilon w_2(t) + \varepsilon^3 w_1^2(t) w_2(t) + 2u_0\varepsilon^2 w_1(t) w_2(t)], \\
\varepsilon\frac{dw_2(t)}{dt} &= \gamma_\Omega[b_2 - u_0^2 v_0 - v_0\varepsilon^2 w_1^2(t) - 2u_0 v_0\varepsilon w_1(t) - u_0^2\varepsilon w_2(t) \\
&\quad - \varepsilon^3 w_1^2(t) w_2(t) - 2u_0\varepsilon^2 w_1(t) w_2(t)], \\
\varepsilon\frac{dw_3(t)}{dt} &= \gamma_\Gamma[a_2 - r_0 - \varepsilon w_3(t) + r_0^2 s_0 + \varepsilon^2 w_3^2(t) s_0 + 2r_0 s_0\varepsilon w_3(t) + r_0^2\varepsilon w_4(t) \\
&\quad + \varepsilon^3 w_3^2(t) w_4(t) + 2r_0\varepsilon^2 w_3(t) w_4(t) - \rho_3 r_0 - \rho_3\varepsilon w_3(t) + \mu u_0 + \mu\varepsilon w_1(t) \\
&\quad + \delta_2 v_0 + \delta_2\varepsilon w_2(t)], \\
\varepsilon\frac{dw_4(t)}{dt} &= \gamma_\Gamma[b_2 - r_0^2 s_0 - \varepsilon^2 w_3^2(t) s_0 - 2r_0 s_0\varepsilon w_3(t) - r_0^2\varepsilon w_4(t) - \varepsilon^3 w_3^2(t) w_4(t) \\
&\quad - 2r_0\varepsilon^2 w_3(t) w_4(t) - \rho_4 s_0 - \rho_4\varepsilon w_4(t) + \mu_1 u_0 + \mu_1\varepsilon w_1(t) + \delta_3 v_0 + \delta_3\varepsilon w_2(t)].
\end{aligned} \tag{2.37}$$

Since we know that at the steady state $f(u_0, v_0, r_0, s_0)$, $g(u_0, v_0, r_0, s_0)$, $h_1(u_0, v_0, r_0, s_0)$ and $h_2(u_0, v_0, r_0, s_0)$ are all equal zero, we can arrange the terms appropritely. Such arrangement of terms is obtained as a step of linearisation process to write

$$\begin{aligned}
\varepsilon\frac{dw_1(t)}{dt} &= \gamma_\Omega[\underbrace{a_2 - u_0 + u_0^2 v_0}_{f(u_0,v_0,r_0,s_0)=0} + \varepsilon w_1(t)(2u_0 v_0 - 1) + \varepsilon w_2(t)(u_0^2) \\
&\quad + \underbrace{v_0\varepsilon^2 w_1^2(t) + \varepsilon^3 w_1^2(t) w_2(t) + 2u_0\varepsilon^2 w_1(t) w_2(t)}_{O(\varepsilon^2)}], \\
\varepsilon\frac{dw_2(t)}{dt} &= \gamma_\Omega[\ \underbrace{b_2 - u_0^2 v_0}_{g(u_0,v_0,r_0,s_0)=0} + \varepsilon w_1(t)(-2u_0 v_0) + \varepsilon w_2(t)(-u_0^2) \\
&\quad - \underbrace{v_0\varepsilon^2 w_1^2(t) - \varepsilon^3 w_1^2(t) w_2(t) - 2u_0\varepsilon^2 w_1(t) w_2(t)}_{O(\varepsilon^2)}], \\
\varepsilon\frac{dw_3(t)}{dt} &= \gamma_\Gamma[\underbrace{a_2 - r_0 + r_0^2 s_0 - \rho_3 r_0 + \mu u_0 + \delta_2 v_0}_{f(u_0,v_0,r_0,s_0) - h_1(u_0,v_0,r_0,s_0)=0} \\
&\quad + \varepsilon w_1(t)(\mu) + \varepsilon w_2(t)(\delta_2) + \varepsilon w_3(t)(2r_0 s_0 - \rho_3 - 1) + \varepsilon w_4(t)(r_0^2) \\
&\quad + \underbrace{\varepsilon^2 w_3^2(t) s_0 + \varepsilon^3 w_3^2(t) w_4(t) + 2r_0\varepsilon^2 w_3(t) w_4(t)}_{O(\varepsilon^2)}],
\end{aligned}$$

$$\varepsilon\frac{dw_4(t)}{dt} = \gamma_\Gamma[\underbrace{b_2 - r_0^2 s_0 - \rho_4 s_0 + \mu_1 u_0 + \delta_3 v_0}_{g(u_0,v_0,r_0,s_0)-h_2(u_0,v_0,r_0,s_0)=0}$$
$$+ \varepsilon w_1(t)(\mu_1) + \varepsilon w_2(t)(\delta_3) + \varepsilon w_3(t)(-2r_0 s_0) + \varepsilon w_4(t)(-r_0^2 - \rho_4)$$
$$- \underbrace{\varepsilon^2 w_3^2(t) s_0 - \varepsilon^3 w_3^2(t) w_4(t) - 2r_0\varepsilon^2 w_3(t) w_4(t)}_{O(\varepsilon^2)}].$$

Performing the algebra, cancelling the expressions for steady state and ignoring higher order terms will transform the equations into the following linearised system:

$$\frac{dw_1(t)}{dt} = \gamma_\Omega[(2u_0v_0 - 1)w_1(t) + u_0^2 w_2(t)], \tag{2.38}$$
$$\frac{dw_2(t)}{dt} = \gamma_\Omega[-2u_0v_0 w_1(t) - u_0^2 w_2(t)], \tag{2.39}$$
$$\frac{dw_3(t)}{dt} = \gamma_\Gamma[\mu w_1(t) + \delta_2 w_2(t) + (2r_0 s_0 - \rho_3 - 1)w_3(t) + r_0^2 w_4(t)], \tag{2.40}$$
$$\frac{dw_4(t)}{dt} = \gamma_\Gamma[\mu_1 w_1(t) + \delta_3 w_2(t) - 2r_0 s_0 w_3(t) + (-r_0^2 - \rho_4)w_4(t)], \tag{2.41}$$

which can be written in matrix notation in the form

$$\begin{pmatrix} \frac{dw_1(t)}{dt} \\ \frac{dw_2(t)}{dt} \\ \frac{dw_3(t)}{dt} \\ \frac{dw_4(t)}{dt} \end{pmatrix} = \begin{pmatrix} (2u_0v_0 - 1)\gamma_\Omega & u_0^2\gamma_\Omega & 0 & 0 \\ -2u_0v_0\gamma_\Omega & -u_0^2\gamma_\Omega & 0 & 0 \\ \mu\gamma_\Gamma & \delta_2\gamma_\Gamma & (2r_0s_0 - \rho_3 - 1)\gamma_\Gamma & r_0^2\gamma_\Gamma \\ \mu_1\gamma_\Gamma & \delta_3\gamma_\Gamma & -2r_0s_0\gamma_\Gamma & (-r_0^2 - \rho_4)\gamma_\Gamma \end{pmatrix} \begin{pmatrix} w_1(t) \\ w_2(t) \\ w_3(t) \\ w_4(t) \end{pmatrix},$$

or equivalently

$$\mathbf{w}_t = \mathbf{A}\mathbf{w}, \tag{2.42}$$

where

$$\mathbf{w} = \begin{pmatrix} w_1(t) \\ w_2(t) \\ w_3(t) \\ w_4(t) \end{pmatrix},$$

$$\mathbf{A} = \begin{pmatrix} (2u_0v_0 - 1)\gamma_\Omega & u_0^2\gamma_\Omega & 0 & 0 \\ -2u_0v_0\gamma_\Omega & -u_0^2\gamma_\Omega & 0 & 0 \\ \mu\gamma_\Gamma & \delta_2\gamma_\Gamma & (2r_0s_0 - \rho_3 - 1)\gamma_\Gamma & r_0^2\gamma_\Gamma \\ \mu_1\gamma_\Gamma & \delta_3\gamma_\Gamma & -2r_0s_0\gamma_\Gamma & (-r_0^2 - \rho_4)\gamma_\Gamma \end{pmatrix}$$
$$= \begin{pmatrix} f_{1u} & f_{1v} & f_{1r} & f_{1s} \\ f_{2u} & f_{2v} & f_{2r} & f_{2s} \\ f_{3u} & f_{3v} & f_{3r} & f_{3s} \\ f_{4u} & f_{4v} & f_{4r} & f_{4s} \end{pmatrix}.$$

This is a coupled system of four ordinary differential equations which has solutions in the form

$$\mathbf{w} = \mathbf{c}e^{\lambda t} \quad \text{where} \quad e^{\lambda t} > 0, \quad \mathbf{c} \neq 0. \tag{2.43}$$

Substituting (2.43) into (2.42) gives us

$$\lambda \mathbf{c} e^{\lambda t} = \mathbf{A}\mathbf{c}e^{\lambda t} \qquad \text{where} \quad e^{\lambda t} > 0, \quad \mathbf{c} \neq 0.$$

Cancelling $e^{\lambda t}$ from both sides, we obtain

$$(\lambda \mathbf{I} - \mathbf{A})\mathbf{c} = 0.$$

Since $\mathbf{c} \neq 0$ then $\mathbf{A}$ is a singular matrix. This leads to the computation of the discrete eigenvalues λ of system (2.42), which is obtained through solving the discrete eigenvalue problem written as

$$\begin{vmatrix} \lambda - \gamma_\Omega(2u_0v_0 - 1) & -\gamma_\Omega(u_0^2) & 0 & 0 \\ \gamma_\Omega(2u_0v_0) & \lambda + \gamma_\Omega(u_0^2) & 0 & 0 \\ -\gamma_\Gamma(\mu) & -\gamma_\Gamma(\delta_2) & \lambda - \gamma_\Gamma(2r_0s_0 - \rho_3 - 1) & -\gamma_\Gamma(r_0^2) \\ -\gamma_\Gamma(\mu_1) & -\gamma_\Gamma(\delta_3) & \gamma_\Gamma(2r_0s_0) & \lambda + \gamma_\Gamma(r_0^2 + \rho_4) \end{vmatrix} = 0. \tag{2.44}$$

We find the eigenvalues of system (2.44) by stating and solving the characteristic polynomial of the matrix, which is

$$(\lambda-\gamma_\Omega(2u_0v_0-1))\begin{vmatrix}\lambda+u_0^2\gamma_\Omega & 0 & 0\\ -\delta_2\gamma_\Gamma & \lambda-\gamma_\Gamma(2r_0s_0-\rho_3-1) & -\gamma_\Gamma(r_0^2)\\ -\delta_3\gamma_\Gamma & \gamma_\Gamma(2r_0s_0) & \lambda+\gamma_\Gamma(r_0^2+\rho_4)\end{vmatrix} \tag{2.45}$$

$$+(u_0^2\gamma_\Omega)\begin{vmatrix}2u_0v_0\gamma_\Omega & 0 & 0\\ -\mu\gamma_\Gamma & \lambda-\gamma_\Gamma(2r_0s_0-\rho_3-1) & -\gamma_\Gamma(r_0^2)\\ -\mu_1\gamma_\Gamma & \gamma_\Gamma(2r_0s_0) & \lambda+\gamma_\Gamma(r_0^2+\rho_4)\end{vmatrix}=0. \tag{2.46}$$

Proceeding with the usual steps we find that the eigenvalues of this matrix are the roots of a degree-four polynomial given by

$$\Big(\lambda-\gamma_\Omega(2u_0v_0-1)\Big)\Big[(\lambda+u_0^2\gamma_\Omega)\Big((\lambda-\gamma_\Gamma(2r_0s_0-\rho_3-1))(\lambda+\gamma_\Gamma(r_0^2+\rho_4))+2r_0^3s_0\gamma_\Gamma^2\Big)\Big]$$
$$+(u_0^2\gamma_\Omega)\Big[(2u_0v_0\gamma_\Omega)\Big((\lambda-\gamma_\Gamma(2r_0s_0-\rho_3-1))(\lambda+\gamma_\Gamma(r_0^2+\rho_4))+2r_0^3s_0\gamma_\Gamma^2\Big)\Big]=0. \tag{2.47}$$

Simplifying the brackets and factoring out the appropriate terms in (2.47) gives

$$\Big[\big(\lambda-\gamma_\Gamma(2r_0s_0-\rho_3-1)\big)\big(\lambda+\gamma_\Gamma(r_0^2+\rho_4)\big)+2r_0^3s_0\gamma_\Gamma^2\Big]$$
$$\Big[\big(\lambda-\gamma_\Omega(2u_0v_0-1)\big)\big(\lambda+u_0^2\gamma_\Omega\big)+2u_0^3v_0\gamma_\Omega^2\Big]=0,$$

which implies to solve two independent quadratic equations written as

$$(\lambda-\gamma_\Gamma(2r_0s_0-\rho_3-1))(\lambda+\gamma_\Gamma(r_0^2+\rho_4))+2r_0^3s_0\gamma_\Gamma^2=0, \tag{2.48}$$

and

$$(\lambda-\gamma_\Omega(2u_0v_0-1))(\lambda+u_0^2\gamma_\Omega)+2u_0^3v_0\gamma_\Omega^2=0. \tag{2.49}$$

In order to find the two eigenvalues in (2.48) we use the equation

$$\lambda^2-\gamma_\Gamma(2r_0s_0-\rho_3-1-r_0^2-\rho_4)\lambda+[2r_0^3s_0-(2r_0s_0-\rho_3-1)(r_0^2+\rho_4)]\gamma_\Gamma^2=0.$$

From this we obtain

$$2\lambda=\gamma_\Gamma(2r_0s_0-\rho_3-1-r_0^2-\rho_4)$$
$$\pm\sqrt{\gamma_\Gamma^2(2r_0s_0-\rho_3-1-r_0^2-\rho_4)^2-4[2r_0^3s_0-(2r_0s_0-\rho_3-1)(r_0^2+\rho_4)]\gamma_\Gamma^2}.$$

We see that for the real part of the two roots to be negative we require the conditions

$$\gamma_\Gamma(2r_0s_0 - \rho_3 - 1 - r_0^2 - \rho_4) < 0, \quad \text{and} \quad [2r_0^3s_0 - (2r_0s_0 - \rho_3 - 1)(r_0^2 + \rho_4)]\gamma_\Gamma^2 > 0, \tag{2.50}$$

which can be equivalently written as

$$f_{3r} + f_{4s} < 0, \quad \text{and} \quad f_{3r}f_{4s} - f_{3s}f_{4r} > 0, \tag{2.51}$$

in terms of the trace and determinant of the last (2×2) block matrix of the system. Similarly we can find the remaining two eigenvalues in (2.49) by using the equation

$$\lambda^2 + \gamma_\Omega(u_0^2 - 2u_0v_0 + 1)\lambda + (u_0^2)\gamma_\Omega^2 = 0.$$

From this we obtain

$$2\lambda = -\gamma_\Omega(u_0^2 - 2u_0v_0 + 1) \pm \sqrt{\gamma_\Omega^2(u_0^2 - 2u_0v_0 + 1)^2 - 4(u_0^2)\gamma_\Omega^2}.$$

We see that for the real part of the final two roots to be negative we require the conditions

$$\gamma_\Omega(u_0^2 - 2u_0v_0 + 1) > 0, \quad \text{and} \quad (u_0^2)\gamma_\Omega^2 > 0, \tag{2.52}$$

which can be equivalently written as

$$f_{1u} + f_{2v} < 0, \quad \text{and} \quad f_{1u}f_{2v} - f_{1v}f_{2u} > 0, \tag{2.53}$$

in terms of the trace and determinant the first (2×2) block matrix of the system. Finally we set out the summary of the necessary and sufficient conditions for $\mathrm{Re}(\lambda) < 0$ in Theorem 2.1.2.

Theorem 2.1.2 *(Necessary and sufficient conditions for $Re(\lambda) < 0$)(Turing, 1952; Murray, 2001) The necessary and sufficient conditions such that the zeros of the polynomial $p_4(\lambda)$ have $Re(\lambda) < 0$ are given by the following conditions:*

$$f_{1u} + f_{2v} < 0, \tag{2.54}$$

$$f_{1u}f_{2v} - f_{1v}f_{2u} > 0, \tag{2.55}$$

$$f_{3r} + f_{4s} < 0, \tag{2.56}$$

$$f_{3r}f_{4s} - f_{3s}f_{4r} > 0. \tag{2.57}$$

Proof 2.1.2 *The proof of this theorem consists of all the steps from (2.42) to (2.53).*□

2.1.3 Linear stability analysis in the presence of diffusion

We start by analysing the system by taking the diffusion terms into account and performing the linear stability analysis. We introduce a small perturbation in the neighbourhood of the steady state namely (u_0, v_0, r_0, s_0). We introduce the small perturbations up to the linear term in the form of

$$\begin{aligned} u(\mathbf{x},t) &= u_0 + \varepsilon w_1(\mathbf{x},t), \\ v(\mathbf{x},t) &= v_0 + \varepsilon w_2(\mathbf{x},t), \\ r(y,t) &= r_0 + \varepsilon w_3(y,t), \\ s(y,t) &= s_0 + \varepsilon w_4(y,t), \\ \text{where} \quad & 0 < \varepsilon << 1. \end{aligned}$$

If we substitute these small perturbations into the system we obtain

$$\begin{aligned} \frac{\partial u(\mathbf{x},t)}{\partial t} &= \frac{\partial (u_0 + \varepsilon w_1(\mathbf{x},t))}{\partial t} = \varepsilon \frac{\partial w_1(\mathbf{x},t)}{\partial t}, \\ \frac{\partial v(\mathbf{x},t)}{\partial t} &= \frac{\partial (v_0 + \varepsilon w_2(\mathbf{x},t))}{\partial t} = \varepsilon \frac{\partial w_2(\mathbf{x},t)}{\partial t}, \\ \frac{\partial r(y,t)}{\partial t} &= \frac{\partial (r_0 + \varepsilon w_3(y,t))}{\partial t} = \varepsilon \frac{\partial w_3(y,t)}{\partial t}, \\ \frac{\partial s(y,t)}{\partial t} &= \frac{\partial (s_0 + \varepsilon w_4(y,t))}{\partial t} = \varepsilon \frac{\partial w_4(y,t)}{\partial t} \end{aligned}$$

and also

$$\begin{aligned} \Delta u(\mathbf{x},t) &= \Delta(u_0 + \varepsilon w_1(\mathbf{x},t)) = \varepsilon \Delta w_1(\mathbf{x},t), \\ d_\Omega \Delta v(\mathbf{x},t) &= d_\Omega \Delta(v_0 + \varepsilon w_2(\mathbf{x},t)) = d_\Omega \varepsilon \Delta w_2(\mathbf{x},t), \\ \Delta_\Gamma r(y,t) &= \Delta_\Gamma(r_0 + \varepsilon w_3(y,t)) = \varepsilon \Delta_\Gamma w_3(y,t), \\ d_\Gamma \Delta_\Gamma s(y,t) &= d_\Gamma \Delta_\Gamma(s_0 + \varepsilon w_4(y,t)) = d_\Gamma \varepsilon \Delta_\Gamma w_4(y,t). \end{aligned}$$

Similarly we substitute such perturbations in the reaction terms to obtain

$$\begin{aligned} \varepsilon \frac{\partial w_1(\mathbf{x},t)}{\partial t} = \frac{\partial u(\mathbf{x},t)}{\partial t} &= \varepsilon \Delta w_1(\mathbf{x},t) + \gamma_\Omega [a_2 - (u_0 + \varepsilon w_1(\mathbf{x},t)) \\ &\quad + (u_0 + \varepsilon w_1(\mathbf{x},t))^2 (v_0 + \varepsilon w_2(\mathbf{x},t))], \\ \varepsilon \frac{\partial w_2(\mathbf{x},t)}{\partial t} = \frac{\partial v(\mathbf{x},t)}{\partial t} &= d_\Omega \varepsilon \Delta w_2(\mathbf{x},t) + \gamma_\Omega [b_2 - (u_0 + \varepsilon w_1(\mathbf{x},t))^2 (v_0 + \varepsilon w_2(\mathbf{x},t))], \\ \varepsilon \frac{\partial w_3(y,t)}{\partial t} = \frac{\partial r(y,t)}{\partial t} &= \varepsilon \Delta_\Gamma w_3(y,t) + \gamma_\Gamma [a_2 - (r_0 + \varepsilon w_3(t)) \\ &\quad + (r_0 + \varepsilon w_3(t))^2 (s_0 + \varepsilon w_4(t)) - \rho_3 (r_0 + \varepsilon w_3(t)) + \mu (u_0 + \varepsilon w_1(t)) \\ &\quad + \delta_2 (v_0 + \varepsilon w_2(t))], \end{aligned}$$

$$\varepsilon\frac{\partial w_4(y,t)}{\partial t} = \frac{\partial s(y,t)}{\partial t} = d_\Gamma \varepsilon \Delta_\Gamma w_4(y,t) + \gamma_\Gamma[b_2 - (r_0+\varepsilon w_3(t))^2(s_0+\varepsilon w_4(t)) - \rho_4(s_0+\varepsilon w_4(t)) + \mu_1(u_0+\varepsilon w_1(t)) + \delta_3(v_0+\varepsilon w_2(t))].$$

Since we know that at the steady state $f(u_0, v_0, r_0, s_0)$, $g(u_0, v_0, r_0, s_0)$, $h_1(u_0, v_0, r_0, s_0)$ and $h_2(u_0, v_0, r_0, s_0)$ are all equal zero, therefore we aim to collect terms in such a way to determine the relative expressions for the steady state in each equation. Furthermore, we aim to perform linear stability analysis,

$$\begin{aligned}
\varepsilon\tfrac{\partial w_1(\mathbf{x},t)}{\partial t} &= \varepsilon\Delta w_1(\mathbf{x},t) + \gamma_\Omega[\underbrace{a_2 - u_0 + u_0^2 v_0}_{f(u_0,v_0,r_0,s_0)=0} + \varepsilon w_1(\mathbf{x},t)(2u_0v_0 - 1) + \varepsilon w_2(\mathbf{x},t)(u_0^2) \\
&\quad + \underbrace{v_0\varepsilon^2 w_1^2(\mathbf{x},t) + \varepsilon^3 w_1^2(\mathbf{x},t)w_2(\mathbf{x},t) + 2u_0\varepsilon^2 w_1(\mathbf{x},t)w_2(\mathbf{x},t)}_{O(\varepsilon^2)}], \\
\varepsilon\tfrac{\partial w_2(\mathbf{x},t)}{\partial t} &= d_\Omega\varepsilon\Delta w_2(\mathbf{x},t) + \gamma_\Omega[\underbrace{b_2 - u_0^2 v_0}_{f(u_0,v_0,r_0,s_0)=0} + \varepsilon w_1(\mathbf{x},t)(-2u_0v_0) + \varepsilon w_2(\mathbf{x},t)(-u_0^2) \\
&\quad - \underbrace{v_0\varepsilon^2 w_1^2(\mathbf{x},t) - \varepsilon^3 w_1^2(\mathbf{x},t)w_2(\mathbf{x},t) - 2u_0\varepsilon^2 w_1(\mathbf{x},t)w_2(\mathbf{x},t)}_{O(\varepsilon^2)}], \\
\varepsilon\tfrac{\partial w_3(y,t)}{\partial t} &= \varepsilon\Delta_\Gamma w_3(y,t) + \gamma_\Gamma[\underbrace{a_2 - r_0 + r_0^2 s_0 - \rho_3 r_0 + \mu u_0 + \delta_2 v_0}_{f(u_0,v_0,r_0,s_0) - h_1(u_0,v_0,r_0,s_0)=0} \\
&\quad + \varepsilon w_1(t)(\mu) + \varepsilon w_2(t)(\delta_2) + \varepsilon w_3(t)(2r_0s_0 - \rho_3 - 1) + \varepsilon w_4(t)(r_0^2) \\
&\quad + \underbrace{\varepsilon^2 w_3^2(t)s_0 + \varepsilon^3 w_3^2(t)w_4(t) + 2r_0\varepsilon^2 w_3(t)w_4(t)}_{O(\varepsilon^2)}], \\
\varepsilon\tfrac{\partial w_4(y,t)}{\partial t} &= d_\Gamma\varepsilon\Delta_\Gamma w_4(y,t) + \gamma_\Gamma[\underbrace{b_2 - r_0^2 s_0 - \rho_4 s_0 + \mu_1 u_0 + \delta_3 v_0}_{g(u_0,v_0,r_0,s_0) - h_2(u_0,v_0,r_0,s_0)=0} \\
&\quad + \varepsilon w_1(t)(\mu_1) + \varepsilon w_2(t)(\delta_3) + \varepsilon w_3(t)(-2r_0s_0) + \varepsilon w_4(t)(-r_0^2 - \rho_4) \\
&\quad - \underbrace{\varepsilon^2 w_3^2(t)s_0 - \varepsilon^3 w_3^2(t)w_4(t) - 2r_0\varepsilon^2 w_3(t)w_4(t)}_{O(\varepsilon^2)}].
\end{aligned}$$

Performing the algebra and cancelling the expressions for steady state and ignoring higher order terms will transform the equations into the following linearised system:

$$\begin{cases} \frac{\partial w_1(\mathbf{x},t)}{\partial t} = \Delta w_1(\mathbf{x},t) + \gamma_\Omega[w_1(\mathbf{x},t)(2u_0v_0 - 1) + w_2(\mathbf{x},t)(u_0^2)], \\ \frac{\partial w_2(\mathbf{x},t)}{\partial t} = d_\Omega\Delta w_2(\mathbf{x},t) + \gamma_\Omega[w_1(\mathbf{x},t)(-2u_0v_0) + w_2(\mathbf{x},t)(-u_0^2)], \end{cases} \quad \mathbf{x}\in\Omega \tag{2.58}$$

$$\begin{cases} \frac{\partial w_3(y,t)}{\partial t} & = \Delta_\Gamma w_3(y,t) + \gamma_\Gamma[w_1(\mathbf{x},t)(\mu) + w_2(\mathbf{x},t)(\delta_2) \\ & \quad + w_3(y,t)(2r_0s_0 - \rho_3 - 1) + w_4(y,t)(r_0^2)], \\ \frac{\partial w_4(y,t)}{\partial t} & = d_\Gamma \Delta_\Gamma w_4(y,t) + \gamma_\Gamma[w_1(\mathbf{x},t)(\mu_1) + w_2(\mathbf{x},t)(\delta_3) \\ & \quad + w_3(y,t)(-2r_0s_0) + w_4(y,t)(-r_0^2 - \rho_4)]. \end{cases} \quad y \in \Gamma \tag{2.59}$$

We also present the boundary conditions using the substitution of linearisation as

$$\begin{cases} \frac{\partial w_1}{\partial \nu} = \gamma_\Gamma[\rho_3 w_3(y,t) - \mu w_1(\mathbf{x},t) - \delta_2 w_2(\mathbf{x},t)], \\ d_\Omega \frac{\partial w_2}{\partial \nu} = \gamma_\Gamma[\rho_4 w_4(y,t) - \mu_1 w_1(\mathbf{x},t) - \delta_3 w_2(\mathbf{x},t)]. \end{cases} \quad \text{on } \Gamma \times (0,T]. \tag{2.60}$$

For the remaining of this work, the analysis is restricted to circular and spherical domains, where the cartesian coordinates are transformed to polar coordinates. The coordinate transformation is done mainly for the convenience of applying the separation variables. Transformation of the Laplace operator from cartesian coordinates to spherical coordinates is a well-known process in (Arfken and Weber, 2005; Chaplain et al., 2001) and it can be shown that in spherical coordinates the usual Laplace is given by

$$\Delta u = \frac{\partial^2 u}{\partial r^2} + \frac{1}{r^2}\frac{\partial^2 u}{\partial \theta^2} + \frac{1}{r^2 \sin^2(\theta)}\frac{\partial^2 u}{\partial \phi^2} + \frac{2}{r}\frac{\partial u}{\partial r} + \frac{\cos(\theta)}{r^2 \sin(\theta)}\frac{\partial u}{\partial \theta}. \tag{2.61}$$

Laplace-Beltrami operator on the surface is given by

$$\Delta_\Gamma u = \frac{\partial^2 u}{\partial \theta^2} + \frac{1}{\sin^2(\theta)}\frac{\partial^2 u}{\partial \phi^2} + \frac{\cos(\theta)}{\sin(\theta)}\frac{\partial u}{\partial \theta}, \tag{2.62}$$

Solving the eigenvalue problem for the Laplace-Beltrami operator given by (2.62), requires the method of separation of variables of the form

$$u(\theta, \phi) = \Theta(\theta)\Phi(\phi), \tag{2.63}$$

which we subtitute into (2.62) to obtain

$$\Theta''\Phi + \frac{\cos(\theta)}{\sin(\theta)}\Theta'\Phi + \frac{1}{\sin^2(\theta)}\Theta\Phi'' = -k^2\Theta\Phi. \tag{2.64}$$

Dividing both sides by $\Theta\Phi$ and multiplying by $\sin^2(\theta)$ results in

$$\sin^2(\theta)\frac{\Theta''}{\Theta} + \cos(\theta)\sin(\theta)\frac{\Theta'}{\Theta} + \frac{\Phi''}{\Phi} = -k^2\sin^2(\theta), \tag{2.65}$$

whose solution satisfies the eigenvalue problem for the Laplace-Beltrami operator of the form

$$\Delta_\Gamma u = -k^2 u, \tag{2.66}$$

with the eigenvalues $k^2 = l(l+1)$. The eigenfunction can be chosen as the spherical harmonics in Chaplain et al. (2001) in the form

$$u_l^m(\theta, \phi) = c_l^m P_l^{|m|}(\cos\theta)\exp(im\phi), \tag{2.67}$$

where $(\theta, \phi) \in [0, \pi] \times [0, 2\pi]$, $l = 0, 1, 2, ...$ and $|m| \leq l$. In Arfken and Weber (2005) and Chaplain et al. (2001) the coefficients c_l^m are given by

$$c_l^m = \sqrt{\frac{2l+1}{4\pi}\frac{(l-m)!}{(l+m)!}},$$

and $P_l^{|m|}(\cos\theta)$ are the associated Legendre function. Using the method of separation of variables, a close a form solution satisfying (2.58) and (2.59) can be written in the form

$$\begin{aligned} w_1(\mathbf{x}, t) &= \psi_{k_{l,m}}(\mathbf{x})u_{l,m}(t), \\ w_2(\mathbf{x}, t) &= \psi_{k_{l,m}}(\mathbf{x})v_{l,m}(t), \\ w_3(y, t) &= \phi(y)r_{l,m}(t), \\ w_4(y, t) &= \phi(y)s_{l,m}(t), \end{aligned}$$

which are substituted in (2.58) and (2.59), to obtain

$$\begin{aligned} \psi_{k_{l,m}}(\mathbf{x})u_{l,m}^{'}(t) &= \Delta\psi_{k_{l,m}}(\mathbf{x})u_{l,m}(t), \\ \psi_{k_{l,m}}(\mathbf{x})v_{l,m}^{'}(t) &= \Delta\psi_{k_{l,m}}(\mathbf{x})v_{l,m}(t), \\ \phi(y)r_{l,m}^{'}(t) &= \Delta_\Gamma\phi(y)r_{l,m}(t), \\ \phi(y)s_{l,m}^{'}(t) &= \Delta_\Gamma\phi(y)s_{l,m}(t). \end{aligned}$$

For equations on the surface the relations may be written as

$$\begin{aligned} \frac{r_{l,m}^{'}(t)}{r_{l,m}(t)} &= \frac{\Delta_\Gamma\phi(y)}{\phi(y)} = -l(l+1), \\ \frac{s_{l,m}^{'}(t)}{s_{l,m}(t)} &= \frac{\Delta_\Gamma\phi(y)}{\phi(y)} = -l(l+1), \end{aligned}$$

whereas for the bulk the relations take the form

$$\begin{aligned} \frac{u_{l,m}^{'}(t)}{u_{l,m}(t)} &= \frac{\Delta\psi_{k_{l,m}}(\mathbf{x})}{\psi_{k_{l,m}}(\mathbf{x})} = -k_{l,m}^2, \\ \frac{v_{l,m}^{'}(t)}{v_{l,m}(t)} &= \frac{\Delta\psi_{k_{l,m}}(\mathbf{x})}{\psi_{k_{l,m}}(\mathbf{x})} = -k_{l,m}^2. \end{aligned}$$

We consider a coordinate transformation in which a vector $\mathbf{x}$ may define every point in the bulk by the variables r (radial distance from the origin) and $\mathbf{y}$ (a point on the surface), with the relationship $\mathbf{x} = r\mathbf{y}$ where $r \in (0,1)$, $\mathbf{y} \in \Gamma$. The eigenvalue of the problem on the surface depends on l itself, where we may consider positive integers only, and m can be any integer with the restriction $|m| \leq l$. This is because the eigenvalues of both problems are equal at $r = 1$. We introduce the continuous eigenvalue problems for the bulk as well as for the surface, in the form of

$$\Delta\psi_{k_{l,m}}(r) = -k_{l,m}^2\psi_{k_{l,m}}(r), \qquad 0 < r < 1 \tag{2.68}$$

and

$$\Delta_\Gamma\phi(y) = -l(l+1)\phi(y), \qquad y \in \Gamma. \tag{2.69}$$

Note that if $r = 1$ for the eigenvalue problem in the bulk, then the eigenvalues associated to the usual diffusion operator must coincide with those associated to the Laplace-Beltrami operator on the surface, which means the relation

$$-k_{l,m}^2 = -l(l+1)$$

must hold. Solutions to such a system can be written in power series representation Arfken and Weber (2005), taking the form

$$\begin{aligned} w_1(ry,t) &= \sum_{l\in\mathbb{N}_0, m\in\mathbb{Z}} u_{l,m}(t)\psi_{k_{l,m}}(r)\phi_{l,m}(y), \\ w_2(ry,t) &= \sum_{l\in\mathbb{N}_0, m\in\mathbb{Z}} v_{l,m}(t)\psi_{k_{l,m}}(r)\phi_{l,m}(y), \\ w_3(y,t) &= \sum_{l\in\mathbb{N}_0, m\in\mathbb{Z}} r_{l,m}(t)\phi_{l,m}(y), \\ w_4(y,t) &= \sum_{l\in\mathbb{N}_0, m\in\mathbb{Z}} s_{l,m}(t)\phi_{l,m}(y), \end{aligned} \tag{2.70}$$

which we substitute for w_1, w_2, w_3 and w_4 the power series solutions (2.70) to turn the system of PDEs into a system of ODEs. First we note that on the surface we have

$$\begin{aligned} \frac{\partial w_3}{\partial t} &= \Delta_\Gamma w_3 + \gamma_\Gamma[w_1(\mu) + w_2(\delta_2) + w_3(2r_0^2 s_0 - \rho_3 - 1) + w_4(r_0^2)] \\ &= \Delta_\Gamma w_3 + \gamma_\Gamma[(2r_0^2 s_0 - 1)w_3 + (r_0^2)w_4] - \gamma_\Gamma[-\mu w_1 - \delta_2 w_2 + \rho_3 w_3], \\ \frac{\partial w_3}{\partial t} &= \frac{d}{dt}(r_{l,m}(t)\phi_{l,m}(y)), \\ &= \frac{dr_{l,m}(t)}{dt}(\phi_{l,m}(y)), \end{aligned}$$

$$\begin{aligned}\tfrac{dr_{l,m}(t)}{dt}(\phi_{l,m}(y)) &= \Delta_\Gamma r_{l,m}(t)\phi_{l,m}(y)\\ &+\gamma_\Gamma\phi_{l,m}(y)[(2r_0^2s_0-1)r_{l,m}(t)+(r_0^2)s_{l,m}(t)]\\ &-\gamma_\Gamma\phi_{l,m}(y)[-\mu u_{l,m}(t)\psi_{k_{l,m}}(1)-\delta_2 v_{l,m}(t)\psi_{k_{l,m}}(1)+(\rho_3)r_{l,m}(t)].\end{aligned} \tag{2.71}$$

Upon substituting (2.69) in (2.71) we are able to write the differential equation for r in the form

$$\begin{aligned}\tfrac{dr_{l,m}(t)}{dt}(\phi_{l,m}(y)) &= -r_{l,m}(t)l(l+1)\phi_{l,m}(y)\\ &+\gamma_\Gamma\phi_{l,m}(y)[(2r_0^2s_0-1)r_{l,m}(t)+(r_0^2)s_{l,m}(t)]\\ &-\gamma_\Gamma\phi_{l,m}(y)[-\mu u_{l,m}(t)\psi_{k_{l,m}}(1)-\delta_2 v_{l,m}(t)\psi_{k_{l,m}}(1)+(\rho_3)r_{l,m}(t)],\end{aligned} \tag{2.72}$$

which upon cancelling $\phi_{l,m}(y)$ from both sides of (2.72), leads to

$$\begin{aligned}\tfrac{dr_{l,m}(t)}{dt} &= -r_{l,m}(t)l(l+1)+\gamma_\Gamma[(2r_0^2s_0-1)r_{l,m}(t)+(r_0^2)s_{l,m}(t)]\\ &-\gamma_\Gamma[-\mu u_{l,m}(t)\psi_{k_{l,m}}(1)-\delta_2 v_{l,m}(t)\psi_{k_{l,m}}(1)+(\rho_3)r_{l,m}(t)].\end{aligned} \tag{2.73}$$

In order to obtain the differential equation for s, through a similar approach we write

$$\begin{aligned}\frac{\partial w_4}{\partial t} &= d_\Gamma\Delta_\Gamma w_4+\gamma_\Gamma[w_1(\mu_1)+w_2(\delta_3)+w_3(-2r_0^2s_0)+w_4(r_0^2-\rho_4)]\\ &= d_\Gamma\Delta_\Gamma w_4+\gamma_\Gamma[(-2r_0^2s_0)w_3-(r_0^2)w_4]-\gamma_\Gamma[-(\mu_1)w_1-(\delta_3)w_2+(\rho_4)w_4],\\ \frac{\partial w_4}{\partial t} &= \frac{d}{dt}(s_{l,m}(t)\phi_{l,m}(y))\\ &= \frac{ds_{l,m}(t)}{dt}(\phi_{l,m}(y)),\end{aligned}$$

which results in

$$\begin{aligned}\tfrac{ds_{l,m}(t)}{dt}(\phi_{l,m}(y)) &= d_\Gamma\Delta_\Gamma s_{l,m}(t)\phi_{l,m}(y)\\ &+\gamma_\Gamma\phi_{l,m}(y)[(-2r_0^2s_0)r_{l,m}(t)-(r_0^2)s_{l,m}(t)]\\ &-\gamma_\Gamma\phi_{l,m}(y)[-(\mu_1)u_{l,m}(t)\psi_{k_{l,m}}(1)-(\delta_3)v_{l,m}(t)\psi_{k_{l,m}}(1)+(\rho_4)s_{l,m}(t)].\end{aligned} \tag{2.74}$$

Substituting (2.69) in (2.74) we obtain

$$\begin{aligned}\tfrac{ds_{l,m}(t)}{dt}(\phi_{l,m}(y)) &= -d_\Gamma s_{l,m}(t)l(l+1)\phi_{l,m}(y)\\ &+\gamma_\Gamma\phi_{l,m}(y)[(-2r_0^2s_0)r_{l,m}(t)-(r_0^2)s_{l,m}(t)]\\ &-\gamma_\Gamma\phi_{l,m}(y)[-(\mu_1)u_{l,m}(t)\psi_{k_{l,m}}(1)-(\delta_3)v_{l,m}(t)\psi_{k_{l,m}}(1)+(\rho_4)s_{l,m}(t)].\end{aligned} \tag{2.75}$$

Cancelling $\phi_{l,m}(y)$ from both sides of (2.75), we obtain

$$\begin{aligned}\tfrac{ds_{l,m}(t)}{dt} &= -d_\Gamma s_{l,m}(t)l(l+1) + \gamma_\Gamma[(-2r_0^2 s_0)r_{l,m}(t) - (r_0^2)s_{l,m}(t)] \\ &-\gamma_\Gamma[-(\mu_1)u_{l,m}(t)\psi_{k_{l,m}}(1) - (\delta_3)v_{l,m}(t)\psi_{k_{l,m}}(1) + (\rho_4)s_{l,m}(t)].\end{aligned} \tag{2.76}$$

Similarly we substitute the power series solution for the equations in the bulk

$$\begin{aligned}\frac{\partial w_1}{\partial t} &= \Delta w_1 + \gamma_\Omega[w_1(2u_0v_0 - 1) + w_2(u_0^2)], \\ \frac{\partial w_1}{\partial t} &= \frac{d(u_{l,m}(t))}{dt}[\psi_{k_{l,m}}(r)\phi_{l,m}(y)],\end{aligned}$$

$$\begin{aligned}\Rightarrow \tfrac{d(u_{l,m}(t))}{dt}[\psi_{k_{l,m}}(r)\phi_{l,m}(y)] &= \Delta u_{l,m}(t)\psi_{k_{l,m}}(r)\phi_{l,m}(y) \\ &+\gamma_\Omega[(2u_0v_0 - 1)u_{l,m}(t)\psi_{k_{l,m}}(r)\phi_{l,m}(y) \\ &+(u_0^2)v_{l,m}(t)\psi_{k_{l,m}}(r)\phi_{l,m}(y)].\end{aligned} \tag{2.77}$$

Upon substituting (2.68) in (2.77) we are able to write the differential equation for u in the form

$$\begin{aligned}\tfrac{d(u_{l,m}(t))}{dt}[\psi_{k_{l,m}}(r)\phi_{l,m}(y)] &= -k_{l,m}^2 u_{l,m}(t)\psi_{k_{l,m}}(r)\phi_{l,m}(y) \\ &+\gamma_\Omega[(2u_0v_0 - 1)u_{l,m}(t)\psi_{k_{l,m}}(r)\phi_{l,m}(y) \\ &+(u_0^2)v_{l,m}(t)\psi_{k_{l,m}}(r)\phi_{l,m}(y)],\end{aligned} \tag{2.78}$$

which upon cancelling $\psi_{k_{l,m}}(r)$ and $\phi_{l,m}(y)$ from both sides of (2.78), leads to

$$\frac{d(u_{l,m}(t))}{dt} = -k_{l,m}^2 u_{l,m}(t) + \gamma_\Omega[(2u_0v_0 - 1)u_{l,m}(t) + (u_0^2)v_{l,m}(t)]. \tag{2.79}$$

In order to obtain the differential equation for v through a similar approach we write

$$\begin{aligned}\frac{\partial w_2}{\partial t} &= d_\Omega \Delta w_2 + \gamma_\Omega[w_1(-2u_0v_0) + w_2(-u_0^2)], \\ \frac{\partial w_2}{\partial t} &= \frac{d(v_{l,m}(t))}{dt}[\psi_{k_{l,m}}(r)\phi_{l,m}(y)],\end{aligned}$$

$$\begin{aligned}\Rightarrow \tfrac{d(v_{l,m}(t))}{dt}[\psi_{k_{l,m}}(r)\phi_{l,m}(y)] &= d_\Omega \Delta v_{l,m}(t)\psi_{k_{l,m}}(r)\phi_{l,m}(y) \\ &+\gamma_\Omega[(-2u_0v_0)u_{l,m}(t)\psi_{k_{l,m}}(r)\phi_{l,m}(y) \\ &-(u_0^2)v_{l,m}(t)\psi_{k_{l,m}}(r)\phi_{l,m}(y)],\end{aligned} \tag{2.80}$$

Substituting (2.68) in (2.80) we obtain

$$\begin{aligned}\tfrac{d(v_{l,m}(t))}{dt}[\psi_{k_{l,m}}(r)\phi_{l,m}(y)] &= -d_\Omega k_{l,m}^2 v_{l,m}(t)\psi_{k_{l,m}}(r)\phi_{l,m}(y) \\ &+\gamma_\Omega[(-2u_0v_0)u_{l,m}(t)\psi_{k_{l,m}}(r)\phi_{l,m}(y) \\ &-(u_0^2)v_{l,m}(t)\psi_{k_{l,m}}(r)\phi_{l,m}(y)],\end{aligned} \tag{2.81}$$

Cancelling $\psi_{k_{l,m}}(r)$ and $\phi_{l,m}(y)$ from both sides of (2.81), results in

$$\frac{d(v_{l,m}(t))}{dt} = -d_\Omega k_{l,m}^2 v_{l,m}(t) + \gamma_\Omega[(-2u_0v_0)u_{l,m}(t) - (u_0^2)v_{l,m}(t)]. \tag{2.82}$$

We apply this substitution to the given boundary conditions to obtain

$$\begin{aligned} \tfrac{\partial w_1}{\partial \nu} &= \gamma_\Gamma[-\mu w_1 - \delta_2 w_2 + (\rho_3)w_3], \\ \tfrac{\partial w_1}{\partial \nu} &= \tfrac{d}{d\nu}(u_{l,m}(t)\psi_{k_{l,m}}(1)\phi_{l,m}(y)) \\ &= u_{l,m}(t)\phi_{l,m}(y)\tfrac{d\psi_{k_{l,m}}(1)}{d\nu}, \end{aligned}$$

$$\begin{aligned} u_{l,m}(t)\phi_{l,m}(y)\tfrac{d\psi_{k_{l,m}}(1)}{d\nu} &= \gamma_\Gamma[-\mu u_{l,m}(t)\psi_{k_{l,m}}(1)\phi_{l,m}(y) - \delta_2 v_{l,m}(t)\psi_{k_{l,m}}(1)\phi_{l,m}(y) \\ &\quad +(\rho_3)r_{l,m}(t)\phi_{l,m}(y)]. \end{aligned} \tag{2.83}$$

Cancelling $\phi_{l,m}(y)$ from both sides of (2.83), we have

$$u_{l,m}(t)\frac{d\psi_{k_{l,m}}(1)}{d\nu} = \gamma_\Gamma\psi_{k_{l,m}}(1)[-\mu u_{l,m}(t) - \delta_2 v_{l,m}(t)] + \gamma_\Gamma(\rho_3)r_{l,m}(t). \tag{2.84}$$

Similarly

$$\begin{aligned} d_\Omega\tfrac{\partial w_2}{\partial \nu} &= \gamma_\Gamma[-\mu_1 w_1 - \delta_3 w_2 + \rho_4 w_4], \\ d_\Omega\tfrac{\partial w_2}{\partial \nu} &= d_\Omega\tfrac{d}{d\nu}(v_{l,m}(t)\psi_{k_{l,m}}(1)\phi_{l,m}(y)), \\ &= d_\Omega v_{l,m}(t)\phi_{l,m}(y)\tfrac{d\psi_{k_{l,m}}(1)}{d\nu}, \end{aligned}$$

$$\begin{aligned} d_\Omega v_{l,m}(t)\phi_{l,m}(y)\tfrac{d\psi_{k_{l,m}}(1)}{d\nu} &= \gamma_\Gamma[-\mu_1 u_{l,m}(t)\psi_{k_{l,m}}(1)\phi_{l,m}(y) - \delta_3 v_{l,m}(t)\psi_{k_{l,m}}(1)\phi_{l,m}(y) \\ &\quad +(\rho_4)s_{l,m}(t)\phi_{l,m}(y)]. \end{aligned} \tag{2.85}$$

Cancelling $\phi_{l,m}(y)$ from both sides of (2.85), we obtain

$$d_\Omega v_{l,m}(t)\frac{d\psi_{k_{l,m}}(1)}{d\nu} = \gamma_\Gamma\psi_{k_{l,m}}(1)[-\mu_1 u_{l,m}(t) - \delta_3 v_{l,m}(t)] + \gamma_\Gamma\rho_4 s_{l,m}(t), \tag{2.86}$$

where $\frac{d\psi_{k_{l,m}}(1)}{d\nu} = \psi'_{k_{l,m}}(1)$. We rewrite (2.79) and (2.82), and we substitute (2.84) and (2.86) into (2.73) and (2.76) respectively to obtain

$$\frac{d(u_{l,m}(t))}{dt} = [-k_{l,m}^2 + 2u_0v_0\gamma_\Omega - \gamma_\Omega]u_{l,m}(t) + [u_0^2\gamma_\Omega]v_{l,m}(t), \tag{2.87}$$

$$\frac{d(v_{l,m}(t))}{dt} = [-2u_0v_0\gamma_\Omega]u_{l,m}(t) + [-d_\Omega k_{l,m}^2 - u_0^2\gamma_\Omega]v_{l,m}(t), \tag{2.88}$$

$$\frac{d(r_{l,m}(t))}{dt} = [-l(l+1) + \gamma_\Gamma(2r_0^2s_0 - 1)]r_{l,m}(t) + [r_0^2\gamma_\Gamma]s_{l,m}(t) + [-\psi'_{k_{l,m}}(1)]u_{l,m}(t), \tag{2.89}$$

$$\frac{d(s_{l,m}(t))}{dt} = [-2r_0^2s_0\gamma_\Gamma]r_{l,m}(t) + [-d_\Gamma l(l+1) - r_0^2\gamma_\Gamma]s_{l,m}(t) + [-d_\Omega\psi'_{k_{l,m}}(1)]v_{l,m}(t), \tag{2.90}$$

which can be written in the form

$$\mathbf{w}_t = \mathbf{M}\mathbf{w}, \tag{2.91}$$

where $\mathbf{w}$ and $\mathbf{M}$ are given by

$$\mathbf{w} = \begin{pmatrix} u_{l,m}(t) \\ v_{l,m}(t) \\ r_{l,m}(t) \\ s_{l,m}(t) \end{pmatrix}$$

and

$$\mathbf{M} = \begin{pmatrix} -k_{l,m}^2 + 2u_0v_0\gamma_\Omega - \gamma_\Omega & u_0^2\gamma_\Omega & 0 & 0 \\ -2u_0v_0\gamma_\Omega & -d_\Omega k_{l,m}^2 - u_0^2\gamma_\Omega & 0 & 0 \\ -\psi'_{k_{l,m}}(1) & 0 & -l(l+1) + \gamma_\Gamma(2r_0^2s_0 - 1) & r_0^2\gamma_\Gamma \\ 0 & -d_\Omega\psi'_{k_{l,m}}(1) & -2r_0^2s_0\gamma_\Gamma & -d_\Gamma l(l+1) - r_0^2\gamma_\Gamma \end{pmatrix}.$$

This is a coupled system of four ODEs which has a solution in the form

$$(u_{l,m}, v_{l,m}, r_{l,m}, s_{l,m})^T = (u_{l,m}^0, v_{l,m}^0, r_{l,m}^0, s_{l,m}^0)^T e^{\lambda t}, \tag{2.92}$$

$$\Rightarrow \mathbf{w} = \mathbf{w^0} e^{\lambda t}, \tag{2.93}$$

where

$$\mathbf{w} = (u_{l,m}, v_{l,m}, r_{l,m}, s_{l,m})^T, \qquad \mathbf{w^0} = (u_{l,m}^0, v_{l,m}^0, r_{l,m}^0, s_{l,m}^0)^T \neq (0,0,0,0)^T, \qquad e^{\lambda t} > 0$$

and λ depends on k^2 for equations in the bulk and it is a function of l for equations on the surface. Substituting (2.93) into (2.91), to obtain

$$\lambda \mathbf{w^0} e^{\lambda t} = \mathbf{M}\mathbf{w^0} e^{\lambda t}, \quad \text{where} \quad e^{\lambda t} > 0.$$

Cancelling $e^{\lambda t}$ from both sides,

$$(\lambda \mathbf{I} - \mathbf{M})\mathbf{w^0} = 0.$$

Since $\mathbf{w^0} = (u_{l,m}^0, v_{l,m}^0, r_{l,m}^0, s_{l,m}^0)^T \neq (0,0,0,0)^T$, then $\mathbf{M}$ is a singular matrix. This leads to the computation of the discrete eigenvalues $\lambda_{l,m}$ associated to the system

(2.91), which is obtained through solving the discrete eigenvalues polynomial given by

$$|\lambda \mathbf{I} - \mathbf{M}| = 0,$$

$$\begin{vmatrix} \lambda+k_{l,m}^2-\gamma_\Omega(2u_0v_0-1) & -\gamma_\Omega(u_0^2) & 0 & 0 \\ \gamma_\Omega(2u_0v_0) & \lambda+d_\Omega k_{l,m}^2+\gamma_\Omega(u_0^2) & 0 & 0 \\ \psi'_{k_{l,m}}(1) & 0 & \lambda+l(l+1)-\gamma_\Gamma(2r_0^2s_0-1) & -\gamma_\Gamma(r_0^2) \\ 0 & d_\Omega\psi'_{k_{l,m}}(1) & \gamma_\Gamma(2r_0^2s_0) & \lambda+d_\Gamma l(l+1)+\gamma_\Gamma(r_0^2) \end{vmatrix} = 0.$$

Proceeding with the usual steps we find that the eigenvalues of this matrix are the roots of a degree-four polynomial given by

$$[(\lambda + l(l+1) - \gamma_\Gamma(2r_0^2s_0 - 1))(\lambda + d_\Gamma l(l+1) + r_0^2\gamma_\Gamma) + 2r_0^3 s_0 \gamma_\Gamma^2]$$
$$[(\lambda + k_{l,m}^2 - \gamma_\Omega(2u_0v_0 - 1))(\lambda + d_\Omega k_{l,m}^2 + u_0^2\gamma_\Omega) + 2u_0^3 v_0 \gamma_\Omega^2] = 0.$$

We observe that

$$(\lambda + l(l+1) - \gamma_\Gamma(2r_0^2s_0 - 1))(\lambda + d_\Gamma l(l+1) + r_0^2\gamma_\Gamma) + 2r_0^3 s_0 \gamma_\Gamma^2 = 0, \tag{2.94}$$

or

$$(\lambda + k_{l,m}^2 - \gamma_\Omega(2u_0v_0 - 1))(\lambda + d_\Omega k_{l,m}^2 + u_0^2\gamma_\Omega) + 2u_0^3 v_0 \gamma_\Omega^2 = 0. \tag{2.95}$$

In order to find the two eigenvalues in (2.94) we use the equation

$$\lambda^2 + \underbrace{\left((1+d_\Gamma)l(l+1) - \gamma_\Gamma(2r_0^2s_0 - r_0^2 - 1)\right)}_{M_1}\lambda$$
$$+ \underbrace{\left(d_\Gamma[l(l+1)]^2 - l(l+1)\gamma_\Gamma[d_\Gamma(2r_0^2s_0 - 1) - r_0^2] + r_0^2\gamma_\Gamma^2\right)}_{H_1} = 0.$$

From this we obtain

$$2\lambda = -M_1 \pm \sqrt{(M_1)^2 - 4H_1}.$$

Let M_1 and H_1 respectively denote the trace and the determinant of the last 2×2 block matrix; then for the uniform steady state (2.26) to be unstable, we require that

$$\mathrm{Re}(\lambda(l(l+1))) > 0 \quad \text{for some } l(l+1) > 0, \tag{2.96}$$

which can be found if and only if

$$M_1 < 0 \quad \text{and} \quad H_1 > 0, \tag{2.97}$$

or

$$M_1 > 0 \quad \text{and} \quad H_1 < 0. \tag{2.98}$$

Since $2r_0s_0 - 1 - r_0^2 < 0$, then $M_1 > 0$ from (2.98). A direct consequence of $H_1 < 0$ is to write

$$H_1(l(l+1)) = d_\Gamma[l(l+1)]^2 - l(l+1)\gamma_\Gamma[d_\Gamma(2r_0^2s_0 - 1) - r_0^2] + r_0^2\gamma_\Gamma^2, \tag{2.99}$$

where we observe that $H_1(l(l+1)) < 0$ if $d_\Gamma(2r_0^2s_0 - 1) - r_0^2 > 0$ which also implies that $d_\Gamma \neq 1$ because $2r_0s_0 - 1 - r_0^2 < 0$.
Therefore

$$d_\Gamma(2r_0^2s_0 - 1) - r_0^2 > 0 \quad \Rightarrow \; d_\Gamma \neq 1, \tag{2.100}$$

which can be equivalently written as

$$d_\Gamma f_{3r} + f_{4s} > 0 \quad \Rightarrow \; d_\Gamma \neq 1, \tag{2.101}$$

is necessary but not sufficient. We find the stationary point of H_1 through differentiating the equation (2.99) with respect to $p = l(l+1)$ and equate it to zero to obtain

$$\frac{dH_1(p)}{dp} = 2d_\Gamma[l(l+1)] - \gamma_\Gamma[d_\Gamma(2r_0^2s_0 - 1) - r_0^2],$$

$$\Rightarrow p = \frac{\gamma_\Gamma[d_\Gamma(2r_0^2s_0 - 1) - r_0^2]}{2d_\Gamma}. \tag{2.102}$$

Substituting (2.102) into (2.99), we obtain

$$H_1(p) = \frac{\gamma_\Gamma^2[d_\Gamma(2r_0^2s_0 - 1) - r_0^2]^2}{4d_\Gamma} - \frac{\gamma_\Gamma^2[d_\Gamma(2r_0^2s_0 - 1) - r_0^2]^2}{2d_\Gamma} + r_0^2\gamma_\Gamma^2 < 0,$$

which implies that

$$r_0^2\gamma_\Gamma^2 < \frac{\gamma_\Gamma^2[d_\Gamma(2r_0^2s_0 - 1) - r_0^2]^2}{4d_\Gamma}. \tag{2.103}$$

By simplifying (2.103) we obtain

$$[d_\Gamma(2r_0^2 s_0 - 1) - r_0^2]^2 - 4d_\Gamma r_0^2 > 0, \tag{2.104}$$

which can be equivalently written as

$$[d_\Gamma f_{3r} + f_{4s}]^2 - 4d_\Gamma(f_{3r}f_{4s} - f_{3s}f_{4r}) > 0. \tag{2.105}$$

Similarly we can find the remaining two eigenvalues in (2.95) by using the equation

$$\lambda^2 + \underbrace{((d_\Omega+1)k_{l,m}^2 - \gamma_\Omega(2u_0v_0 - u_0^2 - 1))}_{M_2}\lambda + \underbrace{(k_{l,m}^4 d_\Omega - k_{l,m}^2\gamma_\Omega[d_\Omega(2u_0v_0-1) - u_0^2] + u_0^2\gamma_\Omega^2)}_{H_2} = 0. \tag{2.106}$$

From this we obtain

$$2\lambda = -M_2 \pm \sqrt{(M_2)^2 - 4H_2}.$$

Let M_2 and H_2 respectively denote the trace and the determinant of the first 2×2 block matrix; then, for the uniform steady state (2.26) to be unstable, we require that

$$\mathrm{Re}(\lambda(k_{l,m}^2)) > 0 \quad \text{for some } k_{l,m}^2 > 0, \tag{2.107}$$

which can be found if and only if

$$M_2 < 0 \quad \text{and} \quad H_2 > 0, \tag{2.108}$$

or

$$M_2 > 0 \quad \text{and} \quad H_2 < 0. \tag{2.109}$$

Since $2u_0v_0 - 1 - u_0^2 < 0$, then $M_2 > 0$ from (2.109). A direct cnsequence of $H_2 < 0$ is to write

$$H_2(k_{l,m}^2) = {k_{l,m}}^4 d_\Omega - {k_{l,m}}^2\gamma_\Omega[d_\Omega(2u_0v_0 - 1) - u_0^2] + u_0^2\gamma_\Omega^2. \tag{2.110}$$

where we observe that $H_2(k_{l,m}^2) < 0$ if $d_\Omega(2u_0v_0 - 1) - u_0^2 > 0$ which implies that $d_\Omega \neq 1$ because $2u_0v_0 - 1 - u_0^2 < 0$. It follows therefore that the condition

$$d_\Omega(2u_0v_0 - 1) - u_0^2 > 0 \quad \Rightarrow \; d_\Omega \neq 1, \tag{2.111}$$

which can be equivalently written as

$$d_\Omega f_{1u} + f_{2v} > 0 \quad \Rightarrow \; d_\Omega \neq 1, \tag{2.112}$$

is necessary but not sufficient. We find the stationary point of H_2 through differentiating the equation (2.110) with respect to $k^2_{l,m}$ and equate it to zero to obtain

$$\frac{dH_2(k^2_{l,m})}{dk^2_{l,m}} = 2{k_{l,m}}^2 d_\Omega - \gamma_\Omega[d_\Omega(2u_0v_0 - 1) - u_0^2],$$

$$\Rightarrow k^2_{l,m} = \frac{\gamma_\Omega[d_\Omega(2u_0v_0 - 1) - u_0^2]}{2d_\Omega}. \tag{2.113}$$

Substituting (2.113) into (2.110), we obtain

$$H_2(k^2_{l,m}) = \frac{\gamma^2_\Omega[d_\Omega(2u_0v_0 - 1) - u_0^2]^2}{4d_\Omega} - \frac{\gamma^2_\Omega[d_\Omega(2u_0v_0 - 1) - u_0^2]^2}{2d_\Omega} + u_0^2\gamma^2_\Omega < 0.,$$

which implies that

$$u_0^2\gamma^2_\Omega < \frac{\gamma^2_\Omega[d_\Omega(2u_0v_0 - 1) - u_0^2]^2}{4d_\Omega}. \tag{2.114}$$

By simplifying (2.114) we obtain

$$[d_\Omega(2u_0v_0 - 1) - u_0^2]^2 - 4d_\Omega u_0^2 > 0, \tag{2.115}$$

which can be equivalently written as

$$[d_\Omega f_{1u} + f_{2v}]^2 - 4d_\Omega(f_{1u}f_{2v} - f_{1v}f_{2u}) > 0. \tag{2.116}$$

Now we summarise the results in the following theorem.

Theorem 2.1.3 *(Turing, 1952; Murray, 2001) The necessary conditions for diffusion-driven instability for the coupled system of BSRDEs (2.15) and (2.16) are given by*

$$f_{1u} + f_{2v} < 0, \tag{2.117}$$

$$f_{1u}f_{2v} - f_{1v}f_{2u} > 0, \tag{2.118}$$

$$f_{3r} + f_{4s} < 0, \tag{2.119}$$

$$f_{3r}f_{4s} - f_{3s}f_{4r} > 0, \tag{2.120}$$

and

$$d_\Omega f_{1u} + f_{2v} > 0 \quad \textit{and} \quad [d_\Omega f_{1u} + f_{2v}]^2 - 4d_\Omega(f_{1u}f_{2v} - f_{1v}f_{2u}) > 0. \tag{2.121}$$

and/or

$$d_\Gamma f_{3r} + f_{4s} > 0 \quad \textit{and} \quad [d_\Gamma f_{3r} + f_{4s}]^2 - 4d_\Gamma(f_{3r}f_{4s} - f_{3s}f_{4r}) > 0. \tag{2.122}$$

Proof 2.1.3 *The proof of this theorem consists of all the steps from* (2.91) *to* (2.116).□

Theoretical predictions

We state from the analytical results about system the following theoretical predictions.

- The bulk dynamics and the surface dynamics can both give rise to pattern formation.

- From conditions (2.117) and (2.121) for the bulk, we write

$$f_{1u} + f_{2v} < 0 \quad \text{and} \quad d_\Omega f_{1u} + f_{2v} > 0.$$

  Combining the inequalities imply $f_{1u} < -f_{2v} < d_\Omega f_{1u}$, which means that for diffusion-driven instability to occur, $f_{1u} < d_\Omega f_{1u} \Rightarrow d_\Omega > 1$. Thus, the inhibitor must diffuse faster than the activator, because $d_\Omega = \frac{D_v}{D_u}$ where D_v is the diffusion coefficient of the inhibitor and D_u is the diffusion coefficient of the activator. It is through a similar argument for diffusion-driven instability to occur on the surface, one finds that $d_\Gamma > 1$ is required. For a detailed mathematical derivation of condition $d > 1$ the interested reader may consult (Madzvamuse et al., 2010, 2015b, 2016).

- Taking $d_\Omega = 1$ and $d_\Gamma > 1$, the surface dynamics may evolve into a spatial pattern while the bulk dynamics can not produce patterns.

- Taking $d_\Omega = 1$ and $d_\Gamma = 1$, the bulk and the surface dynamics fail to produce patterns.

- Taking $d_\Omega > 1$ and $d_\Gamma = 1$, the bulk dynamics may produce pattern while the surface dynamics fail to do so, however, the bulk pattern can induce pattern on the surface as well, even though the surface reaction-diffusion system can not.

- The conditions (2.117) - (2.122) are necessary but not sufficient for the emergence of an inhomogeneous spatial structure. Sufficient conditions will be presented in Chapter 3.

2.2 Linear reaction kinetics on the surface and non-linear reaction kinetics in the bulk

In this system we focus on a system with linear reaction kinetics on the surface and non-linear reaction kinetics in the bulk by considering the following coupled bulk-surface reaction-diffusion equations

$$\begin{cases} \begin{cases} u_t &= D_u\Delta u + f(u,v), \\ v_t &= D_v\Delta v + g(u,v), \end{cases} & \text{in } \Omega\times(0,T] \\ \begin{cases} r_t &= D_r\Delta_\Gamma r - ar + bs - h_1(u,v,r,s), \\ s_t &= D_s\Delta_\Gamma s + cr - ds - h_2(u,v,r,s), \end{cases} & \text{on } \Gamma\times(0,T] \end{cases} \tag{2.123}$$

with coupling boundary conditions

$$\begin{cases} \frac{\partial u}{\partial \nu} = h_1(u,v,r,s), \\ d_\Omega \frac{\partial v}{\partial \nu} = h_2(u,v,r,s), \end{cases} \quad \text{on } \Gamma\times(0,T]. \tag{2.124}$$

The constants a, b, c and d are strictly positive parameters of the system. The coupling conditions of the system is represented in a similar way by h_1 and h_2 which are functions of u, v, r and s, where h_1 and h_2 are given by

$$h_1(u,v,r,s) = \alpha_1 r - \beta_1 u - \kappa_1 v, \tag{2.125}$$

$$h_2(u,v,r,s) = \alpha_2 s - \beta_2 u - \kappa_2 v. \tag{2.126}$$

The constants $\alpha_1, \alpha_2, \beta_1, \beta_2, \kappa_1$ and κ_2 are also positive parameters. The initial conditions are prescribed similar to those given for system (2.1), which are

$$u(\mathbf{x},0) = u^0(\mathbf{x}), \quad v(\mathbf{x},0) = v^0(\mathbf{x}), \quad r(\mathbf{x},0) = r^0(\mathbf{x}), \quad \text{and} \quad s(\mathbf{x},0) = s^0(\mathbf{x}).$$

In the bulk, we focus on an *activator-depleted* type model also known as the Brusselator model (Gierer and Meinhardt, 1972; Schnakenberg, 1979; Lakkis et al., 2013; Prigogine and Lefever, 1968; Venkataraman et al., 2012). In the Brusselator model the reaction kinetics are non-linear and are

$$f(u,v) = k_1 - k_2 u + k_3 u^2 v, \quad \text{and} \quad g(u,v) = k_4 - k_3 u^2 v, \tag{2.127}$$

with positive parameters k_1, k_2, k_3 and k_4.

2.2.1 Non-dimensionalisation

We proceed with a similar approach to that used in Section 2.1.1 of scaling choices to non-dimensionalise a system (2.123), which reads as

$$\begin{cases} \begin{cases} \frac{\partial u}{\partial t} &= \Delta u + \gamma_\Omega[a_2 - u + u^2 v], \\ \frac{\partial v}{\partial t} &= d_\Omega \Delta v + \gamma_\Omega[b_2 - u^2 v], \end{cases} & \text{in } \Omega \times (0,T] \\ \begin{cases} \frac{\partial r}{\partial t} &= \Delta_\Gamma r + \gamma_\Gamma[-r + q_2 s - \rho_3 r + u + \delta_2 v], \\ \frac{\partial s}{\partial t} &= d_\Gamma \Delta_\Gamma s + \gamma_\Gamma[c_2 r - j_2 s - \rho_4 s + u + \delta_3 v]. \end{cases} & \text{on } \Gamma \times (0,T], \end{cases} \tag{2.128}$$

The prescribed choices of rescaling consist of display $d_\Omega = \frac{D_v}{D_u}$, $d_\Gamma = \frac{D_s}{D_r}$, $\gamma_\Omega = \frac{L_b^2 k_2}{D_u}$, $\gamma_\Gamma = \frac{L_s^2 a}{D_r}$, $a_2 = \frac{k_1\sqrt{\frac{k_3}{k_2}}}{k_2}$, $b_2 = \frac{k_4\sqrt{\frac{k_3}{k_2}}}{k_2}$, $q_2 = \frac{b\beta_2}{a\beta_1}$, $c_2 = \frac{c\beta_1}{a\beta_2}$, $j_2 = \frac{d}{a}$, $\rho_3 = \frac{\alpha_1}{a}$, $\rho_4 = \frac{\alpha_2}{a}$, $\delta_2 = \frac{\kappa_1}{\beta_1}$, $\delta_3 = \frac{\kappa_2}{\beta_2}$. The linear boundary conditions for material interface are given by

$$\begin{cases} \nabla u \cdot \nu = \gamma_\Gamma[\rho_3 r - u - \delta_2 v], \\ d_\Omega \nabla v \cdot \nu = \gamma_\Gamma[\rho_4 s - u - \delta_3 v]. \end{cases} \quad \text{on } \Gamma \times (0,T]. \tag{2.129}$$

The non-dimensional initial conditions for all chemical concentrations are exactly the same as prescribed for system (2.15).

2.2.2 Linear stability analysis in the absence of diffusion

We derive the uniform steady state as defined in Definition 2.1.1 by solving the algebraic system

$$f_1(u,v,r,s) = \gamma_\Omega(a_2 - u + u^2 v) = 0, \tag{2.130}$$

$$f_2(u,v,r,s) = \gamma_\Omega(b_2 - u^2 v) = 0, \tag{2.131}$$

$$f_3(u,v,r,s) = \gamma_\Gamma(-r + q_2 s - \rho_3 r + u + \delta_2 v) = 0, \tag{2.132}$$

$$f_4(u,v,r,s) = \gamma_\Gamma(c_2 r - j_2 s - \rho_4 s + u + \delta_3 v) = 0, \tag{2.133}$$

such that the boundary conditions given by (2.129) are also satisfied:

$$\gamma_\Gamma[\rho_3 r - u - \delta_2 v] = 0, \tag{2.134}$$

$$\gamma_\Gamma[\rho_4 s - u - \delta_3 v] = 0. \tag{2.135}$$

We found in Section (2.1.2) that equations (2.130) and (2.131) admit a uniform non-zero steady state of the form

$$u_0 = a_2 + b_2, \tag{2.136}$$

$$v_0 = \frac{b_2}{(a_2 + b_2)^2}. \tag{2.137}$$

Substituting u_0 and v_0 in (2.134) and (2.135) we obtain steady-state values for r_0 and s_0, which read as

$$r_0 = \frac{(a_2 + b_2)^3 + \delta_2 b_2}{\rho_3 (a_2 + b_2)^2}, \tag{2.138}$$

$$s_0 = \frac{(a_2 + b_2)^3 + \delta_3 b_2}{\rho_4 (a_2 + b_2)^2}. \tag{2.139}$$

Therefore, the uniform steady state we wanted to compute is

$$(u_0, v_0, r_0, s_0) = \Big(a_2 + b_2, \frac{b_2}{(a_2 + b_2)^2}, \frac{(a_2 + b_2)^3 + \delta_2 b_2}{\rho_3 (a_2 + b_2)^2}, \frac{(a_2 + b_2)^3 + \delta_3 b_2}{\rho_4 (a_2 + b_2)^2}\Big). \tag{2.140}$$

Substituting (2.140) in (2.132) leads to

$$-\frac{(a_2 + b_2)^3 + \delta_2 b_2}{\rho_3 (a_2 + b_2)^2} + q_2 \frac{(a_2 + b_2)^3 + \delta_3 b_2}{\rho_4 (a_2 + b_2)^2}) = 0$$

$$\Rightarrow q_2 \rho_3 (a_2 + b_2)^3 - \rho_4 (a_2 + b_2)^3 = \rho_4 \delta_2 b_2 - q_2 \rho_3 \delta_3 b_2,$$

$$\Rightarrow (a_2 + b_2)^3 = \frac{b_2(\rho_4 \delta_2 - q_2 \rho_3 \delta_3)}{q_2 \rho_3 - \rho_4}. \tag{2.141}$$

Similarly substituting (2.140) in (2.133) we obtain

$$c_2 (\frac{(a_2 + b_2)^3 + \delta_2 b_2}{\rho_3 (a_2 + b_2)^2}) - j_2 (\frac{(a_2 + b_2)^3 + \delta_3 b_2}{\rho_4 (a_2 + b_2)^2}) = 0$$

$$\Rightarrow c_2 \rho_4 (a_2 + b_2)^3 - j_2 \rho_3 (a_2 + b_2)^3 = j_2 \rho_3 \delta_3 b_2 - c_2 \rho_4 \delta_2 b_2,$$

$$\Rightarrow (a_2 + b_2)^3 = \frac{b_2(j_2 \rho_3 \delta_3 - c_2 \rho_4 \delta_2)}{c_2 \rho_4 - j_2 \rho_3}. \tag{2.142}$$

Combining (2.141) and (2.142) and requiring that (2.140) is a uniform steady state according to Definition 2.1.1, reveals a parameters conditions on values of c_2, q_2 and j_2. This is achived by

$$\frac{b_2(\rho_4 \delta_2 - q_2 \rho_3 \delta_3)}{q_2 \rho_3 - \rho_4} = \frac{b_2(j_2 \rho_3 \delta_3 - c_2 \rho_4 \delta_2)}{c_2 \rho_4 - j_2 \rho_3}$$

$$\Rightarrow (c_2 \rho_4 - j_2 \rho_3)(\rho_4 \delta_2 - q_2 \rho_3 \delta_3) = (q_2 \rho_3 - \rho_4)(j_2 \rho_3 \delta_3 - c_2 \rho_4 \delta_2),$$

$$c_2 q_2 = j_2. \tag{2.143}$$

The results of these finding are summarised in Theorem 2.2.1.

Theorem 2.2.1 *(Existence and uniqueness of the uniform steady state): Madzvamuse et al. (2015a) The coupled system of BSRDEs (2.128) with conditions (2.129) admits a unique steady state given by*

$$(u_0, v_0, r_0, s_0) = \Big(a_2 + b_2, \frac{b_2}{(a_2+b_2)^2}, \frac{(a_2+b_2)^3 + \delta_2 b_2}{\rho_3(a_2+b_2)^2}, \frac{(a_2+b_2)^3 + \delta_3 b_2}{\rho_4(a_2+b_2)^2}\Big), \quad (2.144)$$

provided the following compatibility condition on the cofficients of the coupling is satisfied:

$$c_2 q_2 = j_2. \quad (2.145)$$

Proof 2.2.1 *The proof of this theorem consists of all the steps from (2.130) to (2.143).* □

The next step is to complete the linearisation in the absence of diffusion, which is achieved by omitting the diffusion term from system (2.128). This results in a four-component system of ordinary differential equations written as

$$u_t = f_1(u, v, r, s) = \gamma_\Omega(a_2 - u + u^2 v) \quad (2.146)$$

$$v_t = f_2(u, v, r, s) = \gamma_\Omega(b_2 - u^2 v) \quad (2.147)$$

$$r_t = f_3(u, v, r, s) = \gamma_\Gamma(-r + q_2 s - \rho_3 r + u + \delta_2 v) \quad (2.148)$$

$$s_t = f_4(u, v, r, s) = \gamma_\Gamma(c_2 r - j_2 s - \rho_4 s + u + \delta_3 v). \quad (2.149)$$

We use the approach taken in section 2.1.2 to linearise system (2.146)-(2.149), which reads as

$$\frac{dw_1(t)}{dt} = \gamma_\Omega[(2u_0v_0 - 1)w_1(t) + u_0^2 w_2(t)] \quad (2.150)$$

$$\frac{dw_2(t)}{dt} = \gamma_\Omega[-2u_0v_0 w_1(t) - u_0^2 w_2(t)] \quad (2.151)$$

$$\frac{dw_3(t)}{dt} = \gamma_\Gamma[w_1(t) + \delta_2 w_2(t) + (-\rho_3 - 1)w_3(t) + q_2 w_4(t)] \quad (2.152)$$

$$\frac{dw_4(t)}{dt} = \gamma_\Gamma[w_1(t) + \delta_3 w_2(t) + c_2 w_3(t) + (-\rho_4 - j_2)w_4(t)], \quad (2.153)$$

which can also be written in the form

$$\mathbf{w}_t = \mathbf{A}\mathbf{w}, \quad (2.154)$$

where

$$\mathbf{w} = \begin{pmatrix} w_1(t) \\ w_2(t) \\ w_3(t) \\ w_4(t) \end{pmatrix},$$

$$\mathbf{A} = \begin{pmatrix} \gamma_\Omega(2u_0v_0 - 1) & \gamma_\Omega(u_0^2) & 0 & 0 \\ \gamma_\Omega(-2u_0v_0) & \gamma_\Omega(-u_0^2) & 0 & 0 \\ \gamma_\Gamma(1) & \gamma_\Gamma(\delta_2) & \gamma_\Gamma(-\rho_3 - 1) & \gamma_\Gamma(q_2) \\ \gamma_\Gamma(1) & \gamma_\Gamma(\delta_3) & \gamma_\Gamma(c_2) & \gamma_\Gamma(-\rho_4 - j_2) \end{pmatrix} = \begin{pmatrix} f_{1u} & f_{1v} & f_{1r} & f_{1s} \\ f_{2u} & f_{2v} & f_{2r} & f_{2s} \\ f_{3u} & f_{3v} & f_{3r} & f_{3s} \\ f_{4u} & f_{4v} & f_{4r} & f_{4s} \end{pmatrix}.$$

The system (2.154) requires the solutions in the form

$$\mathbf{w} = \mathbf{c}e^{\lambda t} \quad \text{where} \quad e^{\lambda t} > 0, \quad \mathbf{c} \neq 0, \tag{2.155}$$

which leads to the relevant discrete eigenvalue problem of 4×4 algebraic system in the form

$$\begin{vmatrix} \lambda - \gamma_\Omega(2u_0v_0 - 1) & -\gamma_\Omega(u_0^2) & 0 & 0 \\ \gamma_\Omega(2u_0v_0) & \lambda + \gamma_\Omega(u_0^2) & 0 & 0 \\ -\gamma_\Gamma(1) & -\gamma_\Gamma(\delta_2) & \lambda + \gamma_\Gamma(\rho_3 + 1) & -\gamma_\Gamma(q_2) \\ -\gamma_\Gamma(1) & -\gamma_\Gamma(\delta_3) & -\gamma_\Gamma(c_2) & \lambda + \gamma_\Gamma(\rho_4 + j_2) \end{vmatrix} = 0. \tag{2.156}$$

The eigenvalues of system (2.156) are the roots of a degree-four polynomial which can be factorised in the form

$$\begin{aligned} &[((\lambda + \gamma_\Gamma(\rho_3 + 1))(\lambda + \gamma_\Gamma(\rho_4 + j_2)) - c_2q_2\gamma_\Gamma^2] \\ &[(\lambda - \gamma_\Omega(2u_0v_0 - 1))(\lambda + u_0^2\gamma_\Omega) + 2u_0^3v_0\gamma_\Omega^2] = 0. \end{aligned} \tag{2.157}$$

Equation (2.157) gives rise to two quadratic equations of the form

$$((\lambda + \gamma_\Gamma(\rho_3 + 1))(\lambda + \gamma_\Gamma(\rho_4 + j_2)) - c_2q_2\gamma_\Gamma^2 = 0, \tag{2.158}$$

and

$$(\lambda - \gamma_\Omega(2u_0v_0 - 1))(\lambda + u_0^2\gamma_\Omega) + 2u_0^3v_0\gamma_\Omega^2 = 0, \tag{2.159}$$

both of which are solved to obtain

$$\begin{aligned} 2\lambda = &-\gamma_\Gamma(\rho_3 + \rho_4 + j_2 + 1) \\ &\pm \sqrt{\gamma_\Gamma^2(\rho_3 + \rho_4 + j_2 + 1)^2 - 4(\rho_3\rho_4 + \rho_4 + \rho_3j_2 + j_2 - c_2q_2)\gamma_\Gamma^2}, \end{aligned} \tag{2.160}$$

and

$$2\lambda = -\gamma_\Omega(u_0^2 - 2u_0v_0 + 1) \pm \sqrt{\gamma_\Omega^2(u_0^2 - 2u_0v_0 + 1)^2 - 4(u_0^2)\gamma_\Omega^2}. \tag{2.161}$$

We see that for the real parts of the roots in (2.160) to be negative we require the conditions

$$\gamma_\Gamma(\rho_3 + \rho_4 + j_2 + 1) > 0 \quad \text{and} \quad (\rho_3\rho_4 + \rho_4 + \rho_3 j_2 + j_2 - c_2q_2)\gamma_\Gamma^2 > 0, \tag{2.162}$$

which can be equivalently written as

$$f_{3r} + f_{4s} < 0 \quad \text{and} \quad f_{3r}f_{4s} - f_{3s}f_{4r} > 0, \tag{2.163}$$

in terms of the trace and determinant the corresponding 2×2 block matrix of the system. Similarly for the roots in (2.161) to be negative we also require the conditions

$$\gamma_\Omega(u_0^2 - 2u_0v_0 + 1) > 0, \quad \text{and} \quad (u_0^2)\gamma_\Omega^2 > 0, \tag{2.164}$$

which can be equivalently written as

$$f_{1u} + f_{2v} < 0, \quad \text{and} \quad f_{1u}f_{2v} - f_{1v}f_{2u} > 0, \tag{2.165}$$

in terms of the trace and determinate the corresponding 2×2 block matrix. Finally we set out the summary of the necessary and sufficient conditions for stability of system (2.154) in Theorem 2.2.2.

Theorem 2.2.2 *(Turing, 1952; Murray, 2001) The necessary and sufficient conditions such that all the zeros of the polynomial $p_4(\lambda)$ have $Re(\lambda) < 0$ are given by the following conditions:*

$$f_{1u} + f_{2v} < 0, \tag{2.166}$$

$$f_{1u}f_{2v} - f_{1v}f_{2u} > 0, \tag{2.167}$$

$$f_{3r} + f_{4s} < 0, \tag{2.168}$$

$$f_{3r}f_{4s} - f_{3s}f_{4r} > 0. \tag{2.169}$$

Proof 2.2.2 *The proof of this theorem consists of all the steps from (2.154) to (2.165).* □

2.2.3 Linear stability analysis in the presence of diffusion

We start by analysing system (2.128) by taking the diffusion terms into account and perform the stability analysis. Through identical steps to those taken in section 2.1.3, we obtain

$$\frac{d(u_{l,m}(t))}{dt} = [-k_{l,m}^2 + 2u_0v_0\gamma_\Omega - \gamma_\Omega]u_{l,m}(t) + [u_0^2\gamma_\Omega]v_{l,m}(t), \tag{2.170}$$

$$\frac{d(v_{l,m}(t))}{dt} = [-2u_0v_0\gamma_\Omega]u_{l,m}(t) + [-d_\Omega k_{l,m}^2 - u_0^2\gamma_\Omega]v_{l,m}(t), \tag{2.171}$$

$$\frac{dr_{l,m}(t)}{dt} = [-l(l+1) - \gamma_\Gamma]r_{l,m}(t) + [q_2\gamma_\Gamma]s_{l,m}(t) + [-\psi'_{k_{l,m}}(1)]u_{l,m}(t), \tag{2.172}$$

$$\frac{ds_{l,m}(t)}{dt} = [c_2\gamma_\Gamma]r_{l,m}(t) + [-d_\Gamma l(l+1) - j_2\gamma_\Gamma]s_{l,m}(t) + [-d_\Omega\psi'_{k_{l,m}}(1)]v_{l,m}(t), \tag{2.173}$$

which can be written in the form

$$\mathbf{w}_t = \mathbf{M}\mathbf{w}, \tag{2.174}$$

where

$$\mathbf{w} = \begin{pmatrix} u_{l,m}(t) \\ v_{l,m}(t) \\ r_{l,m}(t) \\ s_{l,m}(t) \end{pmatrix}$$

and

$$\mathbf{M} = \begin{pmatrix} -k_{l,m}^2+2u_0v_0\gamma_\Omega-\gamma_\Omega & u_0^2\gamma_\Omega & 0 & 0 \\ -2u_0v_0\gamma_\Omega & -d_\Omega k_{l,m}^2-u_0^2\gamma_\Omega & 0 & 0 \\ -\psi'_{k_{l,m}}(1) & 0 & -l(l+1)-\gamma_\Gamma & q_2\gamma_\Gamma \\ 0 & -d_\Omega\psi'_{k_{l,m}}(1) & c_2\gamma_\Gamma & -d_\Gamma l(l+1)-j_2\gamma_\Gamma \end{pmatrix}$$

This is a coupled system of four ODEs which has the solution in the form

$$\begin{aligned} (u_{l,m}, v_{l,m}, r_{l,m}, s_{l,m})^T &= (u_{l,m}^0, v_{l,m}^0, r_{l,m}^0, s_{l,m}^0)^T e^{\lambda t}, \\ \Rightarrow \mathbf{w} &= \mathbf{w^0} e^{\lambda t}, \end{aligned} \tag{2.175}$$

where

$$\mathbf{w} = (u_{l,m}, v_{l,m}, r_{l,m}, s_{l,m})^T, \qquad \mathbf{w^0} = (u_{l,m}^0, v_{l,m}^0, r_{l,m}^0, s_{l,m}^0)^T \neq (0,0,0,0)^T, \qquad e^{\lambda t} > 0,$$

which leads to the relevant discrete eigenvalue problem of 4×4 algebraic system in the form

$$\begin{vmatrix} \lambda+k_{l,m}^2-\gamma_\Omega(2u_0v_0-1) & -\gamma_\Omega(u_0^2) & 0 & 0 \\ \gamma_\Omega(2u_0v_0) & \lambda+d_\Omega k_{l,m}^2+\gamma_\Omega(u_0^2) & 0 & 0 \\ \psi'_{k_{l,m}}(1) & 0 & \lambda+l(l+1)+\gamma_\Gamma & -\gamma_\Gamma(q_2) \\ 0 & d_\Omega\psi'_{k_{l,m}}(1) & -\gamma_\Gamma(c_2) & \lambda+d_\Gamma l(l+1)+\gamma_\Gamma(j_2) \end{vmatrix} = 0. \tag{2.176}$$

Proceeding in the usual way we find that the eigenvalues of this matrix in (2.176) are the roots of the polynomial, which can be factorised in the form

$$\begin{aligned} &\Big[\Big(\lambda + l(l+1) + \gamma_\Gamma)(\lambda + d_\Gamma l(l+1) + j_2\gamma_\Gamma\Big) - c_2q_2\gamma_\Gamma^2\Big] \\ &\Big[\Big(\lambda + k_{l,m}^2 - \gamma_\Omega(2u_0v_0 - 1))(\lambda + d_\Omega k_{l,m}^2 + u_0^2\gamma_\Omega\Big) + 2u_0^3v_0\gamma_\Omega^2\Big] = 0. \end{aligned} \tag{2.177}$$

Equation (2.177) gives rise to two quadratic equations of the form

$$(\lambda + l(l+1) + \gamma_\Gamma)(\lambda + d_\Gamma l(l+1) + j_2\gamma_\Gamma) - c_2q_2\gamma_\Gamma^2 = 0, \tag{2.178}$$

and

$$(\lambda + k_{l,m}^2 - \gamma_\Omega(2u_0v_0 - 1))(\lambda + d_\Omega k_{l,m}^2 + u_0^2\gamma_\Omega) + 2u_0^3v_0\gamma_\Omega^2 = 0. \tag{2.179}$$

In order to find the two eigenvalues in (2.178) we use the equation

$$\lambda^2 + \underbrace{\Big((1+d_\Gamma)l(l+1) + \gamma_\Gamma(j_2+1)\Big)}_{M_1}\lambda + \underbrace{\Big(d_\Gamma[l(l+1)]^2 + l(l+1)\gamma_\Gamma(j_2+d_\Gamma) + \gamma_\Gamma^2(j_2 - c_2q_2)\Big)}_{H_1} = 0,$$

from which we obtain

$$2\lambda = -M_1 \pm \sqrt{(M_1)^2 - 4H_1}.$$

We observe that, since $M_1 > 0$ and $H_1 > 0$, the real part of the two roots are negative. For the remaining two eigenvalues in (2.179), a similar procedure to (2.1.3) is followed to obtain the necessary and sufficient conditions for the real part of the eigenvalues to be positive, which reads as

$$d_\Omega f_{1u} + f_{2v} > 0, \quad \text{and} \quad [d_\Omega f_{1u} + f_{2v}]^2 - 4d_\Omega(f_{1u}f_{2v} - f_{1v}f_{2u}) > 0. \tag{2.180}$$

Now we summarise the main result in Theorem 2.2.3.

Theorem 2.2.3 *(Turing, 1952; Murray, 2001) The necessary conditions for diffusion-driven instability for the coupled system of BSRDEs (2.128) and (2.129) are given by*

$$f_{1u} + f_{2v} < 0, \tag{2.181}$$

$$f_{1u}f_{2v} - f_{1v}f_{2u} > 0, \tag{2.182}$$

$$f_{3r} + f_{4s} < 0, \tag{2.183}$$

$$f_{3r}f_{4s} - f_{3s}f_{4r} > 0, \tag{2.184}$$

and

$$d_\Omega f_{1u} + f_{2v} > 0 \quad \textit{and} \quad [d_\Omega f_{1u} + f_{2v}]^2 - 4d_\Omega(f_{1u}f_{2v} - f_{1v}f_{2u}) > 0. \tag{2.185}$$

Proof 2.2.3 *The proof of this theorem consists of all the steps from (2.174) to (2.180).*□

Theoretical predictions

We state from the analytical results the following theoretical predictions.

- The bulk dynamics can give rise to patterning while the surface reaction-diffusion system can not.
- From conditions (2.181) and (2.185) for the bulk, we write

  $$f_{1u} + f_{2v} < 0 \ \text{ and } \ d_\Omega f_{1u} + f_{2v} > 0.$$

  Combining the inequalities imply $f_{1u} < -f_{2v} < d_\Omega f_{1u}$, which means that for diffusion-driven instability to occur, $f_{1u} < d_\Omega f_{1u} \Rightarrow d_\Omega > 1$. For a detailed mathematical derivation of condition $d > 1$ the interested reader may consult (Madzvamuse et al., 2010, 2015b, 2016).
- $d_\Omega > 1$ means that inhibitor must diffuse faster than the activator, because $d_\Omega = \frac{Dv}{Du}$ where Dv is the diffusion coefficient of the inhibitor and Du is the diffusion coefficient of the activator.
- The conditions (2.181) - (2.185) are necessary but not sufficient for the emergence of an inhomogeneous spatial structure. Sufficient conditions will be presented in Chapter 3.

2.3 Linear reaction kinetics in the bulk and non-linear reaction kinetics on the surface

In this system we focus on a system with linear reaction kinetics in the bulk and non-linear reaction kinetics on the surface by considering the following coupled bulk-surface reaction-diffusion equations:

$$\begin{cases} \begin{cases} u_t &= D_u\Delta u - au + bv, \\ v_t &= D_v\Delta v + cu - dv, \end{cases} & \text{in } \Omega \times (0,T] \\ \begin{cases} r_t &= D_r\Delta_\Gamma r + (f(r,s) - h_1(u,v,r,s)), \\ s_t &= D_s\Delta_\Gamma s + (g(r,s) - h_2(u,v,r,s)), \end{cases} & \text{on } \Gamma \times (0,T] \end{cases} \tag{2.186}$$

with coupling boundary conditions

$$\begin{cases} \frac{\partial u}{\partial \nu} = h_1(u,v,r,s), \\ d_\Omega \frac{\partial v}{\partial \nu} = h_2(u,v,r,s). \end{cases} \quad \text{on } \Gamma \times (0,T] \tag{2.187}$$

The coupling conditions of the system are represented in a similar way by h_1 and h_2 which are functions of u, v, r and s, where h_1 and h_2 are given by

$$h_1(u,v,r,s) = \alpha_1 r - \beta_1 u - \kappa_1 v, \tag{2.188}$$

$$h_2(u,v,r,s) = \alpha_2 s - \beta_2 u - \kappa_2 v. \tag{2.189}$$

The constants $\alpha_1, \alpha_2, \beta_1, \beta_2, \kappa_1$ and κ_2 are also positive parameters. The initial conditions are prescribed similar to those given for system (2.123), which are written as

$$u(\mathbf{x},0) = u^0(\mathbf{x}), \quad v(\mathbf{x},0) = v^0(\mathbf{x}), \quad r(\mathbf{x},0) = r^0(\mathbf{x}), \quad \text{and} \quad s(\mathbf{x},0) = s^0(\mathbf{x}).$$

On the surface, we focus on an *activator-depleted* model also known as the Brusselator model (Gierer and Meinhardt, 1972; Schnakenberg, 1979; Lakkis et al., 2013; Prigogine and Lefever, 1968; Venkataraman et al., 2012). In Brusselator model the reaction kinetics are non-linear, given by

$$f(r,s) = k_1 - k_2 r + k_3 r^2 s, \quad \text{and} \quad g(r,s) = k_4 - k_3 r^2 s, \tag{2.190}$$

with non-negative parameters k_1, k_2, k_3 and k_4.

2.3.1 Non-dimensionalisation

We proceed with a similar approach that used in Section 2.1.1 of scaling choices to the non-dimensionalised system (2.186), which reads as

$$\begin{cases} \begin{cases} \frac{\partial u}{\partial t} &= \Delta u + \gamma_\Omega[-u + qv], \\ \frac{\partial v}{\partial t} &= d_\Omega \Delta v + \gamma_\Omega[c_1 u - zv], \end{cases} & \text{in } \Omega \times (0,T] \\ \begin{cases} \frac{\partial r}{\partial t} &= \Delta_\Gamma r + \gamma_\Gamma[a_1 - r + r^2 s - \rho_1 r + u + v], \\ \frac{\partial s}{\partial t} &= d_\Gamma \Delta_\Gamma s + \gamma_\Gamma[b_1 - r^2 s - \rho_2 s + \mu u + \delta v], \end{cases} & \text{on } \Gamma \times (0,T] \end{cases} \tag{2.191}$$

The prescribed choices of rescaling consist of display $d_\Omega = \frac{D_v}{D_u}$, $d_\Gamma = \frac{D_s}{D_r}$, $\gamma_\Omega = \frac{L_b^2 a}{D_u}$, $\gamma_\Gamma = \frac{L_s^2 k_2}{D_r}$, $q = \frac{b\kappa_1}{a\beta_1}$, $c_1 = \frac{c\beta_1}{a\kappa_1}$, $z = \frac{d}{a}$, $a_1 = \frac{k_1\sqrt{\frac{k_3}{k_2}}}{k_2}$, $b_1 = \frac{k_4\sqrt{\frac{k_3}{k_2}}}{k_2}$, $\rho_1 = \frac{\alpha_1}{k_2}$, $\rho_2 = \frac{\alpha_2}{k_2}$, $\mu = \frac{\beta_2}{\beta_1}$, $\delta = \frac{\kappa_2}{\kappa_1}$. The linear boundary conditions are given by

$$\begin{cases} \nabla u \cdot \nu = \gamma_\Gamma[\rho_1 r - u - v], \\ d_\Omega \nabla v \cdot \nu = \gamma_\Gamma[\rho_2 s - \mu u - \delta v]. \end{cases} \quad \text{on } \Gamma \times (0,T] \tag{2.192}$$

The non-dimensional initial conditions for all chemical concentrations are exactly the same as prescribed for the system (2.15).

2.3.2 Linear stability analysis in the absence of diffusion

We derive the uniform steady state as defined in Definition 2.1.1 by solving the algebraic system

$$f_1(u,v,r,s) = \gamma_\Omega(-u + qv) = 0, \tag{2.193}$$

$$f_2(u,v,r,s) = \gamma_\Omega(c_1 u - zv) = 0, \tag{2.194}$$

$$f_3(u,v,r,s) = \gamma_\Gamma(a_1 - r + r^2 s - \rho_1 r + u + v) = 0, \tag{2.195}$$

$$f_4(u,v,r,s) = \gamma_\Gamma(b_1 - r^2 s - \rho_2 s + \mu u + \delta v) = 0, \tag{2.196}$$

such that the boundary conditions given by (2.192) are also satisfied:

$$\gamma_\Gamma[\rho_1 r - u - v] = 0, \tag{2.197}$$

$$\gamma_\Gamma[\rho_2 s - \mu u - \delta v] = 0. \tag{2.198}$$

From (2.193) we observe that

$$u_0 = q v_0, \tag{2.199}$$

which we can substitute into (2.194) to obtain

$$v_0(c_1q - z) = 0. \tag{2.200}$$

Considering (2.200) we have that either of $c_1q - z = 0$ or $v_0 = 0$ must hold for the system to have a unique solution. From the first condition, namely, $c_1q - z = 0$ we deduce that there are infinitely many steady states for all positive real values of v_0 and u_0 . This case is not of much interest for further investigation, because it is impractical. Subject to this observation, we only have to consider the case $v_0 = 0$. Substituting $v_0 = 0$ into (2.199), we get that $u_0 = 0$. Also, substituting $u_0 = 0$ and $v_0 = 0$ into the given boundary conditions, we obtain that $r_0 = 0$ and $s_0 = 0$, for strictly non-negative parameters ρ_1 and ρ_2. We observe that the solution

$$(u_0, v_0, r_0, s_0) = (0, 0, 0, 0), \tag{2.201}$$

is a steady state. However, if we substitute this steady state into the surface reaction kinetics, it results in a contradiction, namely

$$a_1 = 0 \quad \text{and} \quad b_1 = 0. \tag{2.202}$$

Therefore, in order for zero steady state to exist, we require some conditions on parameters of the model, which are presented in theorem (2.3.1).

Theorem 2.3.1 *(Parameter conditions for a uniform steady state) The coupled system given by* (2.191) *with the boundary conditions given by* (2.192) *admits a uniform steady state*

$$(u_0, v_0, r_0, s_0) = (0, 0, 0, 0), \tag{2.203}$$

under the conditions on the non-negative parameters such that

$$a_1 = 0, \quad b_1 = 0 \quad \textit{and} \quad c_1q - z \neq 0. \tag{2.204}$$

Proof 2.3.1 *The proof of this theorem consists of all the steps from* (2.193) *to* (2.202).□

Remark 2.3.1 *The steady state given in Theorem 2.3.1 is a trivial case, which does not provide interesting mathematical implications. However we conduct stability analysis for completeness purposes. In general we require non-zero steady states and in fact all this is saying is that linear kinetics in the bulk is not that interesting. In fact, one could simply take constant solutions in the bulk and study how these affect the surface reaction-diffusion system.*

In the absence of diffusion we note that u, v, r and s must satisfy

$$u_t = f_1(u, v, r, s) = \gamma_\Omega(-u + qv), \tag{2.205}$$
$$v_t = f_2(u, v, r, s) = \gamma_\Omega(c_1 u - zv), \tag{2.206}$$
$$r_t = f_3(u, v, r, s) = \gamma_\Gamma(a_1 - r + r^2 s - \rho_1 r + u + v), \tag{2.207}$$
$$s_t = f_4(u, v, r, s) = \gamma_\Gamma(b_1 - r^2 s - \rho_2 s + \mu u + \delta v). \tag{2.208}$$

We use the approach taken in Section 2.1.2 to linearise system (2.205)-(2.208), which reads as

$$\begin{aligned}
\frac{dw_1(t)}{dt} &= \gamma_\Omega[-w_1(t) + qw_2(t)],\\
\frac{dw_2(t)}{dt} &= \gamma_\Omega[c_1 w_1(t) - zw_2(t)],\\
\frac{dw_3(t)}{dt} &= \gamma_\Gamma[w_1(t) + w_2(t) + (2r_0 s_0 - \rho_1 - 1)w_3(t) + r_0^2 w_4(t)],\\
\frac{dw_4(t)}{dt} &= \gamma_\Gamma[\mu w_1(t) + \delta w_2(t) - 2r_0 s_0 w_3(t) + (-r_0^2 - \rho_2)w_4(t)].
\end{aligned} \tag{2.209}$$

Substituting the uniform steady state in (2.209), we obtain

$$\frac{dw_1(t)}{dt} = \gamma_\Omega[-w_1(t) + qw_2(t)] \tag{2.210}$$
$$\frac{dw_2(t)}{dt} = \gamma_\Omega[c_1 w_1(t) - zw_2(t)] \tag{2.211}$$
$$\frac{dw_3(t)}{dt} = \gamma_\Gamma[w_1(t) + w_2(t) + (-\rho_1 - 1)w_3(t)] \tag{2.212}$$
$$\frac{dw_4(t)}{dt} = \gamma_\Gamma[\mu w_1(t) + \delta w_2(t) - \rho_2 w_4(t)]. \tag{2.213}$$

which can also be written in the form

$$\mathbf{w}_t = \mathbf{A}\mathbf{w} \tag{2.214}$$

where

$$\mathbf{w} = \begin{pmatrix} w_1(t) \\ w_2(t) \\ w_3(t) \\ w_4(t) \end{pmatrix},$$

$$\mathbf{A} = \begin{pmatrix} \gamma_\Omega(-1) & \gamma_\Omega(q) & 0 & 0 \\ \gamma_\Omega(c_1) & \gamma_\Omega(-z) & 0 & 0 \\ \gamma_\Gamma(1) & \gamma_\Gamma(1) & \gamma_\Gamma(-\rho_1 - 1) & 0 \\ \gamma_\Gamma(\mu) & \gamma_\Gamma(\delta) & 0 & \gamma_\Gamma(-\rho_2) \end{pmatrix} = \begin{pmatrix} f_{1u} & f_{1v} & f_{1r} & f_{1s} \\ f_{2u} & f_{2v} & f_{2r} & f_{2s} \\ f_{3u} & f_{3v} & f_{3r} & f_{3s} \\ f_{4u} & f_{4v} & f_{4r} & f_{4s} \end{pmatrix}.$$

This is a system of ordinary differential equations which has the solutions in the form of

$$\mathbf{w} = \mathbf{c}e^{\lambda t} \quad \text{where} \quad e^{\lambda t} > 0, \quad \mathbf{c} \neq 0, \tag{2.215}$$

which leads to the relevant discrete eigenvalue problem of a 4×4 lgebraic system in the form

$$\begin{vmatrix} \lambda - \gamma_\Omega(-1) & -\gamma_\Omega(q) & 0 & 0 \\ -\gamma_\Omega(c_1) & \lambda - \gamma_\Omega(-z) & 0 & 0 \\ -\gamma_\Gamma(1) & -\gamma_\Gamma(1) & \lambda - \gamma_\Gamma(-\rho_1 - 1) & 0 \\ -\gamma_\Gamma(\mu) & -\gamma_\Gamma(\delta) & 0 & \lambda - \gamma_\Gamma(-\rho_2) \end{vmatrix} = 0. \tag{2.216}$$

The eigenvalues of system (2.216) are the roots of a degree-four polynomial which can be factorised in the form

$$(\lambda + \gamma_\Gamma(\rho_1 + 1))(\lambda + \rho_2\gamma_\Gamma)[(\lambda + \gamma_\Omega)(\lambda + z\gamma_\Omega) - (c_1 q\gamma_\Omega^2)] = 0, \tag{2.217}$$

Two of those roots can be easily found by rating that

$$\lambda + \gamma_\Gamma(\rho_1 + 1) = 0, \quad \text{and} \quad \lambda + \rho_2\gamma_\Gamma = 0, \tag{2.218}$$

from which it can be observed that those two roots are negative. In order to find the remaining two eigenvalues we use the equation

$$(\lambda + \gamma_\Omega)(\lambda + z\gamma_\Omega) - (c_1 q\gamma_\Omega^2) = 0, \tag{2.219}$$

$$[\lambda^2 + \gamma_\Omega(z+1)\lambda + (z - c_1 q)\gamma_\Omega^2] = 0.$$

From this we obtain

$$2\lambda = -\gamma_\Omega(z+1) \pm \sqrt{\gamma_\Omega^2(z+1)^2 - 4(z - c_1 q)\gamma_\Omega^2}$$

We see that for the real part of the final two roots to be negative we require the conditions

$$\gamma_\Omega(z+1) > 0, \quad \text{and} \quad (z - c_1 q)\gamma_\Omega^2 > 0, \tag{2.220}$$

which can be equivalently written as

$$f_{1u} + f_{2v} < 0, \quad \text{and} \quad f_{1u} f_{2v} - f_{1v} f_{2u} > 0, \tag{2.221}$$

in terms of the trace and determinant of the first 2×2 block matrix of the system. Finally we set out the summary of the necessary and sufficient conditions for $\mathrm{Re}(\lambda) < 0$ in Theorem 2.3.2.

Theorem 2.3.2 *(Turing, 1952; Murray, 2001) The necessary and sufficient conditions such that the zeros of the polynomial $p_4(\lambda)$ have $Re(\lambda) < 0$ are given by the following conditions:*

$$f_{1u} + f_{2v} < 0, \tag{2.222}$$

$$f_{1u} f_{2v} - f_{1v} f_{2u} > 0. \tag{2.223}$$

Proof 2.3.2 *The proof of this theorem consists of all the steps from (2.214) to (2.221).*□

2.3.3 Linear stability analysis in the presence of diffusion

We start by analysing the system taking the diffusion terms into account and perform the stability analysis. Through identical steps to those taken in Section 2.1.3 we

obtain

$$\begin{aligned}
\frac{d(u_{l,m}(t))}{dt} &= [-k_{l,m}^2 - \gamma_\Omega]u_{l,m}(t) + [q\gamma_\Omega]v_{l,m}(t),\\
\frac{d(v_{l,m}(t))}{dt} &= [c_1\gamma_\Omega]u_{l,m}(t) + [-d_\Omega k_{l,m}^2 - z\gamma_\Omega]v_{l,m}(t),\\
\frac{dr_{l,m}(t)}{dt} &= [-l(l+1) + 2r_0 s_0\gamma_\Gamma - \gamma_\Gamma]r_{l,m}(t) + [r_0^2\gamma_\Gamma]s_{l,m}(t) + [-\psi'_{k_{l,m}}(1)]u_{l,m}(t),\\
\frac{ds_{l,m}(t)}{dt} &= [-2r_0 s_0\gamma_\Gamma]r_{l,m}(t) + [-d_\Gamma l(l+1) - r_0^2\gamma_\Gamma]s_{l,m}(t) + [-d_\Omega\psi'_{k_{l,m}}(1)]v_{l,m}(t).
\end{aligned} \tag{2.224}$$

Substituting the uniform steady state in (2.224) equations, we obtain

$$\frac{d(u_{l,m}(t))}{dt} = [-k_{l,m}^2 - \gamma_\Omega]u_{l,m}(t) + [q\gamma_\Omega]v_{l,m}(t), \tag{2.225}$$

$$\frac{d(v_{l,m}(t))}{dt} = [c_1\gamma_\Omega]u_{l,m}(t) + [-d_\Omega k_{l,m}^2 - z\gamma_\Omega]v_{l,m}(t), \tag{2.226}$$

$$\frac{dr_{l,m}(t)}{dt} = [-l(l+1) - \gamma_\Gamma]r_{l,m}(t) + [0]s_{l,m}(t) + [-\psi'_{k_{l,m}}(1)]u_{l,m}(t), \tag{2.227}$$

$$\frac{ds_{l,m}(t)}{dt} = [0]r_{l,m}(t) + [-d_\Gamma l(l+1)]s_{l,m}(t) + [-d_\Omega\psi'_{k_{l,m}}(1)]v_{l,m}(t), \tag{2.228}$$

which can be written in the form

$$\mathbf{w}_t = \mathbf{M}\mathbf{w}, \tag{2.229}$$

where

$$\mathbf{w} = \begin{pmatrix} u_{l,m}(t)\\ v_{l,m}(t)\\ r_{l,m}(t)\\ s_{l,m}(t)\end{pmatrix}$$

and

$$\mathbf{M} = \begin{pmatrix} -k_{l,m}^2 - \gamma_\Omega & q\gamma_\Omega & 0 & 0\\ c_1\gamma_\Omega & -d_\Omega k_{l,m}^2 - z\gamma_\Omega & 0 & 0\\ -\psi'_{k_{l,m}}(1) & 0 & -l(l+1) - \gamma_\Gamma & 0\\ 0 & -d_\Omega\psi'_{k_{l,m}}(1) & 0 & -d_\Gamma l(l+1)\end{pmatrix}.$$

The system (2.229) has the solution in the form

$$(u_{l,m}, v_{l,m}, r_{l,m}, s_{l,m})^T = (u_{l,m}^0, v_{l,m}^0, r_{l,m}^0, s_{l,m}^0)^T e^{\lambda t}, \tag{2.230}$$

$$\Rightarrow \mathbf{w} = \mathbf{w^0} e^{\lambda t}, \tag{2.231}$$

where

$$\mathbf{w} = (u_{l,m}, v_{l,m}, r_{l,m}, s_{l,m})^T, \qquad \mathbf{w^0} = (u^0_{l,m}, v^0_{l,m}, r^0_{l,m}, s^0_{l,m})^T \neq (0,0,0,0)^T, \qquad e^{\lambda t} > 0,$$

which leads to the relevant discrete eigenvalue problem of a 4×4 algebraic system in the form

$$\begin{vmatrix} \lambda + k^2_{l,m} + \gamma_\Omega & -q\gamma_\Omega & 0 & 0 \\ -c_1\gamma_\Omega & \lambda + d_\Omega k^2_{l,m} + z\gamma_\Omega & 0 & 0 \\ \psi'_{k_{l,m}}(1) & 0 & \lambda + l(l+1) + \gamma_\Gamma & 0 \\ 0 & d_\Omega \psi'_{k_{l,m}}(1) & 0 & \lambda + d_\Gamma l(l+1) \end{vmatrix} = 0. \quad (2.232)$$

The eigenvalues of system (2.232) are the roots of a degree-four polynomial which can be factorised in the form

$$(\lambda + l(l+1) + \gamma_\Gamma)(\lambda + d_\Gamma l(l+1))[(\lambda + k^2_{l,m} + \gamma_\Omega)(\lambda + d_\Omega k^2_{l,m} + z\gamma_\Omega) - (c_1 q \gamma^2_\Omega)] = 0. \quad (2.233)$$

Two of those roots can be found by noting that

$$\lambda + (l(l+1) + \gamma_\Gamma) = 0, \quad (2.234)$$

$$\lambda + d_\Gamma l(l+1) = 0, \quad (2.235)$$

from which it can be observed that those two roots are negative. For the remaining two eigenvalues we solve the quadratic equation

$$[(\lambda + k^2_{l,m} + \gamma_\Omega)(\lambda + d_\Omega k^2_{l,m} + z\gamma_\Omega) - (c_1 q \gamma^2_\Omega)] = 0. \quad (2.236)$$

Expanding the brackets we write this equation in the form

$$\lambda^2 + \underbrace{(d_\Omega k^2_{l,m} + z\gamma_\Omega + k^2_{l,m} + \gamma_\Omega)}_{N}\lambda + \underbrace{(k^4_{l,m} d_\Omega + z\gamma_\Omega k^2_{l,m} + d_\Omega \gamma_\Omega k^2_{l,m} + \gamma^2_\Omega (z - c_1 q))}_{H} = 0.$$

$$\Rightarrow \lambda^2_{l,m} + N\lambda_{l,m} + H = 0, \quad (2.237)$$

where N and H are given by

$$N = d_\Omega k^2_{l,m} + z\gamma_\Omega + k^2_{l,m} + \gamma_\Omega, \quad (2.238)$$

$$H = k^4_{l,m} d_\Omega + z\gamma_\Omega k^2_{l,m} + d_\Omega \gamma_\Omega k^2_{l,m} + \gamma^2_\Omega (z - c_1 q). \quad (2.239)$$

For the uniform steady state to be unstable, we require the real part of the eigenvalues to be strictly positive; that is,

$$\mathrm{Re}(\lambda_{l,m}(k_{l,m}^2)) > 0 \quad \text{for some } k_{l,m}^2 > 0. \tag{2.240}$$

Solving (2.237) we can find that $\mathrm{Re}(\lambda_{l,m}(k_{l,m}^2)) > 0$ if and only if either of the following conditions hold:

$$N < 0 \quad \text{and} \quad H > 0, \tag{2.241}$$

or

$$N > 0 \quad \text{and} \quad H < 0. \tag{2.242}$$

Since every terms in the expression for N is clearly strictly positive, therefore we must proceed with requiring $H < 0$.
In the expression for H we know that

$$\gamma_\Omega^2(z - c_1 q) > 0, \tag{2.243}$$

from the second condition in Theorem 2.3.2. The remaining terms in the expression for H are strictly positive by definition. We notice that the strict positivity of N and H implies that both the remaining roots are negative, which excludes the existence of positive real roots as eigenvalues. This analysis allows us to conclude the results in Theorem 2.3.3.

Theorem 2.3.3 *The zero steady state for bulk-surface reaction-diffusion system with linear reaction kinetics in the bulk and non-linear reaction kinetics on the surface is stable.*

Proof 2.3.3 *The proof of this theorem consists of all the steps from (2.229) to (2.243).*□

2.4 Conclusion

If non-linear reaction kinetics are posed both in the bulk and on the surface, then linear stability theory suggests that both the bulk and surface dynamics are capable of producing spatial patterning, provided that Turing conditions are satisfied and

furthermore, the non-dimensional diffusion ratios satisfy $d_\Omega > 1$ and $d_\Gamma > 1$. If $d_\Omega = 1$ is chosen with $d_\Gamma > 1$, then the coupled system only produces a pattern on the surface with equations in the bulk returning to a constant steady state with no pattern. However, if $d_\Gamma = 1$ and $d_\Omega > 1$ are chosen, then the bulk equations are capable to form a spatial pattern and any pattern that emerges on the surface under this case scenario is the consequence of coupling conditions relating bulk equations to the equations posed on the surface. This means that the dynamics on the surface under such a setting are not capable to produce a pattern. It is the same effect that if $d_\Omega = d_\Gamma = 1$ is chosen then the resulting coupled system is not able to produce any pattern at all. If a set of non-linear reaction kinetics are posed in the bulk that are also coupled with a set of linear reaction kinetics posed on the surface then given that $d_\Omega > 1$ the equations in the bulk are predicted to evolve spatial pattern in the bulk with no pattern produced by the linear reaction kinetics on the surface. The spatial pattern may also extend to emerge on the surface, which is purely due to the coupling conditions imposed at the boundary interface. This is due to the surface in discretised domain being defined as the outer face of the elements in the bulk. If the non-linear reaction kinetics are posed on the surface with linear reaction kinetics in the bulk which are coupled through linear coupling conditions, then the system is expected to evolve a definite behaviour with no spatial pattern at all, which is to converge uniformly to a constant and homogeneous steady state. It must be noted that all the conditions derived for diffusion-driven instability in this chapter are necessary but not sufficient conditions. In order to insure that diffusion-driven instability occurs under either of settings prescribed in this chapter, a further requirement in the form of sufficient conditions must be fulfilled, which is to isolate the excitable wavenumber in order for the pattern to be formed. The next chapter is devoted to presenting a numerical procedure on how to isolate the excitable wavenumber to provide sufficient conditions for spatial pattern formation.

Chapter 3

Mode Isolation and Parameter Space Generation

In this chapter we proceed with the process of deriving sufficient conditions for diffusion-driven instability that complement the necessary conditions found in Chapter 2 to ensure the emergence of spatial patterns. As the standard requirement of this process, we start by extracting excitable wavenumber through the analysis of critical diffusion ratio. Wavenumber is an eigenmode of the Laplace operator that satisfies the criteria for diffusion-driven instability. The results for mode isolation for the excitable wavenumber are employed to computationally find Turing parameter spaces on the real positive parameter plane. We also present the process of coordinate transformation from cartesian to spherical of the usual Laplace operator. Finally, we analyse and compare the shift and dependence of Turing spaces for equations in the bulk with those Turing spaces that are derived for equations on the surface.

3.1 Critical diffusion ratio and excitable wavenumber

For the bulk, the conditions (2.117), (2.118) and (2.121) are necessary but not sufficient for the emergence of an inhomogeneous spatial structure. The sufficient condition requires the existence of some finite wavenumber $k^2 \in (k_-^2, k_+^2)$, where $k_\pm^2$ are the roots of the equation $H_2(k^2) = 0$ as in (2.110). Also, for the surface the conditions (2.119), (2.120) and (2.122) are necessary but not sufficient for diffusion-

driven instability and the sufficient condition requires the existence of some finite wavenumber $l(l+1) \in (l(l+1)_-, l(l+1)_+)$ where $l(l+1)_\pm$ are the roots of the equation $H_1(l(l+1)) = 0$ as in (2.99). When the minimum $H_2(k^2) = 0$, we require that

$$f_{1u}f_{2v} - f_{1v}f_{2u} = \frac{(d_c f_{1u} + f_{2v})^2}{4d_c}. \tag{3.1}$$

For fixed parameters on the kinetics in the bulk, the critical diffusion d_c is required to satisfy

$$f_{1u}f_{2v} - f_{1v}f_{2u} = \frac{d_c^2 f_{1u}^2 + 2d_c f_{1u}f_{2v} + f_{2v}^2}{4d_c}. \tag{3.2}$$

Multiplying both sides of (3.2) by $4d_c$, we obtain

$$4d_c f_{1u}f_{2v} - 4d_c f_{1v}f_{2u} = d_c^2 f_{1u}^2 + 2d_c f_{1u}f_{2v} + f_{2v}^2, \tag{3.3}$$

which can be simplified to

$$d_c^2 f_{1u}^2 - (2f_{1u}f_{2v} - 4f_{1v}f_{2u})d_c + f_{2v}^2 = 0. \tag{3.4}$$

Corresponding to the critical diffusion coefficient d_c, there exists a critical wavenumber k_c^2, which is the root of the polynomial

$$H_2(k_{l,m}^2) = {k_{l,m}}^4 d_\Omega - {k_{l,m}}^2 \gamma_\Omega[d_\Omega f_{1u} + f_{2v}] + (f_{1u}f_{2v} - f_{1v}f_{2u})\gamma_\Omega^2 = 0. \tag{3.5}$$

The expression for k_c^2, given as the root of (3.5) is

$${k_c}^2 = \frac{\gamma_\Omega[d_c f_{1u} + f_{2v}] \pm \sqrt{\gamma_\Omega^2[d_c f_{1u} + f_{2v}]^2 - 4d_c(f_{1u}f_{2v} - f_{1v}f_{2u})\gamma_\Omega^2}}{2d_c}.$$

From (3.3), which is substituted into the expression for k_c^2 to obtain

$$k_c^2 = \pm\gamma_\Omega\sqrt{\frac{(f_{1u}f_{2v} - f_{1v}f_{2u})}{d_c}}. \tag{3.6}$$

This is the critical wavenumber, the sufficient condition for Turing instability with the necessary conditions (2.117), (2.118) and (2.121) satisfied, which leads the system to evolve into spatial pattern. Similarly, the critical diffusion coefficient d_c on the surface can be obtained from the following equation:

$$d_c^2 f_{3r}^2 - (2f_{3r}f_{4s} - 4f_{3s}f_{4r})d_c + f_{4s}^2 = 0. \tag{3.7}$$

The critical wavenumber on the surface is given by

$$l(l+1)_c = \pm\gamma_\Gamma \sqrt{\frac{(f_{3r}f_{4s} - f_{3s}f_{4r})}{d_c}}, \tag{3.8}$$

which provides the sufficient condition for diffusion-driven instability on the surface. For fixed kinetics parameter values $a_2 = 0.1, \quad b_2 = 0.9$ Murray (2001), we use the first derivatives of f_1, f_2, f_3 and f_4 which are given by

$$\begin{aligned}
&f_{1u} = 2u_0v_0 - 1, \quad f_{1v} = u_0^2,\\
&f_{2u} = -2u_0v_0, \quad f_{2v} = -u_0^2,\\
&f_{3u} = 1, \quad f_{3v} = \delta_2, \quad f_{3r} = -(\rho_3 + 1), \quad f_{3s} = q_2,\\
&f_{3u} = 1, \quad f_{3v} = \delta_3, \quad f_{3r} = c_2, \quad f_{3s} = -(\rho_4 + j_2).
\end{aligned}$$

Since

$$u_0 = a_2 + b_2 = 0.1 + 0.9 = 1, \quad v_0 = \frac{b_2}{(a_2 + b_2)^2} = 0.9, \tag{3.9}$$

therefore, we obtain

$$f_{1u} = 0.8, \quad f_{1v} = 1, \quad f_{2u} = -1.8, \quad f_{2v} = -1.$$

Note that $f_{1u} + f_{2v} = -0.2 < 0 \quad$ and $\quad f_{1u}f_{2v} - f_{1v}f_{2u} = 1 > 0$ hold so that the conditions (2.117) and (2.118) are satisfied. Substituting these values into (3.4), one obtains

$$d_c^2(0.64) - (5.6)d_c + 1 = 0,$$

for which the two roots are given by

$$d_c = 8.56762745781 > 1, \tag{3.10}$$

$$d_c = 0.18237254218 < 1. \tag{3.11}$$

Since the diffusion coefficient must be greater than 1, then we only take the critical diffusion coefficient ratio as $d_c = 8.56762745781$. Figure 3.1a shows the plot of $H_2(k^2)$ as a function of k^2, which is defined by (2.110). All three possibilities for diffusion coefficient d with respect to the critical diffusion d_c are plotted. It can be observed that only when $d > d_c$, $H_2(k^2)$ becomes negative for a finite range of $k^2 > 0$. Also Figure 3.1b shows the plot of real part of λ as a function of k^2, which

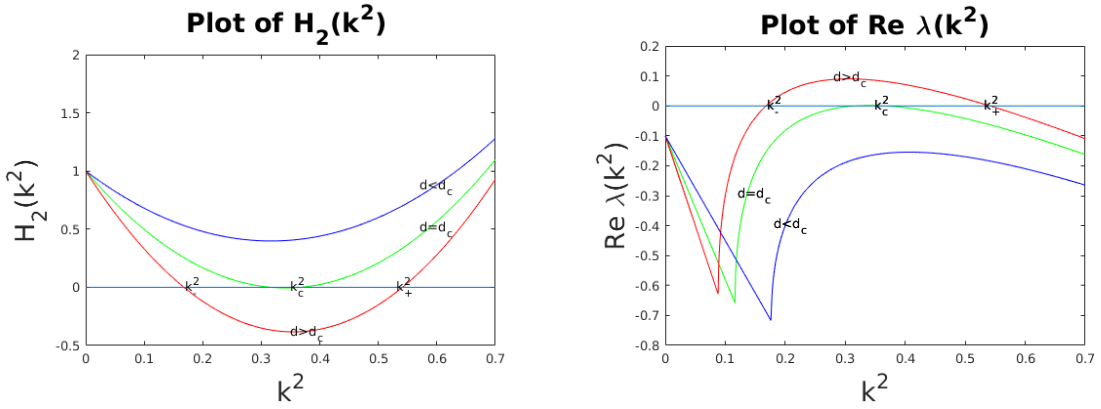

(a) (b)

Figure 3.1: Plot of $H_2(k^2)$ defined by (2.110) is shown in (a). When $d > d_c$, then $H_2(k^2) < 0$ for a finite range of $k^2 > 0$. Plot of the largest of the eigenvalue $\lambda(k^2)$ from (2.106) as a function of k^2 is shown in (b). When $d > d_c$, there is a range of wavenumbers $k_-^2 < k^2 < k_+^2$ which are linearly unstable.

is defined by (2.106). It can be observed that only when $d > d_c$ we have a region in k^2 for which the value of $Re\lambda(k^2)$ is positive. This means that when $d > d_c$, there exist certain wavenumbers k^2 on a finite region which correspond to the frequency of the spatial (Turing) pattern.

To verify that $d < d_c$ does not allow Turing pattern to evolve, the necessary conditions are tested on the parameter space (a_2, b_2) where a_2 and b_2 are the positive constants of the Schnakenberg reaction kinetics. It is found that when $d < d_c$, there is no region in the parameter space that would become unstable due to diffusion in the system. This is shown in Figure 3.2a. Similarly when $d > d_c$, then we see that the unstable region is formed in the parameter space (yellow region in Figure 3.2b), which corresponds to the parameter values that would result in the system to evolve into a Turing pattern.

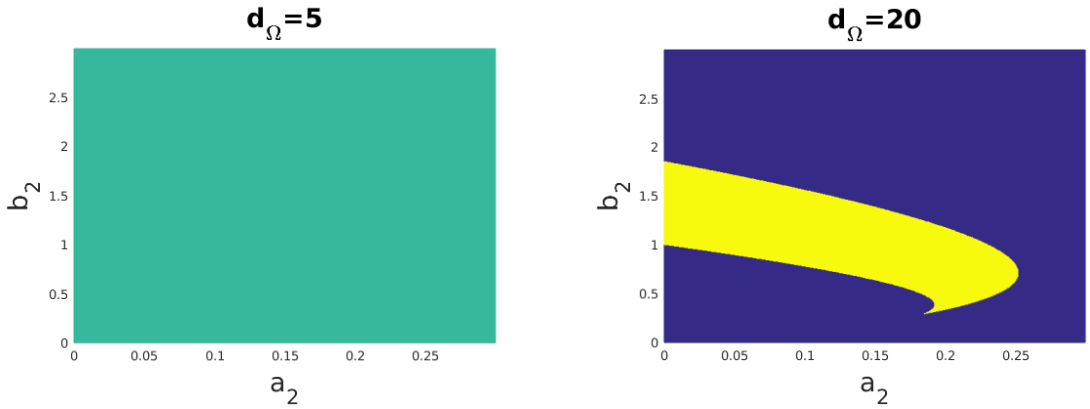

(a) (b)

Figure 3.2: When $d < d_c$, then there is no region in parameter space that corresponds to Turing instability, which is shown in (a). When $d > d_c$, then the diffusion-driven instability region in parameter space exists that corresponds to Turing instability and is shown in (b).

3.2 Mode isolation in the bulk

With the help of linear stability analysis, certain modes can be isolated to help find the admissible set of parameter values d_Ω and γ_Ω for diffusion-driven instability. The necessary conditions for diffusion-driven instability found in Chapter 2 are

$$f_{1u} + f_{2v} < 0, \tag{3.12}$$

$$f_{1u}f_{2v} - f_{1v}f_{2u} > 0, \tag{3.13}$$

$$d_\Omega f_{1u} + f_{2v} > 0 \quad \text{and} \quad [d_\Omega f_{1u} + f_{2v}]^2 - 4d_\Omega(f_{1u}f_{2v} - f_{1v}f_{2u}) > 0. \tag{3.14}$$

One of the sufficient conditions however, for diffusion-driven instability is that the eigenvalues of the Laplace operator should fall in the real interval between the small and the large eigenvalues of the system. It means that

$$\gamma L = k_-^2 < k^2 < k_+^2 = \gamma R \tag{3.15}$$

must hold with L and R expressed by

$$L = \frac{(d_\Omega f_{1u} + f_{2v}) - \sqrt{(d_\Omega f_{1u} + f_{2v})^2 - 4d_\Omega(f_{1u}f_{2v} - f_{1v}f_{2u})}}{2d_\Omega}, \tag{3.16}$$

and

$$R = \frac{(d_\Omega f_{1u} + f_{2v}) + \sqrt{(d_\Omega f_{1u} + f_{2v})^2 - 4d_\Omega(f_{1u}f_{2v} - f_{1v}f_{2u})}}{2d_\Omega}, \tag{3.17}$$

respectively. Therefore, for sufficient condition to exists for diffusion-driven instability, the excitable modes must exist and belong to the interval (3.15). Consider the one-dimensional case, the eigenvalues are $k_l^2 = l^2\pi^2$. In order to find the excitable wavenumbers, in addition to the necessary conditions (3.12), (3.13), (3.14) and (3.15), one requires the sufficient condition of the form

$$k_{l-1}^2 < k_-^2 < k_l^2 < k_+^2 < k_{l+1}^2. \tag{3.18}$$

Figure 3.3 represents the real part of the larger eigenvalue as a function of k^2. In Figure 3.3 the parameter $d_\Omega = 10$ was fixed and the value of γ_Ω was varied according to the values in Madzvamuse (2000), which suggested that when $\gamma_\Omega = 15$ and $\gamma_\Omega = 60$ then no wavenumber excited, however if $\gamma_\Omega = 30$ and $\gamma_\Omega = 90$ then only one wavenumber is excited for each value which are k_1^2 and k_2^2 respectively, with $k_1 = \pi$ and $k_2 = 2\pi$. For $\gamma_\Omega = 187$, there are two excitable wavenumbers which are of the form $k_2^2 = (2\pi)^2$ and $k_3^2 = (3\pi)^2$.

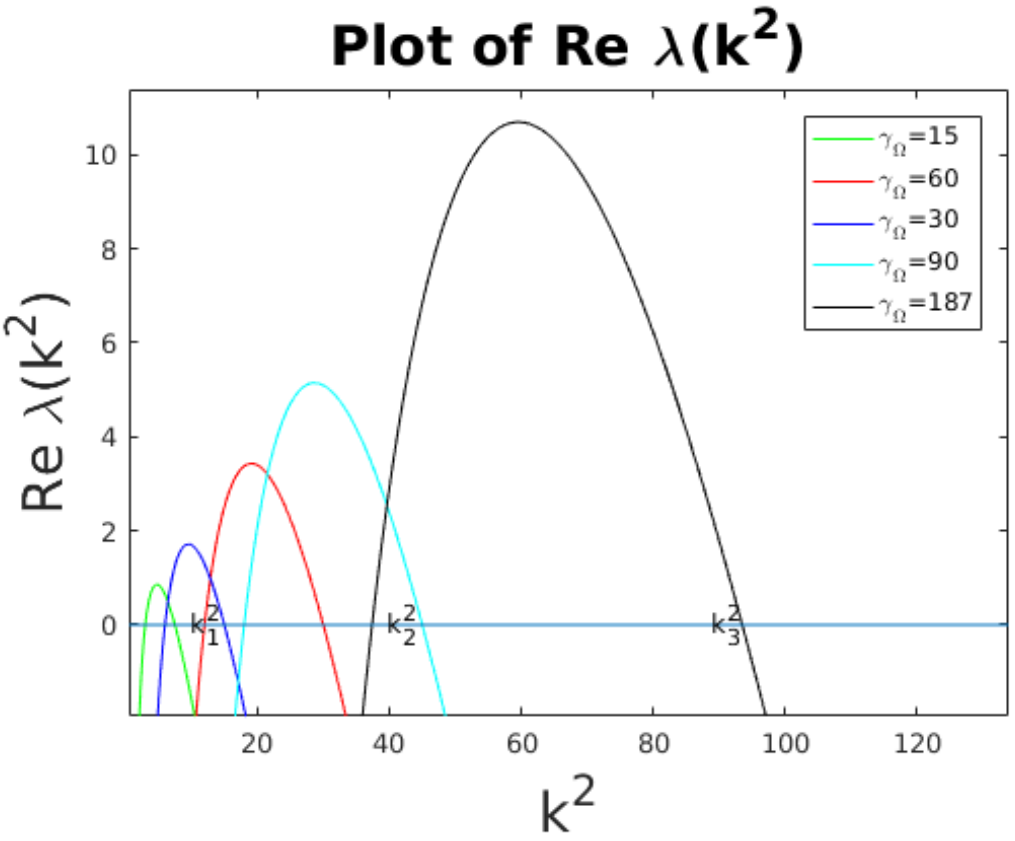

Figure 3.3: Plot of the real part of eigenvalue $\lambda(k^2)$ from (2.106) as a function of k^2. For fixed $d_\Omega = 10$ and increasing γ_Ω, we see that when $\gamma_\Omega = 30$ there is only one wavenumber excited ($k_1^2 = \pi^2$), when $\gamma_\Omega = 90$ there is only one wavenumber excited ($k_2^2 = (2\pi)^2$). There are two excitable wavenumbers namely $k_2^2 = (2\pi)^2$ and $k_3^2 = (3\pi)^2$ when $\gamma_\Omega = 187$.

A similar approach is applied to the case in two dimensions. The values of d_Ω and γ_Ω are computed using the same algorithm used by Madzvamuse (2000). We are interested in finding combination of d_Ω and γ_Ω, such that the curve $\mathrm{Re}(\lambda(k^2))$ encapsulates only one excitable wavenumber. The algorithm is outlined through the following steps.

- Define $d_\Omega = d_c + \epsilon$ where $0 < \epsilon \ll 1$ and $d_c = 8.5676$.
- Compute k_-^2 and k_+^2.
- If $k_{l,m}^2 > k_+^2$ as shown in Figure 3.4 then increase the value of γ_Ω by 1, till the curve includes the wavenumber by shifting to the right.
- If $k_{l,m}^2 < k_-^2$ then decrease the value of γ_Ω by 1, till the curve includes the wavenumber by shifting to the left.
- If there exist two excitable wavenumbers as shown in Figure 3.5a then we decrease ϵ till we obtain a unique excitable wavenumber as shown in Figure 3.5b.

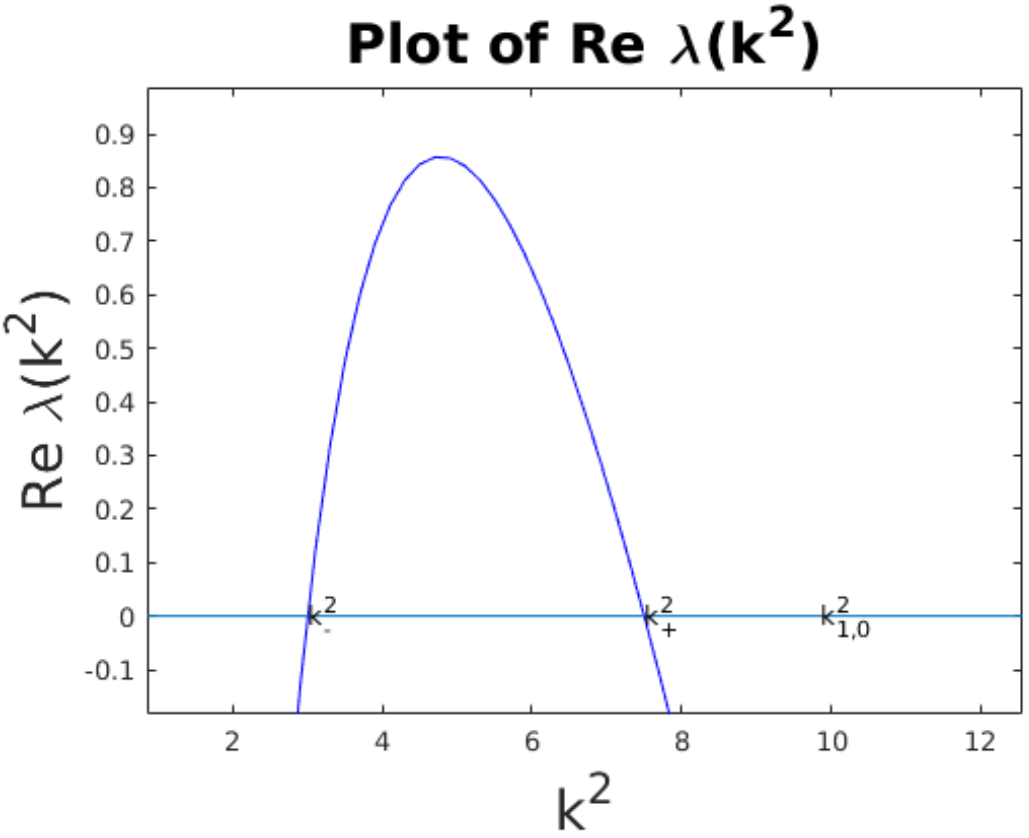

Figure 3.4: Plot of the real part of eigenvalue $\lambda(k^2)$ given by (2.106) as a function of k^2. For all parameter values suitable for diffusion-driven instability, d_Ω and γ_Ω are varied to capture the excitable wavenumber.

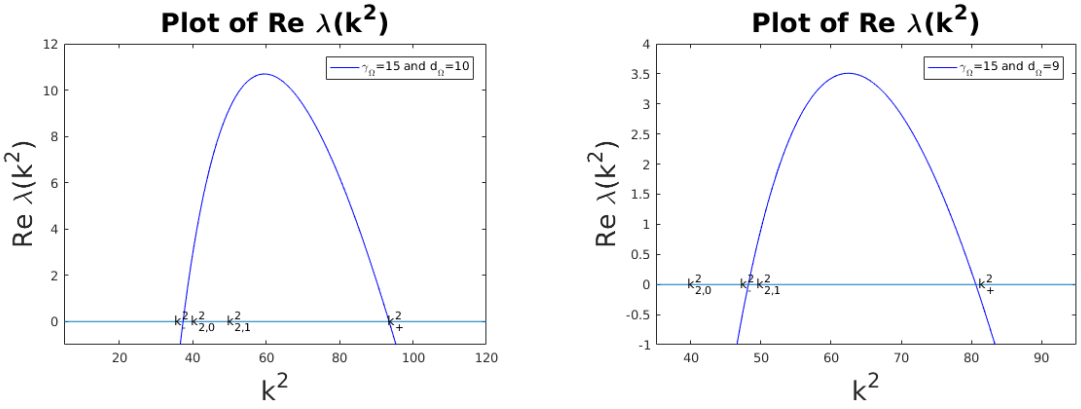

(a) (b)

Figure 3.5: Plot of the real part of eigenvalue $\lambda(k^2)$ given by (2.106) as a function of k^2, where we see that in Figure 3.5a there exist two excitable wavenumbers. By decreasing ϵ we extract a unique excitable wavenumber shown in Figure 3.5b.

3.3 Turing (parameters) space on the surface

In this section we show Turing (parameters) spaces for equations posed on the surface, the conditions for these are obtained in Chapter 2 and outlined as

$$f_{3r} + f_{4s} < 0, \tag{3.19}$$

$$f_{3r}f_{4s} - f_{3s}f_{4r} > 0, \tag{3.20}$$

$$d_\Gamma f_{3r} + f_{4s} > 0 \quad \text{and} \quad [d_\Gamma f_{3r} + f_{4s}]^2 - 4d_\Gamma(f_{3r}f_{4s} - f_{3s}f_{4r}) > 0. \tag{3.21}$$

The parameter spaces are derived on the actual positive real parameter plane (a_2, b_2), for two choices of diffusion ratios namely $d_\Gamma = 20$ and $d_\Gamma = 30$.

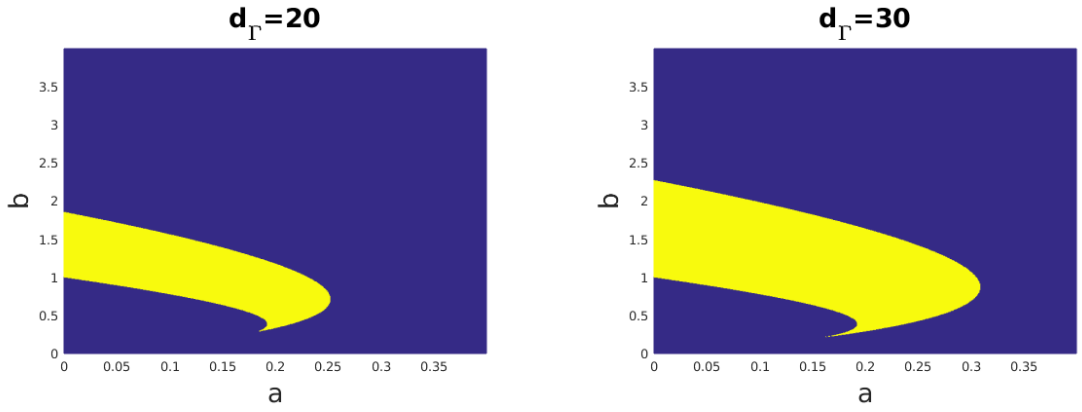

(a) (b)

Figure 3.6: Turing space for Schnakenberg model for different values of d_Γ. Unstable region is shown in the parameter space (yellow region).

3.4 Mode isolation on the surface

A similar procedure may be employed to extract excitable wavenumbers from the spectrum of Laplace-Beltrami operator as a sufficient condition for Turing pattern to be formed on the surface. The spectrum of Laplace-Beltrami operator on spherical surface is studied in great details in Chaplain et al. (2001) where they derive the infinite set of discrete eigenvalues of the form $k^2 = l(l+1)$ corresponding to an infinite set of eigenfunctions given by $u_l^m(\theta, \phi) = c_l^m P_l^{|m|}(\cos\theta)\exp(im\phi)$.

3.5 Turing spaces in the bulk and on the surface

The following sub-figures show diffusion-driven instability spaces for the conditions on diffusion-driven instability given by (2.117)-(2.122) in the bulk and on the surface. We combine the Turing spaces (more than one space) in the bulk and on the surface together. We note that if d_Ω is chosen the same as d_Γ, there is no difference in the region corresponding to Turing space as shown in Sub-figure 3.8a. In Sub-figures 3.8b and 3.8c, it can be seen that for larger values of the diffusion coefficient the Turing space is significantly larger than that for the smaller value of the diffusion coefficient. In the context of pattern formation it means that regions corresponding to diffusion driven instability enlarge with an increase in the diffusion coefficient.

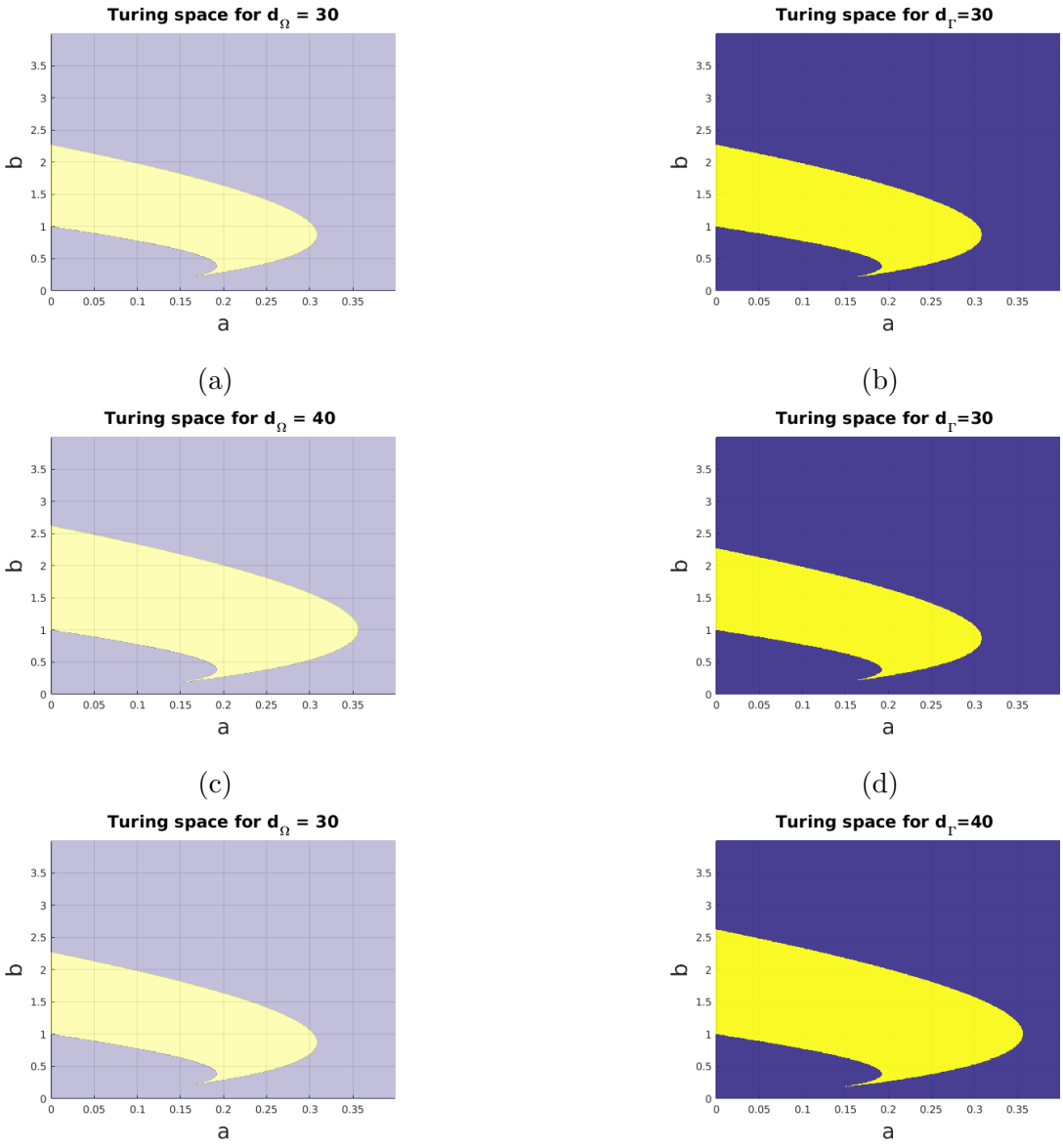

Figure 3.7: First row shows that the Turing space for both the bulk and the surface separately for parameter choices $d_\Gamma = 30$ and $d_\Omega = 30$ respectively. Second and third rows show that the Turing space in the bulk and on the surface separately with different parameter choices (second row $d_\Gamma = 30$ and $d_\Omega = 40$) and (third row $d_\Gamma = 30$ and $d_\Omega = 40$).

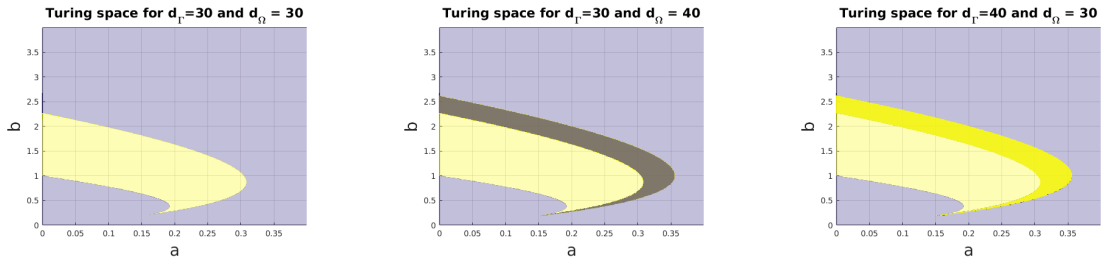

(a) (b) (c)

Figure 3.8: Sub-figure (a) shows that the Turing space for both the bulk and the surface (cream colour) is shown to exactly coincide for parameter choices $d_\Gamma = 30$ and $d_\Omega = 30$. Sub-figure (b) shows that the Turing space on the surface (cream colour) forms a proper subset of those derived for the bulk equations (union of cream and grey regions) when $d_\Gamma = 30$ and $d_\Omega = 40$. Sub-figure (c) shows that the Turing space for equations on the surface (union of yellow and cream colour regions) with $d_\Gamma = 40$ produces larger region, which contains the spaces for the bulk equation with $d_\Omega = 30$ as proper subset, upon submerging.

3.6 Conclusion

As a natural extension from the contents of Chapter 2, where all necessary conditions for diffusion-driven instability are derived, these are also equipped with the sufficient conditions through the contents of this chapter to guarantee achieving spatial pattern formation. Critical diffusion ratio was extracted and analysed. Furthermore, mode isolation algorithm was applied as a technique to extract a single excitable wavenumber. Turing spaces for both the bulk and the surface were computationally found, which are employed for numerical solutions of BSRDEs in Chapter 5. The results of this chapter in relation to Chapter 2 motivates to test the emergence of spatial pattern formation through employing the conditions and constraints obtained in Chapter 2 and Chapter 3, through the formulation and simulation of the finite element numerical scheme. The next chapter is therefore devoted to present the theoretical formulation of the finite element scheme, with strategies for mesh generation and other necessary steps that are required for computational simulation of BSRDEs.

Chapter 4

Finite Element Methods for Reaction-Diffusion Equations on Stationary Volumes

This chapter serves to provide the theoretical formulation required to obtain numerical solutions through the finite element method of all the three systems that were explored in Chapter 2. A brief introduction to Sobolev and Hilbert function spaces is provided as the basis to obtain the weak formulation. The methods of space and time discretisations are described with a brief overview of the time-stepping schemes. We compare the first order IMEX time-stepping scheme with the second order semi-implicit backward differentiation formula (2-SBDF) through the numerical simulations of a reaction-diffusion system on a stationary two-dimensional disc-shape domain. For simplicity the problem is formulated to solve independently in the bulk and on the surface with appropriate boundary settings. Upon achieving such a formulation the method is extended to consider the full four component system of BSRDEs. We present the weak formulation with the corresponding finite element formulation through a fully implicit treatment by employing the extended form of Newton's method for vector valued functions.

4.1 Notations

Before implementing the finite element method, we briefly introduce the necessary function spaces and norms Brenner and Scott (2007) that are utilised in numerical set up of the problem. For a non-negative integer n, we introduce an n-tuple multi-index $\alpha = (\alpha_1, \cdots, \alpha_n)$ with length $|\alpha| = \alpha_1 + \alpha_2 + \cdots + \alpha_n$. Let the operator D^α be defined as

$$D^\alpha = (\frac{\partial}{\partial x_1})^{\alpha_1} \cdots (\frac{\partial}{\partial x_n})^{\alpha_n} = \frac{\partial^{|\alpha|}}{\partial x_1^{\alpha_1} \cdots \partial x_n^{\alpha_n}}.$$

For example, for a function u that depends on three variables x_1, x_2 and x_3, then applying D^α to u generates the third order mixed derivatives of u with respect to all the independent variables, therefore we have

$$\sum_{|\alpha|=3} D^\alpha u = \frac{\partial^3 u}{\partial x_1^3} + \frac{\partial^3 u}{\partial x_2^3} + \frac{\partial^3 u}{\partial x_3^3} + \frac{\partial^3 u}{\partial x_1^2 \partial x_2} + \frac{\partial^3 u}{\partial x_1^2 \partial x_3} + \frac{\partial^3 u}{\partial x_1 \partial x_2^2} + \frac{\partial^3 u}{\partial x_1 \partial x_3^2} + \frac{\partial^3 u}{\partial x_2^2 \partial x_3} + \frac{\partial^3 u}{\partial x_2 \partial x_3^2} + \frac{\partial^3 u}{\partial x_1 \partial x_2 \partial x_3}.$$

For a real number $p \geq 1$ the set of all real valued integrable functions defined on an open subset Ω of R^n are denoted by $L_p(\Omega)$, which are referred to as Lebesgue function spaces. Let the set $L_p(\Omega)$ be equipped with the norm in the form that

$$u \in L_p(\Omega) \Rightarrow \| u \|_{L_p(\Omega)} = \Big(\int_\Omega |u(x)|^p dx \Big)^{\frac{1}{p}} < \infty.$$

Definition 4.1.1 ***Sobolev spaces*** *Brenner and Scott (2007) Let k be a positive integer and $p \in [1, \infty)$, then the set $W_p^k(\Omega)$ is called a Sobolev space of order k where $W_p^k(\Omega)$ is defined by*

$$W_p^k(\Omega) = \{u \in L_p(\Omega) : D^\alpha u \in L_p(\Omega), \quad |\alpha| \leq k\}.$$

The function space $W_p^k(\Omega)$ must also equipped with the norm in form

$$\| u \|_{W_p^k(\Omega)} = \Big(\sum_{|\alpha| \leq k} \| D^\alpha u \|_{L_p(\Omega)}^p \Big)^{\frac{1}{p}} \quad \text{if} \quad 1 \leq p < \infty$$

Hilbert space is a special subset of Sobolev space with $p = 2$, which means that it is the set of all functions that belongs to Sobolev space, with bounded L_2 norm.

By taking $k = 1$, the set $W_2^1(\Omega)$ refers to all functions which are bounded in the L_2 norm as well as their first derivatives are also bounded in the L_2. The usual notation for $W_2^1(\Omega)$ used in literature is $H^1(\Omega)$, which is defined as

$$H^1(\Omega) = \{u \in L_2(\Omega) : \frac{\partial u}{\partial x_i} \in L_2(\Omega), \quad i = 1, \cdots, n\}.$$

We say $u \in H^1(\Omega)$ if u satisfies the following

$$\| u \|_{H^1(\Omega)} = \Big(\| u \|^2_{L_2(\Omega)} + \sum_{i=1}^{n} \| \frac{\partial u}{\partial x_i} \|^2_{L_2(\Omega)} \Big)^{\frac{1}{2}} < \infty.$$

Definition 4.1.2 ***Newton's method*** *Quarteroni et al. (2010) : Assuming that $f \in C^1(\mathcal{I})$ and that $f^{'}(\alpha) \neq 0$ (i.e., α is a simple root of f), if we let*

$$q_k = f^{'}(x_k), \quad \forall k \geq 0$$

and assign the initial value x_0, we obtain the so called Newton method

$$x_{k+1} = x_k - \frac{f(x_k)}{f^{'}(x_k)}, \quad \forall k \geq 0. \tag{4.1}$$

Newton's method can also be employed for vector valued functions as in Quarteroni et al. (2010), Hueso et al. (2009) and Saheya et al. (2016), which means that for a vector valued function with the root $\mathbf{x}_k \in \mathbb{R}^n$, the equivalent algorithm to (4.1) is to find $\mathbf{x}_{k+1}$ through

$$\mathbf{J_F}(\mathbf{x}_{k+1} - \mathbf{x}_k) = -\mathbf{F}(\mathbf{x}_k), \quad k = 0, 1, \cdots. \tag{4.2}$$

where $\mathbf{J_F}$ denotes the corresponding Jacobian matrix associated to the vector valued function $\mathbf{F}$.

4.2 The finite element method in the bulk

We consider a circular two-dimensional simply connected domain $\Omega \subset \mathbb{R}^2$ with a disc-shape geometry and Lipschitz boundary $\partial\Omega \subset \mathbb{R}^2$ which consists of a circle. Let $I = (0, T]$ be some finite time interval. Reaction-diffusion equations with Schnaken-

berg reaction kinetics in its non-dimensional form posed on Ω reads as

$$\begin{cases} \frac{\partial u}{\partial t} - \Delta u = \gamma(a - u + u^2 v) := \gamma f(u,v), \ \text{ in } \ \Omega, \ \ t \in I, \\ \frac{\partial v}{\partial t} - d\Delta v = \gamma(b - u^2 v) := \gamma g(u,v), \ \text{ in } \ \Omega, \ \ t \in I, \\ u(\mathbf{x},0) = u^0(\mathbf{x}) \ \text{ in } \ \Omega, \\ v(\mathbf{x},0) = v^0(\mathbf{x}) \ \text{ in } \ \Omega, \\ \frac{\partial u}{\partial \mathbf{n}} = \frac{\partial v}{\partial \mathbf{n}} = 0 \ \text{ on } \ \partial\Omega, \end{cases} \tag{4.3}$$

for the concentrations $u(\mathbf{x},t)$ and $v(\mathbf{x},t)$ with a, b, d and γ denoting some real positive constants. Here, d represents the ratio of the diffusion coefficients of the v and u variables while γ measures the strength of the reaction. For this system, we have chosen homogeneous Neumann boundary conditions on the entire boundary and initial conditions that are chosen to be small random perturbations about the uniform steady state

$$(u_0, v_0) = \left(a + b, \frac{b}{(a+b)^2}\right). \tag{4.4}$$

In the absence of diffusion, the equilibrium point (4.4) is linearly stable provided that

$$f_u + g_v < 0 \ \text{ and } \ f_u g_v - f_v g_u > 0, \tag{4.5}$$

where the derivatives are evaluated at the equilibrium point (4.4) Madzvamuse and Chung (2014). Upon adding diffusion to the system and provided that conditions for Turing instability namely (4.6)-(4.7), then it is possible that the dynamics of the system evolve to converge to a spatially inhomogeneous (Turing type) steady state. This phenomenon is described as diffusion-driven instability or Turing instability Madzvamuse and Chung (2014). It can be shown that the necessary conditions for diffusion-driven instability are

$$f_u + g_v < 0 \ \text{ and } \ f_u g_v - f_v g_u > 0, \tag{4.6}$$

$$df_u + g_v > 0 \ \text{ and } \ (df_u + g_v)^2 - 4d(f_u g_v - f_v g_u) > 0. \tag{4.7}$$

It is demonstrated in Madzvamuse and Chung (2014) that the numerical values for parameters $a = 0.1$, $b = 0.9$, $d = 10$ and $\gamma = 29$ lead to diffusion-driven instability, which is used in the numerical simulations. For the finite element formulation we require the weak formulation of the reaction-diffusion system, which is derived

through multiplying system (4.3) by a test function $\psi(\mathbf{x},t) \in H^1(\Omega)$ and integrating over Ω which takes the form

$$\begin{aligned} \int_\Omega \psi \frac{\partial u}{\partial t} d\Omega - \int_\Omega \psi \Delta u d\Omega = \gamma \int_\Omega \psi \left(a - u + u^2 v\right) d\Omega \\ \int_\Omega \psi \frac{\partial v}{\partial t} d\Omega - d \int_\Omega \psi \Delta v d\Omega = \gamma \int_\Omega \psi \left(b - u^2 v\right) d\Omega. \end{aligned} \tag{4.8}$$

Application of Green's formula defined by (1.3.2) and enforcing the homogeneous Neumann boundary conditions namely $\frac{\partial u}{\partial \mathbf{n}} = \frac{\partial v}{\partial \mathbf{n}} = 0$ on (4.8) leads to write the weak formulation of system (4.3), which is to find $u(\mathbf{x},t), v(\mathbf{x},t) \in H^1(\Omega)$, $t \in [0,T]$ such that

$$\begin{cases} \int_\Omega \psi \frac{\partial u}{\partial t} d\Omega + \int_\Omega \nabla \psi \cdot \nabla u d\Omega = \gamma \int_\Omega \psi \left(a - u + u^2 v\right) d\Omega, \\ \int_\Omega \psi \frac{\partial v}{\partial t} d\Omega + d \int_\Omega \nabla \psi \cdot \nabla v d\Omega = \gamma \int_\Omega \psi \left(a - u^2 v\right) d\Omega, \end{cases} \tag{4.9}$$

is true for all test functions $\psi(\mathbf{x},t) \in H^1(\Omega)$. Let Ω_h be the discretised domain which is a quadrilateral approximation of Ω. Let T_h denote the triangulation of Ω_h which is made up of non-degenerate rectangular elements K_i such that $T_h = \bigcup_i K_i$. We call each K_i an element of the mesh T_h where h is the diameter of the largest element. For the mesh T_h, we require that it is made up of a finite number of elements and the elements must intersect along a complete edge, or at a vertex or not at all. We define the finite element solution space V_h by

$$V_h = \left\{ v_h \in C^0(\Omega) \ : \ v_h|_{K_i} \text{ is linear} \right\}. \tag{4.10}$$

We seek numerical approximate solutions of system (4.3) in V_h. The finite element formulation entailed by the weak formulation (4.9) of the reaction-diffusion system (4.3) therefore is to find $u_h(\mathbf{x},t), v_h(\mathbf{x},t) \in V_h$ such that

$$\begin{cases} \int_{\Omega_h} \psi_h \frac{\partial u_h}{\partial t} d\Omega_h + \int_{\Omega_h} \nabla \psi_h \cdot \nabla u_h d\Omega_h = \gamma \int_{\Omega_h} \psi_h \left(a - u_h + (u_h)^2 v_h\right) d\Omega_h, \\ \int_{\Omega_h} \psi_h \frac{\partial v_h}{\partial t} d\Omega_h + d \int_{\Omega_h} \nabla \psi_h \cdot \nabla v_h d\Omega_h = \gamma \int_{\Omega_h} \psi_h \left(a - (u_h)^2 v_h\right) d\Omega, \end{cases} \tag{4.11}$$

for all $\psi_h(\mathbf{x},t) \in V_h(\Omega)$. With linear choice of V_h it must have a basis that spans the finite n-dimensional function space. Let $\phi_i(\mathbf{x}) \in V_h$, $i = 1, 2, ..., n$, be the i-th basis function such that

$$\phi_i(p_j) = \begin{cases} 1 \ \text{ if } i = j, \\ 0 \ \text{ if } i \neq j, \end{cases} \tag{4.12}$$

where p_j is the j-th nodal point of the mesh. We seek to find the finite element numerical approximations $u_h(\mathbf{x},t), v_h(\mathbf{x},t) \in V_h$ expressed as the linear combinations of the linear nodal basis functions $\phi_i(\mathbf{x})$ expressed as

$$u_h(\mathbf{x},t) = \sum_{j=1}^{n} U_j(t)\phi_j(\mathbf{x}) \text{ and } v_h(\mathbf{x},t) = \sum_{j=1}^{n} V_j(t)\phi_j(\mathbf{x}), \tag{4.13}$$

where $U_j(t) = u_h(p_j,t)$ and $V_j(t) = v_h(p_j,t)$. Without loss of generality, we also express the test functions $\psi_h(\mathbf{x},t)$ in terms of $\phi_i(\mathbf{x}) \in V_h,\ i = 1,2,...,n$, which leads to write (4.11) as a set of ordinary differential equations in the form

$$\begin{aligned}\sum_{j=1}^{n}\int_{\Omega_h} \phi_i(\mathbf{x})\cdot\phi_j(\mathbf{x})\frac{dU_j(t)}{dt}\,d\Omega_h + \sum_{j=1}^{n}\int_{\Omega_h} \nabla\phi_i(\mathbf{x})\cdot\nabla\phi_j(\mathbf{x})\,U_j(t)\,d\Omega_h = \\ \gamma a\int_{\Omega_h}\phi_i(\mathbf{x})\,d\Omega_h - \gamma\sum_{j=1}^{n}\int_{\Omega_h}\phi_i(\mathbf{x})\cdot\phi_j(\mathbf{x})U_j(t)\,d\Omega_h \\ + \gamma\sum_{j=1}^{n}\int_{\Omega_h}\phi_i(\mathbf{x})\cdot(\phi_j(\mathbf{x})U_j(t))^2\cdot(\phi_j(\mathbf{x})V_j(t))\,d\Omega_h,\end{aligned} \tag{4.14}$$

$$\begin{aligned}\sum_{j=1}^{n}\int_{\Omega_h} \phi_i(\mathbf{x})\cdot\phi_j(\mathbf{x})\frac{dV_j(t)}{dt}\,d\Omega_h + d\sum_{j=1}^{n}\int_{\Omega_h} \nabla\phi_i(\mathbf{x})\cdot\nabla\phi_j(\mathbf{x})\,V_j(t)\,d\Omega_h = \\ \gamma b\int_{\Omega_h}\phi_i(\mathbf{x})\,d\Omega_h - \gamma\sum_{j=1}^{n}\int_{\Omega_h}\phi_i(\mathbf{x})\cdot(\phi_j(\mathbf{x})U_j(t))^2\cdot(\phi_j(\mathbf{x})V_j(t))\,d\Omega_h,\end{aligned} \tag{4.15}$$

respectively, for all $i = 1,2,...,n$ and $\mathbf{x} = (x,y)$. Integrating over the discretised Ω_h gives rise to a set of semi-discrete equations in the form

$$\begin{cases} M\frac{d\mathbf{U}(t)}{dt} + A\mathbf{U}(t) = \gamma a\mathbf{H} - \gamma M\mathbf{U}(t) + \gamma B(\mathbf{U}(t),\mathbf{V}(t))\mathbf{U}(t), \\ M\frac{d\mathbf{V}(t)}{dt} + dA\mathbf{V}(t) = \gamma b\mathbf{H} - \gamma B(\mathbf{U}(t),\mathbf{U}(t))\mathbf{V}(t), \end{cases} \tag{4.16}$$

where $\mathbf{U}(t) = (U_1(t),U_2(t),...,U_n(t))^T$ and $\mathbf{V}(t) = (V_1(t),V_2(t),...,V_n(t))^T$ are the solution vectors, M is the global mass matrix, A is the global stiffness matrix, B is the matrix corresponding to the non-linear terms and $\mathbf{H}$ is the global force vector

with entries

$$\begin{cases} M_{ij} = \int_{\Omega_h} \phi_i(\mathbf{x}) \cdot \phi_j(\mathbf{x})\, d\Omega_h, \quad H_j = \int_{\Omega_h} \phi_j(\mathbf{x})\, d\Omega_h, \quad A_{ij} = \int_{\Omega_h} \nabla\phi_i(\mathbf{x}) \cdot \nabla\phi_j(\mathbf{x})\, d\Omega_h, \\ (B(\mathbf{U},\mathbf{V})\mathbf{U})_{ij} = \int_{\Omega_h} \phi_i(\mathbf{x}) \cdot \phi_j(\mathbf{x}) \cdot (U_j^2\phi_j(\mathbf{x})) \cdot (V_j\phi_j(\mathbf{x}))d\Omega_h, \\ (B(\mathbf{U},\mathbf{U})\mathbf{V})_{ij} = \int_{\Omega_h} \phi_i(\mathbf{x}) \cdot \phi_j(\mathbf{x}) \cdot (U_j^2\phi_j(\mathbf{x})) \cdot (V_j\phi_j(\mathbf{x}))d\Omega_h. \end{cases} \tag{4.17}$$

So far we have formulated the spatial approximation through which we obtain a semi-discrete system of $2n$ ODEs. We proceed to analyse and compare the convergence rate of two time-stepping schemes for solving (4.16).

4.2.1 First order IMEX scheme

The idea of first order IMEX time-stepping scheme is to treat the diffusive term implicitly while the terms in the reaction kinetics are treated explicitly Ruuth (1995); Madzvamuse (2006); Madzvamuse and Chung (2014). Applying this scheme to system (4.16) results in obtaining a fully discrete system of algebraic equations in the form

$$\begin{cases} M\frac{\mathbf{U}^{m+1}-\mathbf{U}^m}{\tau} + A\mathbf{U}^{m+1} = \gamma a\mathbf{H} - \gamma M\mathbf{U}^m + \gamma B(\mathbf{U}^m,\mathbf{V}^m)\mathbf{U}^m, \\ M\frac{\mathbf{V}^{m+1}-\mathbf{V}^m}{\tau} + dA\mathbf{V}^{m+1} = \gamma b\mathbf{H} - \gamma B(\mathbf{U}^m,\mathbf{U}^m)\mathbf{V}^m, \end{cases} \tag{4.18}$$

where τ denotes the time-step size. System (4.18) can be rearranged to obtain an algebraic matrix system whose solution at each time step is the finite element approximate numerical solution of system (4.3) which is written in the form

$$\begin{cases} (M+\tau A)\,\mathbf{U}^{m+1} = \tau\gamma a\mathbf{H} + (1-\tau\gamma)M\mathbf{U}^m + \tau\gamma B(\mathbf{U}^m,\mathbf{V}^m)\mathbf{U}^m, \\ (M+\tau dA)\,\mathbf{V}^{m+1} = \tau\gamma b\mathbf{H} - \tau\gamma B(\mathbf{U}^m,\mathbf{U}^m)\mathbf{V}^m + M\mathbf{V}^m, \end{cases} \tag{4.19}$$

where $\mathbf{U}^m$, $\mathbf{U}^{m+1}$ refers to the approximate numerical solutions for u at time t^m and t^{m+1} respectively. Similarly $\mathbf{V}^m$, $\mathbf{V}^{m+1}$ denote the approximate numerical solutions corresponding to v at time step t^m and t^{m+1} respectively.

4.2.2 Second order semi-implicit backward differentiation formula (2-SBDF)

Using the second order semi-implicit backward differentiation formula to the semi-discrete equations (4.16) gives a discrete scheme also presented in Ruuth (1995);

Madzvamuse (2006) and has the form

$$\begin{cases} M\left(\frac{3\mathbf{U}^{m+1}-4\mathbf{U}^{m}+\mathbf{U}^{m-1}}{2\tau}\right)+A\mathbf{U}^{m+1} & =2(\gamma a\mathbf{H}-\gamma M\mathbf{U}^{m}+\gamma B(\mathbf{U}^{m},\mathbf{V}^{m})\mathbf{U}^{m} \\ & \quad -(\gamma a\mathbf{H}-\gamma M\mathbf{U}^{m-1}+\gamma B(\mathbf{U}^{m-1},\mathbf{V}^{m-1})\mathbf{U}^{m-1}, \\ M\left(\frac{3\mathbf{V}^{m+1}-4\mathbf{V}^{m}+\mathbf{V}^{m-1}}{2\tau}\right)+dA\mathbf{V}^{m+1} & =2(\gamma b\mathbf{H}-\gamma B(\mathbf{U}^{m},\mathbf{U}^{m})\mathbf{V}^{m} \\ & \quad -(\gamma b\mathbf{H}-\gamma B(\mathbf{U}^{m-1},\mathbf{U}^{m-1})\mathbf{V}^{m-1}, \end{cases}$$

where τ is the time-step. Collecting likewise terms and rearranging the equations provide a system of linear equations expressed by

$$\begin{aligned}(3M+2\tau A)\,\mathbf{U}^{m+1} &= 4M\mathbf{U}^{m}-M\mathbf{U}^{m-1}+2\tau\gamma a\mathbf{H}+2\tau\gamma M\mathbf{U}^{m-1} \\ &\quad -2\tau\gamma B(\mathbf{U}^{m-1},\mathbf{V}^{m-1})\mathbf{U}^{m-1}-4\tau\gamma M\mathbf{U}^{m}+4\tau\gamma B(\mathbf{U}^{m},\mathbf{V}^{m})\mathbf{U}^{m}, \quad (4.20)\end{aligned}$$

$$\begin{aligned}(3M+2\tau dA)\,\mathbf{V}^{m+1} &= 4M\mathbf{V}^{m}-M\mathbf{V}^{m-1}+2\tau\gamma b\mathbf{H} \\ &\quad +2\tau\gamma B(\mathbf{U}^{m-1},\mathbf{U}^{m-1})\mathbf{V}^{m-1}-4\tau\gamma B(\mathbf{U}^{m},\mathbf{U}^{m})\mathbf{V}^{m}. \quad (4.21)\end{aligned}$$

Here we notice that we need solutions at both times $t=t_m$ and $t=t_{m-1}$. Solutions for the last two time-steps will therefore need to be stored. For the initial start of the scheme we use a single step of Backward Euler method with the reaction terms treated explicitly to solve for the $\mathbf{U}^1$ and $\mathbf{V}^1$ solutions, which provides sufficient data for the scheme to discretely step forward in time.

4.2.3 Numerical simulations in the bulk

For our simulations, the domain Ω is the unit disc. We employ the deal.ii library Bangerth et al. (2016) to discretise the domain with 5185 degrees of freedom. The initial data is chosen to be random perturbations from the equilibrium points in equation (4.4). The simulations are run until a spatially inhomogeneous steady state is reached as shown in Figures 4.1, 4.2, 4.5 and 4.6. The convergence rate in the L_2-norm of the two time stepping schemes namely first order IMEX and 2-SBDF are compared through the use of $\tau=10^{-3}$ and $\tau=2\times10^{-3}$ for time step sizes. To verify the convergence, we also compute the relative error given by

$$\text{Relative error } =\sqrt{\frac{\sum|U^{n+1}-U^{n}|^2}{\sum|U^{n+1}|^2}}, \quad (4.22)$$

at the final time $t = 10$. The convergence rates corresponding to the variable u using the first order IMEX and 2-SBDF schemes with different values of time step sizes are shown Tables 4.1 and 4.2 respectively. We vary the parameter γ and plot the solutions in Figure 4.11. We plot in logarithmic scale the graph for the L_2-norm with two choices of time-steps shown in Figure 4.3. We plot the convergence history of the simulations conducted on the Schnakenberg model for variable u using the first order IMEX scheme, with different time steps shown in the legend of Figure 4.7 and with refined mesh shown in Figure 4.8. Also, the convergence history of the simulations is plotted for the Schnakenberg model for variable u using 2-SBDF scheme, with different time-steps shown in Figure 4.9 and with refinement of mesh size shown in 4.10. We can observe from Figures 4.4 (a) and (b) that 2-SBDF outperforms first order IMEX in the convergence rate to a spatially inhomogeneous steady state. This can be verified by realising that the values of the discrete L_2-norm of the numerical solutions difference for subsequent time steps for 2-SBFD always remains smaller than those values obtained for first order IMEX.

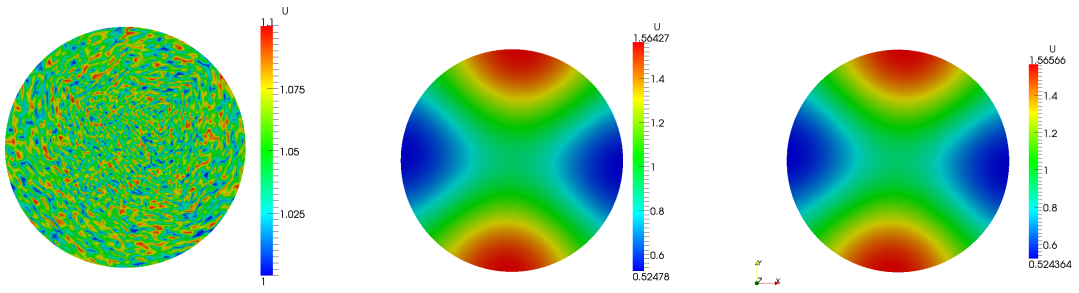

(a) (b) (c)

Figure 4.1: Solutions for variable u of the Schnakenberg model using the first order IMEX scheme. Sub-figure (a) shows the initial condition as random perturbations about steady states. Sub-figures (b) and (c) show the numerical solutions corresponding to u at times $t = 5.8$ and $t = 10$ respectively.

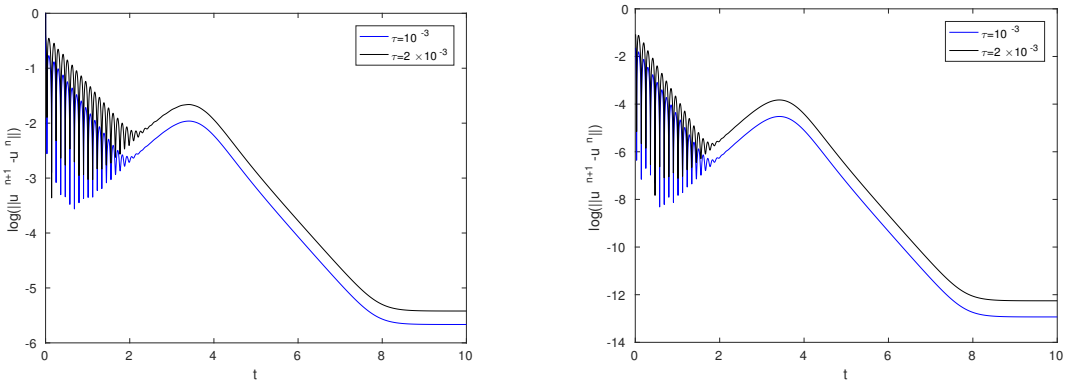

(a) (b)

Figure 4.3: Convergence history of the simulations of the Schnakenberg model for the variable u using (a) the first order IMEX scheme and (b) the 2-SBDF scheme.

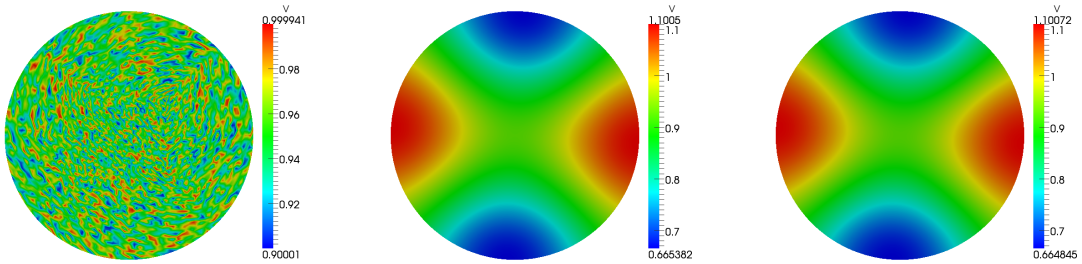

(a) (b) (c)

Figure 4.2: Solutions for variable v of the Schnakenberg model using the first order IMEX scheme. Sub-figure (a) shows the initial condition as random perturbations about steady states. Sub-figures (b) and (c) show the numerical solutions corresponding to v at times $t = 5.8$ and $t = 10$ respectively.

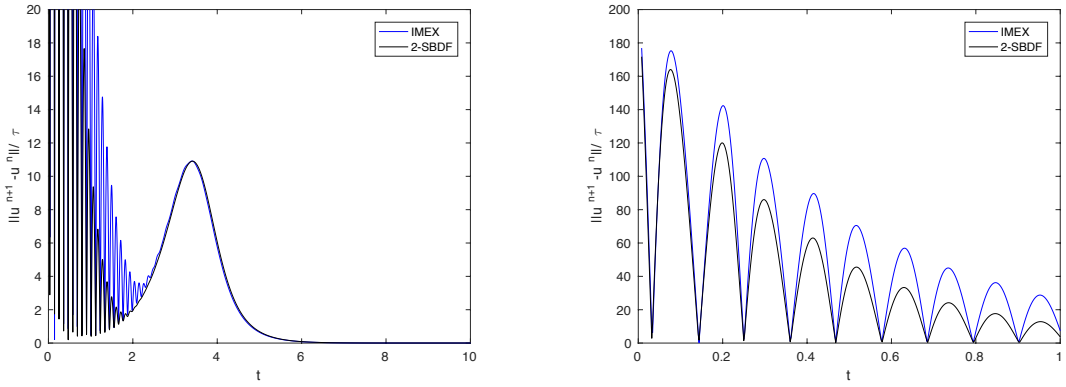

(a) (b)

Figure 4.4: Comparison of the convergence history of the simulations of the Schnakenberg model for the variable u between the first order IMEX and the 2-SBDF schemes with (a) entire time interval and (b) time interval $[0, 1]$ zoomed.

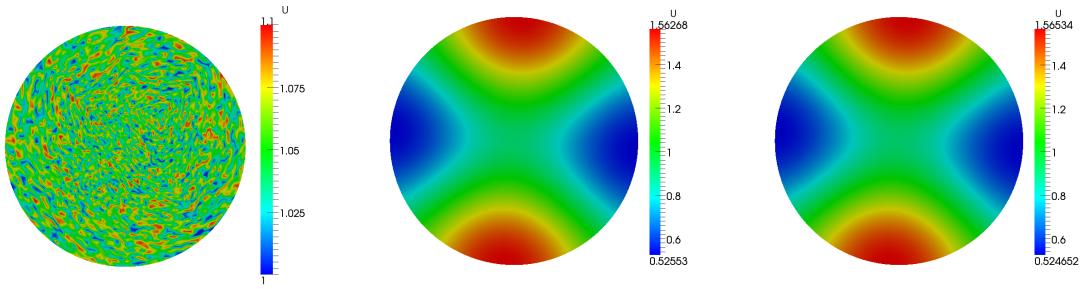

(a) (b) (c)

Figure 4.5: Solutions for variable u of the Schnakenberg model using the 2-SBDF scheme. Sub-figure (a) shows the initial condition as random perturbations about steady states. Sub-figures (b) and (c) show the numerical solutions corresponding to u at times $t = 5.5$ and $t = 10$ respectively.

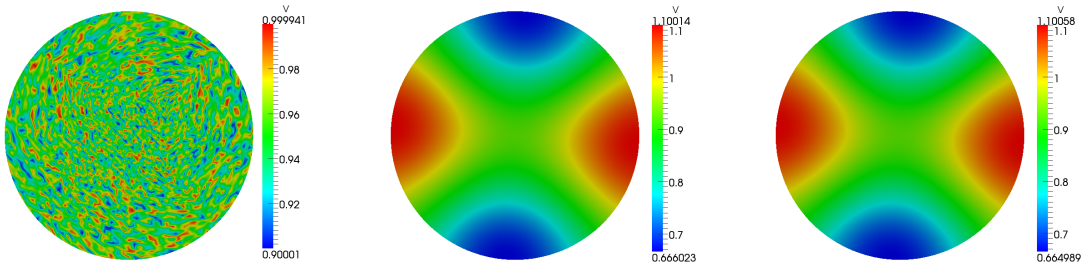

Figure 4.6: Solutions for variable v of the Schnakenberg model using the 2-SBDF scheme. Sub-figure (a) shows the initial condition as random perturbations about steady states. Sub-figures (b) and (c) show the numerical solutions corresponding to v at times $t = 5.5$ and $t = 10$ respectively.

Time-step τ	No. of time steps	Relative error	$\|\frac{u^{n+1}-u^n}{\tau}\|$
1.5×10^{-2}	667	5.86517×10^{-2}	497.647
1.0×10^{-2}	$1,000$	8.49711×10^{-2}	1040.86
9.0×10^{-3}	$1,111$	4.77306×10^{-2}	296.839
8.3×10^{-3}	$1,200$	2.90822×10^{-5}	0.255796
8.0×10^{-3}	$1,250$	1.9956×10^{-5}	0.182218
5.0×10^{-3}	$2,000$	8.03654×10^{-8}	0.00117415

Table 4.1: Convergence of u variable using the first order IMEX scheme with refinement of time steps.

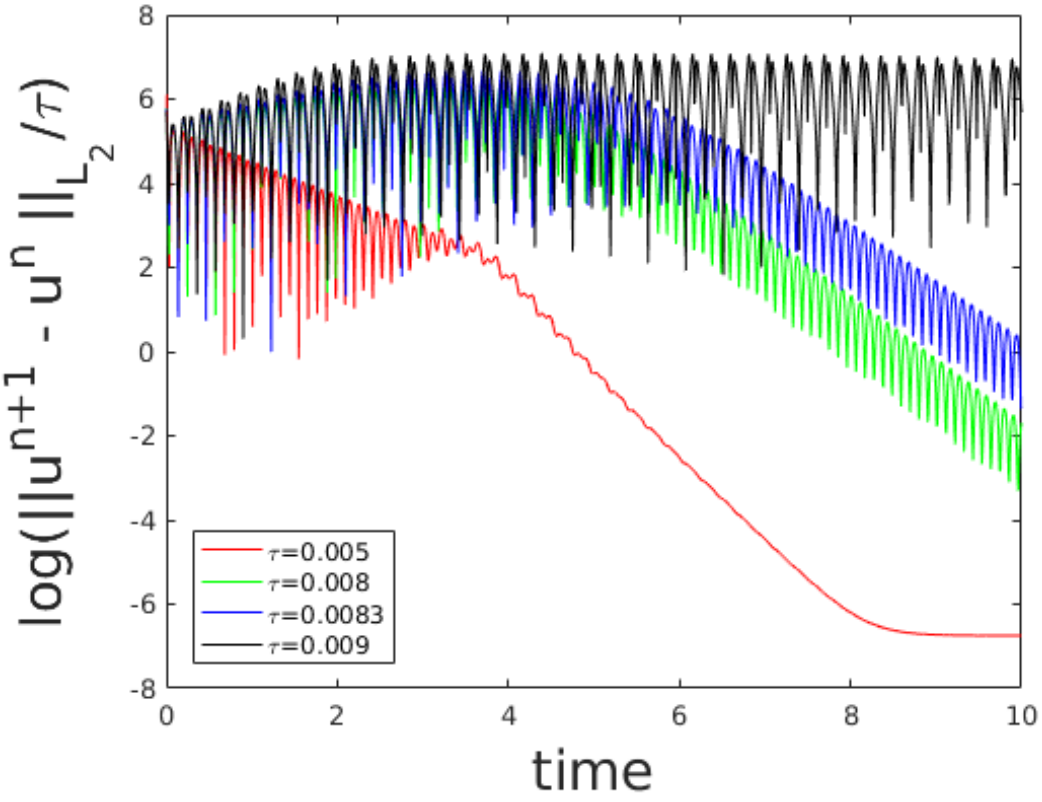

Figure 4.7: Convergence history of the simulations of the Schnakenberg model for the variable u using the first order IMEX scheme with refinement of time steps.

Time-step τ	No. of time steps	Relative error	$\|\frac{u^{n+1}-u^n}{\tau}\|$
2.0×10^{-2}	500	1.57128×10^{-1}	518.582
1.85×10^{-2}	540	9.69243×10^{-4}	3.81838
1.82×10^{-2}	550	1.30074×10^{-6}	0.00522085
1.5×10^{-2}	667	2.62499×10^{-7}	0.00127839
1.0×10^{-2}	$1,000$	2.34805×10^{-7}	0.00171531
9.0×10^{-3}	$1,111$	2.22973×10^{-7}	0.00180987
8.3×10^{-3}	$1,200$	2.13171×10^{-7}	0.00187625
8.0×10^{-3}	$1,250$	2.08573×10^{-7}	0.00190462

Table 4.2: Convergence of u variable using the 2-SBDF scheme with refinement of time steps.

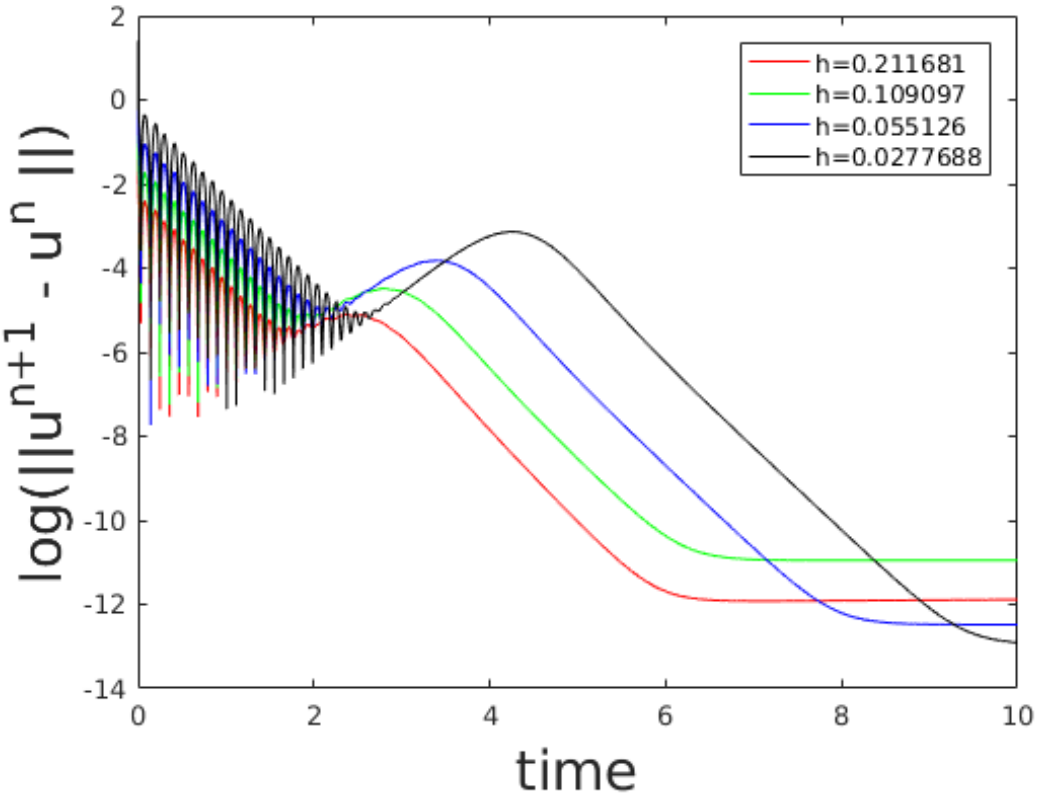

Figure 4.8: Convergence history of the simulations of the Schnakenberg model for the variable u using the first order IMEX scheme with refinement of the mesh.

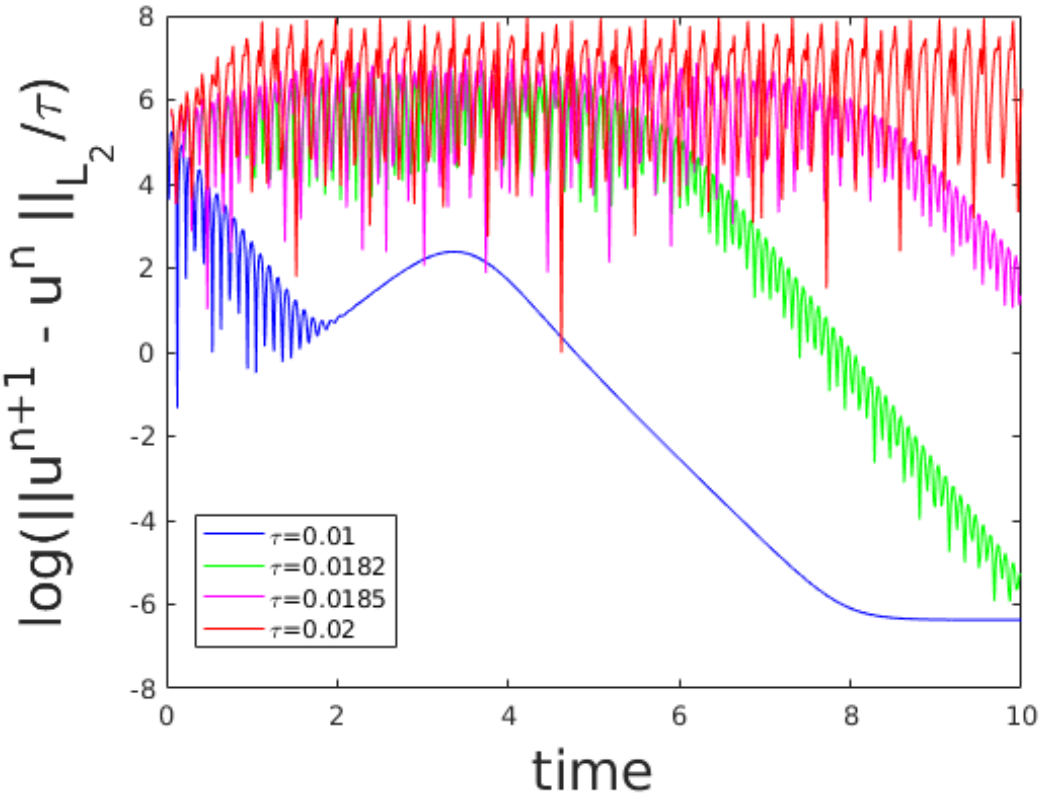

Figure 4.9: Convergence history of the simulations of the Schnakenberg model for the variable u using the 2-SBDF scheme with refinement of time steps.

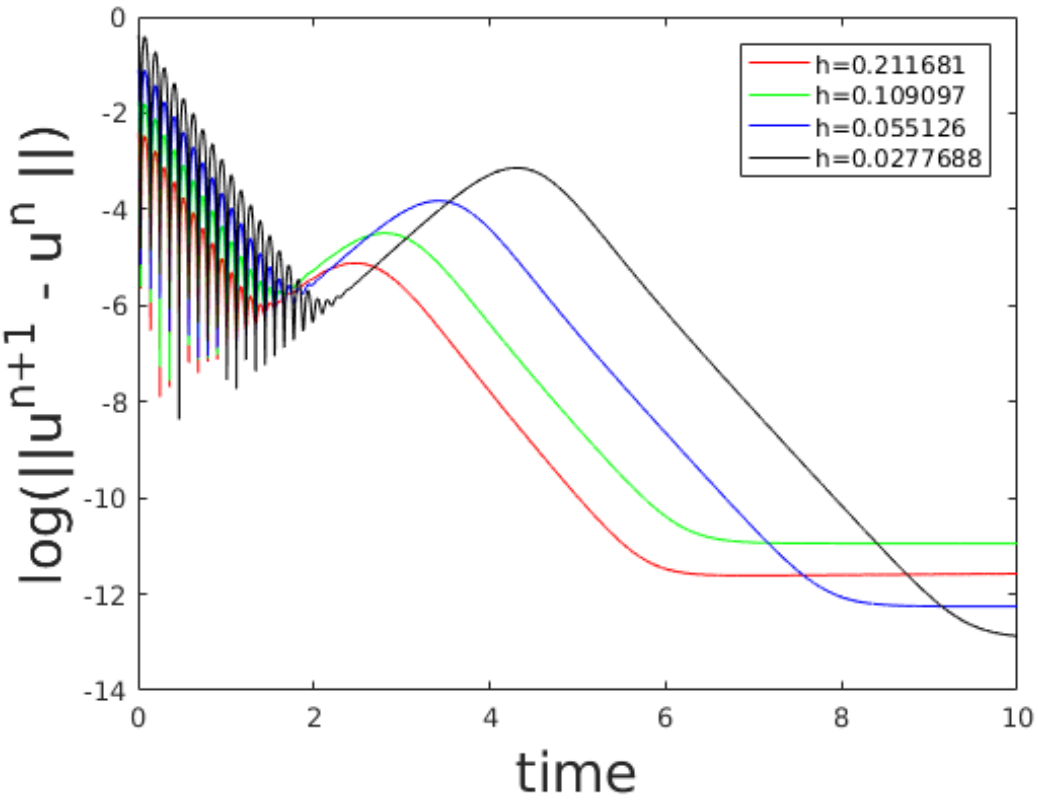

Figure 4.10: Convergence history of the simulations of the Schnakenberg model for the variable u using the 2-SBDF scheme with refinement of the mesh.

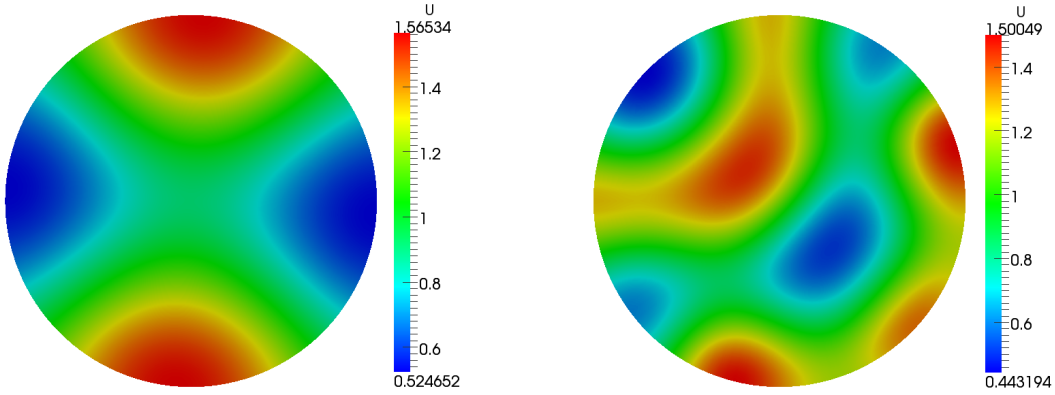

Figure 4.11: Solutions for the variable u of the Schnakenberg model using the 2-SBDF scheme with $a = 0.1$, $b = 0.9$, $d = 10$ and (a) $\gamma = 29$ and (b) $\gamma = 100$.

.

4.3 The surface finite element method

In this section we apply the same procedure used in Section 4.2 to equations posed on a surface domain. It means that material diffusion is represented by Laplace-Beltrami operator Δ_Γ instead of the usual Laplacian in (4.3). The surface finite element method presented in Dziuk and Elliott (2013b), Elliott and Ranner (2014) and Barreira et al. (2011) is employed to get approximate numerical solutions. We also study on the surface finite element method a comparison of the convergence rates of two time-stepping schemes namely first order IMEX scheme and the second order semi-implicit backward Euler differentiation formula (2-SBDF).

4.3.1 Numerical simulations on the surface

For the numerical simulations, Γ is the surface of a sphere and cuboid. Using Deal.II library we discretise the domain with 6146 degrees of freedom. The initial data is chosen (similar to the case of the bulk) to be random perturbations near the uniform steady state in equation (4.4). The simulations were allowed to run until a spatially inhomogeneous steady state was reached as shown in Figures 4.12 and 4.16. The parameter values for simulations on the surface are chosen identical to those for the bulk case, which are $a = 0.1$, $b = 0.9$, $d = 10$ and $\gamma = 29$. For illustration purposes, we have chosen both the first order IMEX and second order semi-implicit backward differentiation formula,2-SBDF, schemes. In first order IMEX scheme, the diffusive term is treated implicitly while the reaction term is treated explicitly. For each of these methods, we have chosen time-step sizes to be $\tau = 1\times10^{-3}$, $\tau = 1.33333\times10^{-3}$ and $\tau = 2\times10^{-3}$ and compare the L_2-norms of the numerical solution difference $\|\frac{u^{n+1}-u^n}{\tau}\|$. In the latter case, we choose to divide the L_2-norm by τ for comparison purposes. We also compute the relative error given by

$$\text{Relative error } = \sqrt{\frac{\sum |U^{n+1}-U^n|^2}{\sum |U^{n+1}|^2}}, \tag{4.23}$$

at the final time $t = 10$. The convergence of the variable u using the first order IMEX scheme with different values of time step is shown in Table 4.3. Also, the convergence of the variable u using the 2-SBDF scheme with different values of time steps is shown in Table 4.4. We plot the graph for the L_2-norms of the solution differences

Time-step τ	No. of time steps	Relative error	$\|\frac{u^{n+1}-u^n}{\tau}\|$
7.5×10^{-3}	$1,333$	0.000349925	3.78871
7.4×10^{-3}	$1,351$	6.33246×10^{-5}	0.695777
7.0×10^{-3}	$1,428$	2.51018×10^{-5}	0.29199
6.0×10^{-3}	$1,666$	6.94301×10^{-7}	0.00942279
5.0×10^{-3}	$2,000$	5.04293×10^{-7}	0.0082124
2.0×10^{-3}	$5,000$	1.7363×10^{-7}	0.00706762
10^{-3}	$10,000$	8.0948×10^{-8}	0.00658958

Table 4.3: Convergence of the variable u using the first order IMEX scheme with refinement of time steps.

versus time, shown in Figures 4.13 and 4.17. We plot the convergence history of the simulations of the Schnakenberg model for the variable u, using first order IMEX scheme, with different time steps as shown in 4.14 and with refinement in the mesh as shown in 4.15. Also, we plot the convergence history of the simulations of the Schnakenberg model for the variable u, using the 2-SBDF scheme, with different time steps as shown in 4.18 and with mesh refinements as shown in 4.19

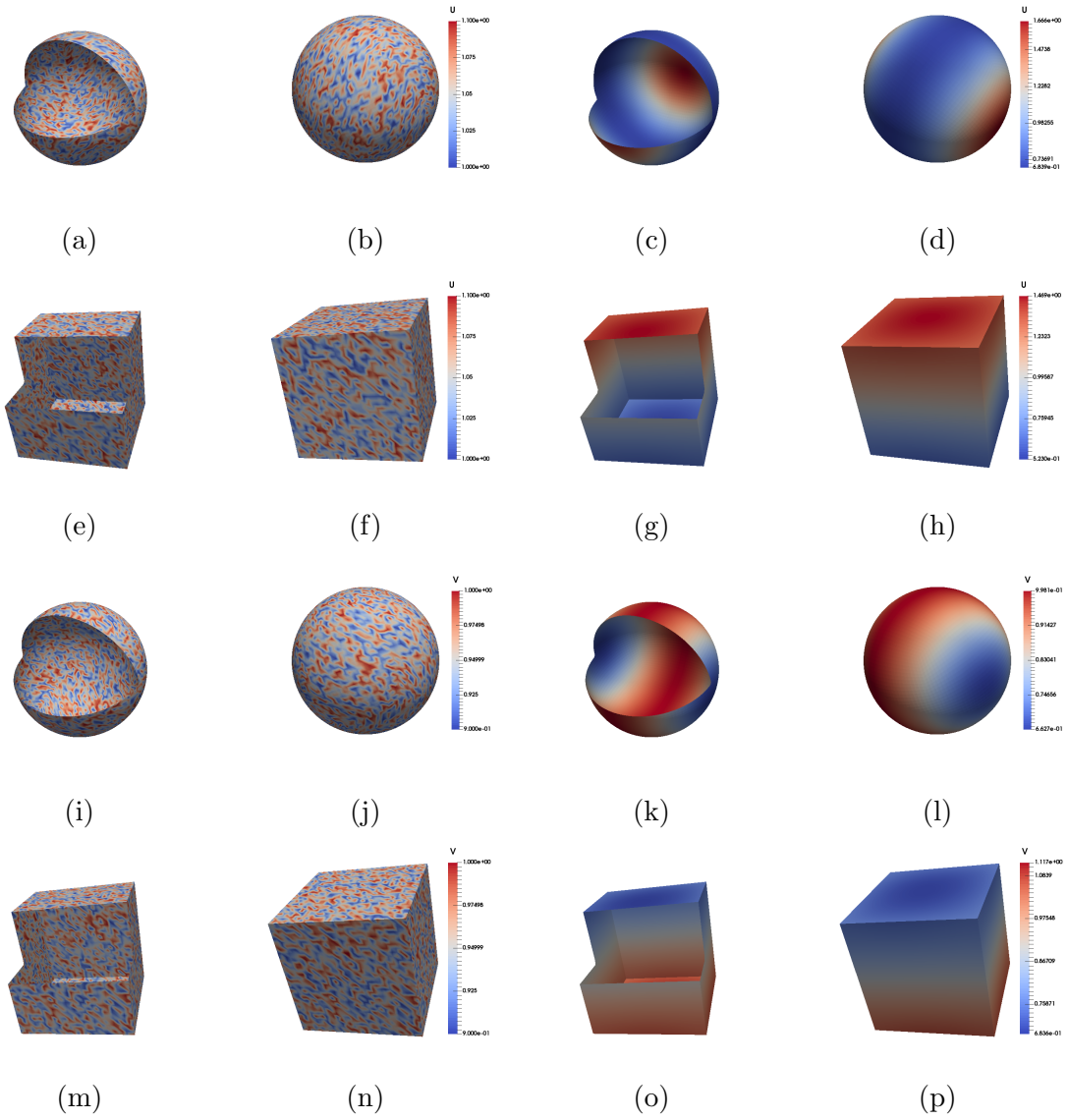

Figure 4.12: Surface finite element solutions for the variable u "first and second rows" and the variable v "third and fourth rows" of the Schnakenberg model using the first order IMEX scheme at $\tau = 10^{-3}$. First and second columns show initial condition as random perturbations about steady states. Third and fourth columns show solution at the final time $t = 10$ showing convergence to an inhomogeneous steady state.

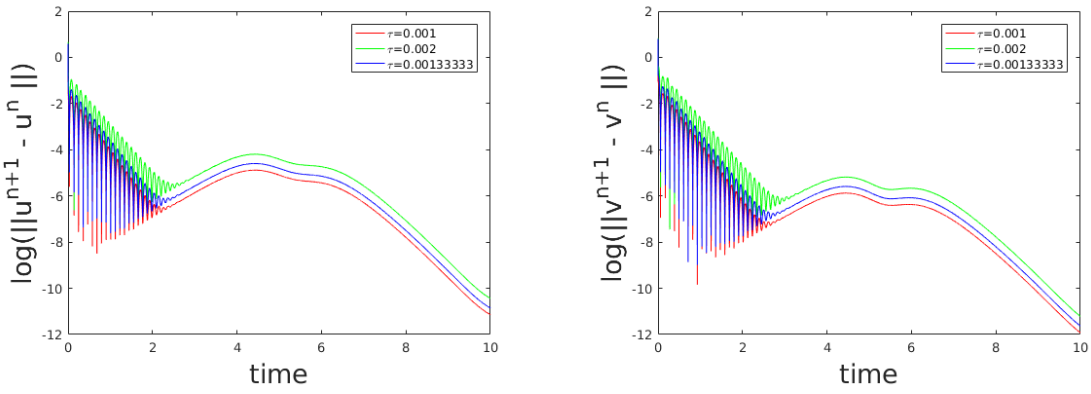

(a) (b)

Figure 4.13: Convergence history of the simulations of the Schnakenberg model using the first order IMEX scheme (a) for the variable u, (b) for the variable v.

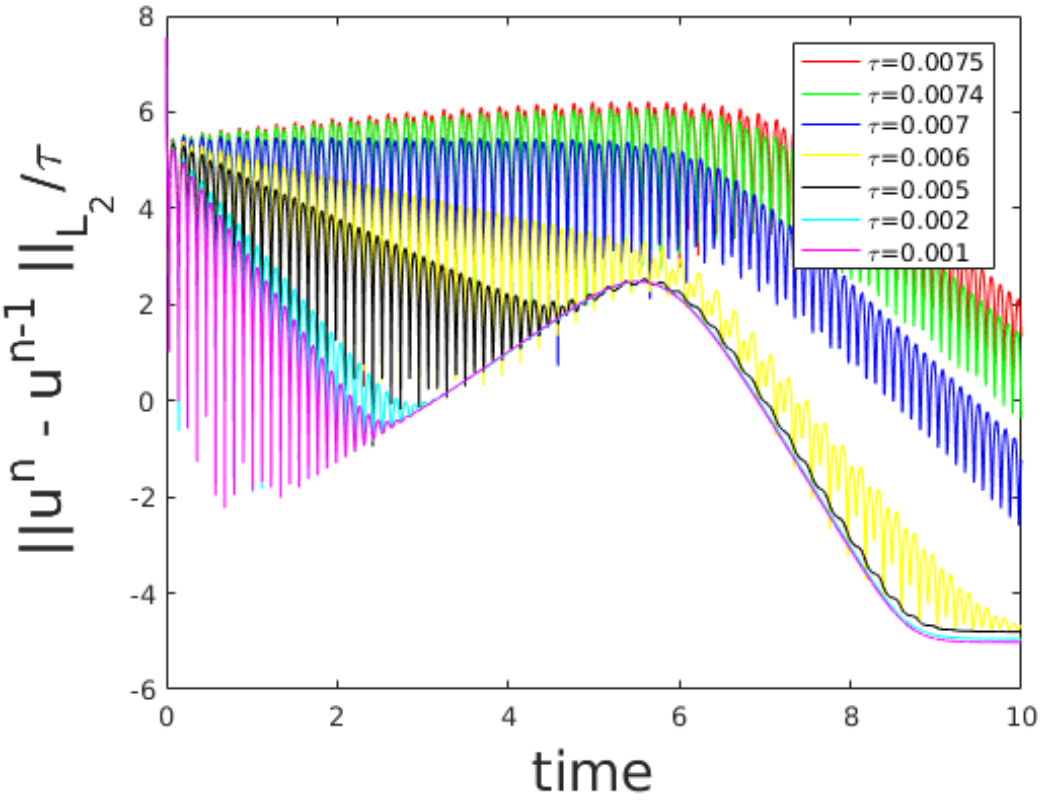

Figure 4.14: Convergence history of the simulations of the Schnakenberg model for the variable u using the 2-SBDF scheme with refinement of time steps.

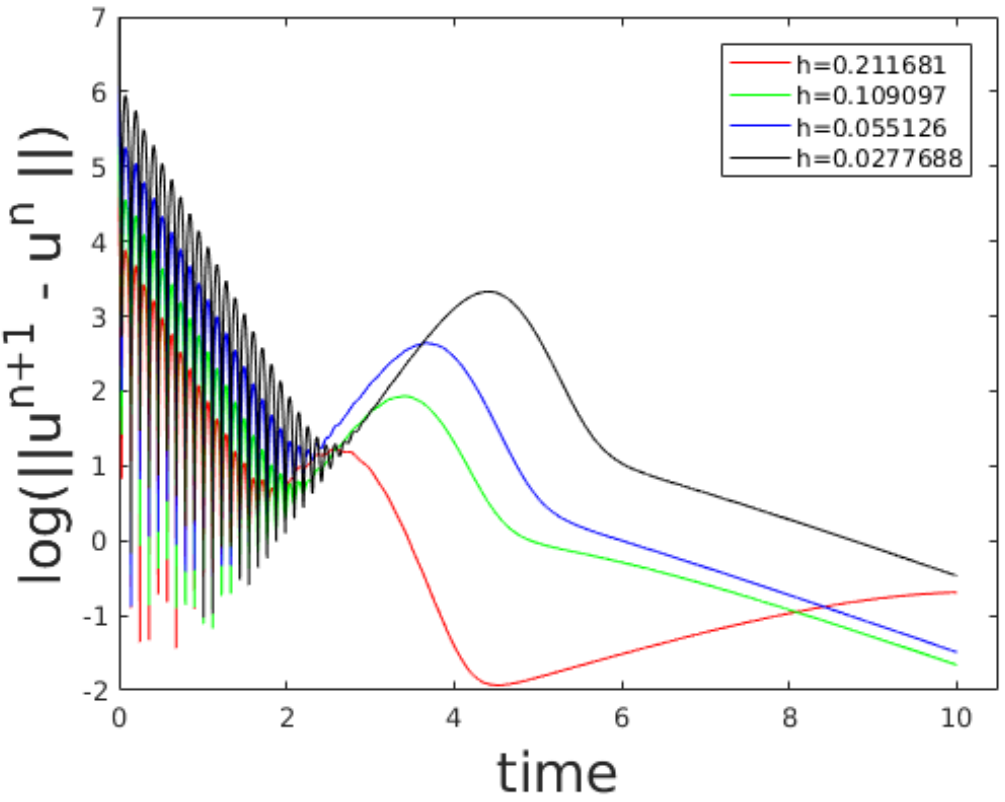

Figure 4.15: Convergence history of the simulations of the Schnakenberg model for the variable u using the first order IMEX scheme with refinement of the mesh.

Time-step τ	No. of time steps	Relative error	$\|\frac{u^{n+1}-u^n}{\tau}\|$
2.0×10^{-2}	500	0.157484	566.497
1.8×10^{-2}	556	0.0560895	232.541
1.7×10^{-2}	588	1.75893×10^{-6}	0.00842489
10^{-2}	$1,000$	9.20586×10^{-7}	0.00749488
5.0×10^{-3}	$2,000$	4.06565×10^{-7}	0.00661931
2.0×10^{-3}	$5,000$	1.51609×10^{-7}	0.0061706
10^{-3}	$10,000$	7.47409×10^{-8}	0.00608396

Table 4.4: Convergence of the variable u using the 2-SBDF scheme with refinement of time steps.

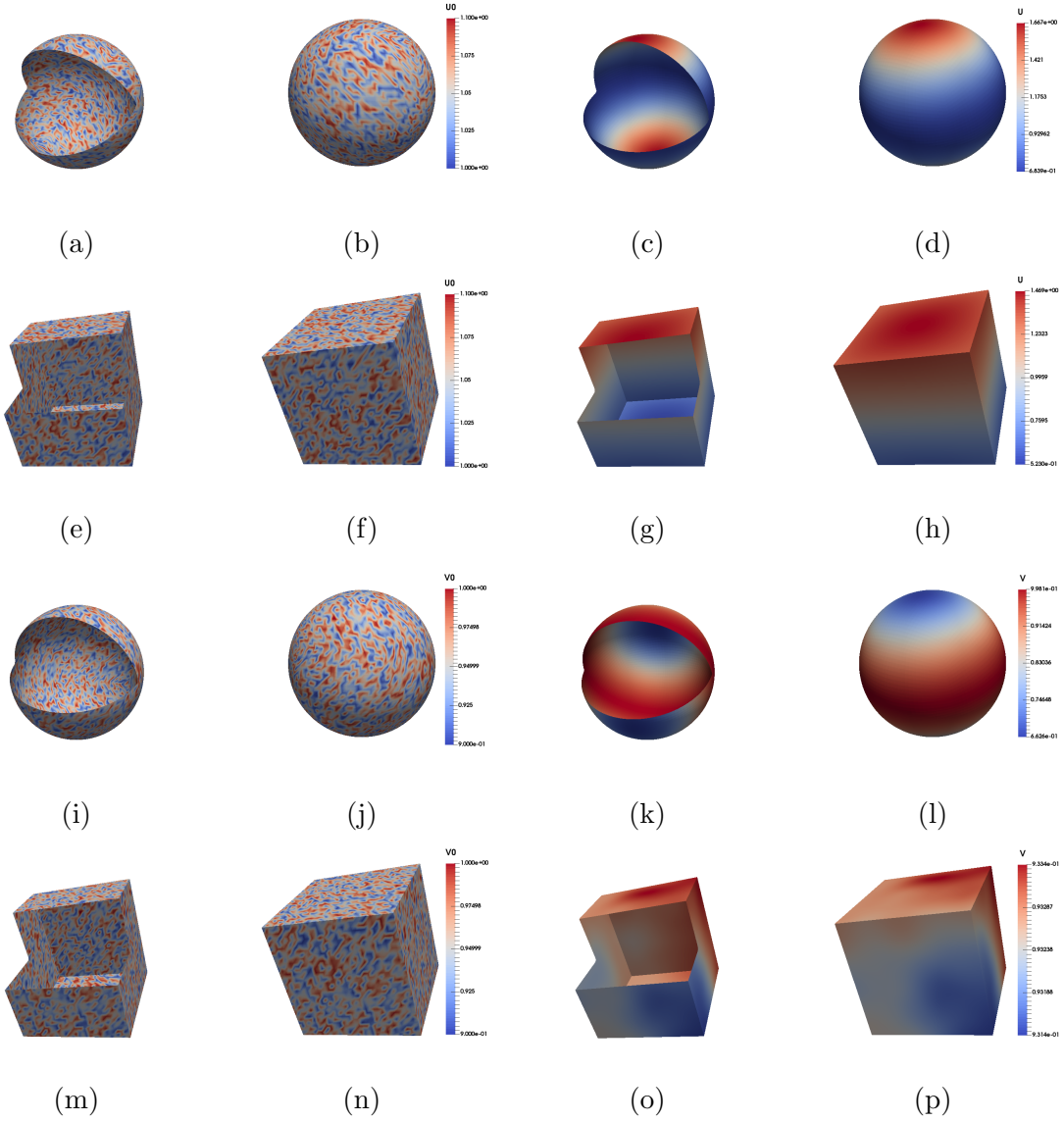

Figure 4.16: Surface finite element solutions for the variable u "first and second rows" and the variable v "third and fourth rows" of the Schnakenberg model using the 2-SBDF scheme at $\tau = 10^{-3}$. First and second columns show initial condition as random perturbations about steady states. Third and fourth columens show solution at the final time $t = 10$ showing convergence to an inhomogeneous steady state.

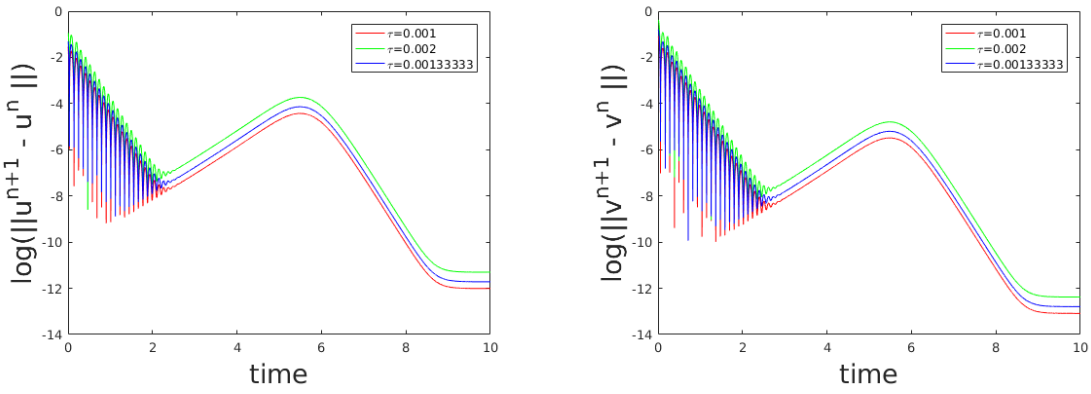

(a) (b)

Figure 4.17: Convergence history of the simulations of the Schnakenberg model using the 2-BSDF scheme (a) for the variable u, (b) for the variable v.

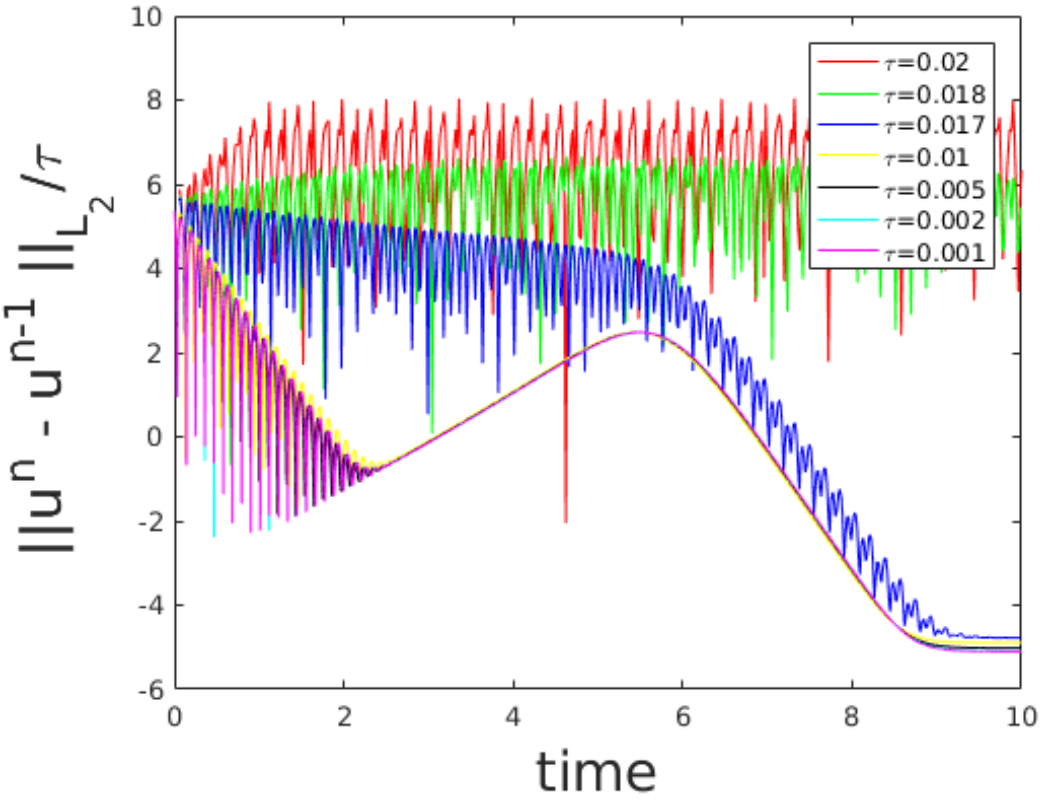

Figure 4.18: Convergence history of the simulations of the Schnakenberg model for the variable u using the 2-SBDF scheme with refinement of time steps.

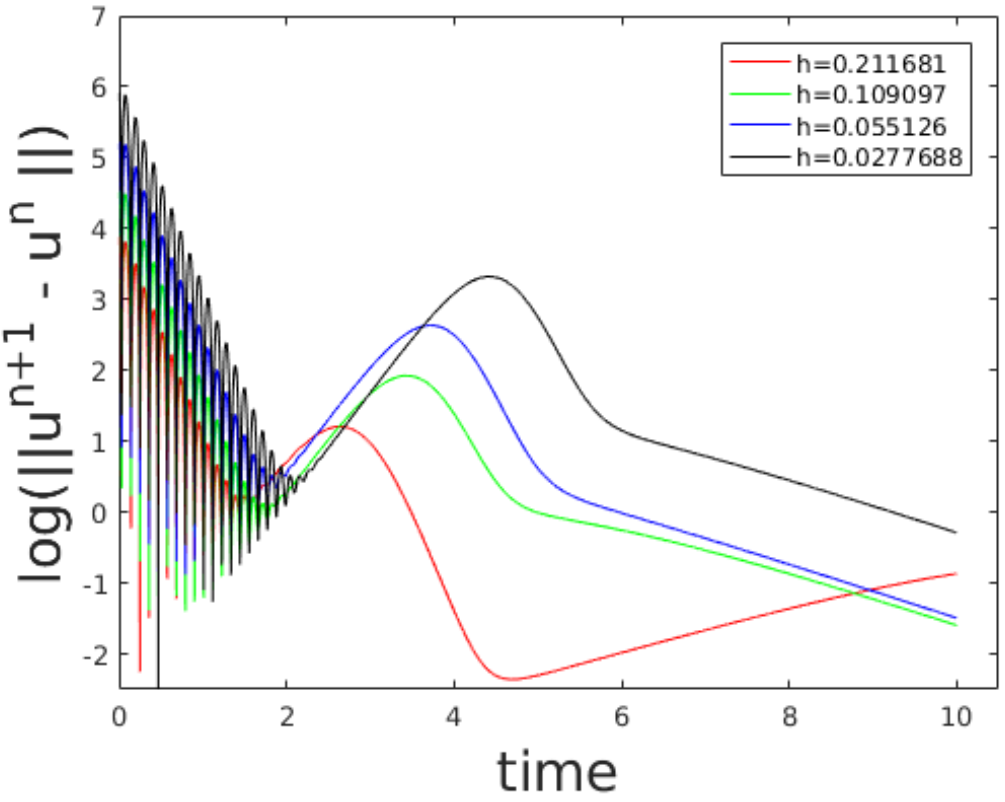

Figure 4.19: Convergence history of the simulations of the Schnakenberg model for the variable u using the 2-SBDF scheme with refinement of the mesh.

In Sections 4.2 and 4.3 we compared first order IMEX and 2-SBDF time-stepping schemes through the implementation of the finite element method. We use discrete time-derivative of the numerical solution in the discrete L_2 norm and the relative error of the same to conduct a quantitative comparison and found that 2-SBDF time-stepping scheme outperforms the first order IMEX in convergence rate to a Turing type spatially patterned steady state. Next we implement the finite element method with a fully implicit time-stepping scheme through the application of extended Newton's method.

4.4 The bulk-surface finite element method

In Chapters 2 and 3 we derived the necessary and sufficient conditions for diffusion-driven instability for the coupled system of bulk-surface reaction-diffusion equations on stationary volumes. In this chapter we present the finite element formulation for coupled bulk-surface reaction-diffusion system on stationary volumes. We employ a fully implicit time integrator for stepping forward in time, which is implemented through the application of Newton's extended method for vector valued functions.

4.5 Non-linear reaction kinetics both in the bulk and on the surface

We rewrite the non-dimensional bulk-surface reaction-diffusion systems given by (2.15) in Chapter 2,

$$\begin{cases} \begin{cases} \frac{\partial u}{\partial t} &= \Delta u + f_1(u,v,r,s), \\ \frac{\partial v}{\partial t} &= d_\Omega \Delta v + f_2(u,v,r,s), \end{cases} & \text{in } \Omega \times (0,T] \\ \begin{cases} \frac{\partial r}{\partial t} &= \Delta_\Gamma r + f_3(u,v,r,s), \\ \frac{\partial s}{\partial t} &= d_\Gamma \Delta_\Gamma s + f_4(u,v,r,s), \end{cases} & \text{on } \Gamma \times (0,T]. \end{cases} \tag{4.24}$$

where

$$f_1(u,v,r,s) = \gamma_\Omega(a_2 - u + u^2 v), \tag{4.25}$$

$$f_2(u,v,r,s) = \gamma_\Omega(b_2 - u^2 v), \tag{4.26}$$

$$f_3(u,v,r,s) = \gamma_\Gamma(a_2 - r + r^2 s - \rho_3 r + \mu u + \delta_2 v), \tag{4.27}$$

$$f_4(u,v,r,s) = \gamma_\Gamma(b_2 - r^2 s - \rho_4 s + \mu_1 u + \delta_3 v). \tag{4.28}$$

The linear boundary conditions have the form

$$\begin{cases} \nabla u \cdot \nu = \gamma_\Gamma[\rho_3 r - \mu u - \delta_2 v], \\ d_\Omega \nabla v \cdot \nu = \gamma_\Gamma[\rho_4 s - \mu_1 u - \delta_3 v]. \end{cases} \quad \text{on } \Gamma \times (0,T]. \tag{4.29}$$

The non-dimensional initial conditions for all chemical concentrations are given by

$$u(\mathbf{x},0) = u^0(\mathbf{x}), \quad v(\mathbf{x},0) = v^0(\mathbf{x}), \quad r(\mathbf{x},0) = r^0(\mathbf{x}) \quad \text{and} \quad s(\mathbf{x},0) = s^0(\mathbf{x}). \tag{4.30}$$

4.5.1 Weak formulation

In order to derive the weak formulation, we multiply (4.24) by a test function say $\varphi \in H^1(\Omega)$ for the bulk and $\psi \in H^1(\Gamma)$ for the surface and integrate over Ω for the bulk and over Γ for the surface written as

$$\begin{aligned}
\int_\Omega \frac{\partial u}{\partial t}\varphi \, \mathrm{d}\Omega - \int_\Omega \Delta u\varphi \, \mathrm{d}\Omega &= \gamma_\Omega \int_\Omega [a_2 - u + u^2 v]\varphi \, \mathrm{d}\Omega, \\
\int_\Omega \frac{\partial v}{\partial t}\varphi \, \mathrm{d}\Omega - \int_\Omega d_\Omega \Delta v\varphi \, \mathrm{d}\Omega &= \gamma_\Omega \int_\Omega [b_2 - u^2 v]\varphi \, \mathrm{d}\Omega, \qquad \text{in } \Omega \times (0,T] \\
\int_\Gamma \frac{\partial r}{\partial t}\psi \, \mathrm{d}\Gamma - \int_\Gamma \Delta_\Gamma r\psi \, \mathrm{d}\Gamma &= \gamma_\Gamma \int_\Gamma [a_2 - r + r^2 s - \rho_3 r + \mu u + \delta_2 v]\psi \, \mathrm{d}\Gamma, \\
\int_\Gamma \frac{\partial s}{\partial t}\psi \, \mathrm{d}\Gamma - \int_\Gamma d_\Gamma \Delta_\Gamma s\psi \, \mathrm{d}\Gamma &= \gamma_\Gamma \int_\Gamma [b_2 - r^2 s - \rho_4 s + \mu_1 u + \delta_3 v]\psi \, \mathrm{d}\Gamma, \quad \text{on } \Gamma \times (0,T].
\end{aligned}$$

Using the Green's formula for the second terms in the above with the boundary conditions (4.29), we obtain

$$\begin{aligned}
\int_\Omega \frac{\partial u}{\partial t}\varphi \, \mathrm{d}\Omega + \int_\Omega \nabla u \cdot \nabla \varphi \, \mathrm{d}\Omega &= \gamma_\Omega \int_\Omega [a_2 - u + u^2 v]\varphi \, \mathrm{d}\Omega \\
&\quad + \gamma_\Gamma \int_\Gamma (\rho_3 r - \mu u - \delta_2 v)\varphi \, \mathrm{d}\Gamma, \\
\int_\Omega \frac{\partial v}{\partial t}\varphi \, \mathrm{d}\Omega + d_\Omega \int_\Omega \nabla v \cdot \nabla \varphi \, \mathrm{d}\Omega &= \gamma_\Omega \int_\Omega [b_2 - u^2 v]\varphi \, \mathrm{d}\Omega \\
&\quad + \gamma_\Gamma \int_\Gamma (\rho_4 s - \mu_1 u - \delta_3 v)\varphi \, \mathrm{d}\Gamma, \quad \text{in } \Omega \times (0,T] \\
\int_\Gamma \frac{\partial r}{\partial t}\psi \, \mathrm{d}\Gamma + \int_\Gamma \nabla_\Gamma r \cdot \nabla_\Gamma \psi \, \mathrm{d}\Gamma &= \gamma_\Gamma \int_\Gamma [a_2 - r + r^2 s - \rho_3 r + \mu u + \delta_2 v]\psi \, \mathrm{d}\Gamma, \\
\int_\Gamma \frac{\partial s}{\partial t}\psi \, \mathrm{d}\Gamma + d_\Gamma \int_\Gamma \nabla_\Gamma s \cdot \nabla_\Gamma \psi \, \mathrm{d}\Gamma &= \gamma_\Gamma \int_\Gamma [b_2 - r^2 s - \rho_4 s + \mu_1 u + \delta_3 v]\psi \, \mathrm{d}\Gamma, \text{on } \Gamma \times (0,T].
\end{aligned}$$

4.5.2 Spatial discretisation of the weak formulation

We discretise the original domain Ω and its boundary Γ to obtain Ω_h and Γ_h where $\Omega_h \subset \Omega$ and $\Gamma_h \subset \Gamma$ with N_Ω and N_Γ the number of vertices associated to their respective discretisation. Let V_{Ω_h} and V_{Γ_h} denote the finite element function spaces associated to the discretised domains Ω_h and Γ_h respectively. The finite element formulation is then to seek $u_h,\ v_h \in V_{\Omega_h}$ and $r_h,\ s_h \in V_{\Gamma_h}$ such that for $t > 0$ the

equations

$$\begin{aligned}
\int_{\Omega_h} \frac{\partial u_h}{\partial t}\varphi_h \, \mathrm{d}\Omega_h + \int_{\Omega_h} \nabla u_h \cdot \nabla \varphi_h \, \mathrm{d}\Omega_h &= \gamma_\Omega \int_{\Omega_h} [a_2 - u_h + u_h^2 v_h]\varphi_h \, \mathrm{d}\Omega_h \\
&+ \gamma_\Gamma \int_{\Gamma_h} (\rho_3 r_h - \mu u_h - \delta_2 v_h)\varphi_h \, \mathrm{d}\Gamma_h, \\
\int_{\Omega_h} \frac{\partial v_h}{\partial t}\varphi_h \, \mathrm{d}\Omega_h + d_\Omega \int_{\Omega_h} \nabla v_h \cdot \nabla \varphi_h \, \mathrm{d}\Omega_h &= \gamma_\Omega \int_{\Omega_h} [b_2 - u_h^2 v_h]\varphi_h \, \mathrm{d}\Omega_h \\
&+ \gamma_\Gamma \int_{\Gamma_h} (\rho_4 s_h - \mu_1 u_h - \delta_3 v_h)\varphi_h \, \mathrm{d}\Gamma_h,
\end{aligned}$$

$$\begin{aligned}
\int_{\Gamma_h} \frac{\partial r_h}{\partial t}\psi_h \, \mathrm{d}\Gamma_h + \int_{\Gamma_h} \nabla_\Gamma r_h \cdot \nabla_\Gamma \psi_h \, \mathrm{d}\Gamma_h &= \gamma_\Gamma \int_{\Gamma_h} [a_2 - r_h + r_h^2 s_h \\
&- \rho_3 r_h + \mu u_h + \delta_2 v_h]\psi_h \, \mathrm{d}\Gamma_h, \\
\int_{\Gamma_h} \frac{\partial s_h}{\partial t}\psi_h \, \mathrm{d}\Gamma_h + d_\Gamma \int_{\Gamma_h} \nabla_\Gamma s_h \cdot \nabla_\Gamma \psi_h \, \mathrm{d}\Gamma_h &= \gamma_\Gamma \int_{\Gamma_h} [b_2 - r_h^2 s_h \\
&- \rho_4 s_h + \mu_1 u_h + \delta_3 v_h]\psi_h \, \mathrm{d}\Gamma_h,
\end{aligned}$$

are true for all test functions $\varphi_h \in V_{\Omega_h}$ and $\psi_h \in V_{\Gamma_h}$ respectively. Let $\{\varphi_i\}_{i=1}^{N_\Omega}$ and $\{\psi_i\}_{i=1}^{N_\Gamma}$ be the set of piecewise bilinear basis functions. It is known that the spaces V_{Ω_h} and V_{Γ_h} are spanned by the basis functions $\{\varphi_i\}_{i=1}^{N_\Omega}$ and $\{\psi_i\}_{i=1}^{N_\Gamma}$ respectively Brenner and Scott (2007). Thus, u_h, v_h, r_h and s_h may be expanded in terms of linear combinations of its corresponding basis functions namely $\{\varphi_i\}_{i=1}^{N_\Omega}$ and $\{\psi_i\}_{i=1}^{N_\Gamma}$. Substituting the expressions $u_h = \sum_{i=1}^{N_\Omega} U_i\varphi_i$, $v_h = \sum_{i=1}^{N_\Omega} V_i\varphi_i$, $r_h = \sum_{i=1}^{N_\Gamma} R_i\psi_i$, and $s_h = \sum_{i=1}^{N_\Gamma} S_i\psi_i$ in the finite element formulations leads to a system of differential equations written in matrix notation as

$$\begin{aligned}
M_0\mathbf{U_t} + \gamma_\Omega M_0\mathbf{U} + A_0\mathbf{U} - \gamma_\Omega B_0(\mathbf{U},\mathbf{V})\mathbf{U} \\
- \gamma_\Gamma(\rho_3 M_{10}\mathbf{R} - \mu M_{00}\mathbf{U} - \delta_2 M_{00}\mathbf{V}) = \gamma_\Omega a_2 \mathbf{C_0}, \\
M_0\mathbf{V_t} + d_\Omega A_0\mathbf{V} + \gamma_\Omega B_0(\mathbf{U},\mathbf{U})\mathbf{V} \\
- \gamma_\Gamma(\rho_4 M_{10}\mathbf{S} - \mu_1 M_{00}\mathbf{U} - \delta_3 M_{00}\mathbf{V}) = \gamma_\Omega b_2 \mathbf{C_0}, \\
M_1\mathbf{R_t} + \gamma_\Gamma M_1\mathbf{R} + A_1\mathbf{R} - \gamma_\Gamma B_1(\mathbf{R},\mathbf{S})\mathbf{R} \\
+ \gamma_\Gamma(\rho_3 M_{11}\mathbf{R} - \mu M_{01}\mathbf{U} - \delta_2 M_{01}\mathbf{V}) = \gamma_\Gamma a_2 \mathbf{C_1}, \\
M_1\mathbf{S_t} + d_\Gamma A_1\mathbf{S} + \gamma_\Gamma B_1(\mathbf{R},\mathbf{R})\mathbf{S} \\
+ \gamma_\Gamma(\rho_4 M_{11}\mathbf{S} - \mu_1 M_{01}\mathbf{U} - \delta_3 M_{01}\mathbf{V}) = \gamma_\Gamma a_2 \mathbf{C_1},
\end{aligned}$$

where the matrices with their corresponding entries are given by

$$(M_0)_{ij} = \int_{\Omega_h} \varphi_i \varphi_j \mathrm{d}\Omega_h, \quad (A_0)_{ij} = \int_{\Omega_h} \nabla\varphi_i \cdot \nabla\varphi_j \mathrm{d}\Omega_h, \quad \mathbf{C_0} = \int_{\Omega_h} \varphi_j \mathrm{d}\Omega_h,$$
$$(B_0(\mathbf{U}, \mathbf{V}))_{ij} = \int_{\Omega_h} (U_i\varphi_i)(V_i\varphi_i)\varphi_i\varphi_j \mathrm{d}\Omega_h, \quad (B_0(\mathbf{U}, \mathbf{U}))_{ij} = \int_{\Omega_h} (U_i\varphi_i)(U_i\varphi_i)\varphi_i\varphi_j \mathrm{d}\Omega_h,$$

and the entries for $M_1, A_1, B_1(\mathbf{R}, \mathbf{S})$ and $\mathbf{C_1}$, are expressed in similar way to those expressed for matrices with subscript 0. The entries of the matrices that are constructed from the combination of function spaces defined in the bulk and on the surface are defined by

$$(M_{10})_{ij} = \int_{\Gamma_h} \psi_i \varphi_j \mathrm{d}\Gamma_h, \quad (M_{01})_{ij} = \int_{\Gamma_h} \varphi_i \psi_j \mathrm{d}\Gamma_h,$$
$$(M_{00})_{ij} = \int_{\Gamma_h} \varphi_i \varphi_j \mathrm{d}\Gamma_h, \quad (M_{11})_{ij} = \int_{\Gamma_h} \psi_i \psi_j \mathrm{d}\Gamma_h,$$

where M is the mass matrix and A is the stiffness matrix, B is the matrix corresponding to the non-linear terms and $\mathbf{C}$ is the column vector.

4.5.3 Mesh generation (using deal.II Bangerth et al. (2016))

The usual approach to discretising Ω and Γ is such that, Ω is first discretised and denoted by Ω_h. The union of those elements from Ω_h whose vertices lie on $\partial\Omega$ is considered as the discretisation of Γ, which is denoted by Γ_h. Bulk is discretised by quadrilateral elements each with uniform structure throughout Ω_h. Triangulation Γ_h is also a uniform set of 2-dimensional quadrilaterals consisting of the external faces of all the bulk elements that have at least one vertex on Γ_h.

4.5.4 Time discretisation

We discretise the time interval $[0, T]$ into a finite number of uniform subintervals such that $0 = t_0 < t_1 \cdots < t_J = T$. Let τ be the time steps and J be a fixed positive integer, then $T = J\tau$. We denote the approximate solution at time $t_n = n\tau$ by $u_h^n = u_h(., t_n)$ where $n = 0, 1, \cdots, J$ and similar for the other variables. A fully implicit Euler scheme is used to solve the system in time. The fully implicit scheme is applied to the uniform time discretisation. We can obtain the fully discretised

system as

$$
\begin{aligned}
M_0\frac{\mathbf{U}^n-\mathbf{U}^{n-1}}{\tau}+\gamma_\Omega M_0\mathbf{U}^n+A_0\mathbf{U}^n-\gamma_\Omega B_0(\mathbf{U}^n,\mathbf{V}^n)\mathbf{U}^n&\\
-\gamma_\Gamma(\rho_3 M_{10}\mathbf{R}^n-\mu M_{00}\mathbf{U}^n-\delta_2 M_{00}\mathbf{V}^n)=\gamma_\Omega a_2\mathbf{C_0},&\\
M_0\frac{\mathbf{V}^n-\mathbf{V}^{n-1}}{\tau}+d_\Omega A_0\mathbf{V}^n+\gamma_\Omega B_0(\mathbf{U}^n,\mathbf{U}^n)\mathbf{V}^n&\\
-\gamma_\Gamma(\rho_4 M_{10}\mathbf{S}^n-\mu_1 M_{00}\mathbf{U}^n-\delta_3 M_{00}\mathbf{V}^n)=\gamma_\Omega b_2\mathbf{C_0},&\\
M_1\frac{\mathbf{R}^n-\mathbf{R}^{n-1}}{\tau}+\gamma_\Gamma M_1\mathbf{R}^n+A_1\mathbf{R}^n-\gamma_\Gamma B_1(\mathbf{R}^n,\mathbf{S}^n)\mathbf{R}^n&\\
+\gamma_\Gamma(\rho_3 M_{11}\mathbf{R}^n-\mu M_{01}\mathbf{U}^n-\delta_2 M_{01}\mathbf{V}^n)=\gamma_\Gamma a_2\mathbf{C_1},&
\end{aligned}
$$

$$
\begin{aligned}
M_1\frac{\mathbf{S}^n-\mathbf{S}^{n-1}}{\tau}+d_\Gamma A_1\mathbf{S}^n+\gamma_\Gamma B_1(\mathbf{R}^n,\mathbf{R}^n)\mathbf{S}^n&\\
+\gamma_\Gamma(\rho_4 M_{11}\mathbf{S}^n-\mu_1 M_{01}\mathbf{U}^n-\delta_3 M_{01}\mathbf{V}^n)=\gamma_\Gamma b_2\mathbf{C_1}.&
\end{aligned}
$$

Algebraic manipulation and rearrangement of each equation, leads to write the system in a different form which is

$$
\begin{aligned}
\mathbf{F_1}(\mathbf{U}^n,\mathbf{V}^n,\mathbf{R}^n,\mathbf{S}^n)=0,\\
\mathbf{F_2}(\mathbf{U}^n,\mathbf{V}^n,\mathbf{R}^n,\mathbf{S}^n)=0,\\
\mathbf{F_3}(\mathbf{U}^n,\mathbf{V}^n,\mathbf{R}^n,\mathbf{S}^n)=0,\\
\mathbf{F_4}(\mathbf{U}^n,\mathbf{V}^n,\mathbf{R}^n,\mathbf{S}^n)=0,
\end{aligned}
$$

where

$$
\begin{aligned}
\mathbf{F_1}(\mathbf{U}^n,\mathbf{V}^n,\mathbf{R}^n,\mathbf{S}^n)&=((\frac{1}{\tau}+\gamma_\Omega)M_0+A_0)\mathbf{U}^n-\gamma_\Omega B_0(\mathbf{U}^n,\mathbf{V}^n)\mathbf{U}^n\\
&-\gamma_\Gamma(\rho_3 M_{10}\mathbf{R}^n-\mu M_{00}\mathbf{U}^n-\delta_2 M_{00}\mathbf{V}^n)-\gamma_\Omega a_2\mathbf{C_0}-\frac{1}{\tau}M_0\mathbf{U}^{n-1},\\
\mathbf{F_2}(\mathbf{U}^n,\mathbf{V}^n,\mathbf{R}^n,\mathbf{S}^n)&=(\frac{1}{\tau}M_0+d_\Omega A_0)\mathbf{V}^n+\gamma_\Omega B_0(\mathbf{U}^n,\mathbf{U}^n)\mathbf{V}^n\\
&-\gamma_\Gamma(\rho_4 M_{10}\mathbf{S}^n-\mu_1 M_{00}\mathbf{U}^n-\delta_3 M_{00}\mathbf{V}^n)-\gamma_\Omega b_2\mathbf{C_0}-\frac{1}{\tau}M_0\mathbf{V}^{n-1},\\
\mathbf{F_3}(\mathbf{U}^n,\mathbf{V}^n,\mathbf{R}^n,\mathbf{S}^n)&=((\frac{1}{\tau}+\gamma_\Gamma)M_1+A_1)\mathbf{R}^n-\gamma_\Gamma B_1(\mathbf{R}^n,\mathbf{S}^n)\mathbf{R}^n\\
&+\gamma_\Gamma(\rho_3 M_{11}\mathbf{R}^n-\mu M_{01}\mathbf{U}^n-\delta_2 M_{01}\mathbf{V}^n)-\gamma_\Gamma a_2\mathbf{C_1}-\frac{1}{\tau}M_1\mathbf{R}^{n-1},\\
\mathbf{F_4}(\mathbf{U}^n,\mathbf{V}^n,\mathbf{R}^n,\mathbf{S}^n)&=(\frac{1}{\tau}M_1+d_\Gamma A_1)\mathbf{S}^n+\gamma_\Gamma B_1(\mathbf{R}^n,\mathbf{R}^n)\mathbf{S}^n\\
&+\gamma_\Gamma(\rho_4 M_{11}\mathbf{S}^n-\mu_1 M_{01}\mathbf{U}^n-\delta_3 M_{01}\mathbf{V}^n)-\gamma_\Gamma b_2\mathbf{C_1}-\frac{1}{\tau}M_1\mathbf{S}^{n-1}.
\end{aligned}
$$

In order to solve the system of non-linear equations, we employ the extended form of Newton's method for vector valued functions leads to

$$\mathbf{J}_{\mathbf{F}\imath}\mid_{(\mathbf{u}_k^n,\mathbf{v}_k^n,\mathbf{r}_k^n,\mathbf{s}_k^n)}(\mathbf{u}_{k+1}^n-\mathbf{u}_k^n,\mathbf{v}_{k+1}^n-\mathbf{v}_k^n,\mathbf{r}_{k+1}^n-\mathbf{r}_k^n,\mathbf{s}_{k+1}^n-\mathbf{s}_k^n)=-\mathbf{F}_\imath(\mathbf{u}_k^n,\mathbf{v}_k^n,\mathbf{r}_k^n,\mathbf{s}_k^n), \tag{4.31}$$

where the index $\imath=1,2,3,4$ and

$$\mathbf{J}_{\mathbf{F}}\mid_{(\mathbf{u}_k^n,\mathbf{v}_k^n,\mathbf{r}_k^n,\mathbf{s}_k^n)}=\begin{pmatrix}\frac{\partial\mathbf{F}_1(\mathbf{u}_k^n,\mathbf{v}_k^n,\mathbf{r}_k^n,\mathbf{s}_k^n)}{\partial\mathbf{u}_k^n} & \frac{\partial\mathbf{F}_1(\mathbf{u}_k^n,\mathbf{v}_k^n,\mathbf{r}_k^n,\mathbf{s}_k^n)}{\partial\mathbf{v}_k^n} & \frac{\partial\mathbf{F}_1(\mathbf{u}_k^n,\mathbf{v}_k^n,\mathbf{r}_k^n,\mathbf{s}_k^n)}{\partial\mathbf{r}_k^n} & \frac{\partial\mathbf{F}_1(\mathbf{u}_k^n,\mathbf{v}_k^n,\mathbf{r}_k^n,\mathbf{s}_k^n)}{\partial\mathbf{s}_k^n}\\ \frac{\partial\mathbf{F}_2(\mathbf{u}_k^n,\mathbf{v}_k^n,\mathbf{r}_k^n,\mathbf{s}_k^n)}{\partial\mathbf{u}_k^n} & \frac{\partial\mathbf{F}_2(\mathbf{u}_k^n,\mathbf{v}_k^n,\mathbf{r}_k^n,\mathbf{s}_k^n)}{\partial\mathbf{v}_k^n} & \frac{\partial\mathbf{F}_2(\mathbf{u}_k^n,\mathbf{v}_k^n,\mathbf{r}_k^n,\mathbf{s}_k^n)}{\partial\mathbf{r}_k^n} & \frac{\partial\mathbf{F}_2(\mathbf{u}_k^n,\mathbf{v}_k^n,\mathbf{r}_k^n,\mathbf{s}_k^n)}{\partial\mathbf{s}_k^n}\\ \frac{\partial\mathbf{F}_3(\mathbf{u}_k^n,\mathbf{v}_k^n,\mathbf{r}_k^n,\mathbf{s}_k^n)}{\partial\mathbf{u}_k^n} & \frac{\partial\mathbf{F}_3(\mathbf{u}_k^n,\mathbf{v}_k^n,\mathbf{r}_k^n,\mathbf{s}_k^n)}{\partial\mathbf{v}_k^n} & \frac{\partial\mathbf{F}_3(\mathbf{u}_k^n,\mathbf{v}_k^n,\mathbf{r}_k^n,\mathbf{s}_k^n)}{\partial\mathbf{r}_k^n} & \frac{\partial\mathbf{F}_3(\mathbf{u}_k^n,\mathbf{v}_k^n,\mathbf{r}_k^n,\mathbf{s}_k^n)}{\partial\mathbf{s}_k^n}\\ \frac{\partial\mathbf{F}_4(\mathbf{u}_k^n,\mathbf{v}_k^n,\mathbf{r}_k^n,\mathbf{s}_k^n)}{\partial\mathbf{u}_k^n} & \frac{\partial\mathbf{F}_4(\mathbf{u}_k^n,\mathbf{v}_k^n,\mathbf{r}_k^n,\mathbf{s}_k^n)}{\partial\mathbf{v}_k^n} & \frac{\partial\mathbf{F}_4(\mathbf{u}_k^n,\mathbf{v}_k^n,\mathbf{r}_k^n,\mathbf{s}_k^n)}{\partial\mathbf{r}_k^n} & \frac{\partial\mathbf{F}_4(\mathbf{u}_k^n,\mathbf{v}_k^n,\mathbf{r}_k^n,\mathbf{s}_k^n)}{\partial\mathbf{s}_k^n}\end{pmatrix}, \tag{4.32}$$

and the entries of $\mathbf{J}_{\mathbf{F}}$ are expressed by

$$\begin{aligned}
\frac{\partial\mathbf{F}_1(\mathbf{u}_k^n,\mathbf{v}_k^n,\mathbf{r}_k^n,\mathbf{s}_k^n)}{\partial\mathbf{u}_k^n}&=(\frac{1}{\tau}+\gamma_\Omega)M_0+A_0-2\gamma_\Omega B_0(\mathbf{u}_k^n,\mathbf{v}_k^n)+\gamma_\Gamma\mu M_{00},\\
\frac{\partial\mathbf{F}_1(\mathbf{u}_k^n,\mathbf{v}_k^n,\mathbf{r}_k^n,\mathbf{s}_k^n)}{\partial\mathbf{v}_k^n}&=-\gamma_\Omega B_0(\mathbf{u}_k^n,\mathbf{u}_k^n)+\gamma_\Gamma\delta_2 M_{00},\\
\frac{\partial\mathbf{F}_1(\mathbf{u}_k^n,\mathbf{v}_k^n,\mathbf{r}_k^n,\mathbf{s}_k^n)}{\partial\mathbf{r}_k^n}&=-\gamma_\Gamma\rho_3 M_{10},\\
\frac{\partial\mathbf{F}_1(\mathbf{u}_k^n,\mathbf{v}_k^n,\mathbf{r}_k^n,\mathbf{s}_k^n)}{\partial\mathbf{s}_k^n}&=0,\\
\frac{\partial\mathbf{F}_2(\mathbf{u}_k^n,\mathbf{v}_k^n,\mathbf{r}_k^n,\mathbf{s}_k^n)}{\partial\mathbf{u}_k^n}&=2\gamma_\Omega B_0(\mathbf{u}_k^n,\mathbf{v}_k^n)+\gamma_\Gamma\mu_1 M_{00},\\
\frac{\partial\mathbf{F}_2(\mathbf{u}_k^n,\mathbf{v}_k^n,\mathbf{r}_k^n,\mathbf{s}_k^n)}{\partial\mathbf{v}_k^n}&=\frac{1}{\tau}M_0+d_\Omega A_0+\gamma_\Omega B_0(\mathbf{u}_k^n,\mathbf{u}_k^n)+\gamma_\Gamma\delta_3 M_{00},\\
\frac{\partial\mathbf{F}_2(\mathbf{u}_k^n,\mathbf{v}_k^n,\mathbf{r}_k^n,\mathbf{s}_k^n)}{\partial\mathbf{r}_k^n}&=0,\\
\frac{\partial\mathbf{F}_2(\mathbf{u}_k^n,\mathbf{v}_k^n,\mathbf{r}_k^n,\mathbf{s}_k^n)}{\partial\mathbf{s}_k^n}&=-\gamma_\Gamma\rho_4 M_{10},\\
\frac{\partial\mathbf{F}_3(\mathbf{u}_k^n,\mathbf{v}_k^n,\mathbf{r}_k^n,\mathbf{s}_k^n)}{\partial\mathbf{u}_k^n}&=-\gamma_\Gamma\mu M_{01},\\
\frac{\partial\mathbf{F}_3(\mathbf{u}_k^n,\mathbf{v}_k^n,\mathbf{r}_k^n,\mathbf{s}_k^n)}{\partial\mathbf{v}_k^n}&=-\gamma_\Gamma\delta_2 M_{01},\\
\frac{\partial\mathbf{F}_3(\mathbf{u}_k^n,\mathbf{v}_k^n,\mathbf{r}_k^n,\mathbf{s}_k^n)}{\partial\mathbf{r}_k^n}&=(\frac{1}{\tau}+\gamma_\Gamma)M_1+A_1-2\gamma_\Gamma B_1(\mathbf{r}_k^n,\mathbf{s}_k^n)+\gamma_\Gamma\rho_3 M_{11},\\
\frac{\partial\mathbf{F}_3(\mathbf{u}_k^n,\mathbf{v}_k^n,\mathbf{r}_k^n,\mathbf{s}_k^n)}{\partial\mathbf{s}_k^n}&=-\gamma_\Gamma B_1(\mathbf{r}_k^n,\mathbf{r}_k^n),\\
\frac{\partial\mathbf{F}_4(\mathbf{u}_k^n,\mathbf{v}_k^n,\mathbf{r}_k^n,\mathbf{s}_k^n)}{\partial\mathbf{u}_k^n}&=-\gamma_\Gamma\mu_1 M_{01},\\
\frac{\partial\mathbf{F}_4(\mathbf{u}_k^n,\mathbf{v}_k^n,\mathbf{r}_k^n,\mathbf{s}_k^n)}{\partial\mathbf{v}_k^n}&=-\gamma_\Gamma\delta_3 M_{01},
\end{aligned}$$

$$\frac{\partial \mathbf{F}_4(\mathbf{u}_k^n, \mathbf{v}_k^n, \mathbf{r}_k^n, \mathbf{s}_k^n)}{\partial \mathbf{r}_k^n} = 2\gamma_\Gamma B_1(\mathbf{r}_k^n, \mathbf{s}_k^n),$$
$$\frac{\partial \mathbf{F}_4(\mathbf{u}_k^n, \mathbf{v}_k^n, \mathbf{r}_k^n, \mathbf{s}_k^n)}{\partial \mathbf{s}_k^n} = \frac{1}{\tau}M_1 + d_\Gamma A_1 + \gamma_\Gamma B_1(\mathbf{r}_k^n, \mathbf{r}_k^n) + \gamma_\Gamma \rho_4 M_{11}.$$

Substituting (4.32) in (4.31) and simplifying, we obtain

$$\begin{aligned}[(\frac{1}{\tau}+\gamma_\Omega)M_0 + A_0 - 2\gamma_\Omega B_0(\mathbf{u}_k^n, \mathbf{v}_k^n)](\mathbf{u}_{k+1}^n) + [-\gamma_\Omega B_0(\mathbf{u}_k^n, \mathbf{u}_k^n)](\mathbf{v}_{k+1}^n)\\ - \gamma_\Gamma[(\rho_3 M_{10})\mathbf{r}_{k+1}^n - (\mu M_{00})\mathbf{u}_{k+1}^n - (\delta_2 M_{00})\mathbf{v}_{k+1}^n]\\ = -2\gamma_\Omega B_0(\mathbf{u}_k^n, \mathbf{v}_k^n)\mathbf{u}_k^n + \gamma_\Omega a_2 \mathbf{C_0} + \frac{1}{\tau}M_0\mathbf{u}^{n-1},\end{aligned}$$

$$\begin{aligned}[2\gamma_\Omega B_0(\mathbf{u}_k^n, \mathbf{v}_k^n)](\mathbf{u}_{k+1}^n) + [\frac{1}{\tau}M_0 + d_\Omega A_0 + \gamma_\Omega B_0(\mathbf{u}_k^n, \mathbf{u}_k^n)](\mathbf{v}_{k+1}^n)\\ - \gamma_\Gamma[(\rho_4 M_{10})\mathbf{s}_{k+1}^n - (\mu_1 M_{00})\mathbf{u}_{k+1}^n - (\delta_3 M_{00})\mathbf{u}_{k+1}^n]\\ = 2\gamma_\Omega B_0(\mathbf{u}_k^n, \mathbf{u}_k^n)\mathbf{v}_k^n + \gamma_\Omega b_2 \mathbf{C_0} + \frac{1}{\tau}M_0\mathbf{v}^{n-1},\end{aligned}$$

$$\begin{aligned}[(\frac{1}{\tau}+\gamma_\Gamma)M_1 + A_1 - 2\gamma_\Gamma B_1(\mathbf{r}_k^n, \mathbf{s}_k^n)](\mathbf{r}_{k+1}^n) + [-\gamma_\Gamma B_1(\mathbf{r}_k^n, \mathbf{r}_k^n)](\mathbf{s}_{k+1}^n)\\ + \gamma_\Gamma[(\rho_3 M_{11})\mathbf{r}_{k+1}^n - (\mu M_{01})\mathbf{u}_{k+1}^n - (\delta_2 M_{01})\mathbf{v}_{k+1}^n]\\ = -2\gamma_\Gamma B_1(\mathbf{r}_k^n, \mathbf{s}_k^n)\mathbf{r}_k^n + \gamma_\Gamma a_2 \mathbf{C_1} + \frac{1}{\tau}M_1\mathbf{r}^{n-1},\end{aligned}$$

$$\begin{aligned}[2\gamma_\Gamma B_1(\mathbf{r}_k^n, \mathbf{s}_k^n)](\mathbf{r}_{k+1}^n) + [\frac{1}{\tau}M_1 + d_\Gamma A_1 + \gamma_\Gamma B_1(\mathbf{r}_k^n, \mathbf{r}_k^n)](\mathbf{s}_{k+1}^n)\\ + \gamma_\Gamma[(\rho_4 M_{11})\mathbf{s}_{k+1}^n - (\mu_1 M_{01})\mathbf{u}_{k+1}^n - (\delta_3 M_{01})\mathbf{v}_{k+1}^n]\\ = 2\gamma_\Gamma B_1(\mathbf{r}_k^n, \mathbf{r}_k^n)\mathbf{s}_k^n + \gamma_\Gamma b_2 \mathbf{C_1} + \frac{1}{\tau}M_1\mathbf{s}^{n-1},\end{aligned}$$

which can be written in matrix form as

$$\begin{pmatrix} \frac{\partial \mathbf{F}_1(\mathbf{u}_k^n,\mathbf{v}_k^n,\mathbf{r}_k^n,\mathbf{s}_k^n)}{\partial \mathbf{u}_k^n} & \frac{\partial \mathbf{F}_1(\mathbf{u}_k^n,\mathbf{v}_k^n,\mathbf{r}_k^n,\mathbf{s}_k^n)}{\partial \mathbf{v}_k^n} & \frac{\partial \mathbf{F}_1(\mathbf{u}_k^n,\mathbf{v}_k^n,\mathbf{r}_k^n,\mathbf{s}_k^n)}{\partial \mathbf{r}_k^n} & \frac{\partial \mathbf{F}_1(\mathbf{u}_k^n,\mathbf{v}_k^n,\mathbf{r}_k^n,\mathbf{s}_k^n)}{\partial \mathbf{s}_k^n} \\ \frac{\partial \mathbf{F}_2(\mathbf{u}_k^n,\mathbf{v}_k^n,\mathbf{r}_k^n,\mathbf{s}_k^n)}{\partial \mathbf{u}_k^n} & \frac{\partial \mathbf{F}_2(\mathbf{u}_k^n,\mathbf{v}_k^n,\mathbf{r}_k^n,\mathbf{s}_k^n)}{\partial \mathbf{v}_k^n} & \frac{\partial \mathbf{F}_2(\mathbf{u}_k^n,\mathbf{v}_k^n,\mathbf{r}_k^n,\mathbf{s}_k^n)}{\partial \mathbf{r}_k^n} & \frac{\partial \mathbf{F}_2(\mathbf{u}_k^n,\mathbf{v}_k^n,\mathbf{r}_k^n,\mathbf{s}_k^n)}{\partial \mathbf{s}_k^n} \\ \frac{\partial \mathbf{F}_3(\mathbf{u}_k^n,\mathbf{v}_k^n,\mathbf{r}_k^n,\mathbf{s}_k^n)}{\partial \mathbf{u}_k^n} & \frac{\partial \mathbf{F}_3(\mathbf{u}_k^n,\mathbf{v}_k^n,\mathbf{r}_k^n,\mathbf{s}_k^n)}{\partial \mathbf{v}_k^n} & \frac{\partial \mathbf{F}_3(\mathbf{u}_k^n,\mathbf{v}_k^n,\mathbf{r}_k^n,\mathbf{s}_k^n)}{\partial \mathbf{r}_k^n} & \frac{\partial \mathbf{F}_3(\mathbf{u}_k^n,\mathbf{v}_k^n,\mathbf{r}_k^n,\mathbf{s}_k^n)}{\partial \mathbf{s}_k^n} \\ \frac{\partial \mathbf{F}_4(\mathbf{u}_k^n,\mathbf{v}_k^n,\mathbf{r}_k^n,\mathbf{s}_k^n)}{\partial \mathbf{u}_k^n} & \frac{\partial \mathbf{F}_4(\mathbf{u}_k^n,\mathbf{v}_k^n,\mathbf{r}_k^n,\mathbf{s}_k^n)}{\partial \mathbf{v}_k^n} & \frac{\partial \mathbf{F}_4(\mathbf{u}_k^n,\mathbf{v}_k^n,\mathbf{r}_k^n,\mathbf{s}_k^n)}{\partial \mathbf{r}_k^n} & \frac{\partial \mathbf{F}_4(\mathbf{u}_k^n,\mathbf{v}_k^n,\mathbf{r}_k^n,\mathbf{s}_k^n)}{\partial \mathbf{s}_k^n} \end{pmatrix} \begin{pmatrix} \mathbf{u}_{k+1}^n \\ \mathbf{v}_{k+1}^n \\ \mathbf{r}_{k+1}^n \\ \mathbf{s}_{k+1}^n \end{pmatrix}$$

$$= \begin{pmatrix} -2\gamma_\Omega B_0(\mathbf{u}_k^n, \mathbf{v}_k^n)\mathbf{u}_k^n + \gamma_\Omega a_2 \mathbf{C_0} + \frac{1}{\tau}M_0\mathbf{u}^{n-1} \\ 2\gamma_\Omega B_0(\mathbf{u}_k^n, \mathbf{u}_k^n)\mathbf{v}_k^n + \gamma_\Omega b_2 \mathbf{C_0} + \frac{1}{\tau}M_0\mathbf{v}^{n-1} \\ -2\gamma_\Gamma B_1(\mathbf{r}_k^n, \mathbf{s}_k^n)\mathbf{r}_k^n + \gamma_\Gamma a_2 \mathbf{C_1} + \frac{1}{\tau}M_1\mathbf{r}^{n-1} \\ 2\gamma_\Gamma B_1(\mathbf{r}_k^n, \mathbf{r}_k^n)\mathbf{s}_k^n + \gamma_\Gamma b_2 \mathbf{C_1} + \frac{1}{\tau}M_1\mathbf{s}^{n-1} \end{pmatrix}.$$

4.6 Linear reaction kinetics on the surface and non-linear reaction kinetics in the bulk

In this system we consider linear reaction kinetics on the surface and non-linear reaction kinetics in the bulk. We rewrite the non-dimensional bulk-surface reaction-diffusion systems given by (2.128) in Chapter 2,

$$\begin{cases} \begin{cases} \frac{\partial u}{\partial t} &= \Delta u + f_1(u,v,r,s), \\ \frac{\partial v}{\partial t} &= d_\Omega \Delta v + f_2(u,v,r,s), \end{cases} & \text{in } \Omega \times (0,T] \\ \begin{cases} \frac{\partial r}{\partial t} &= \Delta_\Gamma r + f_3(u,v,r,s), \\ \frac{\partial s}{\partial t} &= d_\Gamma \Delta_\Gamma s + f_4(u,v,r,s), \end{cases} & \text{on } \Gamma \times (0,T]. \end{cases} \tag{4.33}$$

where

$$f_1(u,v,r,s) = \gamma_\Omega(a_2 - u + u^2 v), \tag{4.34}$$

$$f_2(u,v,r,s) = \gamma_\Omega(b_2 - u^2 v), \tag{4.35}$$

$$f_3(u,v,r,s) = \gamma_\Gamma(-r + q_2 s - \rho_3 r + u + \delta_2 v), \tag{4.36}$$

$$f_4(u,v,r,s) = \gamma_\Gamma(c_2 r - j_2 s - \rho_4 s + u + \delta_3 v). \tag{4.37}$$

The linear boundary conditions have the form

$$\begin{cases} \nabla u \cdot \nu = \gamma_\Gamma[\rho_3 r - u - \delta_2 v], \\ d_\Omega \nabla v \cdot \nu = \gamma_\Gamma[\rho_4 s - u - \delta_3 v]. \end{cases} \quad \text{on } \Gamma \times (0,T]. \tag{4.38}$$

The non-dimensional initial conditions for all chemical concentrations are given by

$$u(\mathbf{x},0) = u^0(\mathbf{x}), \quad v(\mathbf{x},0) = v^0(\mathbf{x}), \quad r(\mathbf{x},0) = r^0(\mathbf{x}) \quad \text{and} \quad s(\mathbf{x},0) = s^0(\mathbf{x}). \tag{4.39}$$

An analogous approach to that employed in Section 4.5 gives rise to a system of non-linear algebraic equations which are solved by Newton's method. The set of non-linear equations can be written in the form

$$\mathbf{F_1}(\mathbf{U}^n, \mathbf{V}^n, \mathbf{R}^n, \mathbf{S}^n) = 0,$$

$$\mathbf{F_2}(\mathbf{U}^n, \mathbf{V}^n, \mathbf{R}^n, \mathbf{S}^n) = 0,$$

$$\mathbf{F_3}(\mathbf{U}^n, \mathbf{V}^n, \mathbf{R}^n, \mathbf{S}^n) = 0,$$

$$\mathbf{F_4}(\mathbf{U}^n, \mathbf{V}^n, \mathbf{R}^n, \mathbf{S}^n) = 0,$$

where

$$
\begin{aligned}
\mathbf{F_1}(\mathbf{U}^n,\mathbf{V}^n,\mathbf{R}^n,\mathbf{S}^n) &= M_0\mathbf{U}^n + \tau\gamma_\Omega M_0\mathbf{U}^n + \tau A_0\mathbf{U}^n - \tau\gamma_\Omega B_0(\mathbf{U}^n,\mathbf{V}^n)\mathbf{U}^n \\
&\quad - \tau\gamma_\Gamma(\rho_3 M_{10}\mathbf{R}^n - M_{00}\mathbf{U}^n - \delta_2 M_{00}\mathbf{V}^n) - \tau\gamma_\Omega a_2\mathbf{C_0} - M_0\mathbf{U}^{n-1}, \\
\mathbf{F_2}(\mathbf{U}^n,\mathbf{V}^n,\mathbf{R}^n,\mathbf{S}^n) &= M_0\mathbf{V}^n + \tau d_\Omega A_0\mathbf{V}^n + \tau\gamma_\Omega B_0(\mathbf{U}^n,\mathbf{U}^n)\mathbf{V}^n \\
&\quad - \tau\gamma_\Gamma(\rho_4 M_{10}\mathbf{S}^n - M_{00}\mathbf{U}^n - \delta_3 M_{00}\mathbf{V}^n) - \tau\gamma_\Omega b_2\mathbf{C_0} - M_0\mathbf{V}^{n-1}, \\
\mathbf{F_3}(\mathbf{U}^n,\mathbf{V}^n,\mathbf{R}^n,\mathbf{S}^n) &= M_1\mathbf{R}^n + \tau\gamma_\Gamma M_1\mathbf{R}^n + \tau A_1\mathbf{R}^n - \tau q_2\gamma_\Gamma M_1\mathbf{S}^n \\
&\quad + \tau\gamma_\Gamma(\rho_3 M_1\mathbf{R}^n - M_{01}\mathbf{U}^n - \delta_2 M_{01}\mathbf{V}^n) - M_1\mathbf{R}^{n-1}, \\
\mathbf{F_4}(\mathbf{U}^n,\mathbf{V}^n,\mathbf{R}^n,\mathbf{S}^n) &= M_1\mathbf{S}^n + \tau j_2\gamma_\Gamma M_1\mathbf{S}^n + \tau d_\Gamma A_1\mathbf{S}^n - \tau c_2\gamma_\Gamma M_1\mathbf{R}^n \\
&\quad + \tau\gamma_\Gamma(\rho_4 M_1\mathbf{S}^n - M_{01}\mathbf{U}^n - \delta_3 M_{01}\mathbf{V}^n) - M_1\mathbf{S}^{n-1},
\end{aligned}
$$

In order to solve the system of non-linear equation, the employing the extended form of Newton's method for vector valued functions lead to write

$$
\mathbf{J}_{\mathbf{F}\imath}\mid_{(\mathbf{u}_k^n,\mathbf{v}_k^n,\mathbf{r}_k^n,\mathbf{s}_k^n)}(\mathbf{u}_{k+1}^n-\mathbf{u}_k^n,\mathbf{v}_{k+1}^n-\mathbf{v}_k^n,\mathbf{r}_{k+1}^n-\mathbf{r}_k^n,\mathbf{s}_{k+1}^n-\mathbf{s}_k^n) = -\mathbf{F}_\imath(\mathbf{u}_k^n,\mathbf{v}_k^n,\mathbf{r}_k^n,\mathbf{s}_k^n), \quad (4.40)
$$

where the index $\imath = 1,2,3,4$ and

$$
\mathbf{J}_{\mathbf{F}}\mid_{(\mathbf{u}_k^n,\mathbf{v}_k^n,\mathbf{r}_k^n,\mathbf{s}_k^n)} = \begin{pmatrix}
\frac{\partial\mathbf{F}_1(\mathbf{u}_k^n,\mathbf{v}_k^n,\mathbf{r}_k^n,\mathbf{s}_k^n)}{\partial\mathbf{u}_k^n} & \frac{\partial\mathbf{F}_1(\mathbf{u}_k^n,\mathbf{v}_k^n,\mathbf{r}_k^n,\mathbf{s}_k^n)}{\partial\mathbf{v}_k^n} & \frac{\partial\mathbf{F}_1(\mathbf{u}_k^n,\mathbf{v}_k^n,\mathbf{r}_k^n,\mathbf{s}_k^n)}{\partial\mathbf{r}_k^n} & \frac{\partial\mathbf{F}_1(\mathbf{u}_k^n,\mathbf{v}_k^n,\mathbf{r}_k^n,\mathbf{s}_k^n)}{\partial\mathbf{s}_k^n} \\
\frac{\partial\mathbf{F}_2(\mathbf{u}_k^n,\mathbf{v}_k^n,\mathbf{r}_k^n,\mathbf{s}_k^n)}{\partial\mathbf{u}_k^n} & \frac{\partial\mathbf{F}_2(\mathbf{u}_k^n,\mathbf{v}_k^n,\mathbf{r}_k^n,\mathbf{s}_k^n)}{\partial\mathbf{v}_k^n} & \frac{\partial\mathbf{F}_2(\mathbf{u}_k^n,\mathbf{v}_k^n,\mathbf{r}_k^n,\mathbf{s}_k^n)}{\partial\mathbf{r}_k^n} & \frac{\partial\mathbf{F}_2(\mathbf{u}_k^n,\mathbf{v}_k^n,\mathbf{r}_k^n,\mathbf{s}_k^n)}{\partial\mathbf{s}_k^n} \\
\frac{\partial\mathbf{F}_3(\mathbf{u}_k^n,\mathbf{v}_k^n,\mathbf{r}_k^n,\mathbf{s}_k^n)}{\partial\mathbf{u}_k^n} & \frac{\partial\mathbf{F}_3(\mathbf{u}_k^n,\mathbf{v}_k^n,\mathbf{r}_k^n,\mathbf{s}_k^n)}{\partial\mathbf{v}_k^n} & \frac{\partial\mathbf{F}_3(\mathbf{u}_k^n,\mathbf{v}_k^n,\mathbf{r}_k^n,\mathbf{s}_k^n)}{\partial\mathbf{r}_k^n} & \frac{\partial\mathbf{F}_3(\mathbf{u}_k^n,\mathbf{v}_k^n,\mathbf{r}_k^n,\mathbf{s}_k^n)}{\partial\mathbf{s}_k^n} \\
\frac{\partial\mathbf{F}_4(\mathbf{u}_k^n,\mathbf{v}_k^n,\mathbf{r}_k^n,\mathbf{s}_k^n)}{\partial\mathbf{u}_k^n} & \frac{\partial\mathbf{F}_4(\mathbf{u}_k^n,\mathbf{v}_k^n,\mathbf{r}_k^n,\mathbf{s}_k^n)}{\partial\mathbf{v}_k^n} & \frac{\partial\mathbf{F}_4(\mathbf{u}_k^n,\mathbf{v}_k^n,\mathbf{r}_k^n,\mathbf{s}_k^n)}{\partial\mathbf{r}_k^n} & \frac{\partial\mathbf{F}_4(\mathbf{u}_k^n,\mathbf{v}_k^n,\mathbf{r}_k^n,\mathbf{s}_k^n)}{\partial\mathbf{s}_k^n}
\end{pmatrix}, \quad (4.41)
$$

and the entries of $\mathbf{J}_{\mathbf{F}}$ are expressed by

$$
\begin{aligned}
\frac{\partial\mathbf{F}_1(\mathbf{u}_k^n,\mathbf{v}_k^n,\mathbf{r}_k^n,\mathbf{s}_k^n)}{\partial\mathbf{u}_k^n} &= (1+\tau\gamma_\Omega)M_0 + \tau A_0 - 2\tau\gamma_\Omega B_0(\mathbf{u}_k^n,\mathbf{v}_k^n) + \tau\gamma_\Gamma M_{00}, \\
\frac{\partial\mathbf{F}_1(\mathbf{u}_k^n,\mathbf{v}_k^n,\mathbf{r}_k^n,\mathbf{s}_k^n)}{\partial\mathbf{v}_k^n} &= -\tau\gamma_\Omega B_0(\mathbf{u}_k^n,\mathbf{u}_k^n) + \tau\gamma_\Gamma\delta_2 M_{00}, \\
\frac{\partial\mathbf{F}_1(\mathbf{u}_k^n,\mathbf{v}_k^n,\mathbf{r}_k^n,\mathbf{s}_k^n)}{\partial\mathbf{r}_k^n} &= -\tau\gamma_\Gamma\rho_3 M_{10}, \\
\frac{\partial\mathbf{F}_1(\mathbf{u}_k^n,\mathbf{v}_k^n,\mathbf{r}_k^n,\mathbf{s}_k^n)}{\partial\mathbf{s}_k^n} &= 0,
\end{aligned}
$$

$$\frac{\partial \mathbf{F}_2(\mathbf{u}_k^n, \mathbf{v}_k^n, \mathbf{r}_k^n, \mathbf{s}_k^n)}{\partial \mathbf{u}_k^n} = 2\tau\gamma_\Omega B_0(\mathbf{u}_k^n, \mathbf{v}_k^n) + \tau\gamma_\Gamma M_{00},$$
$$\frac{\partial \mathbf{F}_2(\mathbf{u}_k^n, \mathbf{v}_k^n, \mathbf{r}_k^n, \mathbf{s}_k^n)}{\partial \mathbf{v}_k^n} = M_0 + \tau d_\Omega A_0 + \tau\gamma_\Omega B_0(\mathbf{u}_k^n, \mathbf{u}_k^n) + \tau\gamma_\Gamma \delta_3 M_{00},$$
$$\frac{\partial \mathbf{F}_2(\mathbf{u}_k^n, \mathbf{v}_k^n, \mathbf{r}_k^n, \mathbf{s}_k^n)}{\partial \mathbf{r}_k^n} = 0,$$
$$\frac{\partial \mathbf{F}_2(\mathbf{u}_k^n, \mathbf{v}_k^n, \mathbf{r}_k^n, \mathbf{s}_k^n)}{\partial \mathbf{s}_k^n} = -\tau\gamma_\Gamma \rho_4 M_{10},$$
$$\frac{\partial \mathbf{F}_3(\mathbf{u}_k^n, \mathbf{v}_k^n, \mathbf{r}_k^n, \mathbf{s}_k^n)}{\partial \mathbf{u}_k^n} = -\tau\gamma_\Gamma M_{01},$$
$$\frac{\partial \mathbf{F}_3(\mathbf{u}_k^n, \mathbf{v}_k^n, \mathbf{r}_k^n, \mathbf{s}_k^n)}{\partial \mathbf{v}_k^n} = -\tau\gamma_\Gamma \delta_2 M_{01},$$
$$\frac{\partial \mathbf{F}_3(\mathbf{u}_k^n, \mathbf{v}_k^n, \mathbf{r}_k^n, \mathbf{s}_k^n)}{\partial \mathbf{r}_k^n} = (1 + \tau\gamma_\Gamma) M_1 + \tau A_1 + \tau\gamma_\Gamma \rho_3 M_1,$$
$$\frac{\partial \mathbf{F}_3(\mathbf{u}_k^n, \mathbf{v}_k^n, \mathbf{r}_k^n, \mathbf{s}_k^n)}{\partial \mathbf{s}_k^n} = -\tau q_2 \gamma_\Gamma M_1,$$
$$\frac{\partial \mathbf{F}_4(\mathbf{u}_k^n, \mathbf{v}_k^n, \mathbf{r}_k^n, \mathbf{s}_k^n)}{\partial \mathbf{u}_k^n} = -\tau\gamma_\Gamma M_{01},$$
$$\frac{\partial \mathbf{F}_4(\mathbf{u}_k^n, \mathbf{v}_k^n, \mathbf{r}_k^n, \mathbf{s}_k^n)}{\partial \mathbf{v}_k^n} = -\tau\gamma_\Gamma \delta_3 M_{01},$$
$$\frac{\partial \mathbf{F}_4(\mathbf{u}_k^n, \mathbf{v}_k^n, \mathbf{r}_k^n, \mathbf{s}_k^n)}{\partial \mathbf{r}_k^n} = -\tau c_2 \gamma_\Gamma M_1,$$
$$\frac{\partial \mathbf{F}_4(\mathbf{u}_k^n, \mathbf{v}_k^n, \mathbf{r}_k^n, \mathbf{s}_k^n)}{\partial \mathbf{s}_k^n} = (1 + \tau j_2 \gamma_\Gamma) M_1 + \tau d_\Gamma A_1 + \tau\gamma_\Gamma \rho_4 M_1.$$

Substituting (4.41) in (4.40), we obtain

$$\begin{aligned}[(1+\tau\gamma_\Omega)M_0 + \tau A_0 - 2\tau\gamma_\Omega B_0(\mathbf{u}_k^n, \mathbf{v}_k^n) + \tau\gamma_\Gamma M_{00}](\mathbf{u}_{k+1}^n) \\ + [-\tau\gamma_\Omega B_0(\mathbf{u}_k^n, \mathbf{u}_k^n) + \tau\gamma_\Gamma \delta_2 M_{00}](\mathbf{v}_{k+1}^n) + [-\tau\gamma_\Gamma \rho_3 M_{10}](\mathbf{r}_{k+1}^n) \\ = -2\tau\gamma_\Omega B_0(\mathbf{u}_k^n, \mathbf{v}_k^n)\mathbf{u}_k^n + \tau\gamma_\Omega a_2 \mathbf{C_0} + M_0 \mathbf{u}^{n-1},\end{aligned}$$

$$\begin{aligned}[2\tau\gamma_\Omega B_0(\mathbf{u}_k^n, \mathbf{v}_k^n) + \tau\gamma_\Gamma M_{00}](\mathbf{u}_{k+1}^n) + [M_0 + \tau d_\Omega A_0 + \tau\gamma_\Omega B_0(\mathbf{u}_k^n, \mathbf{u}_k^n) + \tau\gamma_\Gamma \delta_3 M_{00}](\mathbf{v}_{k+1}^n) \\ + [-\tau\gamma_\Gamma \rho_4 M_{10}](\mathbf{s}_{k+1}^n) = 2\tau\gamma_\Omega B_0(\mathbf{u}_k^n, \mathbf{u}_k^n)\mathbf{v}_k^n + \tau\gamma_\Omega b_2 \mathbf{C_0} + M_0 \mathbf{v}^{n-1},\end{aligned}$$

$$\begin{aligned}[-\tau\gamma_\Gamma M_{01}](\mathbf{u}_{k+1}^n) + [-\tau\gamma_\Gamma \delta_2 M_{01}](\mathbf{v}_{k+1}^n) + [(1+\tau\gamma_\Gamma)M_1 + \tau A_1 + \tau\gamma_\Gamma \rho_3 M_1](\mathbf{r}_{k+1}^n) \\ + [-\tau q_2 \gamma_\Gamma M_1](\mathbf{s}_{k+1}^n) = M_1 \mathbf{r}^{n-1},\end{aligned}$$

$$\begin{aligned}[-\tau\gamma_\Gamma M_{01}](\mathbf{u}_{k+1}^n) + [-\tau\gamma_\Gamma \delta_3 M_{01}](\mathbf{v}_{k+1}^n) + [-\tau c_2 \gamma_\Gamma M_1](\mathbf{r}_{k+1}^n) \\ + [(1+\tau j_2\gamma_\Gamma)M_1 + \tau d_\Gamma A_1 + \tau\gamma_\Gamma \rho_4 M_1](\mathbf{s}_{k+1}^n) = M_1 \mathbf{s}^{n-1},\end{aligned}$$

which can be written in a matrix form as

$$\begin{pmatrix} \frac{\partial \mathbf{F}_1(\mathbf{u}_k^n,\mathbf{v}_k^n,\mathbf{r}_k^n,\mathbf{s}_k^n)}{\partial \mathbf{u}_k^n} & \frac{\partial \mathbf{F}_1(\mathbf{u}_k^n,\mathbf{v}_k^n,\mathbf{r}_k^n,\mathbf{s}_k^n)}{\partial \mathbf{v}_k^n} & \frac{\partial \mathbf{F}_1(\mathbf{u}_k^n,\mathbf{v}_k^n,\mathbf{r}_k^n,\mathbf{s}_k^n)}{\partial \mathbf{r}_k^n} & \frac{\partial \mathbf{F}_1(\mathbf{u}_k^n,\mathbf{v}_k^n,\mathbf{r}_k^n,\mathbf{s}_k^n)}{\partial \mathbf{s}_k^n} \\ \frac{\partial \mathbf{F}_2(\mathbf{u}_k^n,\mathbf{v}_k^n,\mathbf{r}_k^n,\mathbf{s}_k^n)}{\partial \mathbf{u}_k^n} & \frac{\partial \mathbf{F}_2(\mathbf{u}_k^n,\mathbf{v}_k^n,\mathbf{r}_k^n,\mathbf{s}_k^n)}{\partial \mathbf{v}_k^n} & \frac{\partial \mathbf{F}_2(\mathbf{u}_k^n,\mathbf{v}_k^n,\mathbf{r}_k^n,\mathbf{s}_k^n)}{\partial \mathbf{r}_k^n} & \frac{\partial \mathbf{F}_2(\mathbf{u}_k^n,\mathbf{v}_k^n,\mathbf{r}_k^n,\mathbf{s}_k^n)}{\partial \mathbf{s}_k^n} \\ \frac{\partial \mathbf{F}_3(\mathbf{u}_k^n,\mathbf{v}_k^n,\mathbf{r}_k^n,\mathbf{s}_k^n)}{\partial \mathbf{u}_k^n} & \frac{\partial \mathbf{F}_3(\mathbf{u}_k^n,\mathbf{v}_k^n,\mathbf{r}_k^n,\mathbf{s}_k^n)}{\partial \mathbf{v}_k^n} & \frac{\partial \mathbf{F}_3(\mathbf{u}_k^n,\mathbf{v}_k^n,\mathbf{r}_k^n,\mathbf{s}_k^n)}{\partial \mathbf{r}_k^n} & \frac{\partial \mathbf{F}_3(\mathbf{u}_k^n,\mathbf{v}_k^n,\mathbf{r}_k^n,\mathbf{s}_k^n)}{\partial \mathbf{s}_k^n} \\ \frac{\partial \mathbf{F}_4(\mathbf{u}_k^n,\mathbf{v}_k^n,\mathbf{r}_k^n,\mathbf{s}_k^n)}{\partial \mathbf{u}_k^n} & \frac{\partial \mathbf{F}_4(\mathbf{u}_k^n,\mathbf{v}_k^n,\mathbf{r}_k^n,\mathbf{s}_k^n)}{\partial \mathbf{v}_k^n} & \frac{\partial \mathbf{F}_4(\mathbf{u}_k^n,\mathbf{v}_k^n,\mathbf{r}_k^n,\mathbf{s}_k^n)}{\partial \mathbf{r}_k^n} & \frac{\partial \mathbf{F}_4(\mathbf{u}_k^n,\mathbf{v}_k^n,\mathbf{r}_k^n,\mathbf{s}_k^n)}{\partial \mathbf{s}_k^n} \end{pmatrix} \begin{pmatrix} \mathbf{u}_{k+1}^n \\ \mathbf{v}_{k+1}^n \\ \mathbf{r}_{k+1}^n \\ \mathbf{s}_{k+1}^n \end{pmatrix}$$

$$= \begin{pmatrix} -2\tau\gamma_\Omega B_0(\mathbf{u}_k^n,\mathbf{v}_k^n)\mathbf{u}_k^n + \tau\gamma_\Omega a_2\mathbf{C_0} + M_0\mathbf{u}^{n-1} \\ 2\tau\gamma_\Omega B_0(\mathbf{u}_k^n,\mathbf{u}_k^n)\mathbf{v}_k^n + \tau\gamma_\Omega b_2\mathbf{C_0} + M_0\mathbf{v}^{n-1} \\ M_1\mathbf{r}^{n-1} \\ M_1\mathbf{s}^{n-1} \end{pmatrix}.$$

4.7 Linear reaction kinetics in the bulk and non-linear reaction kinetics on the surface

In this system we consider linear reaction kinetics in the bulk and non-linear reaction kinetics on the surface. We rewrite the non-dimensional bulk-surface reaction-diffusion systems given by (2.191) in Chapter 2,

$$\begin{cases} \begin{cases} \frac{\partial u}{\partial t} &= \Delta u + f_1(u,v,r,s), \\ \frac{\partial v}{\partial t} &= d_\Omega \Delta v + f_2(u,v,r,s), \end{cases} & \text{in } \Omega \times (0,T] \\ \begin{cases} \frac{\partial r}{\partial t} &= \Delta_\Gamma r + f_3(u,v,r,s), \\ \frac{\partial s}{\partial t} &= d_\Gamma \Delta_\Gamma s + f_4(u,v,r,s), \end{cases} & \text{on } \Gamma \times (0,T]. \end{cases} \tag{4.42}$$

where

$$f_1(u,v,r,s) = \gamma_\Omega(-u + qv), \tag{4.43}$$

$$f_2(u,v,r,s) = \gamma_\Omega(c_1 u - zv), \tag{4.44}$$

$$f_3(u,v,r,s) = \gamma_\Gamma(a_1 - r + r^2 s - \rho_1 r + u + v), \tag{4.45}$$

$$f_4(u,v,r,s) = \gamma_\Gamma(b_1 - r^2 s - \rho_2 s + \mu u + \delta v). \tag{4.46}$$

The linear boundary conditions have the form

$$\begin{cases} \nabla u \cdot \nu = \gamma_\Gamma[\rho_1 r - u - v] \\ d_\Omega \nabla v \cdot \nu = \gamma_\Gamma[\rho_2 s - \mu u - \delta v] \end{cases} \text{on } \Gamma \times (0,T]. \tag{4.47}$$

The non-dimensional initial conditions for all chemical concentrations are given by

$$u(\mathbf{x},0)=u^0(\mathbf{x}),\quad v(\mathbf{x},0)=v^0(\mathbf{x}),\quad r(\mathbf{x},0)=r^0(\mathbf{x})\ \text{ and }\ s(\mathbf{x},0)=s^0(\mathbf{x}). \tag{4.48}$$

An analogous approach to that employed in Section 4.5 gives rise to a system of non-linear algebraic equations which are solved by Newton's method. The set of non-linear equations can be written in the form

$$\begin{aligned}
\mathbf{F_1}(\mathbf{U}^n,\mathbf{V}^n,\mathbf{R}^n,\mathbf{S}^n)&=0,\\
\mathbf{F_2}(\mathbf{U}^n,\mathbf{V}^n,\mathbf{R}^n,\mathbf{S}^n)&=0,\\
\mathbf{F_3}(\mathbf{U}^n,\mathbf{V}^n,\mathbf{R}^n,\mathbf{S}^n)&=0,\\
\mathbf{F_4}(\mathbf{U}^n,\mathbf{V}^n,\mathbf{R}^n,\mathbf{S}^n)&=0,
\end{aligned}$$

where

$$\begin{aligned}
\mathbf{F_1}(\mathbf{U}^n,\mathbf{V}^n,\mathbf{R}^n,\mathbf{S}^n)&=((\frac{1}{\tau}+\gamma_\Omega)M_0+A_0)\mathbf{U}^n-\gamma_\Omega q M_0\mathbf{V}^n\\
&\quad-\gamma_\Gamma(\rho_1 M_{10}\mathbf{R}^n-M_{00}\mathbf{U}^n-M_{00}\mathbf{V}^n)-\frac{1}{\tau}M_0\mathbf{U}^{n-1},\\
\mathbf{F_2}(\mathbf{U}^n,\mathbf{V}^n,\mathbf{R}^n,\mathbf{S}^n)&=((\frac{1}{\tau}+\gamma_\Omega z)M_0+d_\Omega A_0)\mathbf{V}^n-\gamma_\Omega c_1 M_0\mathbf{U}^n\\
&\quad-\gamma_\Gamma(\rho_2 M_{10}\mathbf{S}^n-\mu M_{00}\mathbf{U}^n-\delta M_{00}\mathbf{V}^n)-\frac{1}{\tau}M_0\mathbf{V}^{n-1},\\
\mathbf{F_3}(\mathbf{U}^n,\mathbf{V}^n,\mathbf{R}^n,\mathbf{S}^n)&=((\frac{1}{\tau}+\gamma_\Gamma)M_1+A_1)\mathbf{R}^n-\gamma_\Gamma B_1(\mathbf{R}^n,\mathbf{S}^n)\mathbf{R}^n\\
&\quad+\gamma_\Gamma(\rho_1 M_{11}\mathbf{R}^n-M_{01}\mathbf{U}^n-M_{01}\mathbf{V}^n)-\gamma_\Gamma a_1\mathbf{C_1}-\frac{1}{\tau}M_1\mathbf{R}^{n-1},\\
\mathbf{F_4}(\mathbf{U}^n,\mathbf{V}^n,\mathbf{R}^n,\mathbf{S}^n)&=(\frac{1}{\tau}M_1+d_\Gamma A_1)\mathbf{S}^n+\gamma_\Gamma B_1(\mathbf{R}^n,\mathbf{R}^n)\mathbf{S}^n\\
&\quad+\gamma_\Gamma(\rho_2 M_{11}\mathbf{S}^n-\mu M_{01}\mathbf{U}^n-\delta M_{01}\mathbf{V}^n)-\gamma_\Gamma b_1\mathbf{C_1}-\frac{1}{\tau}M_1\mathbf{S}^{n-1}.
\end{aligned}$$

In order to solve the system of non-linear equation, the employing the extended form of Newton's method for vector valued functions lead to write

$$\mathbf{J}_{\mathbf{F}_i}\,|_{(\mathbf{u}_k^n,\mathbf{v}_k^n,\mathbf{r}_k^n,\mathbf{s}_k^n)}\,(\mathbf{u}_{k+1}^n-\mathbf{u}_k^n,\mathbf{v}_{k+1}^n-\mathbf{v}_k^n,\mathbf{r}_{k+1}^n-\mathbf{r}_k^n,\mathbf{s}_{k+1}^n-\mathbf{s}_k^n)=-\mathbf{F}_i(\mathbf{u}_k^n,\mathbf{v}_k^n,\mathbf{r}_k^n,\mathbf{s}_k^n), \tag{4.49}$$

where the index $\imath = 1, 2, 3, 4$ and

$$\mathbf{J_F}\mid_{(\mathbf{u}_k^n,\mathbf{v}_k^n,\mathbf{r}_k^n,\mathbf{s}_k^n)}= \begin{pmatrix} \frac{\partial \mathbf{F}_1(\mathbf{u}_k^n,\mathbf{v}_k^n,\mathbf{r}_k^n,\mathbf{s}_k^n)}{\partial \mathbf{u}_k^n} & \frac{\partial \mathbf{F}_1(\mathbf{u}_k^n,\mathbf{v}_k^n,\mathbf{r}_k^n,\mathbf{s}_k^n)}{\partial \mathbf{v}_k^n} & \frac{\partial \mathbf{F}_1(\mathbf{u}_k^n,\mathbf{v}_k^n,\mathbf{r}_k^n,\mathbf{s}_k^n)}{\partial \mathbf{r}_k^n} & \frac{\partial \mathbf{F}_1(\mathbf{u}_k^n,\mathbf{v}_k^n,\mathbf{r}_k^n,\mathbf{s}_k^n)}{\partial \mathbf{s}_k^n} \\ \frac{\partial \mathbf{F}_2(\mathbf{u}_k^n,\mathbf{v}_k^n,\mathbf{r}_k^n,\mathbf{s}_k^n)}{\partial \mathbf{u}_k^n} & \frac{\partial \mathbf{F}_2(\mathbf{u}_k^n,\mathbf{v}_k^n,\mathbf{r}_k^n,\mathbf{s}_k^n)}{\partial \mathbf{v}_k^n} & \frac{\partial \mathbf{F}_2(\mathbf{u}_k^n,\mathbf{v}_k^n,\mathbf{r}_k^n,\mathbf{s}_k^n)}{\partial \mathbf{r}_k^n} & \frac{\partial \mathbf{F}_2(\mathbf{u}_k^n,\mathbf{v}_k^n,\mathbf{r}_k^n,\mathbf{s}_k^n)}{\partial \mathbf{s}_k^n} \\ \frac{\partial \mathbf{F}_3(\mathbf{u}_k^n,\mathbf{v}_k^n,\mathbf{r}_k^n,\mathbf{s}_k^n)}{\partial \mathbf{u}_k^n} & \frac{\partial \mathbf{F}_3(\mathbf{u}_k^n,\mathbf{v}_k^n,\mathbf{r}_k^n,\mathbf{s}_k^n)}{\partial \mathbf{v}_k^n} & \frac{\partial \mathbf{F}_3(\mathbf{u}_k^n,\mathbf{v}_k^n,\mathbf{r}_k^n,\mathbf{s}_k^n)}{\partial \mathbf{r}_k^n} & \frac{\partial \mathbf{F}_3(\mathbf{u}_k^n,\mathbf{v}_k^n,\mathbf{r}_k^n,\mathbf{s}_k^n)}{\partial \mathbf{s}_k^n} \\ \frac{\partial \mathbf{F}_4(\mathbf{u}_k^n,\mathbf{v}_k^n,\mathbf{r}_k^n,\mathbf{s}_k^n)}{\partial \mathbf{u}_k^n} & \frac{\partial \mathbf{F}_4(\mathbf{u}_k^n,\mathbf{v}_k^n,\mathbf{r}_k^n,\mathbf{s}_k^n)}{\partial \mathbf{v}_k^n} & \frac{\partial \mathbf{F}_4(\mathbf{u}_k^n,\mathbf{v}_k^n,\mathbf{r}_k^n,\mathbf{s}_k^n)}{\partial \mathbf{r}_k^n} & \frac{\partial \mathbf{F}_4(\mathbf{u}_k^n,\mathbf{v}_k^n,\mathbf{r}_k^n,\mathbf{s}_k^n)}{\partial \mathbf{s}_k^n} \end{pmatrix}, \tag{4.50}$$

and the entries of $\mathbf{J_F}$ are expressed by

$$\begin{aligned}
\frac{\partial \mathbf{F}_1(\mathbf{u}_k^n,\mathbf{v}_k^n,\mathbf{r}_k^n,\mathbf{s}_k^n)}{\partial \mathbf{u}_k^n} &= (\frac{1}{\tau}+\gamma_\Omega)M_0 + A_0 + \gamma_\Gamma M_{00},\\
\frac{\partial \mathbf{F}_1(\mathbf{u}_k^n,\mathbf{v}_k^n,\mathbf{r}_k^n,\mathbf{s}_k^n)}{\partial \mathbf{v}_k^n} &= -\gamma_\Omega q M_0 + \gamma_\Gamma M_{00},\\
\frac{\partial \mathbf{F}_1(\mathbf{u}_k^n,\mathbf{v}_k^n,\mathbf{r}_k^n,\mathbf{s}_k^n)}{\partial \mathbf{r}_k^n} &= -\gamma_\Gamma \rho_1 M_{10},\\
\frac{\partial \mathbf{F}_1(\mathbf{u}_k^n,\mathbf{v}_k^n,\mathbf{r}_k^n,\mathbf{s}_k^n)}{\partial \mathbf{s}_k^n} &= 0,\\
\frac{\partial \mathbf{F}_2(\mathbf{u}_k^n,\mathbf{v}_k^n,\mathbf{r}_k^n,\mathbf{s}_k^n)}{\partial \mathbf{u}_k^n} &= -\gamma_\Omega c_1 M_0 + \gamma_\Gamma \mu M_{00},\\
\frac{\partial \mathbf{F}_2(\mathbf{u}_k^n,\mathbf{v}_k^n,\mathbf{r}_k^n,\mathbf{s}_k^n)}{\partial \mathbf{v}_k^n} &= (\frac{1}{\tau}+\gamma_\Omega z)M_0 + d_\Omega A_0 + \gamma_\Gamma \delta M_{00},\\
\frac{\partial \mathbf{F}_2(\mathbf{u}_k^n,\mathbf{v}_k^n,\mathbf{r}_k^n,\mathbf{s}_k^n)}{\partial \mathbf{r}_k^n} &= 0,\\
\frac{\partial \mathbf{F}_2(\mathbf{u}_k^n,\mathbf{v}_k^n,\mathbf{r}_k^n,\mathbf{s}_k^n)}{\partial \mathbf{s}_k^n} &= -\gamma_\Gamma \rho_2 M_{10},\\
\frac{\partial \mathbf{F}_3(\mathbf{u}_k^n,\mathbf{v}_k^n,\mathbf{r}_k^n,\mathbf{s}_k^n)}{\partial \mathbf{u}_k^n} &= -\gamma_\Gamma M_{01},\\
\frac{\partial \mathbf{F}_3(\mathbf{u}_k^n,\mathbf{v}_k^n,\mathbf{r}_k^n,\mathbf{s}_k^n)}{\partial \mathbf{v}_k^n} &= -\gamma_\Gamma M_{01},\\
\frac{\partial \mathbf{F}_3(\mathbf{u}_k^n,\mathbf{v}_k^n,\mathbf{r}_k^n,\mathbf{s}_k^n)}{\partial \mathbf{r}_k^n} &= (\frac{1}{\tau}+\gamma_\Gamma)M_1 + A_1 - 2\gamma_\Gamma B_1(\mathbf{r}_k^n,\mathbf{s}_k^n) + \gamma_\Gamma \rho_1 M_{11},\\
\frac{\partial \mathbf{F}_3(\mathbf{u}_k^n,\mathbf{v}_k^n,\mathbf{r}_k^n,\mathbf{s}_k^n)}{\partial \mathbf{s}_k^n} &= -\gamma_\Gamma B_1(\mathbf{r}_k^n,\mathbf{r}_k^n),\\
\frac{\partial \mathbf{F}_4(\mathbf{u}_k^n,\mathbf{v}_k^n,\mathbf{r}_k^n,\mathbf{s}_k^n)}{\partial \mathbf{u}_k^n} &= -\gamma_\Gamma \mu M_{01},\\
\frac{\partial \mathbf{F}_4(\mathbf{u}_k^n,\mathbf{v}_k^n,\mathbf{r}_k^n,\mathbf{s}_k^n)}{\partial \mathbf{v}_k^n} &= -\gamma_\Gamma \delta M_{01},\\
\frac{\partial \mathbf{F}_4(\mathbf{u}_k^n,\mathbf{v}_k^n,\mathbf{r}_k^n,\mathbf{s}_k^n)}{\partial \mathbf{r}_k^n} &= 2\gamma_\Gamma B_1(\mathbf{r}_k^n,\mathbf{s}_k^n),\\
\frac{\partial \mathbf{F}_4(\mathbf{u}_k^n,\mathbf{v}_k^n,\mathbf{r}_k^n,\mathbf{s}_k^n)}{\partial \mathbf{s}_k^n} &= \frac{1}{\tau}M_1 + d_\Gamma A_1 + \gamma_\Gamma B_1(\mathbf{r}_k^n,\mathbf{r}_k^n) + \gamma_\Gamma \rho_2 M_{11}.
\end{aligned}$$

Substituting (4.50) in (4.49) and simplifying, we obtain

$$[(\frac{1}{\tau}+\gamma_\Omega)M_0 + A_0](\mathbf{u}^n_{k+1}) + [-\gamma_\Omega q M_0](\mathbf{v}^n_{k+1}) \\ - \gamma_\Gamma[(\rho_1 M_{10})\mathbf{r}^n_{k+1} - (M_{00})\mathbf{u}^n_{k+1} - (M_{00})\mathbf{v}^n_{k+1}] = \frac{1}{\tau}M_0\mathbf{u}^{n-1},$$

$$[-\gamma_\Omega c_1 M_0](\mathbf{u}^n_{k+1}) + [(\frac{1}{\tau} + \gamma_\Omega z)M_0 + d_\Omega A_0](\mathbf{v}^n_{k+1}) \\ - \gamma_\Gamma[(\rho_2 M_{10})\mathbf{s}^n_{k+1} - (\mu M_{00})\mathbf{u}^n_{k+1} - (\delta M_{00})\mathbf{v}^n_{k+1}] = \frac{1}{\tau}M_0 v^{n-1},$$

$$[(\frac{1}{\tau}+\gamma_\Gamma)M_1 + A_1 - 2\gamma_\Gamma B_1(\mathbf{r}^n_k, \mathbf{s}^n_k)](\mathbf{r}^n_{k+1}) + [-\gamma_\Gamma B_1(\mathbf{r}^n_k, \mathbf{r}^n_k)](\mathbf{s}^n_{k+1}) \\ + \gamma_\Gamma[(\rho_1 M_{11})\mathbf{r}^n_{k+1} - (M_{01})\mathbf{u}^n_{k+1} - (M_{01})\mathbf{v}^n_{k+1}] \\ = -2\gamma_\Gamma B_1(\mathbf{r}^n_k, \mathbf{s}^n_k)\mathbf{r}^n_k + \gamma_\Gamma a_1\mathbf{C_1} + \frac{1}{\tau}M_1\mathbf{r}^{n-1},$$

$$[2\gamma_\Gamma B_1(\mathbf{r}^n_k, \mathbf{s}^n_k)](\mathbf{r}^n_{k+1}) + [\frac{1}{\tau}M_1 + d_\Gamma A_1 + \gamma_\Gamma B_1(\mathbf{r}^n_k, \mathbf{r}^n_k)](\mathbf{s}^n_{k+1}) \\ + \gamma_\Gamma[(\rho_2 M_{11})\mathbf{s}^n_{k+1} - (\mu M_{01})\mathbf{u}^n_{k+1} - (\delta M_{01})\mathbf{v}^n_{k+1}] \\ = 2\gamma_\Gamma B_1(\mathbf{r}^n_k, \mathbf{r}^n_k)\mathbf{s}^n_k + \gamma_\Gamma b_1\mathbf{C_1} + \frac{1}{\tau}M_1\mathbf{s}^{n-1},$$

which can be written in a matrix form as

$$\begin{pmatrix} \frac{\partial \mathbf{F}_1(\mathbf{u}^n_k,\mathbf{v}^n_k,\mathbf{r}^n_k,\mathbf{s}^n_k)}{\partial \mathbf{u}^n_k} & \frac{\partial \mathbf{F}_1(\mathbf{u}^n_k,\mathbf{v}^n_k,\mathbf{r}^n_k,\mathbf{s}^n_k)}{\partial \mathbf{v}^n_k} & \frac{\partial \mathbf{F}_1(\mathbf{u}^n_k,\mathbf{v}^n_k,\mathbf{r}^n_k,\mathbf{s}^n_k)}{\partial \mathbf{r}^n_k} & \frac{\partial \mathbf{F}_1(\mathbf{u}^n_k,\mathbf{v}^n_k,\mathbf{r}^n_k,\mathbf{s}^n_k)}{\partial \mathbf{s}^n_k} \\ \frac{\partial \mathbf{F}_2(\mathbf{u}^n_k,\mathbf{v}^n_k,\mathbf{r}^n_k,\mathbf{s}^n_k)}{\partial \mathbf{u}^n_k} & \frac{\partial \mathbf{F}_2(\mathbf{u}^n_k,\mathbf{v}^n_k,\mathbf{r}^n_k,\mathbf{s}^n_k)}{\partial \mathbf{v}^n_k} & \frac{\partial \mathbf{F}_2(\mathbf{u}^n_k,\mathbf{v}^n_k,\mathbf{r}^n_k,\mathbf{s}^n_k)}{\partial \mathbf{r}^n_k} & \frac{\partial \mathbf{F}_2(\mathbf{u}^n_k,\mathbf{v}^n_k,\mathbf{r}^n_k,\mathbf{s}^n_k)}{\partial \mathbf{s}^n_k} \\ \frac{\partial \mathbf{F}_3(\mathbf{u}^n_k,\mathbf{v}^n_k,\mathbf{r}^n_k,\mathbf{s}^n_k)}{\partial \mathbf{u}^n_k} & \frac{\partial \mathbf{F}_3(\mathbf{u}^n_k,\mathbf{v}^n_k,\mathbf{r}^n_k,\mathbf{s}^n_k)}{\partial \mathbf{v}^n_k} & \frac{\partial \mathbf{F}_3(\mathbf{u}^n_k,\mathbf{v}^n_k,\mathbf{r}^n_k,\mathbf{s}^n_k)}{\partial \mathbf{r}^n_k} & \frac{\partial \mathbf{F}_3(\mathbf{u}^n_k,\mathbf{v}^n_k,\mathbf{r}^n_k,\mathbf{s}^n_k)}{\partial \mathbf{s}^n_k} \\ \frac{\partial \mathbf{F}_4(\mathbf{u}^n_k,\mathbf{v}^n_k,\mathbf{r}^n_k,\mathbf{s}^n_k)}{\partial \mathbf{u}^n_k} & \frac{\partial \mathbf{F}_4(\mathbf{u}^n_k,\mathbf{v}^n_k,\mathbf{r}^n_k,\mathbf{s}^n_k)}{\partial \mathbf{v}^n_k} & \frac{\partial \mathbf{F}_4(\mathbf{u}^n_k,\mathbf{v}^n_k,\mathbf{r}^n_k,\mathbf{s}^n_k)}{\partial \mathbf{r}^n_k} & \frac{\partial \mathbf{F}_4(\mathbf{u}^n_k,\mathbf{v}^n_k,\mathbf{r}^n_k,\mathbf{s}^n_k)}{\partial \mathbf{s}^n_k} \end{pmatrix} \begin{pmatrix} \mathbf{u}^n_{k+1} \\ \mathbf{v}^n_{k+1} \\ \mathbf{r}^n_{k+1} \\ \mathbf{s}^n_{k+1} \end{pmatrix}$$

$$= \begin{pmatrix} \frac{1}{\tau}M_0\mathbf{u}^{n-1} \\ \frac{1}{\tau}M_0\mathbf{v}^{n-1} \\ -2\gamma_\Gamma B_1(\mathbf{r}^n_k, \mathbf{s}^n_k)\mathbf{r}^n_k + \gamma_\Gamma a_1\mathbf{C_1} + \frac{1}{\tau}M_1\mathbf{r}^{n-1} \\ 2\gamma_\Gamma B_1(\mathbf{r}^n_k, \mathbf{r}^n_k)\mathbf{s}^n_k + \gamma_\Gamma b_1\mathbf{C_1} + \frac{1}{\tau}M_1\mathbf{s}^{n-1} \end{pmatrix}.$$

4.8 Conclusion

A fully implicit time-stepping scheme is employed with the finite element method through the application of the extended form of Newton's formula to discretise the four-component bulk-surface reaction-diffusion systems both in space and in

time. The theoretical set-up for the finite element method is provided with the required definitions of function spaces and other abstract concepts. Two time-stepping schemes namely first order IMEX and 2-SBDF are compared and it is found that 2-SBDF is a faster time-stepping scheme. We also obtain a fully discretised system of algebraic equations of BSRDEs with linear coupling conditions. The finite element formulation is verified by considering well known parameters from the Turing space that give rise to pattern formation. In particular, convergence of the numerical method is shown both in the bulk and on the surface. In the next chapter, we carry out detailed numerical solutions of the coupled system of bulk-surface reaction-diffusion equations with an eye to verifying theoretical results obtained by linear stability analysis in previous chapters.

Chapter 5

Numerical Solution for Coupled Bulk-Surface Reaction-Diffusion Equations

In this chapter we carry out the numerical simulations on all three systems that were explored in Chapter 2. We employ a fully implicit time-stepping scheme based on the extended form of Newton's method with the finite element formulation presented in Chapter 4 to proceed with obtaining numerical approximate solutions both in space and in time. We perform the finite element simulations on two types of bulk-surface domains. The first is a cuboid forming the bulk and its six quadrilateral faces forming the corresponding surface. The second domain is a three dimensional ball forming the bulk and hollow sphere bounding the ball forming the corresponding surface. The cuboid has volume 1 in dimensionless units and it occupies the space defined by C_b, where $C_b = \{(x, y, z) \in \mathbb{R}^3 : 0 < x < 1, 0 < y < 1, 0 < z < 1\}$ and the surface consists of six quadrilaterals that bound the unit-volume cube. The second domain is a three-dimensional ball of radios that forms the bulk B_b, given by $B_b = \{(x, y, z) \in \mathbb{R}^3 : x^2+y^2+z^2 < 1\}$, which is bounded by the surface that consists of all points satisfying the definition of a two-dimensional hollow sphere expressed by $B_s = \{(x, y, z) \in \mathbb{R}^3 : x^2 + y^2 + z^2 = 1\}$. In each simulation we use the L_2-norms of the discrete time derivatives of the numerical solutions to observe diffusion-driven instability. The discretised cuboid Ω_h possesses 9826 vertices (also known as degrees of freedom) of which 3076 belong to the corresponding surface Γ_h. The spherical

discretised domain Ω_h possesses 7634 degrees of freedom of which 772 belong to the discretised hollow surface Γ_h. The initial conditions in all the simulations are taken to be random small perturbation near the uniform steady state.

5.1 Non-linear kinetics both in the bulk and on the surface

The finite element library deal.ii Bangerth et al. (2016) is employed to simulate the numerical solutions of the coupled system of bulk-surface reaction-diffusion equations (4.24) on both the cubic and spherical bulk-surface domains respectively. In all simulations for the coupled system of bulk-surface reaction-diffusion equations (4.24) we use the values $a_2 = 0.1$ and $b_2 = 0.9$ for parameters in Schnakenberg reaction kinetics. These values are chosen because they lie within a region in parameter spaces corresponding to Turing instability Murray (2001); Madzvamuse (2000); Madzvamuse et al. (2015a), and therefore satisfies conditions (2.117)-(2.122). The other parameters are chosen as $\rho_3 = \frac{2}{5}$, $\rho_4 = 3$, $\mu = \frac{2}{5}$, $\mu_1 = 0$, $\delta_2 = 0$, and $\delta_3 = 3$, so that they all satisfy the parameter compatibility condition (2.32). We present simulations corresponding to four different cases, so that we ensure to include all possible behaviors of pattern formation corresponding to different combinations between diffusion ratios namely d_Ω and d_Γ in the bulk and on the surface respectively. In particular the four combinations of values chosen for the current simulations consist of $(d_\Omega, d_\Gamma) = (1,1), (30,30), (1,30), (30,1)$. The theoretical results proposed by Theorem 2.1.3 are verified numerically by observing that the numerical solution of the coupled system of bulk-surface reaction-diffusion equations (4.24) induces no spatial pattern in the bulk or on the surface with a choice of diffusion ratios given by $d_\Omega = d_\Gamma = 1$. Figures 5.1 and 5.2 provide a numerical verification of the absence of any spatial pattern under the parameter settings $d_\Omega = d_\Gamma = 1$, which is in agreement with Theorem 2.1.3 for both the cubic and spherical domains. If the values of the diffusion ratios are chosen such that $d_\Omega = 30 > 1$ and $d_\Gamma = 30 > 1$, then the finite element numerical solution of the coupled system of bulk-surface reaction-diffusion equations (4.24) reveals pattern formation in the bulk, on the surface and on the layer of interface where the coupling terms interact

through the boundary conditions. It is therefore, when non-linear reaction kinetics are posed both in the bulk and on the surface, with parameter compatibility conditions (2.32) satisfied and d_Ω, d_Γ much larger than 1, that one may expect the numerical solutions of the coupled system of bulk-surface reaction-diffusion equations (4.24) to form a spatial pattern everywhere. Figures 5.4 and 5.5 show results in agreement with this prediction, which means that spatial pattern can be observed everywhere. When the diffusion ratios are chosen such that $d_\Omega = 1$ and $d_\Gamma = 30 > 1$, then spatial pattern is emerged on the surface and it extends by forming a boundary layer without inducing spatial pattern into the interior of the bulk. This is observed to be the case in Figures 5.7 and 5.8 for spherical and cubic domains respectively. Figures 5.10 and 5.11 reveal the case where we choose $d_\Omega = 30$ and $d_\Gamma = 1$ for which it was predicted through the results of stability analysis that the reaction kinetics inside the bulk produces spatial pattern with a potential possibility that this pattern may emerge on the surface as well. It is therefore, if a spatial pattern emerges on the surface under this kind of parameter settings then it does not mean that surface reaction kinetics with $d_\Gamma = 1$ is capable of evolving spatial pattern, in fact it only means that the emergence of spatial pattern on the surface is a consequence of the spatial pattern formed in the bulk and extends through the coupling conditions to appear on the surface.

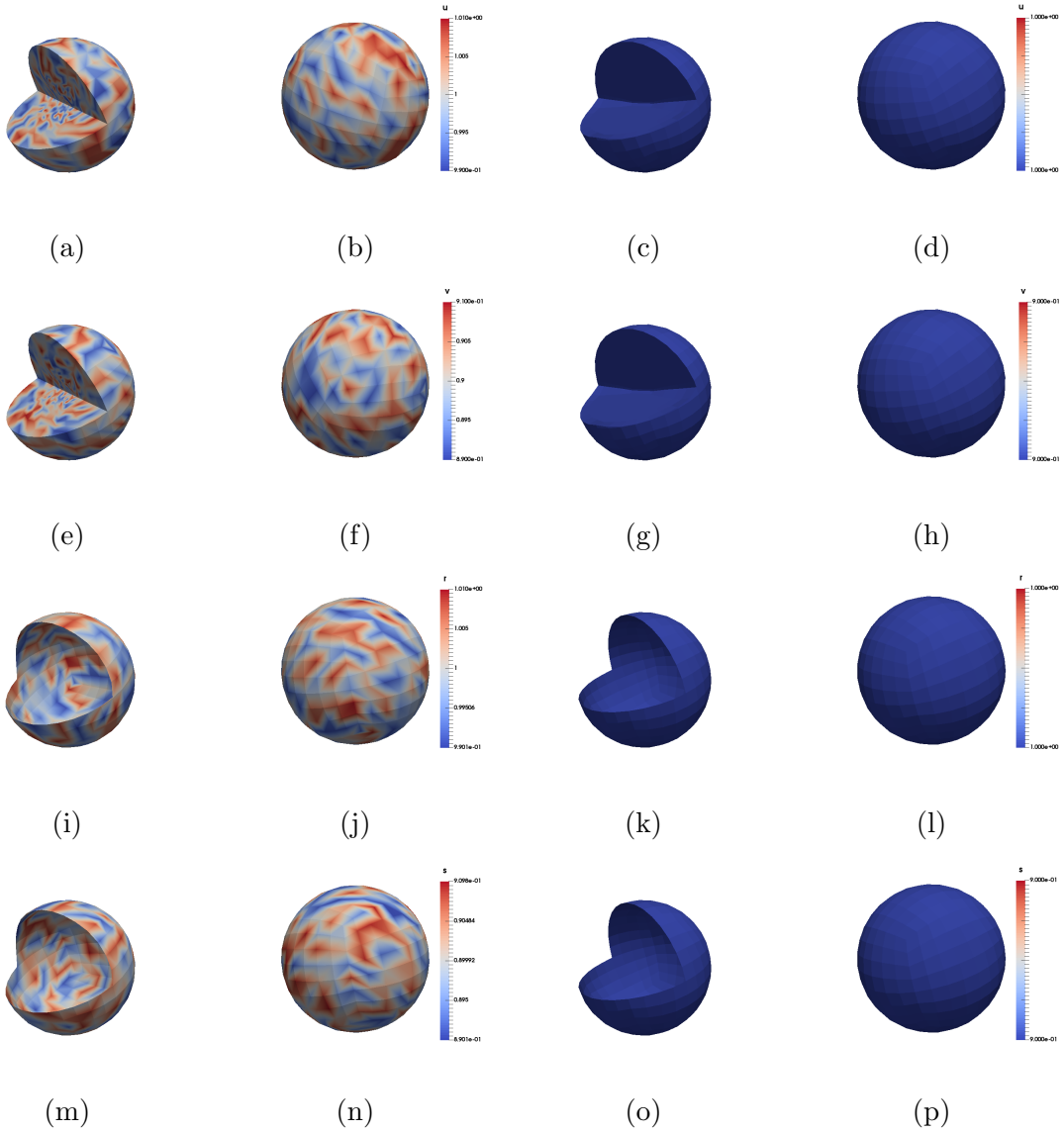

Figure 5.1: Numerical solutions corresponding to the coupled system of BSRDEs given by (4.24) with $d_\Omega = 1$ and $d_\Gamma = 1$ and $\gamma_\Omega = \gamma_\Gamma = 300$. The rows correspond to variables u, v, r and s respectively. The first two columns show the initial profile of concentration with random perturbation near the uniform steady state. The third and fourth columns show the bulk-surface finite element numerical solutions at the final time step at time $t = 10$.

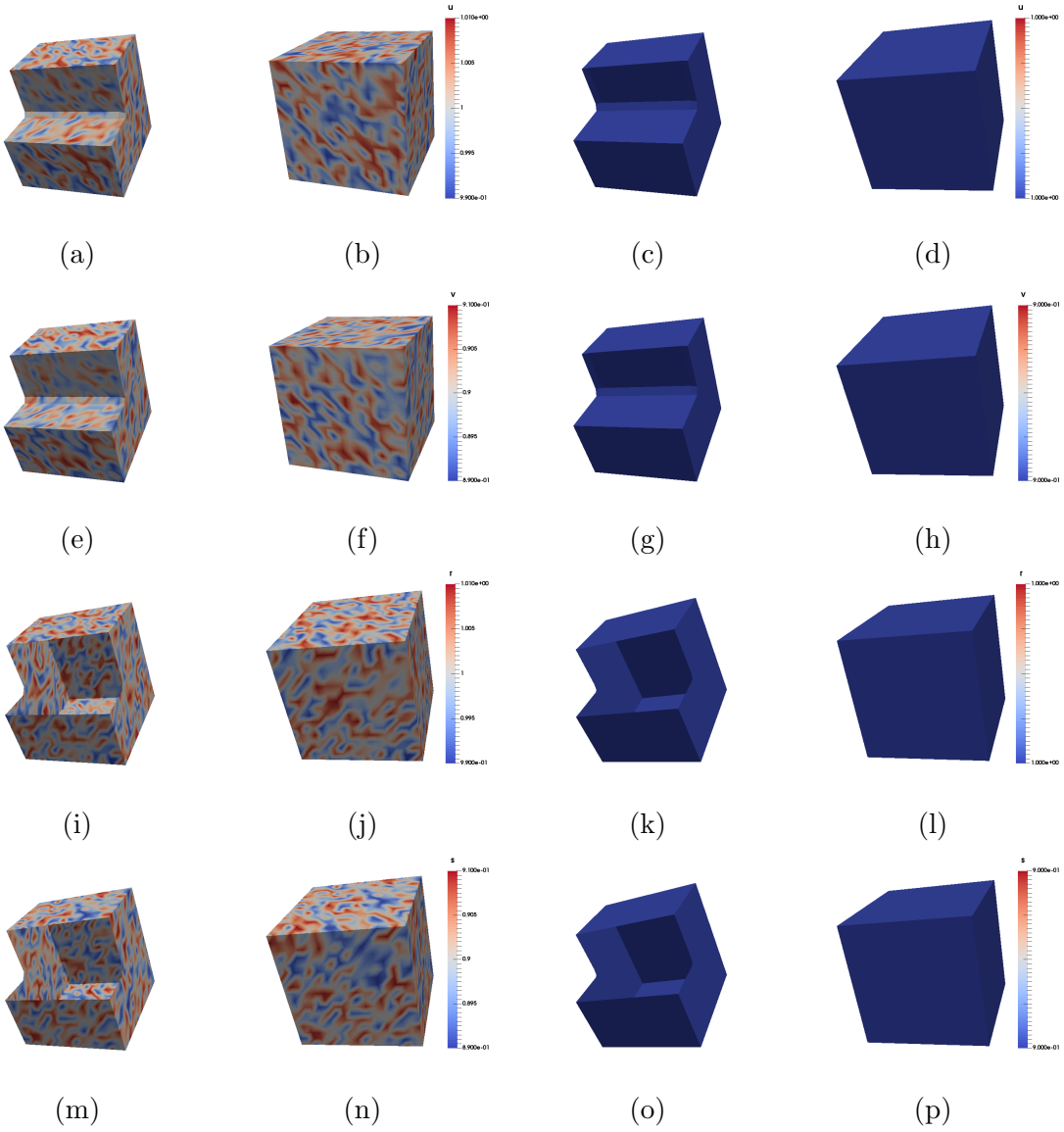

Figure 5.2: Numerical solutions corresponding to the coupled system of BSRDEs given by (4.24) with $d_\Omega = 1$ and $d_\Gamma = 1$ and $\gamma_\Omega = \gamma_\Gamma = 300$. The rows correspond to variables u, v, r and s respectively. The first two columns show the initial profile of concentration with random perturbation near the uniform steady state. The third and fourth columns show the bulk-surface finite element numerical solutions at the final time step at time $t = 10$.

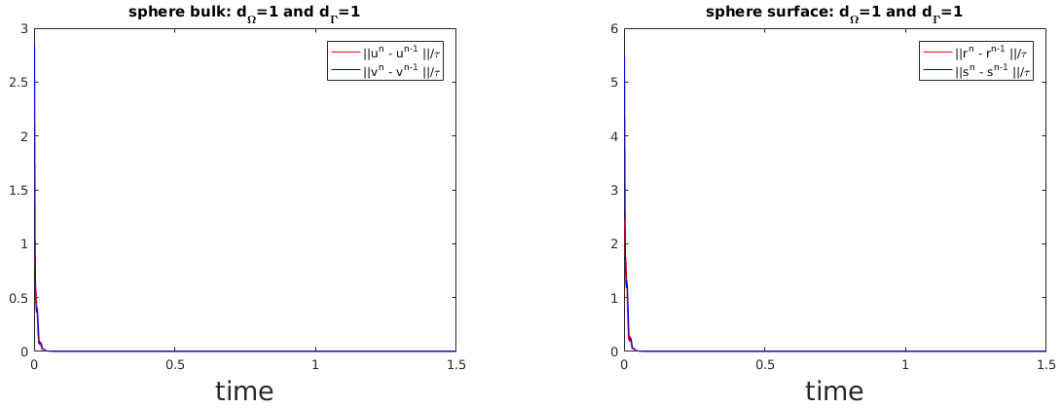

(a) (b)

Figure 5.3: Convergence history corresponding to the coupled system of BSRDEs given by (4.24) with $d_\Omega = 1$, $d_\Gamma = 1$ and $\gamma_\Omega = \gamma_\Gamma = 300$ is shown in the L_2 norm of the discrete time derivative. Sub-figure (a) shows the convergence history for the equations in the bulk, whereas Sub-figure (b) shows the same for equations on the surface.

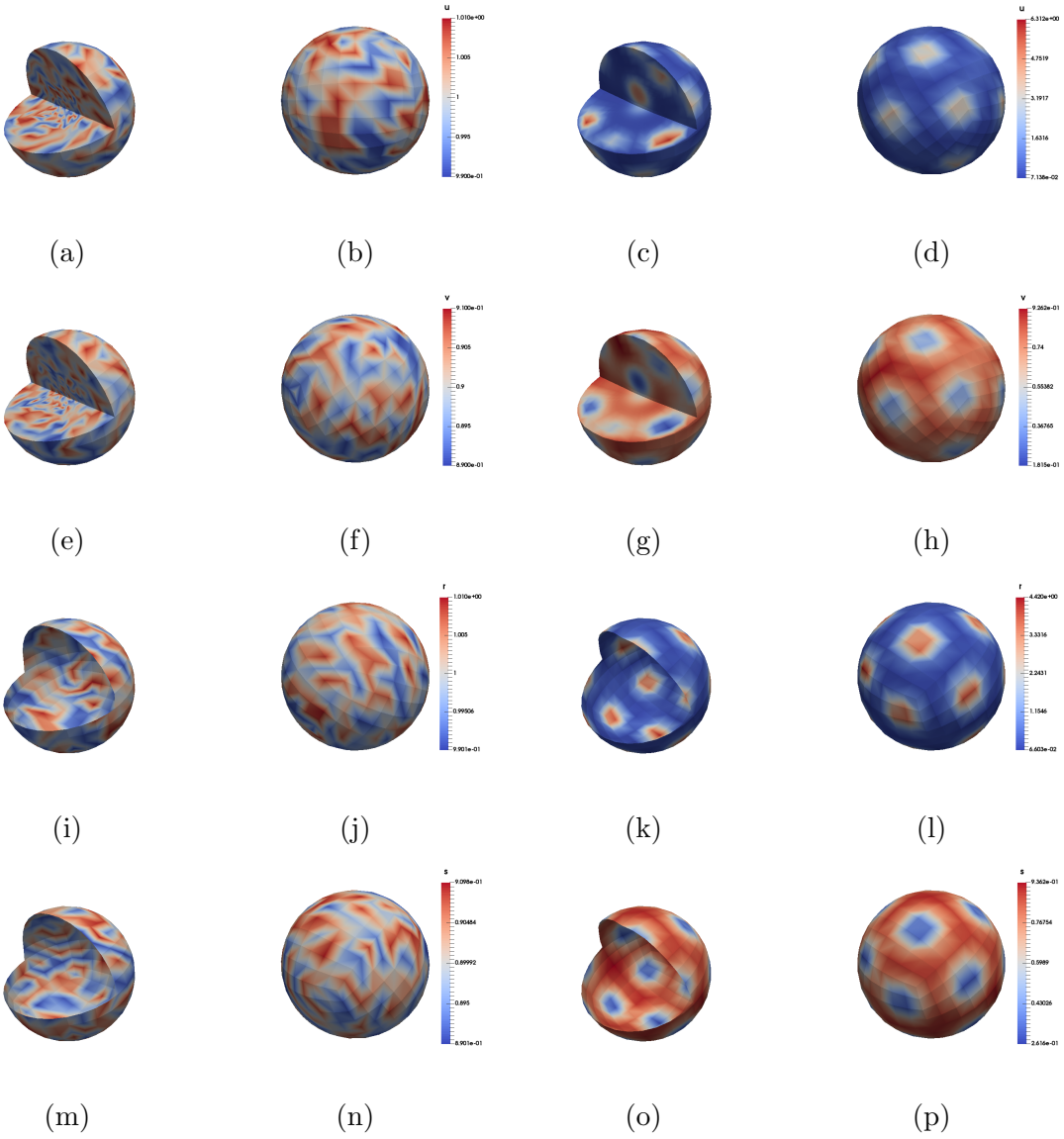

Figure 5.4: Numerical solutions corresponding to the coupled system of BSRDEs given by (4.24) with $d_\Omega = 30$ and $d_\Gamma = 30$ and $\gamma_\Omega = \gamma_\Gamma = 300$. The rows correspond to variables u, v, r and s respectively. The first two columns show the initial profile of concentration with random perturbation near the uniform steady state. The third and fourth columns show the bulk-surface finite element numerical solutions at the final time step at time $t = 10$.

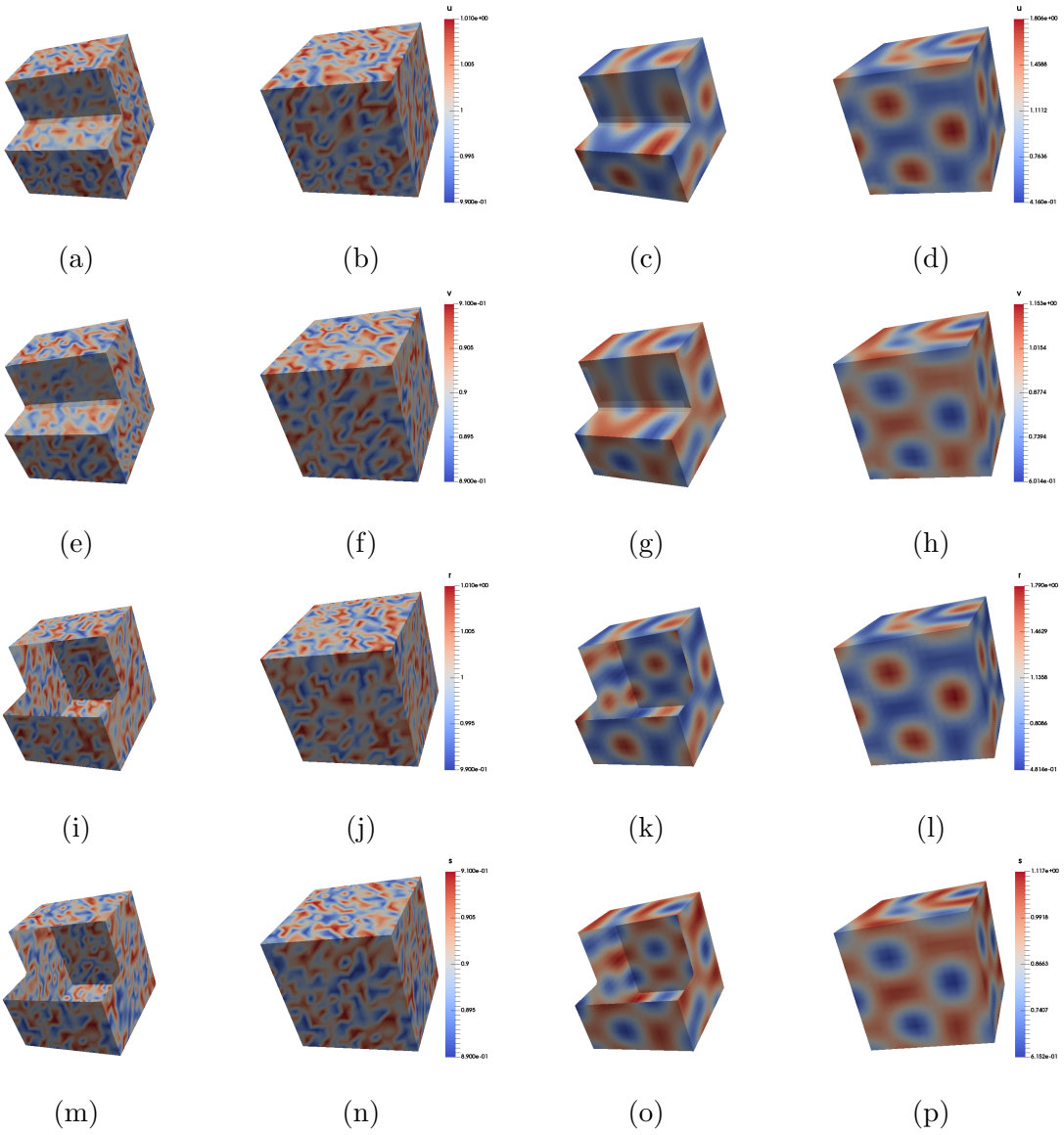

Figure 5.5: Numerical solutions corresponding to the coupled system of BSRDEs given by (4.24) with $d_\Omega = 30$ and $d_\Gamma = 30$ and $\gamma_\Omega = \gamma_\Gamma = 300$. The rows correspond to variables u, v, r and s respectively. The first two columns show the initial profile of concentration with random perturbation near the uniform steady state. The third and fourth columns show the bulk-surface finite element numerical solutions at the final time step at time $t = 10$.

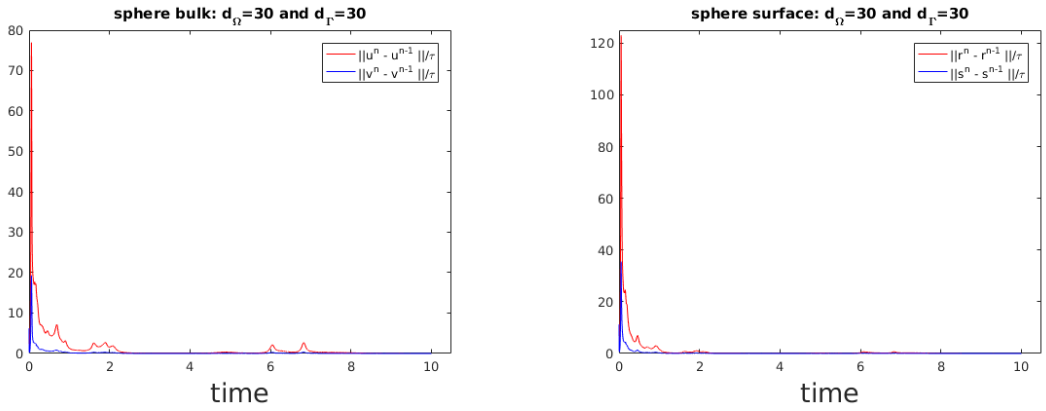

(a) (b)

Figure 5.6: Convergence history corresponding to the coupled system of BSRDEs given by (4.24) with $d_\Omega = 30$, $d_\Gamma = 30$ and $\gamma_\Omega = \gamma_\Gamma = 300$ is shown in the L_2 norm of the discrete time derivative. Sub-figure (a) shows the convergence history for the equations in the bulk, whereas Sub-figure (b) shows the same for equations on the surface

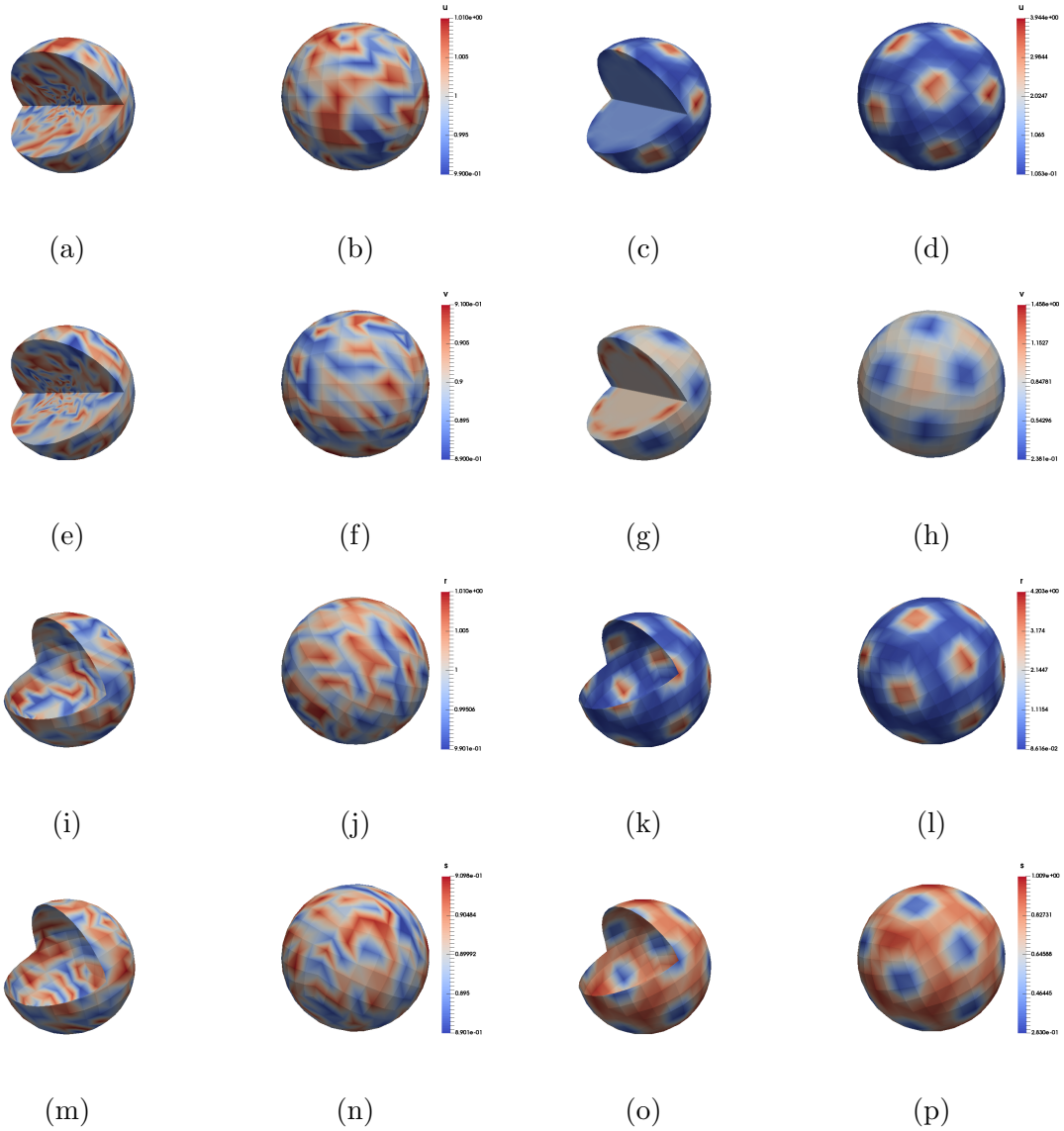

Figure 5.7: Numerical solutions corresponding to the coupled system of BSRDEs given by (4.24) with $d_\Omega = 1$ and $d_\Gamma = 30$ and $\gamma_\Omega = \gamma_\Gamma = 300$. The rows correspond to variables u, v, r and s respectively. The first two columns show the initial profile of concentration with random perturbation near the uniform steady state. The third and fourth columns show the bulk-surface finite element numerical solutions at the final time step at time $t = 10$.

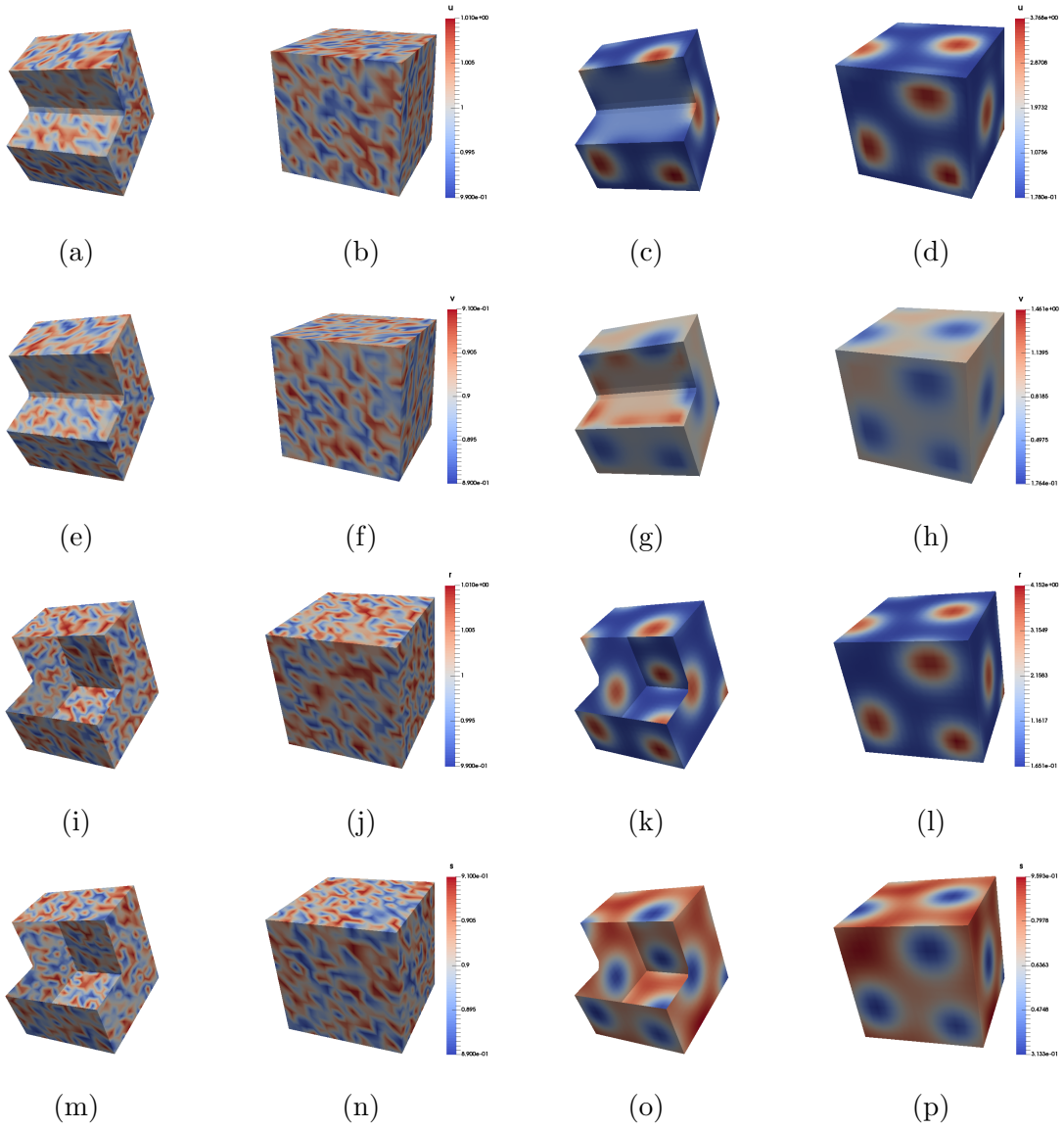

Figure 5.8: Numerical solutions corresponding to the coupled system of BSRDEs given by (4.24) with $d_\Omega = 1$ and $d_\Gamma = 30$ and $\gamma_\Omega = \gamma_\Gamma = 300$. The rows correspond to variables u, v, r and s respectively. The first two columns show the initial profile of concentration with random perturbation near the uniform steady state. The third and fourth columns show the bulk-surface finite element numerical solutions at the final time step at time $t = 10$.

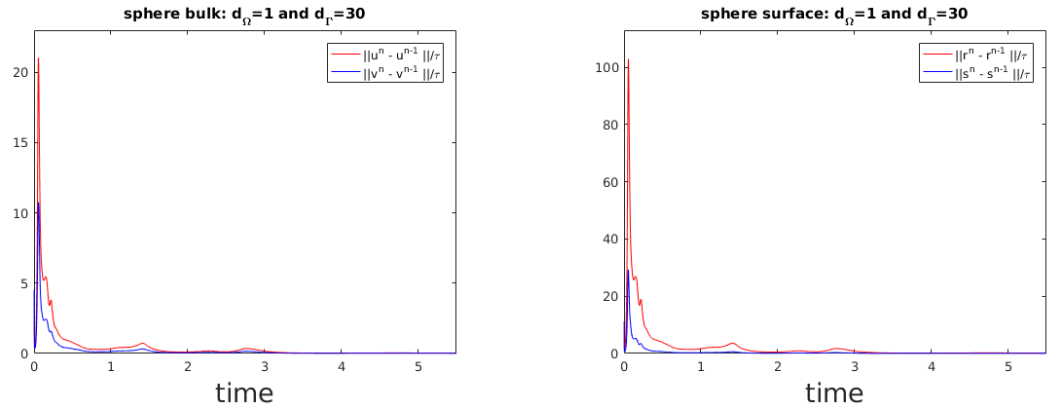

(a) (b)

Figure 5.9: Convergence history corresponding to the coupled system of BSRDEs given by (4.24) with $d_\Omega = 1$, $d_\Gamma = 30$ and $\gamma_\Omega = \gamma_\Gamma = 300$ is shown in the L_2 norm of the discrete time derivative. Sub-figure (a) shows the convergence history for the equations in the bulk, whereas Sub-figure (b) shows the same for equations on the surface.

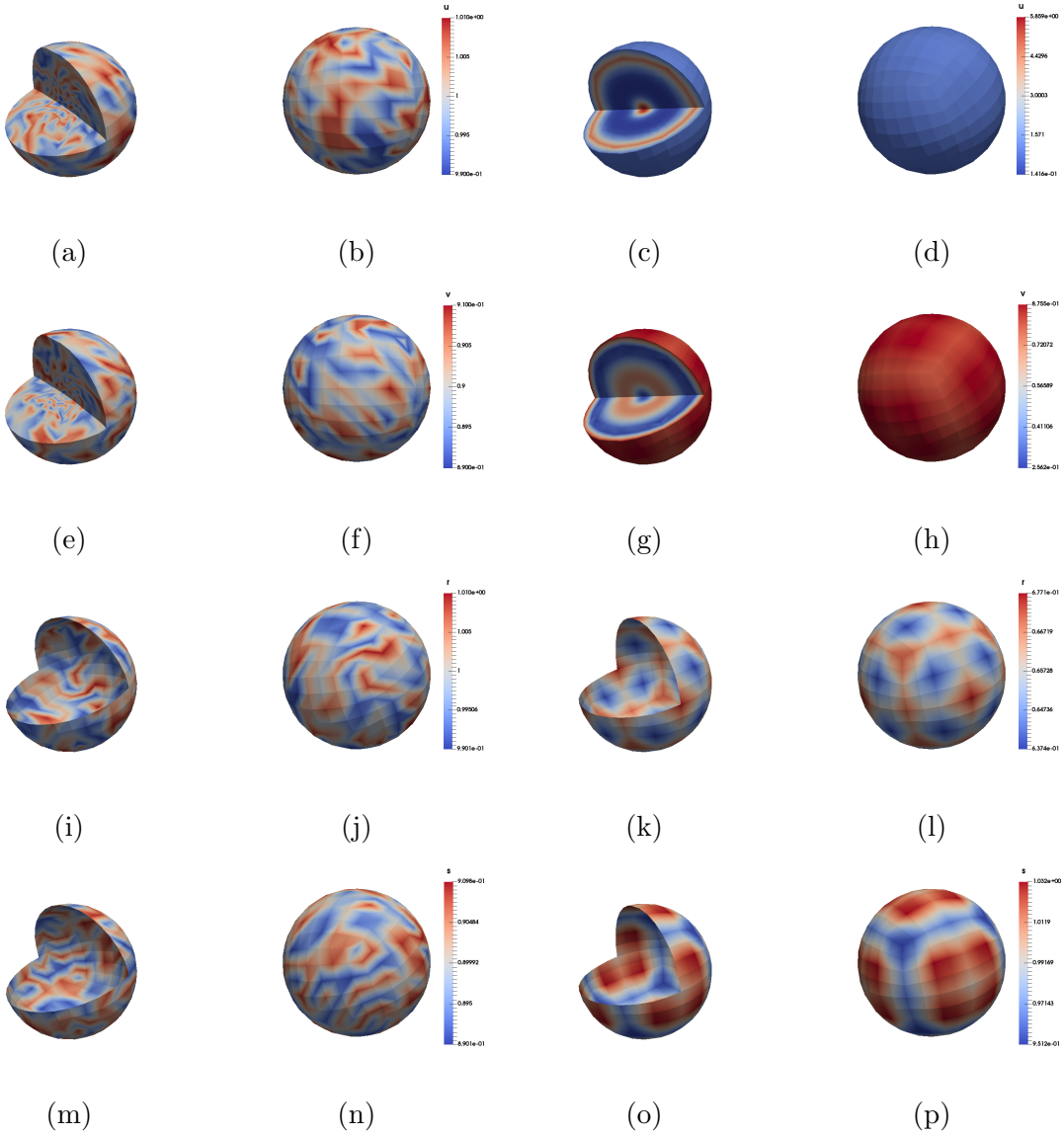

Figure 5.10: Numerical solutions corresponding to the coupled system of BSRDEs given by (4.24) with $d_\Omega = 30$ and $d_\Gamma = 1$ and $\gamma_\Omega = \gamma_\Gamma = 300$. The rows correspond to variables u, v, r and s respectively. The first two columns show the initial profile of concentration with random perturbation near the uniform steady state. The third and fourth columns show the bulk-surface finite element numerical solutions at the final time step at time $t = 10$.

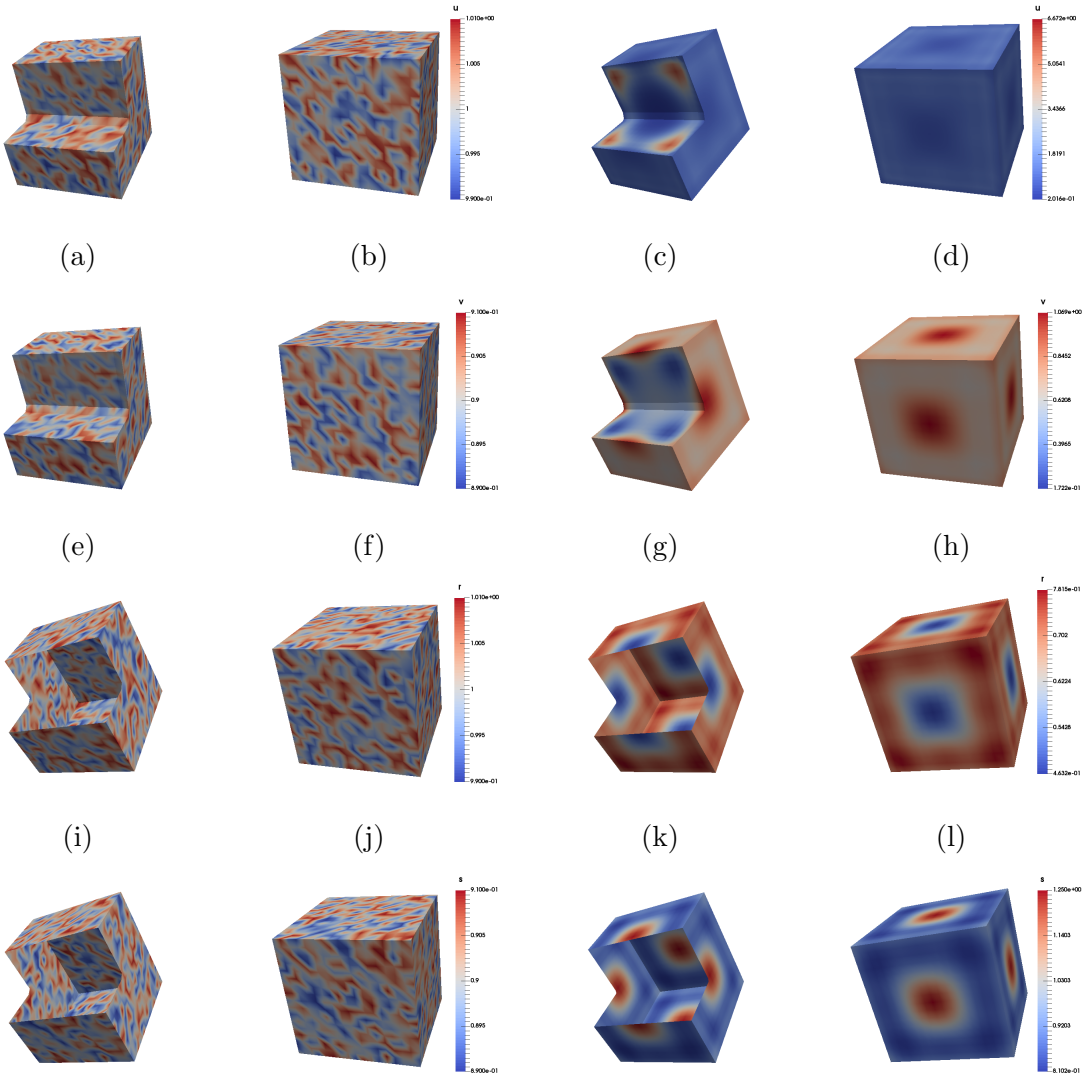

Figure 5.11: Numerical solutions corresponding to the coupled system of BSRDEs given by (4.24) with $d_\Omega = 30$ and $d_\Gamma = 1$ and $\gamma_\Omega = \gamma_\Gamma = 300$. The rows correspond to variables u, v, r and s respectively. The first two columns show the initial profile of concentration with random perturbation near the uniform steady state. The third and fourth columns show the bulk-surface finite element numerical solutions at the final time step at time $t = 10$.

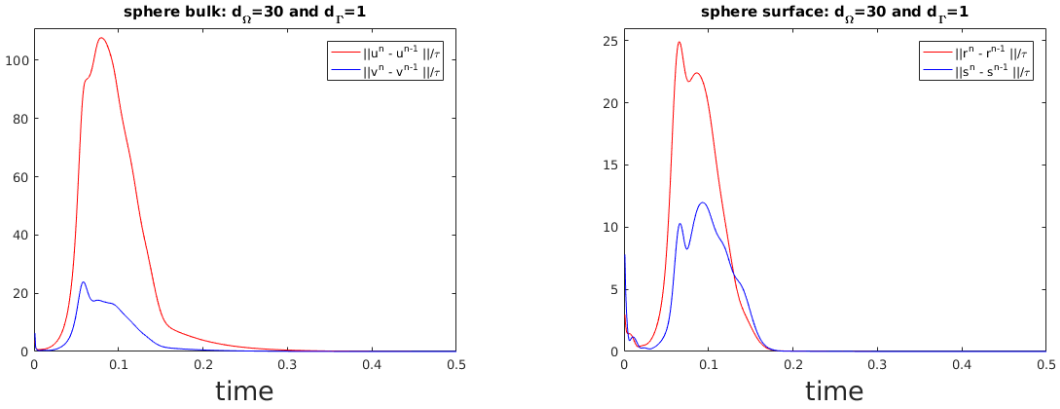

(a) (b)

Figure 5.12: Convergence history corresponding to the coupled system of BSRDEs given by (4.24) with $d_\Omega = 30$, $d_\Gamma = 1$ and $\gamma_\Omega = \gamma_\Gamma = 300$ is shown in the L_2 norm of the discrete time derivative. Sub-figure (a) shows the convergence history for the equations in the bulk, whereas Sub-figure (b) shows the same for equations on the surface.

5.2 Linear reaction kinetics on the surface and non-linear reaction kinetics in the bulk

In simulations for the coupled system of bulk-surface reaction-diffusion equations (4.33) the parameter values are chosen same as in Section 5.1, which are $a_2 = 0.1$ and $b_2 = 0.9$ for Schnakenberg model (Murray, 2001; Madzvamuse, 2000; Madzvamuse et al., 2015a). These values lie within Turing region in parameter spaces Murray (2001); Madzvamuse (2000); Madzvamuse et al. (2015a), and therefore satisfy conditions (2.181)-(2.185). The other parameters are chosen as $q_2 = 2$, $c_2 = 3$ and $j_2 = 6$ which satisfy the compatibility condition (2.145). The proposed theoretical predictions in Theorem 2.2.3 are numerically verified in the sense that the coupled system of bulk-surface reaction-diffusion equations (4.33) exhibits similar properties to those obtained for the case $d_\Omega = 30$ and $d_\Gamma = 1$, where spatial pattern is formed inside the bulk with a possibility to emerge on the surface and also leaving a homogeneous and pattern-less boundary layer. Figures 5.13 and 5.14 reveal the numerical results of such verification, where the reaction kinetics inside the bulk produce spatial pattern which extends to emerge on the surface as well. It is therefore important to realise that the emergence of spatial pattern on the surface under this kind of reaction kinetics does not necessarily imply that the pattern is formed by diffusion-reaction kinetics on the surface, in fact it only means that the emergence of spatial pattern on the surface is a consequence of the spatial pattern formed in the bulk and extends through the coupling conditions to appear on the surface. A distinction that makes the numerical results of this system different from the results obtained for $d_\Omega > 1$ and $d_\Gamma > 1$ in Section 5.1 is that here, the boundary layer where the coupling conditions interact between the bulk and the surface remain pattern-less during the evolution.

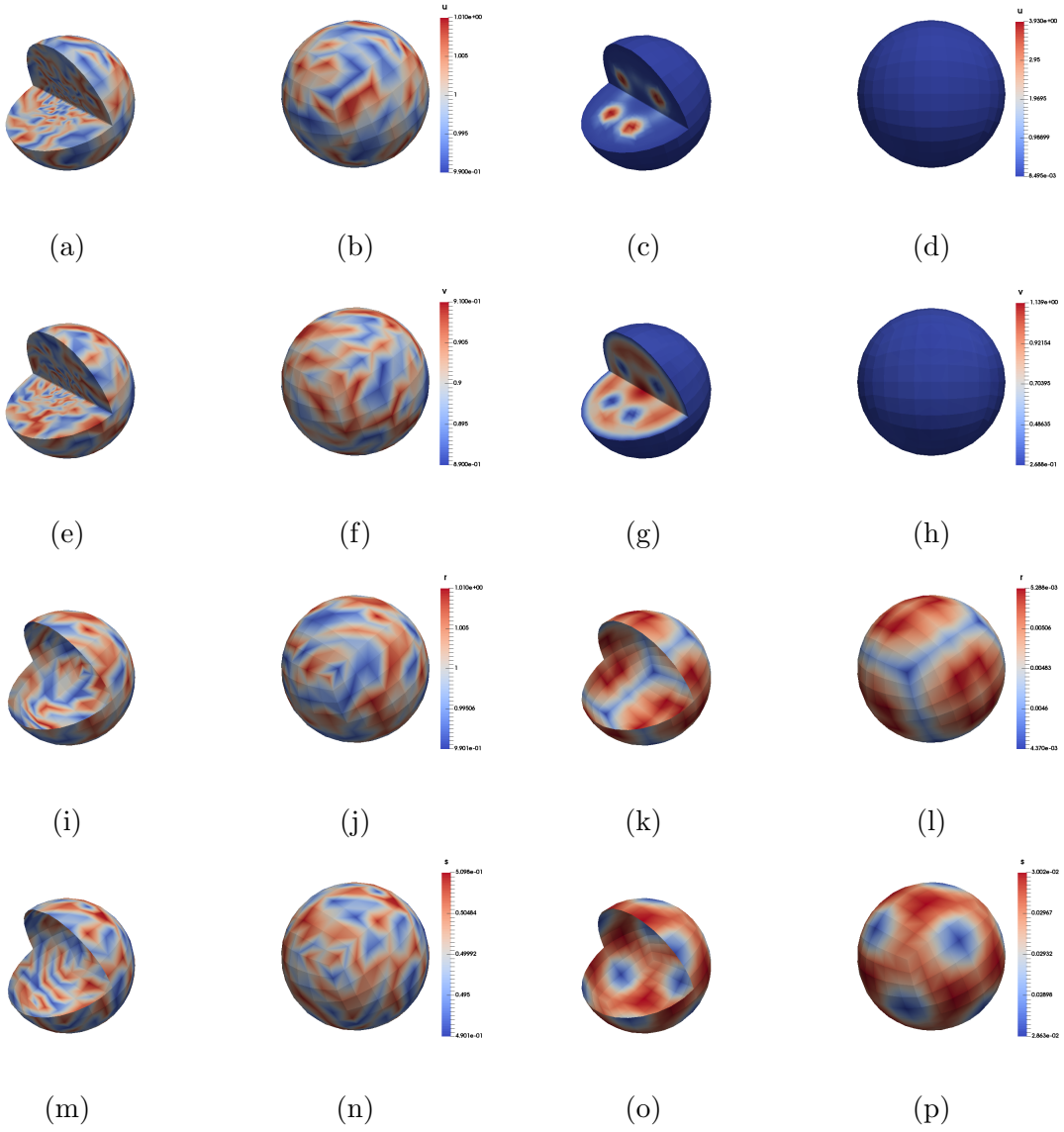

Figure 5.13: Numerical solutions corresponding to the coupled system of BSRDEs given by (4.33) with $d_\Omega = 20$, $d_\Gamma = 20$, $\gamma_\Omega = 500$ and $\gamma_\Gamma = 500$. The rows correspond to variables u, v, r and s respectively. The first two columns show the initial profile of concentration with random perturbation near the uniform steady state. The third and fourth columns show the bulk-surface finite element numerical solutions at the final time step.

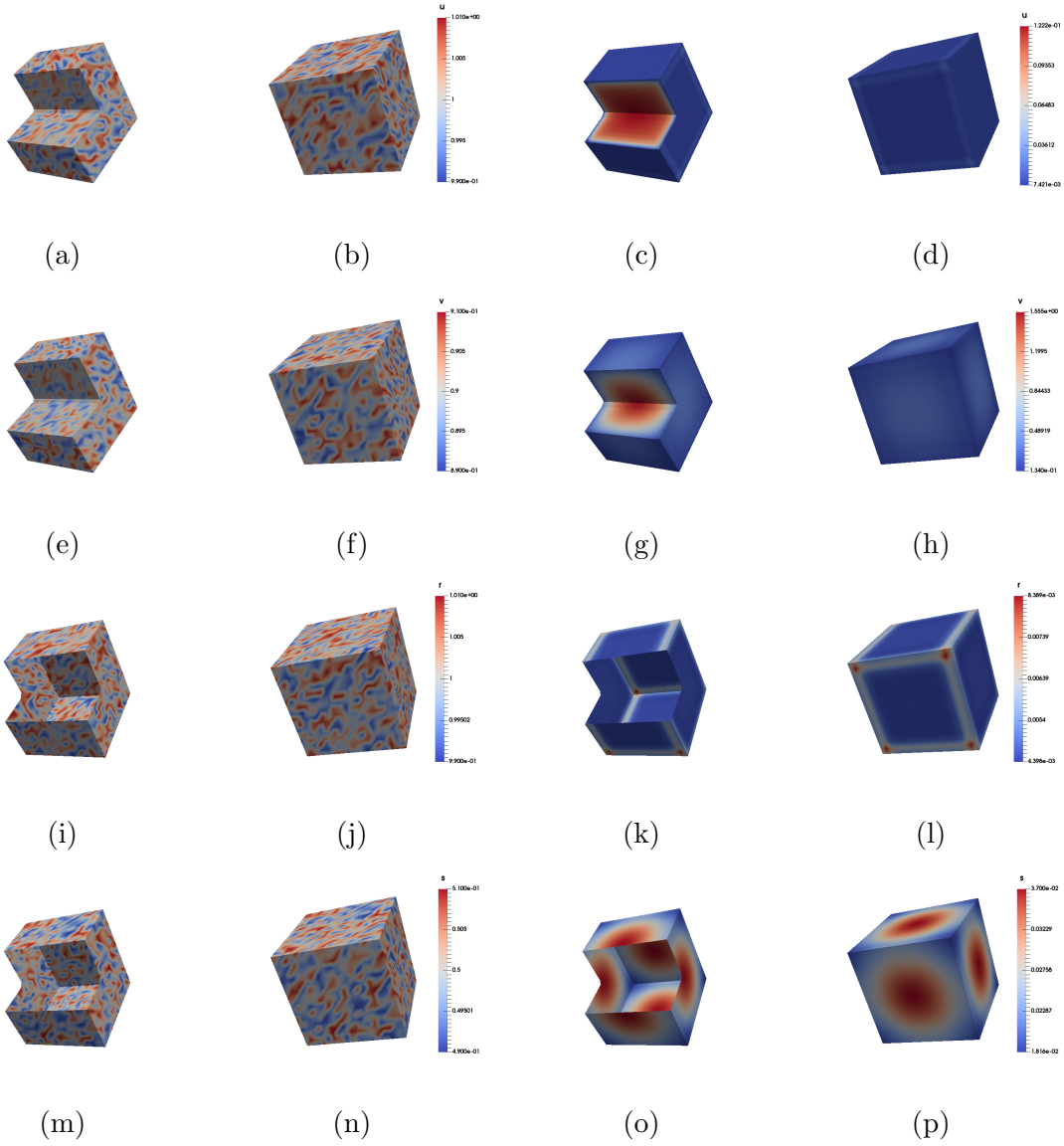

Figure 5.14: Numerical solutions corresponding to the coupled system of BSRDEs given by (4.33) with $d_\Omega = 20$, $d_\Gamma = 20$, $\gamma_\Omega = 500$ and $\gamma_\Gamma = 500$. The rows correspond to variables u, v, r and s respectively. The first two columns show the initial profile of concentration with random perturbation near the uniform steady state. The third and fourth columns show the bulk-surface finite element numerical solutions at the final time step.

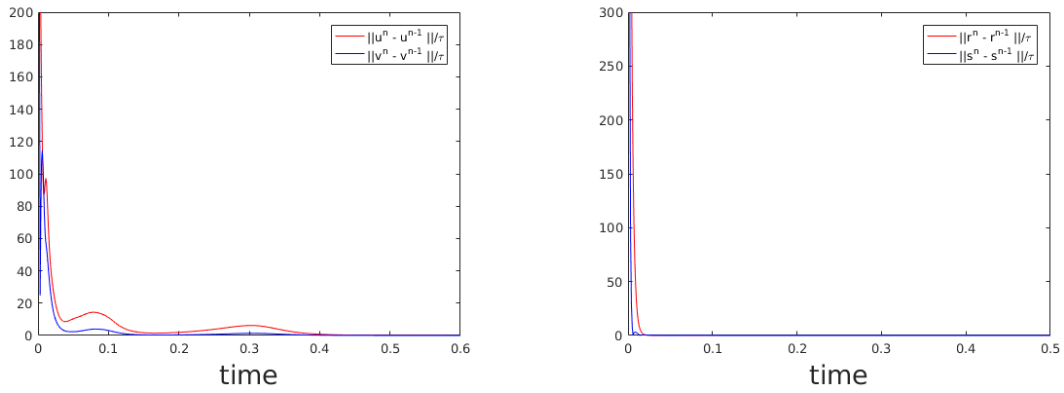

(a) (b)

Figure 5.15: Convergence history corresponding to the coupled system of BSRDEs given by (4.33) with $d_\Omega = 20$, $d_\Gamma = 20$ and $\gamma_\Omega = \gamma_\Gamma = 500$ is shown in the L_2 norm of the discrete time derivative. Sub-figure (a) shows the convergence history for the equations in the bulk, whereas Sub-figure (b) shows the same for equations on the surface.

5.3 Linear reaction kinetics in the bulk and non-linear reaction kinetics on the surface

This section presents numerical simulations verifying the proposed predictions for the coupled system of bulk-surface reaction-diffusion equations (4.42) in Theorem 2.3.3. For the numerical simulations for the coupled system of bulk-surface reaction-diffusion equations (4.42) the parameter values are chosen as $a_2 = 0, \quad b_2 = 0, \quad q = 3, \quad c_1 = 2$ and $z = 4$ which satisfy conditions (2.204). The theoretical results are verified numerically by observing that the numerical solution of the coupled system of bulk-surface reaction-diffusion equations (4.42), induces no spatial pattern in the bulk or on the surface. Figures 5.16, 5.17 and 5.18 provide a numerical verification of the absence of any spatial pattern under the parameter settings in Theorem 2.3.1, and the results are in agreement with Theorem 2.3.3 for both the cubic and spherical domains.

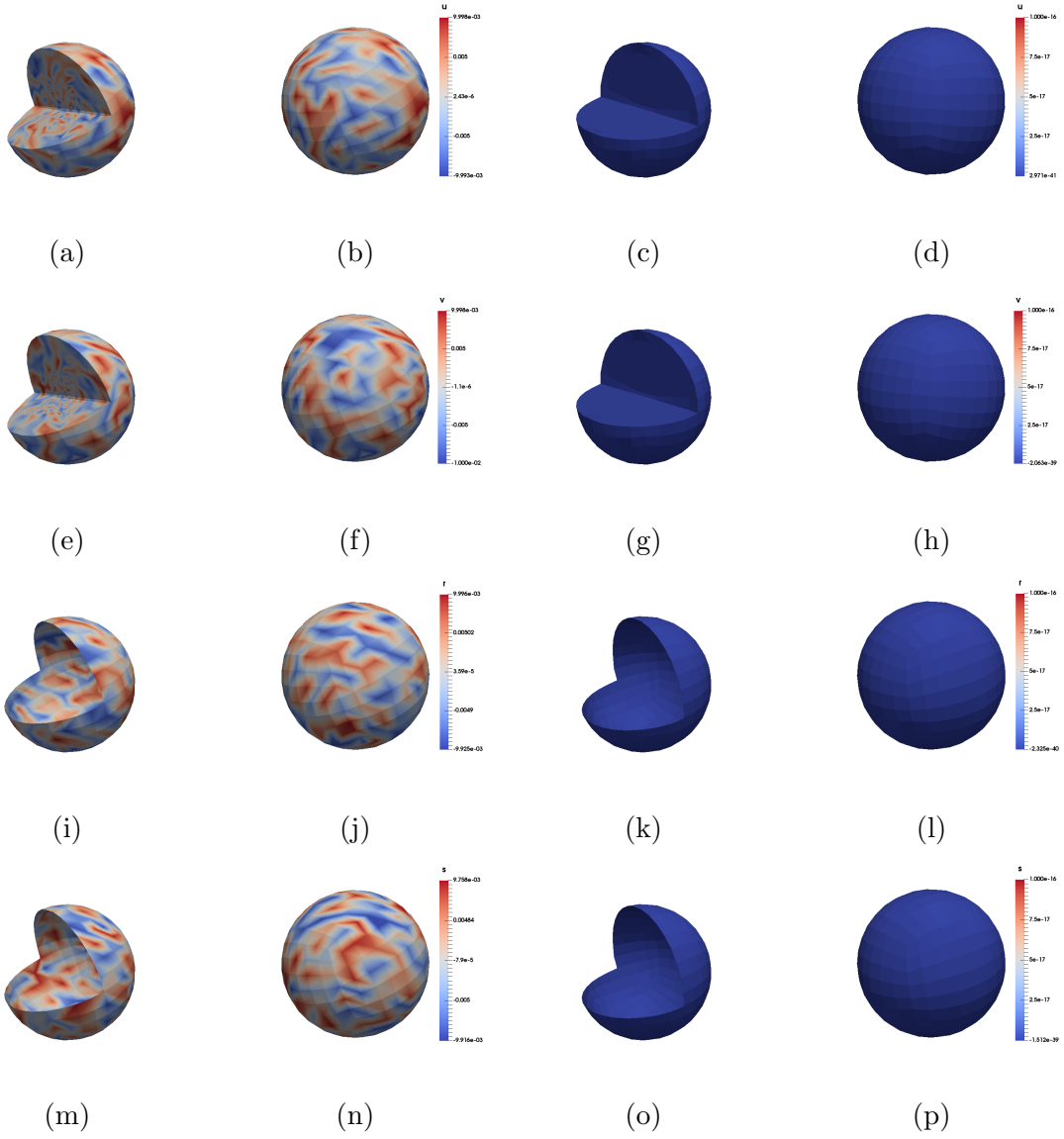

Figure 5.16: Numerical solutions corresponding to the coupled system of BSRDEs given by (4.42) with $d_\Omega = 50$, $d_\Gamma = 50$, $\gamma_\Omega = 240$ and $\gamma_\Gamma = 240$. The rows correspond to variables u, v, r and s respectively. The first two columns show the initial profile of concentration with random perturbation near the uniform steady state. The third and fourth columns show the bulk-surface finite element numerical solutions at the final time step.

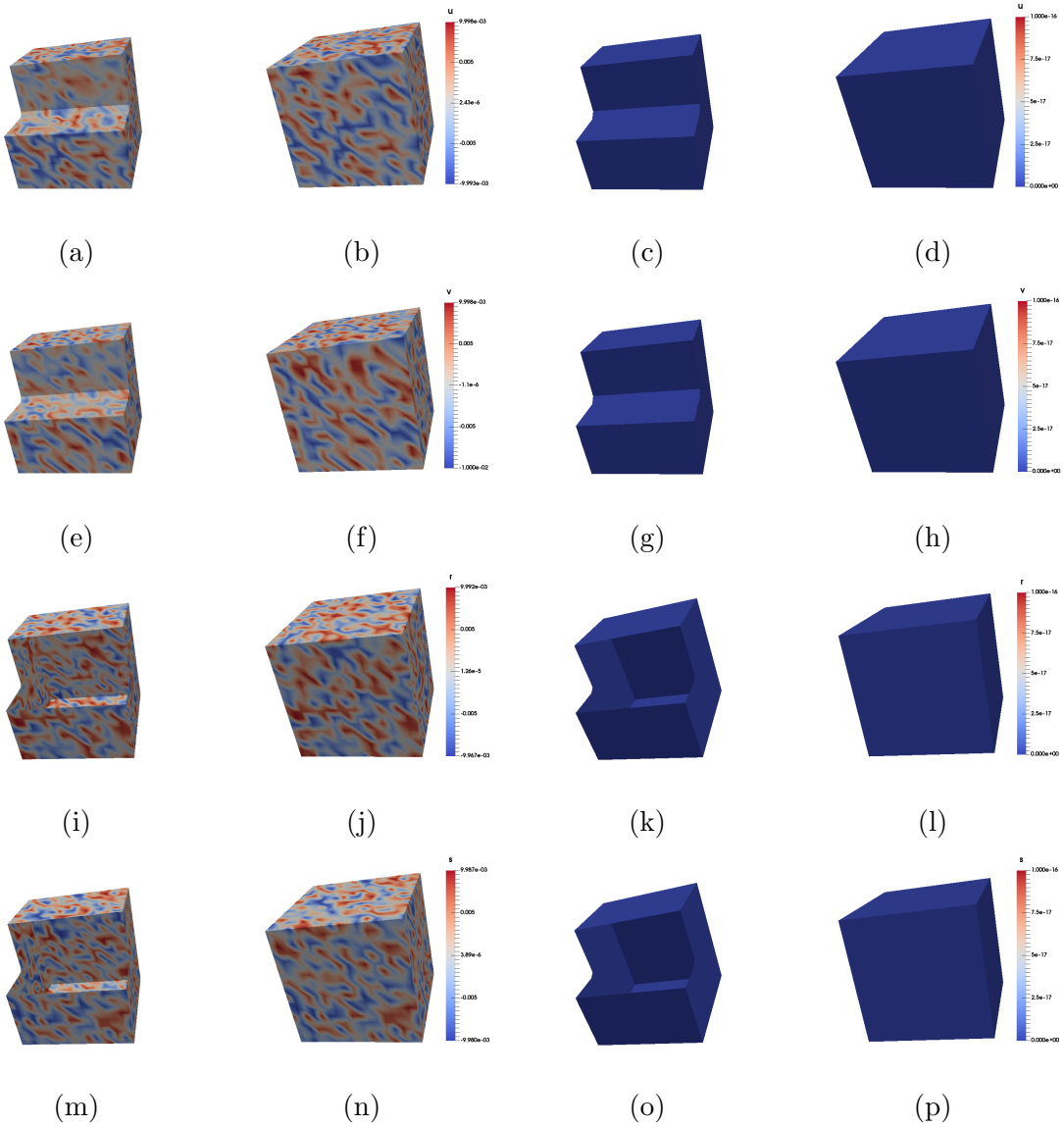

Figure 5.17: Numerical solutions corresponding to the coupled system of BSRDEs given by (4.42) with $d_\Omega = 50$, $d_\Gamma = 50$, $\gamma_\Omega = 240$ and $\gamma_\Gamma = 240$. The rows correspond to variables u, v, r and s respectively. The first two columns show the initial profile of concentration with random perturbation near the uniform steady state. The third and fourth columns show the bulk-surface finite element numerical solutions at the final time step.

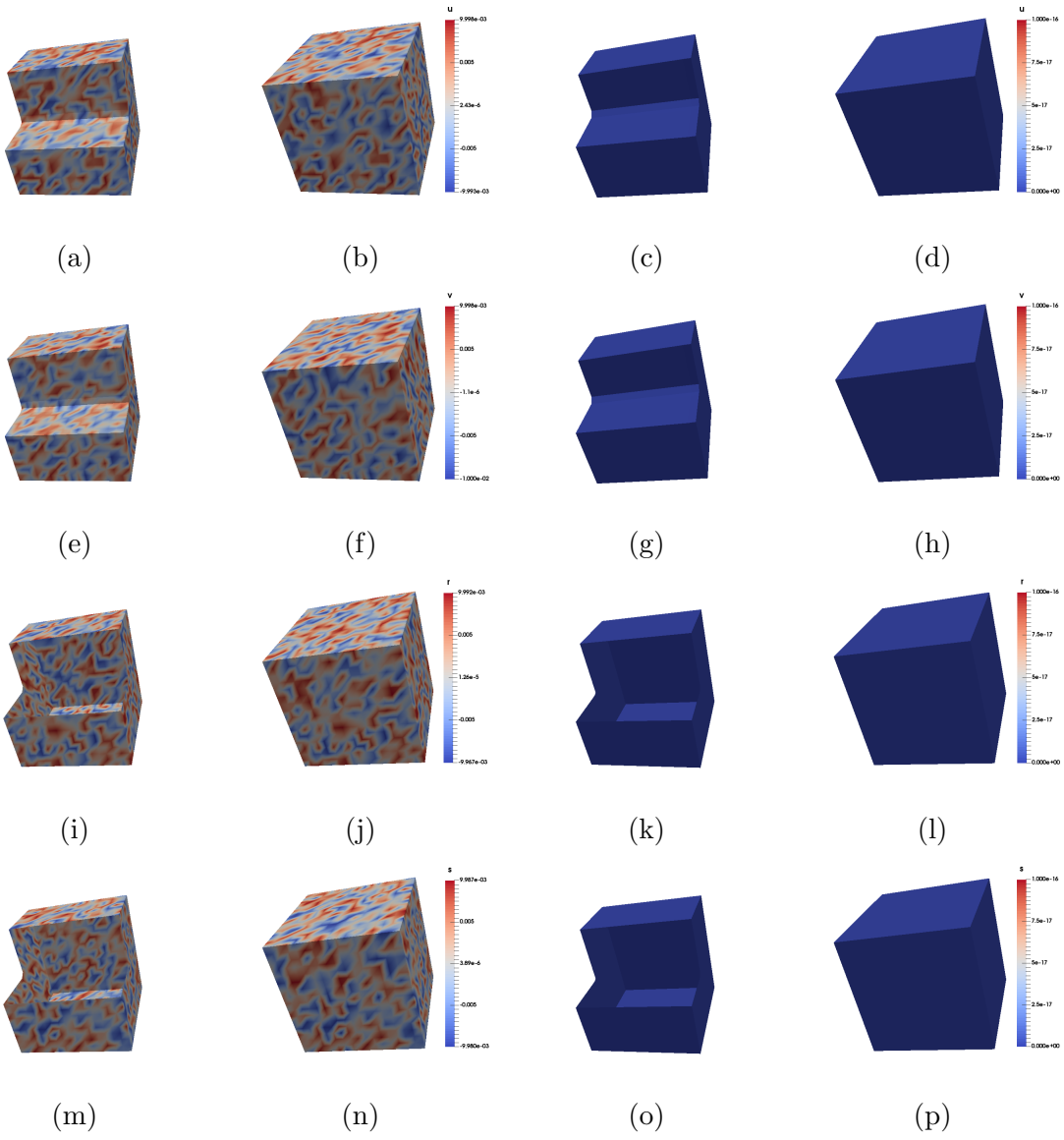

Figure 5.18: Numerical solutions corresponding to the coupled system of BSRDEs given by (4.42) with $d_\Omega = 10$, $d_\Gamma = 10$, $\gamma_\Omega = 500$ and $\gamma_\Gamma = 500$. The rows correspond to variables u, v, r and s respectively. The first two columns show the initial profile of concentration with random perturbation near the uniform steady state. The third and fourth columns show the bulk-surface finite element numerical solutions at the final time step.

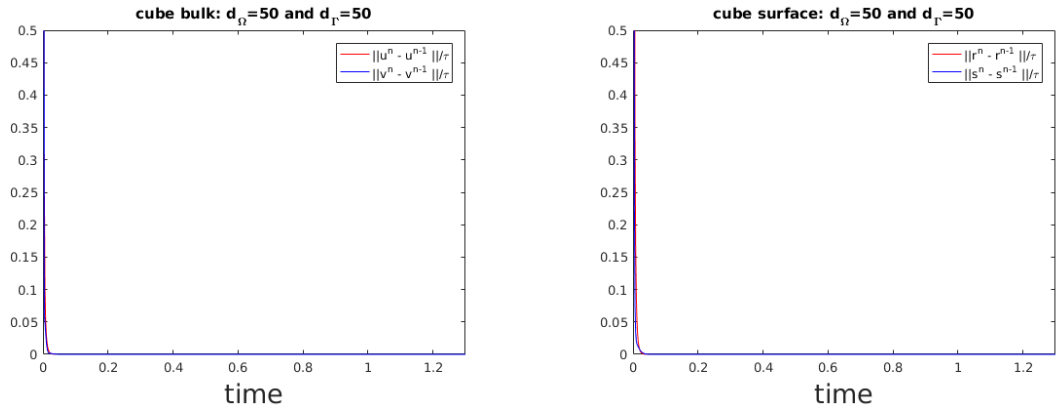

(a) (b)

Figure 5.19: Convergence history corresponding to the coupled system of BSRDEs given by (4.42) with $d_\Omega = 50$, $d_\Gamma = 50$ and $\gamma_\Omega = \gamma_\Gamma = 240$ is shown in the L_2 norm of the discrete time derivative. Sub-figure (a) shows the convergence history for the equations in the bulk, whereas Sub-figure (b) shows the same for equations on the surface.

5.4 Conclusion

The bulk-surface finite element formulation provided in the contents of Chapter 4 was employed to simulate a numerical scheme for all three systems studied in Chapter 2. Parameter choices for all simulations were chosen subject to the admissibility of the necessary and sufficient conditions presented in Chapter 2 and 3 respectively. First the coupled system of bulk-surface reaction-diffusion equations (4.24) with non-linear reaction kinetics in the bulk and on the surface is explored for four different combinations of diffusion ratios. The coupled system of bulk-surface reaction-diffusion equations (4.24) admits the formation of spatial pattern everywhere in the bulk and on the surface provided that the diffusion ratios both in the bulk and on the surface are values greater than 1. If both the diffusion ratios are chosen to be 1, then the coupled system of bulk-surface reaction-diffusion equations (4.24) returns to the uniform steady state forming no pattern at all. If the diffusion ratio only in the bulk is larger than 1, then spatial pattern is admitted inside the bulk with possible emergence on the surface as well, which is due to the coupling conditions between the bulk and its boundary (surface). If the diffusion ratio only on the surface is chosen greater than 1, then spatial patterns can be formed on the surface,

which also forms a patterned boundary layer and the dynamics fail to induce any pattern in the interior of the bulk. In the coupled system of bulk-surface reaction-diffusion equations (4.33), non-linear kinetics are posed inside the bulk which are coupled with linear reaction-kinetics on the surface. Numerical simulation for this system produces pattern in the interior of the bulk as well as on the surface, with no pattern on the interface of the bulk near the surface. In the coupled system of bulk-surface reaction-diffusion equations (4.42) linear reaction kinetics are posed inside the bulk, which are coupled with non-linear kinetics on the surface. This system only admits a trivial zero steady state, which induces a parameter condition for stability on equations in the bulk, such that it prevents diffusion-driven instability from happening and hence the system fails to produce spatial pattern at all.

Chapter 6

Conclusion and Future Work

6.1 Conclusion

Bulk-surface reaction-diffusion systems are explored through studying combinations of linear and non-linear reaction kinetics with linear Robin-type boundary conditions. If non-linear reaction kinetics are posed both in the bulk and on the surface, then with appropriate parameter choices, such a system is able to give rise to pattern formation everywhere. Parameters can also be chosen for this system such that pattern emerges in the bulk and extends to the surface, however it forms no pattern on the internal boundary layer. It is worth noting that the emergence of no pattern in the internal boundary layer is a consequence of parameter choice in the first system and not the exhaustive results associated to it. The results with patterned bulk and surface and no pattern on the internal boundary layer can also be obtained through the second system with non-linear reaction kinetics in the bulk and linear reaction kinetics on the surface. This combination of reaction kinetics is not capable of giving rise to pattern everywhere and the pattern that it emerges on the surface is a consequence of patterning extension from the bulk since linear kinetics on the surface do not satisfy the necessary conditions for diffusion-driven instability. If linear reaction kinetics are posed in the bulk with non-linear reaction kinetics on the surface, then the system is found to evolve with no spatial pattern at all. It means that this combination of reaction kinetics prevents all the necessary conditions required for diffusion-driven instability. It happens mainly because with this combination of reaction kinetics the only uniform steady state admitted

is the trivial zero steady state, therefore, failing to satisfy conditions for diffusion-driven instability. Hence, the dynamics uniformly converge to the trivial zero steady state. The existence of a unique excitable wavenumber is found through employing critical diffusion ratio. The existence of critical wavenumber together with computationally derived (through the results of Chapter 2) provide a full set of necessary and sufficient conditions for diffusion-driven instability. Two types of time-stepping schemes namely first order IMEX and 2-SBDF were considered on a decoupled bulk-surface reaction-diffusion system to explore their respective convergence rates and it was found that 2-SBDF outperforms the first order IMEX. The weak formulation of coupled bulk-surface reaction-diffusion system was obtained to set-up the premises for discretisation in space through employing the standard finite element method. The full coupled system of BSRDEs was simulated using a fully implicit time-stepping scheme through the application of an extended form of Newton's method for vector valued functions. Using a fully implicit time-stepping scheme, we numerically demonstrate that the first system allows patterns to emerge everywhere and the second system emerges pattern inside the bulk and on the surface with a pattern-less boundary layer. Finally, we also demonstrated that the third system evolves to only converge to a homogeneous uniform steady state without any pattern formation at all.

6.2 Future work

A possible direction to extend the current framework is to explore a system with different types of non-linear reaction kinetics such as Gierer-Meinhardt reaction kinetics in the bulk and Schnakenberg reaction kinetics on the surface or vice versa. It is interesting to reveal whether the pattern formation properties found in the scope of this thesis continue to be true for other types of non-linear reaction kinetics. In the third system in Chapter 2 we found that if the coupled system fails to satisfy conditions for diffusion-driven instability then no spatial pattern emerges. This poses an interesting question to study whether employing non-linear Robin-type coupling conditions (instead of linear Robin-type) could change these results or is it that the non-existence of spatial pattern is embedded in the choice of reaction

kinetics posed on the surface and in the bulk. A further direction for extending this framework is to include domain-growth in the formulation. Studying reaction-diffusion systems on time-dependent domains is important because the formulation of such systems from real-world applications usually take place on continuously evolving domains. The results of the current thesis can also be employed to explore the dynamics responsible for cell motility, which is one of the most studied areas of research in mathematical biology. Application of the results of this study could improve our insight on the idea of symmetry breaking in animal embryos, which is an attractive topic in developmental biology. This can be achieved by using a bulk-surface approach to the process of symmetry breaking instead of the routinely used approach of standard reaction-diffusion system. The results of bulk-surface reaction-diffusion system on spherical geometries can also be employed to model the reaction-diffusion process of chemo-taxis inside and on the surface of a solid tumour.

Bibliography

Arfken, G. and Weber, H. (2005). Mathematical methods for physicists 6th ed. by george b. *Arfken and Hans J. Weber. Published: Amsterdam*. 8, 19, 27, 28, 29

Bangerth, W., Heister, T., Heltai, L., Kanschat, G., Kronbichler, M., Maier, M., Turcksin, B., et al. (2016). The deal. ii library, version 8.3. *Archive of Numerical Software*, 4(100):1–11. vii, 6, 79, 99, 112

Barreira, R., Elliott, C. M., and Madzvamuse, A. (2011). The surface finite element method for pattern formation on evolving biological surfaces. *Journal of mathematical biology*, 63(6):1095–1119. 88

Brenner, S. and Scott, R. (2007). *The mathematical theory of finite element methods*, volume 15. springer science & business media, Germany. 73, 98

Bruce, A., Johnson, A., Lewis, J., Raff, M., Roberts, K., and Walter, P. (2007). Molecular biology of the cell 5th edn (new york: Garland science). 7

Castets, V., Dulos, E., Boissonade, J., and De Kepper, P. (1990). Experimental evidence of a sustained standing turing-type nonequilibrium chemical pattern. *Physical Review Letters*, 64(24):2953. 2

Chaplain, M. A., Ganesh, M., and Graham, I. G. (2001). Spatio-temporal pattern formation on spherical surfaces: numerical simulation and application to solid tumour growth. *Journal of mathematical biology*, 42(5):387–423. 27, 28, 68

Chechkin, A. V., Zaid, I. M., Lomholt, M. A., Sokolov, I. M., and Metzler, R. (2012). Bulk-mediated diffusion on a planar surface: full solution. *Physical Review E*, 86(4):041101. 2

De Boer, R. J., Segel, L. A., and Perelson, A. S. (1992). Pattern formation in one-and two-dimensional shape-space models of the immune system. *Journal of theoretical biology*, 155(3):295–333. 1

Dziuk, G. and Elliott, C. M. (2013a). Finite element methods for surface pdes. *Acta Numerica*, 22:289–396. 9, 10

Dziuk, G. and Elliott, C. M. (2013b). Finite element methods for surface pdes. *Acta Numerica*, 22:289–396. 88

Elliott, C. M. and Ranner, T. (2013). Finite element analysis for a coupled bulk–surface partial differential equation. *IMA Journal of Numerical Analysis*, 33(2):377–402. 3, 4

Elliott, C. M. and Ranner, T. (2014). A computational approach to an optimal partition problem on surfaces. *arXiv preprint arXiv:1408.2355*. 88

Elliott, C. M., Ranner, T., and Venkataraman, C. (2017). Coupled bulk-surface free boundary problems arising from a mathematical model of receptor-ligand dynamics. *SIAM Journal on Mathematical Analysis*, 49(1):360–397. 4

Evans, L. (1998). Partial differential equations (graduate studies in mathematics vol 19)(providence, ri: American mathematical society). 9

Gantmacher, F., Brenner, J., Bushaw, D., Evanusa, S., and Morse, P. M. (1960). Applications of the theory of matrices. *Physics Today*, 13:56. 9

Garcke, H., Kampmann, J., Rätz, A., and Röger, M. (2016). A coupled surface-cahn–hilliard bulk-diffusion system modeling lipid raft formation in cell membranes. *Mathematical Models and Methods in Applied Sciences*, 26(06):1149–1189. 7

George, U. Z. (2012). *A numerical approach to studying cell dynamics*. PhD thesis, University of Sussex, UK. 14, 15

Gierer, A. and Meinhardt, H. (1972). A theory of biological pattern formation. *Kybernetik*, 12(1):30–39. 10, 14, 39, 48

Gilbarg, D. and Trudinger, N. S. (2015). *Elliptic partial differential equations of second order*. springer. 8

Hagberg, A. and Meron, E. (1994). Pattern formation in non-gradient reaction-diffusion systems: the effects of front bifurcations. *Nonlinearity*, 7(3):805. 5

Hahn, A., Held, K., and Tobiska, L. (2014). Modelling of surfactant concentration in a coupled bulk surface problem. *PAMM*, 14(1):525–526. 7

Hansbo, P., Larson, M. G., and Zahedi, S. (2016). A cut finite element method for coupled bulk-surface problems on time-dependent domains. *Computer Methods in Applied Mechanics and Engineering*, 307:96–116. 3

Hueso, J. L., Martínez, E., and Torregrosa, J. R. (2009). Modified newtons method for systems of nonlinear equations with singular jacobian. *Journal of Computational and Applied Mathematics*, 224(1):77–83. 74

Hutson, V. (1988). Reaction-diffusion equations and their applications to biology. *Bulletin of the London Mathematical Society*, 20(2):185–186. 1

Iron, D., Wei, J., and Winter, M. (2004). Stability analysis of turing patterns generated by the schnakenberg model. *Journal of mathematical biology*, 49(4):358–390. 5

Janssen, H.-K. (1981). On the nonequilibrium phase transition in reaction-diffusion systems with an absorbing stationary state. *Zeitschrift für Physik B Condensed Matter*, 42(2):151–154. 1

Keener, J. P. and Sneyd, J. (1998). *Mathematical physiology*, volume 1. Springer. 1

Kondo, S. and Asai, R. (1995). A reaction–diffusion wave on the skin of the marine angelfish pomacanthus. *Nature*, 376(6543):765. 1

Krischer, K. and Mikhailov, A. (1994). Bifurcation to traveling spots in reaction-diffusion systems. *Physical review letters*, 73(23):3165. 5

Lakkis, O., Madzvamuse, A., and Venkataraman, C. (2013). Implicit–explicit timestepping with finite element approximation of reaction–diffusion systems on evolving domains. *SIAM Journal on Numerical Analysis*, 51(4):2309–2330. 10, 14, 39, 48

Levine, H. and Rappel, W.-J. (2005). Membrane-bound turing patterns. *Physical Review E*, 72(6):061912. 2, 6

Logan, J. D. (2008). *An introduction to nonlinear partial differential equations*, volume 89. John Wiley & Sons. 1

Madzvamuse, A. (2000). *A numerical approach to the study of spatial pattern formation.* PhD thesis, University of Oxford, UK. 10, 14, 15, 63, 65, 112, 126

Madzvamuse, A. (2006). Time-stepping schemes for moving grid finite elements applied to reaction–diffusion systems on fixed and growing domains. *Journal of computational physics*, 214(1):239–263. 78, 79

Madzvamuse, A. and Chung, A. H. (2014). Fully implicit time-stepping schemes and non-linear solvers for systems of reaction–diffusion equations. *Applied Mathematics and Computation*, 244:361–374. 4, 75, 78

Madzvamuse, A., Chung, A. H., and Venkataraman, C. (2015a). Stability analysis and simulations of coupled bulk-surface reaction–diffusion systems. In *Proc. R. Soc. A*, volume 471, page 20140546. The Royal Society. 5, 6, 14, 19, 42, 112, 126

Madzvamuse, A., Gaffney, E. A., and Maini, P. K. (2010). Stability analysis of non-autonomous reaction-diffusion systems: the effects of growing domains. *Journal of mathematical biology*, 61(1):133–164. 38, 47

Madzvamuse, A., Ndakwo, H. S., and Barreira, R. (2015b). Cross-diffusion-driven instability for reaction-diffusion systems: analysis and simulations. *Journal of mathematical biology*, 70(4):709–743. 38, 47

Madzvamuse, A., Ndakwo, H. S., and Barreira, R. (2016). Stability analysis of reaction-diffusion models on evolving domains: the effects of cross-diffusion. *Discrete and Continuous Dynamical Systems-Series A*, 36(4):2133–2170. 38, 47

Mullins, M. C., Hammerschmidt, M., Kane, D. A., Odenthal, J., Brand, M., Van Eeden, F., Furutani-Seiki, M., Granato, M., Haffter, P., Heisenberg, C.-P., et al. (1996). Genes establishing dorsoventral pattern formation in the zebrafish embryo: the ventral specifying genes. *Development*, 123(1):81–93. 1

Murray, J. D. (1981). A pre-pattern formation mechanism for animal coat markings. *Journal of Theoretical Biology*, 88(1):161–199. 1

Murray, J. D. (2001). *Mathematical Biology. II Spatial Models and Biomedical Applications* {*Interdisciplinary Applied Mathematics V. 18*}. Springer-Verlag New York Incorporated. 2, 14, 17, 24, 37, 44, 47, 53, 60, 112, 126

Novak, I. L., Gao, F., Choi, Y.-S., Resasco, D., Schaff, J. C., and Slepchenko, B. M. (2007). Diffusion on a curved surface coupled to diffusion in the volume: Application to cell biology. *Journal of computational physics*, 226(2):1271–1290. 3

Ouyang, Q. and Swinney, H. L. (1991). Transition from a uniform state to hexagonal and striped turing patterns. *Nature*, 352(6336):610. 3

Prigogine, I. and Lefever, R. (1968). Symmetry breaking instabilities in dissipative systems. ii. *The Journal of Chemical Physics*, 48(4):1695–1700. 10, 14, 39, 48

Quarteroni, A., Sacco, R., and Saleri, F. (2010). *Numerical mathematics*, volume 37. springer science & business media, Germany. 74

Rätz, A. and Röger, M. (2014). Symmetry breaking in a bulk–surface reaction–diffusion model for signalling networks. *Nonlinearity*, 27(8):1805. 6, 7

Ruuth, S. J. (1995). Implicit-explicit methods for reaction-diffusion problems in pattern formation. *Journal of Mathematical Biology*, 34(2):148–176. 78

Saheya, B., Chen, G.-q., Sui, Y.-k., and Wu, C.-y. (2016). A new newton-like method for solving nonlinear equations. *SpringerPlus*, 5(1):1269. 74

Schnakenberg, J. (1979). Simple chemical reaction systems with limit cycle behaviour. *Journal of theoretical biology*, 81(3):389–400. 10, 14, 39, 48

Segel, L. A. and Jackson, J. L. (1972). Dissipative structure: an explanation and an ecological example. *Journal of theoretical biology*, 37(3):545–559. 1

Turing, A. M. (1952). The chemical basis of morphogenesis. *Philosophical Transactions of the Royal Society of London. Series B, Biological Sciences*, 237(641):37–72. 2, 17, 24, 37, 44, 47, 53

Venkataraman, C., Lakkis, O., and Madzvamuse, A. (2012). Global existence for semilinear reaction–diffusion systems on evolving domains. *Journal of mathematical biology*, 64(1-2):41–67. 10, 14, 39, 48

Wei, J. and Winter, M. (2015). Existence and stability of a spike in the central component for a consumer chain model. *Journal of Dynamics and Differential Equations*, 27(3-4):1141–1171. 5

Yang, W. and Rånby, B. (1996a). Bulk surface photografting process and its applications. i. reactions and kinetics. *Journal of Applied Polymer Science*, 62(3):533–543. 6

Yang, W. and Rånby, B. (1996b). Bulk surface photografting process and its applications. ii. principal factors affecting surface photografting. *Journal of applied polymer science*, 62(3):545–555. 6